

THE UNIVERSITY OF CALGARY

COMPUTER SIMULATION OF AN INDUSTRIAL QUENCH COOLER
ON A LARGE ETHANE CRACKING FURNACE

by:

Richard S. Huntrods

A THESIS

SUBMITTED TO THE FACULTY OF GRADUATE STUDIES
IN PARTIAL FULFILLMENT OF THE REQUIREMENTS FOR THE DEGREE OF
MASTER OF ENGINEERING

DEPARTMENT OF CHEMICAL AND PETROLEUM ENGINEERING

CALGARY, ALBERTA, CANADA

SEPTEMBER, 1988

© RICHARD S. HUNTRODS, 1988

Permission has been granted to the National Library of Canada to microfilm this thesis and to lend or sell copies of the film.

The author (copyright owner) has reserved other publication rights, and neither the thesis nor extensive extracts from it may be printed or otherwise reproduced without his/her written permission.

L'autorisation a été accordée à la Bibliothèque nationale du Canada de microfilmer cette thèse et de prêter ou de vendre des exemplaires du film.

L'auteur (titulaire du droit d'auteur) se réserve les autres droits de publication; ni la thèse ni de longs extraits de celle-ci ne doivent être imprimés ou autrement reproduits sans son autorisation écrite.

ISBN 0-315-46610-3

THE UNIVERSITY OF CALGARY

FACULTY OF GRADUATE STUDIES

The undersigned certify that they have read, and recommend to the Faculty of Graduate Studies for acceptance, a thesis entitled,

"COMPUTER SIMULATION OF AN INDUSTRIAL QUENCH COOLER
ON A LARGE ETHANE CRACKING FURNACE"

submitted by Richard Stanley Huntrods in partial fulfillment of the requirements for the degree of Master of Engineering.



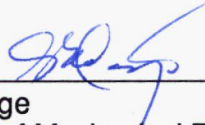
Dr. L.A. Behie, Chairman
Department of Chemical & Petroleum Engineering



Dr. F. Berruti,
Department of Chemical & Petroleum Engineering



Dr. M. Trebble,
Department of Chemical & Petroleum Engineering



Dr. A.G. Doige
Department of Mechanical Engineering

September 15, 1988.
Date

ABSTRACT

An ethane pyrolysis quench cooler, also called a transfer line exchanger (TLX), designed to indirectly cool the exit gases from a pyrolysis furnace producing ethylene from ethane is simulated using the Advanced Continuous Simulation Language (ACSL). The TLX is rigorously modelled using molecular reaction kinetic data. The mass, energy, and momentum balances are solved simultaneously to determine the molar flow of each component and the pressure and temperature profiles along the cooler length.

Transfer line exchangers from the Alberta Gas Ethylene (AGE) pyrolysis plant at Joffre, Alberta are successfully simulated using this model. An excellent history match of the supplied data is achieved both at clean tube conditions and also after 42 days total elapsed operational time. The model predicts a total reaction quench of 20 milliseconds under clean tube conditions. A history match shows 33% of the coke formed in the TLX is deposited on the tube walls. The model indicates the TLX must be shut down for decoking after 48 to 54 days total elapsed operational time.

Additional runs are carried out using data for another TLX simulation obtained from the literature. As with the AGE simulation, an excellent match of this data is obtained

with the simulation model proposed in this work.

A series of runs using the model to observe the effect of mass flux, tube diameter, steam dilution, and heat transfer coefficients is carried out. The most important parameters in the model are found to be the mass flux, the coke deposition ratio, and the coke thermal conductivity. The computer model also indicates that changes in the TLX tube inside diameter due to coke deposition affect the temperature and pressure profiles in the tube, increasing the time required to quench the reaction from 22 milliseconds for a clean tube to 36 milliseconds for a heavily coked tube.

Two different approaches for modelling the deposition of coke on the walls of the quench cooler tube are investigated. A model which calculates incremental changes in the coke thickness at each simulation time step by numerically integrating the coke thickness equation is found to be superior to a model which calculates the total coke thickness at each simulation time step using an integrated form of the coke equation.

The simulation model produced in this work is a fairly detailed computer simulation tool. It is useful for examining the complex interaction of various parameters involved in design, optimization, and better understanding of an industrial ethane to ethylene pyrolysis quench cooler.

ACKNOWLEDGMENTS

I would first like to thank Dr. Leo Behie, under whose supervision this work was carried out, for his assistance and guidance.

I would like to thank Alberta Gas Ethylene, especially Bob Nabata and Hans Wiesner, for supplying the industrial quench cooler data which I used in my simulation work, and also for permitting me to use this data in my thesis.

My friend and colleague, Mr. Dan Henderson provided valuable assistance with the simulation results post-processing. His expertise on PC systems and software is greatly appreciated.

Similarly, Mr. John McRae of the University of Calgary has provided invaluable help with the operation of ACSL in the University environment.

I would also like to thank those I work for and with at Canadian Hunter, especially Mr. Jim Gray, for their support and assistance in the final preparation of this thesis.

Finally, I must thank my wife Linda, and my children Sarah and David. Their continued support and enthusiasm for me and this work has been a great blessing: it made the task of completing this thesis both possible and enjoyable.

TABLE OF CONTENTS

	<u>page</u>
Abstract	iii
Acknowledgments	v
Table of Contents	vi
List of Tables	xv
List of Figures	xvii
List of Symbols	xxxii
1.0 Introduction	1
1.1 Ethylene Pyrolysis Feedstocks	1
1.2 Ethane Pyrolysis Products	8
1.3 Current Ethylene Production	8
1.4 Ethane Pyrolysis Cooling	10
2.0 Ethane Pyrolysis	12
2.1 Pyrolysis Process Description	12
2.2 Pyrolysis Plant Description	12
2.3 Feedstock Chosen for Study	16

	<u>page</u>
3.0 Quench Cooler Applications	17
3.1 Quench Cooler Process Description	17
3.2 Quench Cooler Types and Requirements	17
3.3 Direct Quench versus Indirect Quench	18
3.4 Additional Considerations	21
4.0 Ethane Pyrolysis Model Development	22
4.1 Reaction Schemes	23
4.2 Simple Reaction Scheme	24
4.3 Free-Radical Based Reaction Scheme	26
4.4 Component Based Reaction Scheme	31
4.5 Discussion - Reaction Scheme Chosen	33
5.0 Coke Production in Ethane Pyrolysis	35
5.1 Theories of Coke Formation	35
5.1.1 Surface Reactions	36
5.1.2 Bulk Gas Reactions	38
5.2 Coking Problems in Pyrolysis Systems	41
5.3 Simulation Problems with Coke Formation	44

	<u>page</u>
6.0 Computer Simulation of the Quench Cooler	46
6.1 Computer Model	46
6.2 Computer Model Assumptions	49
6.2.1 Assumption of Plug Flow	49
6.2.2 Assumption of Constant Steam Temperature at the Tube Wall	50
6.2.3 Assumption of Steam Inertness	50
6.2.4 Assumption of Horizontal Flow	52
6.2.5 Assumption of Smooth Pipe	52
6.2.6 Assumption of Pseudo Steady State	53
6.2.7 Assumption of Constant Changes Between Simulation Time Steps	54
6.3 Treatments of Coke Formation	54
6.4 Discussion - Computer Simulation	55
7.0 Computer Simulation Input and Results	58
7.1 Design Conditions and Input Variables	58
7.2 Parametric Simulation - General Discussion	60
7.2.1 Model Assumptions	60

	<u>page</u>
7.2.2 Model Theories	61
7.2.3 Sensitivity	61
7.3 Effect of Total Elapsed Operational Time	61
7.4 Effect of Feed Mass Flux	62
7.5 Effect of Tube Inside Diameter	63
7.6 Effect of Steam Dilution	63
7.7 Effect of Steam Temperature	65
7.8 Effect of Steam Heat Transfer Coefficient	66
7.9 Effect of Coke Laydown Parameter	66
7.10 Effect of Coke Thermal Conductivity	67
7.11 Comparison of Different Coke Formation Models	67
7.12 Comparison with Experimental Results	68
7.13 Comparison with Other Simulators	69
8.0 Discussion of Computer Simulation Results	70
8.1 Effect of Total Elapsed Operational Time	71
8.2 Effect of Feed Mass Flux	89
8.3 Effect of Tube Inside Diameter	95
8.4 Effect of Steam Dilution	100
8.5 Effect of Steam Temperature	105

	<u>page</u>
8.6 Effect of Steam Heat Transfer Coefficient	110
8.7 Effect of Coke Laydown Parameter	116
8.8 Effect of Coke Thermal Conductivity	127
8.9 Discussion - Coke Parameters	138
8.10 Comparison of Different Coke Formation Models	140
8.11 Discussion - Cases Studied	143
8.12 Discussion - Assumptions	146
8.13 Comparison with Experimental Results	146
8.14 Comparison with Other Simulators	147
9.0 Simulation of the Alberta Gas Ethylene Plant	152
9.1 Description of the Alberta Gas Ethylene Plant	152
9.2 Modifications to the Computer Model	153
9.3 Simulation Input Variables	155
9.4 Simulation Results	157
9.5 Discussion of Results	168
9.5.1 History Match for Clean Tube Conditions	169
9.5.2 History Match for Coked Tube Conditions	171
9.6 Simulation Conclusions	172
9.7 Special Considerations - Recommendations	173

	<u>page</u>
10.0 Conclusions and Further Study	177
10.1 Areas not Covered in Simulation	178
10.2 Design Considerations	180
10.3 Experimental Work	180
11.0 References	183
12.0 Appendices	190
Appendix A. General Equations	191
A.1 Pipe Diameters	191
A.2 Cross Sectional Area of Pipe	193
A.3 Inside Perimeter of the Pipe	193
A.4 Reynolds Number	194
A.5 Prandtl Number	194
A.6 Fluid Heat Capacity	195
A.7 Component Viscosity	197
A.8 Process Stream Mixed Viscosities	198
A.9 Average Process Stream Molecular Weight	198

	<u>page</u>
A.10 Total Molar Flow Rate and Mole Fractions	198
A.11 Conversion	199
A.12 Process Stream Density	200
A.13 Fluid Velocity	200
A.14 Mass Flux	200
A.15 Residence Time	201
Appendix B. Continuity Equation	202
B.1 Flowing Component Mass Balance	202
B.2 Units	206
Appendix C. Heat Transfer Equation	207
C.1 Heat Generated or Removed by Reaction	207
C.1.1 Heats of Reaction	208
C.1.2 Heat Capacities	209
C.2 Heat Transfer	211
C.2.1 Inner (Process Stream) Thermal Resistance	212

	<u>page</u>
C.2.2 Process Stream Heat Transfer Coefficient	213
C.2.3 Outer (Shell Side) Thermal Resistance	213
C.2.4 Tube Wall Thermal Resistance	214
C.2.5 Coke Thermal Resistance	214
C.3 Units	215
 Appendix D. Momentum Equation	 216
D.1 Pressure Drop	216
D.1.1 Friction Factor	216
D.2 Units	217
 Appendix E. Reaction Rates	 218
E.1 Reaction Rate Equations	218
E.2 Reaction Rate Constants	218
E.3 Equilibrium Constants	220

	<u>page</u>
Appendix F. Coke Thickness	223
F.1 Derivation of the Basic Coke Thickness Equation	223
F.2 Integrated Coke Thickness Equation	224
F.2.1 Units	227
F.3 Differential Coke Thickness Equation	228
F.3.1 Units	231
Appendix G. Quench Cooler Computer Program Flowchart	232
Appendix H. Summary of Computer Runs and Results	243
Appendix I. Typical Computer Run Output Listing - Run 6	250
Appendix J. Quench Cooler ACSL Program Listings	258
Appendix K. Program Run Post Processing	280

LIST OF TABLES

	<u>page</u>
Table 1.1 Ethylene and Related Petrochemical Production in Canada for 1988	2
Table 1.2 Typical Ethane Pyrolysis Product Distribution	9
Table 4.1 Simple Ethane Reaction Scheme	25
Table 4.2 Free Radical Ethane Reaction Scheme	27
Table 4.3 Component Based Ethane Reaction Scheme	32
Table 6.1 Ethane Reaction Molecular Species	47
Table 7.1 Parametric Simulation Base Case (Rase, 1977b)	59
Table 9.1 Alberta Gas Ethylene Plant Data	156
Table A.1 Component Thermal Properties	196
Table E.1 Ethane Pyrolysis Reaction Rates	219

	<u>page</u>
Table E.2 Ethane Pyrolysis Rate Constants	221
Table H.1 Description of Parametric Simulation Cases	244
Table H.2 Parametric Simulation Results - Part 1	245
Table H.2 Parametric Simulation Results - Part 2	246
Table H.2 Parametric Simulation Results - Part 3	247
Table H.3 Alberta Gas Ethylene Simulation Results - Part 1	248
Table H.3 Alberta Gas Ethylene Simulation Results - Part 2	249

LIST OF FIGURES

	<u>page</u>
Figure 1.1 Flowchart Showing Typical Finished Petrochemical Products Obtained from Ethylene	3
Figure 1.2 Flowchart Showing Typical Finished Petrochemical Products Obtained from Propylene, an Ethane Pyrolysis By-product	4
Figure 1.3 Flowchart Showing Typical Finished Petrochemical Products Obtained from Butadiene, an Ethane Pyrolysis By-product	5
Figure 1.4 Flowchart Showing Typical Finished Petrochemical Products Obtained from Methane, an Ethane Pyrolysis By-product	6
Figure 2.1 Typical Ethane Pyrolysis Process Steps	13
Figure 2.2 Schematic Diagram of a Typical Ethane Pyrolysis Process	15

	<u>page</u>
Figure 3.1 Schematic Diagram of a Typical Shell and Tube Quench Cooler (TLX)	20
Figure 5.1 Coke Producing Reactions	39
Figure 8.1.1 TLX Temperature profiles at different total elapsed operational times using coke model 1 (base case)	72
Figure 8.1.2 TLX Pressure profiles at different total elapsed operational times using coke model 1 (base case)	73
Figure 8.1.3 TLX Ethane conversion profiles at different total elapsed operational times using coke model 1 (base case)	74
Figure 8.1.4 TLX Coke thickness profiles at different total elapsed operational times using coke model 1 (base case)	75
Figure 8.1.5 TLX Coke rate profiles at different total elapsed operational times using coke model 1 (base case)	76

	<u>page</u>
Figure 8.1.6 TLX Temperature profiles at different total elapsed operational times using coke model 2 (base case)	77
Figure 8.1.7 TLX Pressure profiles at different total elapsed operational times using coke model 2 (base case)	78
Figure 8.1.8 TLX Ethane conversion profiles at different total elapsed operational times using coke model 2 (base case)	79
Figure 8.1.9 TLX Coke thickness profiles at different total elapsed operational times using coke model 2 (base case)	80
Figure 8.1.10 TLX Coke rate profiles at different total elapsed operational times using coke model 2 (base case)	81
Figure 8.1.11 TLX Temperature profiles at different total elapsed operational times using coke model 2 (base case)	82
Figure 8.1.12 TLX Pressure profiles at different total elapsed operational times using coke model 2 (base case)	83

	<u>page</u>
Figure 8.1.13 TLX Ethane conversion profiles at different total elapsed operational times using coke model 2 (base case)	84
Figure 8.1.14 TLX Coke thickness profiles at different total elapsed operational times using coke model 2 (base case)	85
Figure 8.1.15 TLX Coke rate profiles at different total elapsed operational times using coke model 2 (base case)	86
Figure 8.2.1 TLX Temperature profiles for different feed mass fluxes at clean tube conditions using either coke model	90
Figure 8.2.2 TLX Pressure profiles for different feed mass fluxes at clean tube conditions using either coke model	91
Figure 8.2.3 TLX Ethane conversion profiles for different feed mass fluxes at clean tube conditions using either coke model	92

	<u>page</u>
Figure 8.2.4 TLX Coke rate profiles for different feed mass fluxes at clean tube conditions using either coke model	93
Figure 8.3.1 TLX Temperature profiles for various TLX tube inside diameters at clean tube conditions using either coke model	96
Figure 8.3.2 TLX Pressure profiles for various TLX tube inside diameters at clean tube conditions using either coke model	97
Figure 8.3.3 TLX Ethane conversion profiles for various TLX tube inside diameters at clean tube conditions using either coke model	98
Figure 8.3.4 TLX Coke rate profiles for various TLX tube inside diameters at clean tube conditions using either coke model	99

	<u>page</u>
Figure 8.4.1 TLX Temperature profiles for different steam - hydrocarbon ratios at clean tube conditions using either coke model	101
Figure 8.4.2 TLX Pressure profiles for different steam - hydrocarbon ratios at clean tube conditions using either coke model	102
Figure 8.4.3 TLX Ethane conversion profiles for different steam - hydrocarbon ratios at clean tube conditions using either coke model	103
Figure 8.4.4 TLX Coke rate profiles for different steam - hydrocarbon ratios at clean tube conditions using either coke model	104
Figure 8.5.1 TLX Temperature profiles for different shell side steam temperatures at clean tube conditions using either coke model	106

	<u>page</u>
Figure 8.5.2 TLX Pressure profiles for different shell side steam temperatures at clean tube conditions using either coke model	107
Figure 8.5.3 TLX Ethane conversion profiles for different shell side steam temperatures at clean tube conditions using either coke model	108
Figure 8.5.4 TLX Coke rate profiles for different shell side steam temperatures at clean tube conditions using either coke model	109
Figure 8.6.1 TLX Temperature profiles for different steam heat transfer coefficients at clean tube conditions using either coke model	111
Figure 8.6.2 TLX Pressure profiles for different steam heat transfer coefficients at clean tube conditions using either coke model	112

	<u>page</u>
Figure 8.6.3 TLX Ethane conversion profiles for different steam heat transfer coefficients at clean tube conditions using either coke model	113
Figure 8.6.4 TLX Coke rate profiles for different steam heat transfer coefficients at clean tube conditions using either coke model	114
Figure 8.7.1 TLX Temperature profiles for different coke deposition ratios at 12 days total elapsed operational time using coke model 1	117
Figure 8.7.2 TLX Pressure profiles for different coke deposition ratios at 12 days total elapsed operational time using coke model 1	118
Figure 8.7.3 TLX Ethane conversion profiles for different coke deposition ratios at 12 days total elapsed operational time using coke model 1	119

	<u>page</u>
Figure 8.7.4 TLX Coke thickness profiles for different coke deposition ratios at 12 days total elapsed operational time using coke model 1	120
Figure 8.7.5 TLX Coke rate profiles for different coke deposition ratios at 12 days total elapsed operational time using coke model 1	121
Figure 8.7.6 TLX Temperature profiles for different coke deposition ratios at 12 days total elapsed operational time using coke model 2	122
Figure 8.7.7 TLX Pressure profiles for different coke deposition ratios at 12 days total elapsed operational time using coke model 2	123
Figure 8.7.8 TLX Ethane conversion profiles for different coke deposition ratios at 12 days total elapsed operational time using coke model 2	124

	<u>page</u>
Figure 8.7.9 TLX Coke thickness profiles for different coke deposition ratios at 12 days total elapsed operational time using coke model 2	125
Figure 8.7.10 TLX Coke rate profiles for different coke deposition ratios at 12 days total elapsed operational time using coke model 2	126
Figure 8.8.1 TLX Temperature profiles for different coke thermal conductivities at 12 days total elapsed time using coke model 1	128
Figure 8.8.2 TLX Pressure profiles for different coke thermal conductivities at 12 days total elapsed time using coke model 1	129
Figure 8.8.3 TLX Ethane conversion profiles for different coke thermal conductivities at 12 days total elapsed time using coke model 1	130

	<u>page</u>
Figure 8.8.4 TLX Coke thickness profiles for different coke thermal conductivities at 12 days total elapsed time using coke model 1	131
Figure 8.8.5 TLX Coke rate profiles for different coke thermal conductivities at 12 days total elapsed time using coke model 1	132
Figure 8.8.6 TLX Temperature profiles for different coke thermal conductivities at 12 days total elapsed time using coke model 2	133
Figure 8.8.7 TLX Pressure profiles for different coke thermal conductivities at 12 days total elapsed time using coke model 2	134
Figure 8.8.8 TLX Ethane conversion profiles for different coke thermal conductivities at 12 days total elapsed time using coke model 2	135

	<u>page</u>
Figure 8.8.9 TLX Coke thickness profiles for different coke thermal conductivities at 12 days total elapsed time using coke model 2	136
Figure 8.8.10 TLX Coke rate profiles for different coke thermal conductivities at 12 days total elapsed time using coke model 2	137
Figure 8.14.1 TLX Outlet Temperatures at different mass fluxes comparing this simulation model to the simulation of Rase (1977b)	148
Figure 8.14.2 TLX Outlet Pressure Drops at different mass fluxes comparing this simulation model to the simulation of Rase (1977b)	149
Figure 8.14.3 TLX Outlet Conversions at different mass fluxes comparing this simulation model to the simulation of Rase (1977b)	150

	<u>page</u>	
Figure 9.1	TLX Temperature profiles at different total elapsed operational times for the Alberta Gas Ethylene TLX simulation	158
Figure 9.2	TLX Pressure profiles at different total elapsed operational times for the Alberta Gas Ethylene TLX simulation	159
Figure 9.3	TLX Ethane conversion profiles at different total elapsed operational times for the Alberta Gas Ethylene TLX simulation	160
Figure 9.4	TLX Coke thickness profiles at different total elapsed operational times for the Alberta Gas Ethylene TLX simulation	161
Figure 9.5	TLX Coke rate profiles at different total elapsed operational times for the Alberta Gas Ethylene TLX simulation	162

	<u>page</u>
Figure 9.6 TLX Temperature profiles at different total elapsed operational times for the Alberta Gas Ethylene TLX simulation	163
Figure 9.7 TLX Outlet Temperatures at different feed mass fluxes for the Alberta Gas Ethylene Simulation	164
Figure 9.8 TLX Outlet Pressures at different feed mass fluxes for the Alberta Gas Ethylene Simulation	165
Figure 9.9 TLX Outlet Temperatures at different coke deposition ratios for the Alberta Gas Ethylene Simulation	166
Figure 9.10 TLX Outlet Pressures at different coke deposition ratios for the Alberta Gas Ethylene Simulation	167
Figure A.1 Differential Element of a Plug Flow Reactor Showing Pertinent Calculation Variables	192

page

Figure B.1 Ethane Pyrolysis Reactions 203

Figure E.1 Plot of Equilibrium Constants for Ethane 222
Pyrolysis Reactions 1 and 3

LIST OF SYMBOLS

- A - Tube inner cross-sectional area
(m^2 or cm^2)
- A' - Rate constant pre-exponentiation factor
($1/s$, $cm^3/mol \cdot s$ or $g_{ck} \cdot cm/g_{c4+} \cdot s$)
- A_{ck} - Cross-sectional area of deposited coke
(m^2 or cm^2)
- ACSL - Advanced Continuous Simulation Language
- b_{ck} - Deposited coke thickness
(m or cm)
- C_{pi} - Component heat capacity
($J/mol \cdot K$ or $cal/mol \cdot K$)
- ΔC_{pi} - Change in component heat capacity
($J/mol \cdot K$ or $cal/mol \cdot K$)
- C_{pj} - Reaction heat capacity
($J/mol \cdot K$ or $cal/mol \cdot K$)
- C_{pm} - Average fluid heat capacity
($J/mol \cdot K$ or $cal/mol \cdot K$)
- C_{pA} - Constant in heat capacity expression
- C_{pB} - Constant in heat capacity expression
- C_{pC} - Constant in heat capacity expression
- C_{pD} - Constant in heat capacity expression

- C_{pN} - General form of the heat capacity constant
where N represents either A, B, C or D
- C_{vm} - Average fluid volumetric heat capacity
(J/mol·K or cal/mol·K)
- d - Tube inside diameter available for
process fluid flow
(mm or cm)
- d_i - Initial (clean) tube inside diameter
(mm or cm)
- d_o - Tube outside diameter
(mm or cm)
- D - Mean tube diameter (tube + wall)
(mm or cm)
- D_{ck} - Mean tube diameter (tube + coke)
(mm or cm)
- E - Reaction rate activation energy
(J/mol or cal/mol)
- f - Fanning friction factor
- F_i - Component molar flow rate
(mol/s)
- F_i^o - Initial component molar flow rate
(mol/s)
- F_{tot} - Total molar flow rate
(mol/s)

- F_{tothc} - Total hydrocarbon molar flow rate
 (mol/s)
- g_c - Gravitation constant
 (9.80 kg·m/kg_f·s² or 980.7 g·cm/g_f·s²)
- G - Fluid mass flux
 (kg/m²·s or g/cm²·s)
- h_i - Inner heat transfer coefficient
 (W/m²·K or Btu/hr·ft²·F)
- h_o - Outer heat transfer coefficient
 (W/m²·K or Btu/hr·ft²·F)
- ΔH_{fi}° - Component heat of formation at
 standard conditions
 (J/mol or cal/mol)
- ΔH_r - Overall heat of reaction at temperature
 (J/mol or cal/mol)
- ΔH_r° - Overall heat of reaction at standard
 temperature
 (J/mol or cal/mol)
- ΔH_{rj} - Heat of reaction
 (J/mol or cal/mol)
- ΔH_{rj}° - Heat of reaction at standard conditions
 (J/mol or cal/mol)
- kc_j - Equilibrium constant
 (mol/L)

- k_{ck} - Coke heat transfer coefficient
 (W/m·K or Btu/hr·ft·F)
- k_{fm} - Fluid heat transfer coefficient
 (W/m·K or Btu/hr·ft·F)
- k_j - Reaction rate coefficient
 (1/s, cm³/mol·s or g_{ck}·cm/g_{c4+}·s)
- k_{wall} - Tube wall heat transfer coefficient
 (W/m·K or Btu/hr·ft·F)
- L - Total quench cooler length
 (m or cm)
- Mw_i - Component molecular weight
 (kg/mol or g/mol)
- Mw_m - Average fluid molecular weight
 (kg/mol or g/mol)
- nc - Number of components
- n_{ck} - Moles of coke produced by reaction
- Pr - Prandtl number
 (dimensionless)
- P - Pressure (absolute)
 (MPa, kPa or atm)
- P_c - Critical Pressure
 (kPa or atm)
- P_i - Partial pressure
 (kPa or atm)

P_t	- Total Pressure (absolute) (MPa, kPa or atm)
r_j	- Reaction rate (mol/cm ³ ·s or mol/cm ² ·s)
R	- Gas constant (1.987 cal/mol·K)
Re	- Reynold's number (dimensionless)
R_g	- Gas constant (82.05 cm ³ ·atm/mol·K)
s_{ij}	- Stoichiometric coefficient
S	- Tube inner perimeter (m or cm)
Δt	- Time step size (s)
t	- Time from start of run (s or days)
t_r	- Fluid residence time (ms)
T	- Fluid temperature (K)
T_c	- Critical temperature (K)

T_{far}	- Fluid temperature (F)
T_o	- Heat of reaction base temperature (K)
T_r	- Reduced temperature
T_{wall}	- Temperature of coolant steam (K)
TLX	- Transfer Line Exchanger (Quench Cooler)
U_o	- Overall heat transfer coefficient ($W/m^2 \cdot K$, $Btu/hr \cdot ft^2 \cdot F$ or $cal/s \cdot cm^2 \cdot K$)
U_m	- Average fluid velocity (cm/s)
x_i	- Hydrocarbon based mole fraction
X_i	- Conversion
x_{wall}	- Tube wall thickness (mm or cm)
Y_i	- Mole fraction
z	- Quench cooler length (m or cm)

Greek Symbols:

- α - Fraction of produced coke deposited on
the tube wall
- ρ_f - Average fluid density
(kg/m^3 or g/cm^3)
- μ_i - Component viscosity
($\text{Pa}\cdot\text{s}$, cP, $\text{g/s}\cdot\text{cm}$ or $\text{lb/hr}\cdot\text{ft}$)
- μ_{cr} - Viscosity calculation term
- μ_m - Average fluid viscosity
($\text{Pa}\cdot\text{s}$, cP, $\text{g/s}\cdot\text{cm}$ or $\text{lb/hr}\cdot\text{ft}$)
- μ_r - Viscosity calculation term

1.0 Introduction

Ethylene is an extremely important chemical in the modern petrochemical industry. Table 1.1 shows the current production of ethylene in Canada. Figures 1.1 to 1.4 show the finished products which may be formed from the pyrolysis products of ethylene manufacture. Table 1.1 also shows the current Canadian production of the various final petrochemical products which use ethylene as a feedstock. Ethylene is produced from two primary sources, as a separation product from the processing of rich natural gas, and as the result of a pyrolysis reaction.

Pyrolysis of feedstock to ethylene involves the addition of heat to the feedstock in order to drive the endothermic cracking reactions required to produce ethylene. Because the common feedstocks are gases, tubular flow reactors are most commonly used for the production of ethylene.

1.1 Ethylene Pyrolysis Feedstocks

A number of feedstocks are used to produce ethylene by pyrolysis.

Ethane and propane are the most popular feedstocks for pyrolysis plant designs, as the secondary pyrolysis reactions are minimized with these feedstocks. Plant design is

**Table 1.1 Ethylene and Related Petrochemical Production
in Canada for 1988 (Oilweek, 1988)**

A. Ethylene Production				
Company	Plant Location	Feedstock	Products	Annual Capacity
Alberta Gas Ethylene	Red Deer, Alberta	Ethane	Ethylene	3 Billion Lbs.
Esso Chemicals Canada	Sarnia, Ontario	Petroleum Fractions	Ethylene Propylene	220 000 Tonnes 75 000 Tonnes
Polysar (Petrosar)	Sarnia, Ontario	Naphtha Gas Oils Propane	Ethylene Propylene Butadiene, Butylene	1 Billion Lbs. 725 Million Lbs. 480 Million Lbs.
Petromont	Varenes, Quebec	Ethane/Propane Mix Naphthas	Ethylene Butadiene, Butylene	225 000 Tonnes 50 000 Tonnes
B. Petrochemical Production				
Company	Plant Location	Feedstock	Products	Annual Capacity
C-I-L Inc.	Edmonton, Alberta	Ethylene,	Polyethylene, Vinyl Acetate	75 000 Tonnes
Celanese Canada Inc.	Edmonton, Alberta	Ethylene	Pentaerythritol,	26 000 Tonnes
Dow Chemical Canada Inc.	Fort Sask., Alberta	Ethylene	Ethylene Oxide, Ethylene Glycols	---
Novacor Chemicals	Red Deer, Alberta	Ethylene	Polyethylene	800 Million Lbs.
Shell Canada	Scotford, Alberta	Benzene, Ethylene	Styrene	300 000 Tonnes
Union Carbide	Prentiss, Alberta	Ethylene	Ethylene Glycol	230 000 Tonnes
Celanese	Millhaven, Ontario	Ethylene Glycol	Polyester Fibre	---
Dow Chemical Canada Inc.	Sarnia, Ontario	Ethylene, Butadiene	Polyethylene, Polystyrene, Vinyl Chloride, others	---
Dow Chemical Canada Inc.	Weston, Ontario	Polystyrene	Styrofoam	---
Du Pont Canada Inc.	Sarnia, Ontario	Ethylene	Polyethylene	235 000 Tonnes
Ethyl Canada Ltd.	Corunna, Ontario	Ethylene	Ethyl Chloride	30 000 Tonnes
Esso Chemical Canada	Sarnia, Ontario	Ethylene	Polyethylene	135 000 Tonnes
Novacor	Hoore Twp., Ontario	Ethylene	Polyethylene	230 Million Lbs.
Polysar Ltd.	Sarnia, Ontario	Ethylene Butadiene Styrene	Styrene Synthetic Rubber	372 000 Tonnes 310 000 Tonnes
Polysar Ltd.	Cambridge, Ontario	Styrene	Polystyrene	30 000 Tonnes
Commercial Alcohols Ltd.	Varenes, Quebec	Ethylene	Ethyl Alcohol	60 000 Tonnes
Dow Chemical Canada Ltd.	Varenes, Quebec	Styrene, Butadiene, Polystyrene	Polystyrene, Styrofoam	--- ---
Hilmont Canada Ltd.	Varenes, Quebec	Propylene, Ethylene	Polypropylene	90 000 Tonnes
Union Carbide Canada	Montreal, Quebec	Ethylene, Ethylene Oxide	Ethylene Oxide, Ethylene Glycol	68 000 Tonnes 95 000 Tonnes

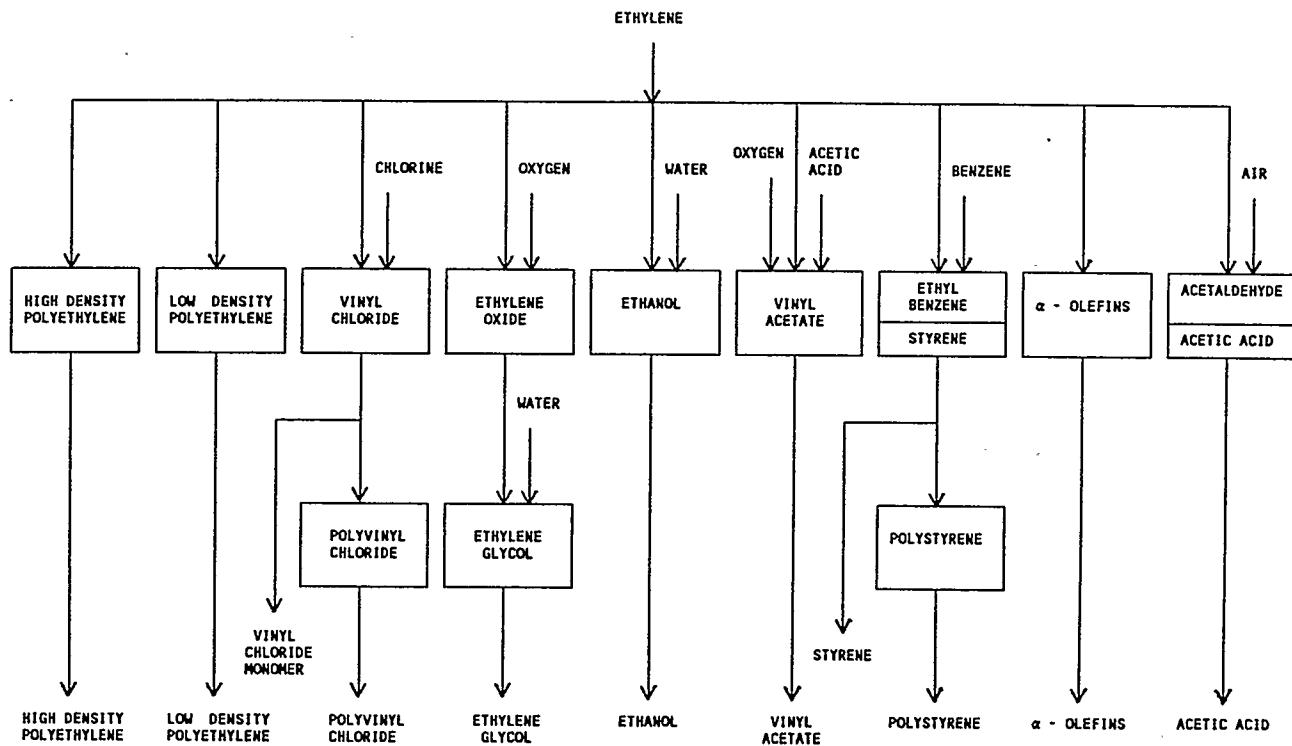


Figure 1.1 Flowchart Showing Typical Finished Petrochemical Products Obtained from Ethylene
(Albright, Crynes and Corcoran, 1983)

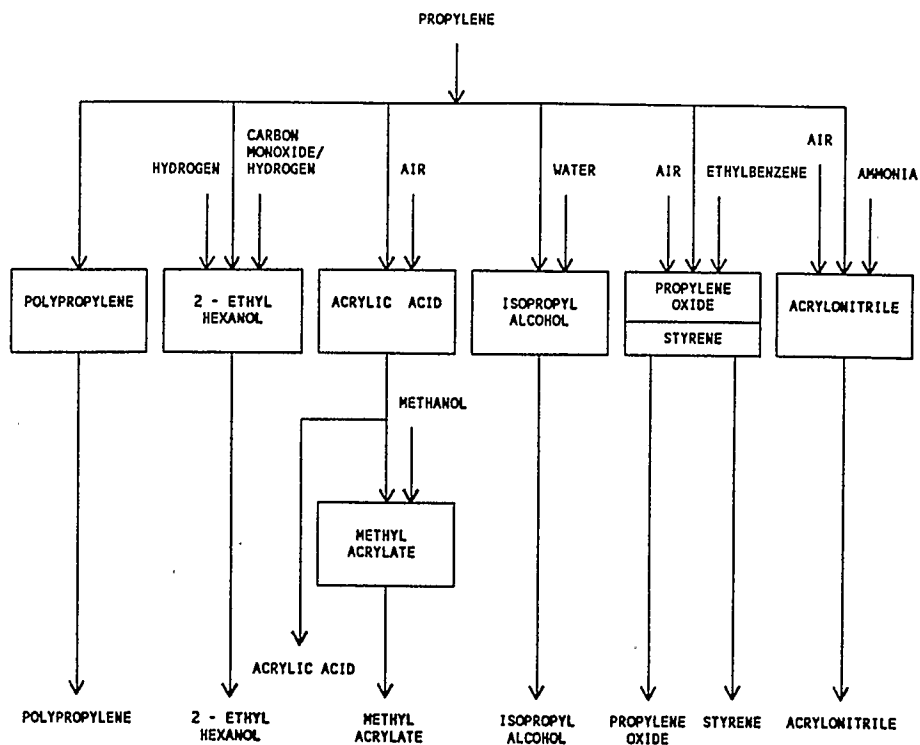


Figure 1.2 Flowchart Showing Typical Finished Petrochemical Products Obtained from Propylene, an Ethane Pyrolysis By-product
(Albright, Crynes and Corcoran, 1983)

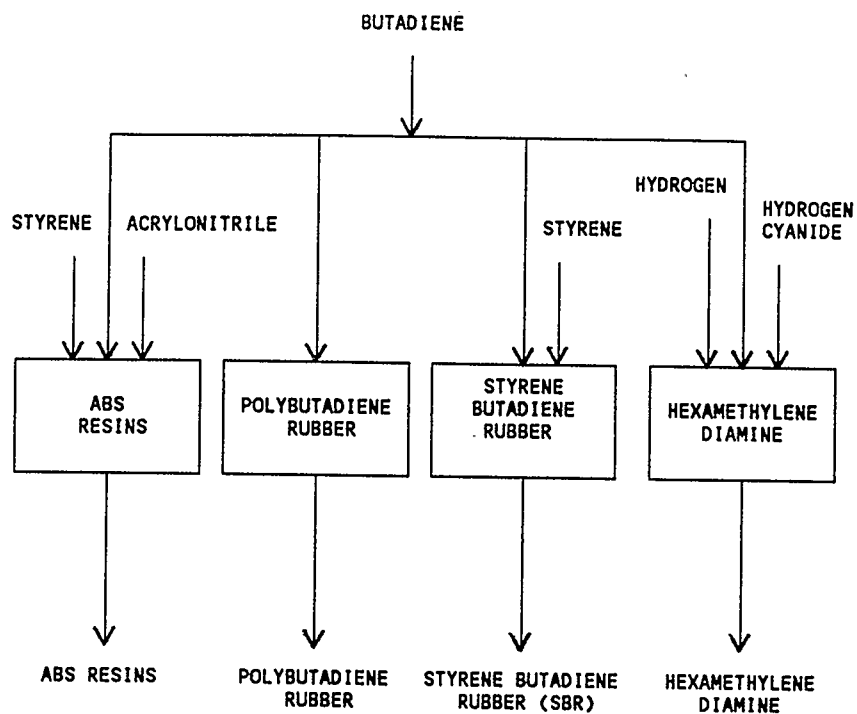


Figure 1.3 Flowchart Showing Typical Finished Petrochemical Products Obtained from Butadiene, an Ethane Pyrolysis By-product
(Albright, Crynes and Corcoran, 1983)

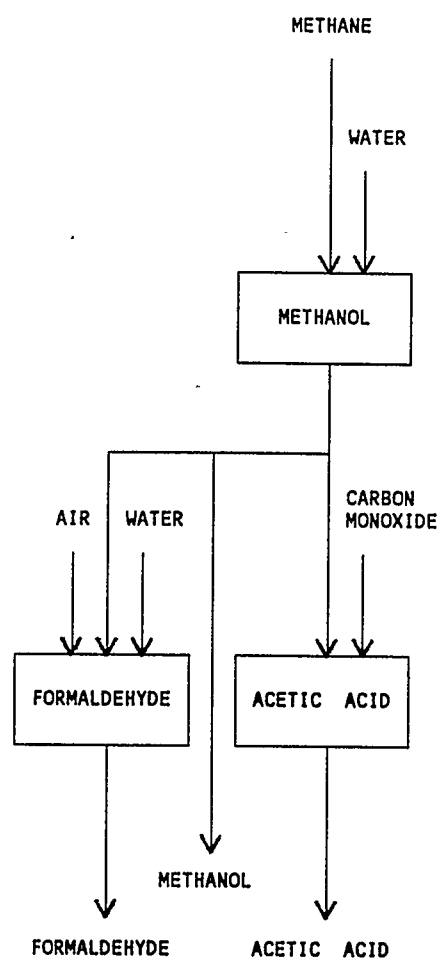


Figure 1.4 Flowchart Showing Typical Finished Petrochemical Products Obtained from Methane, an Ethane Pyrolysis By-product
(Albright, Crynes and Corcoran, 1983)

also made easier since the reacting gases and all of the lighter products (except coke and the various tars and heavy polymers) are non-condensing at all conditions and temperatures of the process.

The most commonly used feedstocks are the naphthas, due to their great worldwide availability. These feedstocks produce more secondary reaction by-products, but those products are often sold for good value. Some problems with condensing products must be considered when designing these coolers, and outlet temperature from the reaction quench must be kept above the dew point of the heavier components.

In recent years, vacuum oils, crude oils, and shale oils have all been considered as feedstocks for ethylene manufacture. Work with these feedstocks is still in its infancy, with problems associated with condensing components and unwanted secondary reactions currently being encountered. Further developments with these heavy feedstocks depends much on world oil prices.

There has been research into the use of methanol from bio-gas plants as a feedstock for non-pyrolytic ethylene manufacture, and even some research into the direct biological production of ethylene from biomass by suitable bacteria, however, none of these methods are economically feasible at this time.

In countries where natural gas is plentiful, the feedstock of choice is ethane, propane, or a mixture of the two.

Pyrolysis of such feedstocks to produce ethylene is a rather straight forward reaction with high yields and low production of side products compared to other feedstocks. The reaction scheme, while not simple, is understood well enough to be numerically modelled with modern computers. Table 1.2 shows the amounts of typical pyrolysis products produced by pyrolysis of ethane, propane, butane, and naphtha.

When all feedstocks are available, economics will usually decide which will be used. The cost of either feedstock, in terms of either direct purchase price, or as lost sales revenue is the first economic factor influencing the feedstock choice. The second is the value of the pyrolysis side reaction products produced by each feedstock.

1.2 Ethane Pyrolysis Products

The products of ethane pyrolysis are shown in Table 1.2. These products can be further reacted to produce some of the petrochemicals shown in Figures 1.1 to 1.4. The most common finished product of the pyrolysis of ethane is polyethylene, as shown in Table 1.1

1.3 Current Ethylene Production

Table 1.1 shows the current (1988) production of both

Table 1.2 Typical Ethane Pyrolysis Product Distribution
(Zdonik, Green and Hallee ,1970)

Feedstock or Product	Product Distribution - Weight %					
	Ethane 60%	Propane 90%	Butane 96%	Naphtha Mild	Naphtha Moderate	Naphtha Severe
Fuel Gas	13.9	28.4	24.2	10.4	16.8	19.8
Ethylene (90% C ₂ H ₄)	80.3	45.6	36.5	19.7	26.7	29.1
C ₃ 's (99.8% C ₃ H ₆)	2.4	15.1	18.2	15.2	16.8	16.5
C ₄ 's (60% C ₄ H ₈)	1.9	2.6	7.9	10.5	10.3	9.3
C ₅ +	1.5	8.3	13.2	44.2	29.4	25.3

ethylene and final petrochemical products in Canada (Oilweek, 1988). Since ethylene is used in such a wide variety of petrochemicals it is easy to understand why the role of ethylene is so important to the petrochemical industry.

1.4 Ethane Pyrolysis Cooling

The economic production of ethylene from ethane requires very high temperatures in the furnace portion of the production facility. Once ethane has been converted into ethylene, a number of undesirable secondary reactions can occur which will form additional by-products from the ethylene, such as acetylene, propane, propylene and heavier compounds, and finally coke. These secondary reactions are undesirable because the products are generated in such small quantities that their separation from the ethylene costs more than the products are worth.

Coke is a very undesirable secondary reaction product, because coke will coat the walls of the furnace and TLX, the elbows in the reactor and the inlet manifold of the quench cooler, causing the plant to be shut down on the average of every 30-60 days for cleaning. Consequently, stopping the reaction by quenching at the point of maximum ethylene production but minimum by-product production is an important step in the process. Computer modelling of ethylene plants

can be invaluable in locating this point.

This quenching of reaction products is accomplished by the rapid cooling of the process by 300 K to 400 K from around 1200 K in as short a time as possible (less than 1 second). This stops the undesirable secondary reactions and minimizes the secondary reaction products. Furthermore, it is standard practice in industry to remove the heat indirectly with conventional heat exchangers called transfer line exchangers (TLX) or quench coolers. The reaction quench thus becomes an important step in controlling the product distribution from the ethylene pyrolysis reaction.

2.0 Ethane Pyrolysis

2.1 Pyrolysis Process Description

The production of ethylene from ethane and other hydrocarbon feedstocks is a highly endothermic process which requires a very large input of heat. This heat is usually provided to the reaction by large furnaces containing many burners, which may be gas or oil fired, in the floor and walls of the furnace. Since the feedstock in current commercial pyrolysis plants is a gas, a tubular flow reactor scheme is employed. Pipes containing the feedstock gases pass through the furnace and are heated to several hundred degrees Kelvin. This initiates the main pyrolysis reactions, producing ethylene from the feedstock. The hot product gases must then be rapidly cooled to stop further reaction. Finally, separation of the various products from the process gas stream must be accomplished. Figure 2.1 shows the typical processing steps for producing ethylene from ethane or propane pyrolysis.

2.2 Pyrolysis Plant Description

The typical ethylene pyrolysis plant consists of three main process units.

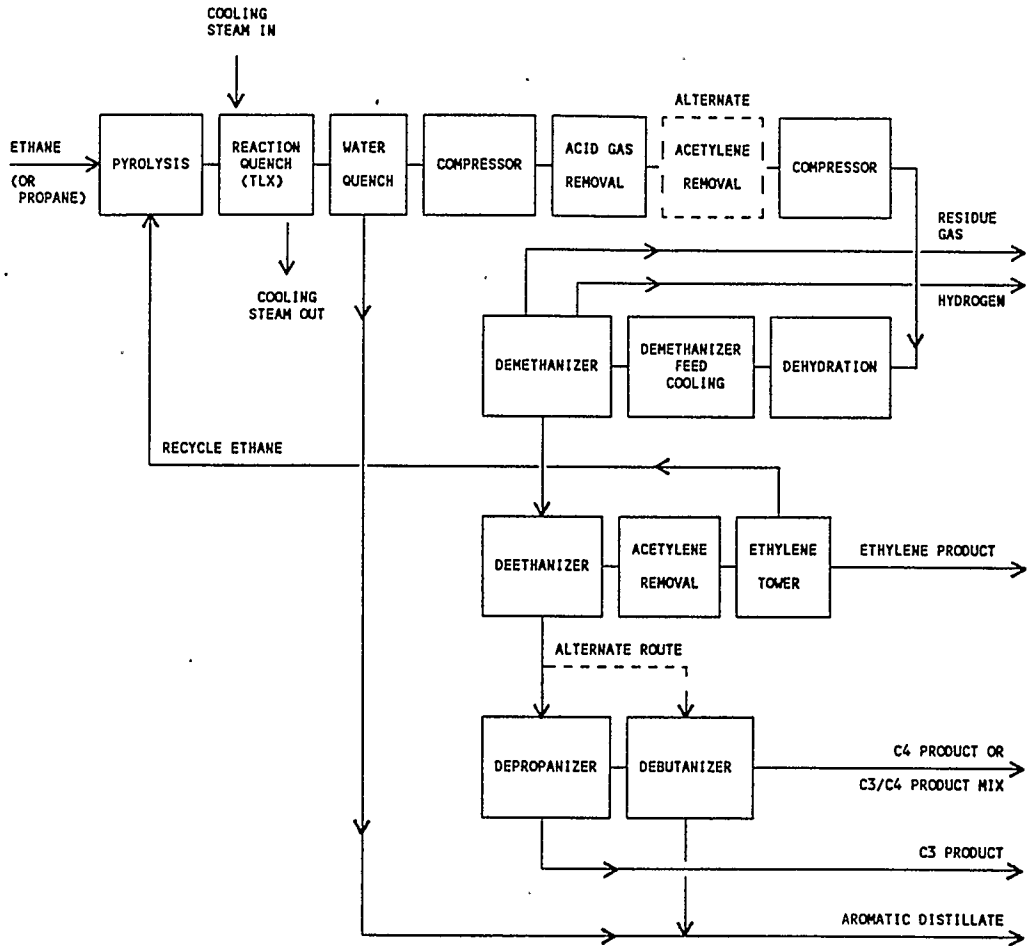


Figure 2.1 Typical Ethane Pyrolysis Process Steps
(Albright, Crynes and Corcoran, 1983)

The first is the pyrolysis furnace, where the heat to promote the pyrolysis reaction is added to the process stream. The furnace usually has two sections, the preheat chamber, where the inlet gases are heated to near the process temperature, usually by heat exchange with the burner exit gases. The second section of the furnace is the radiant heating section. Here the furnace tubes pass extremely close to the heating burners and the process stream is rapidly heated to the pyrolysis temperature, where the feedstock is converted to ethylene.

The second process unit is the quench cooler, commonly called the transfer line exchanger (TLX). Here the product stream is rapidly cooled to stop further reaction and thus prevent the excess production of undesirable by-products. Two types of quench coolers are currently in common use: the shell and tube heat exchanger and the double pipe heat exchanger, arranged either horizontally or vertically to suit the overall plant layout.

The third process unit is the separation facilities, which separate the various compounds produced by the pyrolysis reaction into marketable commodities. A schematic diagram of these process units is shown in Figure 2.2

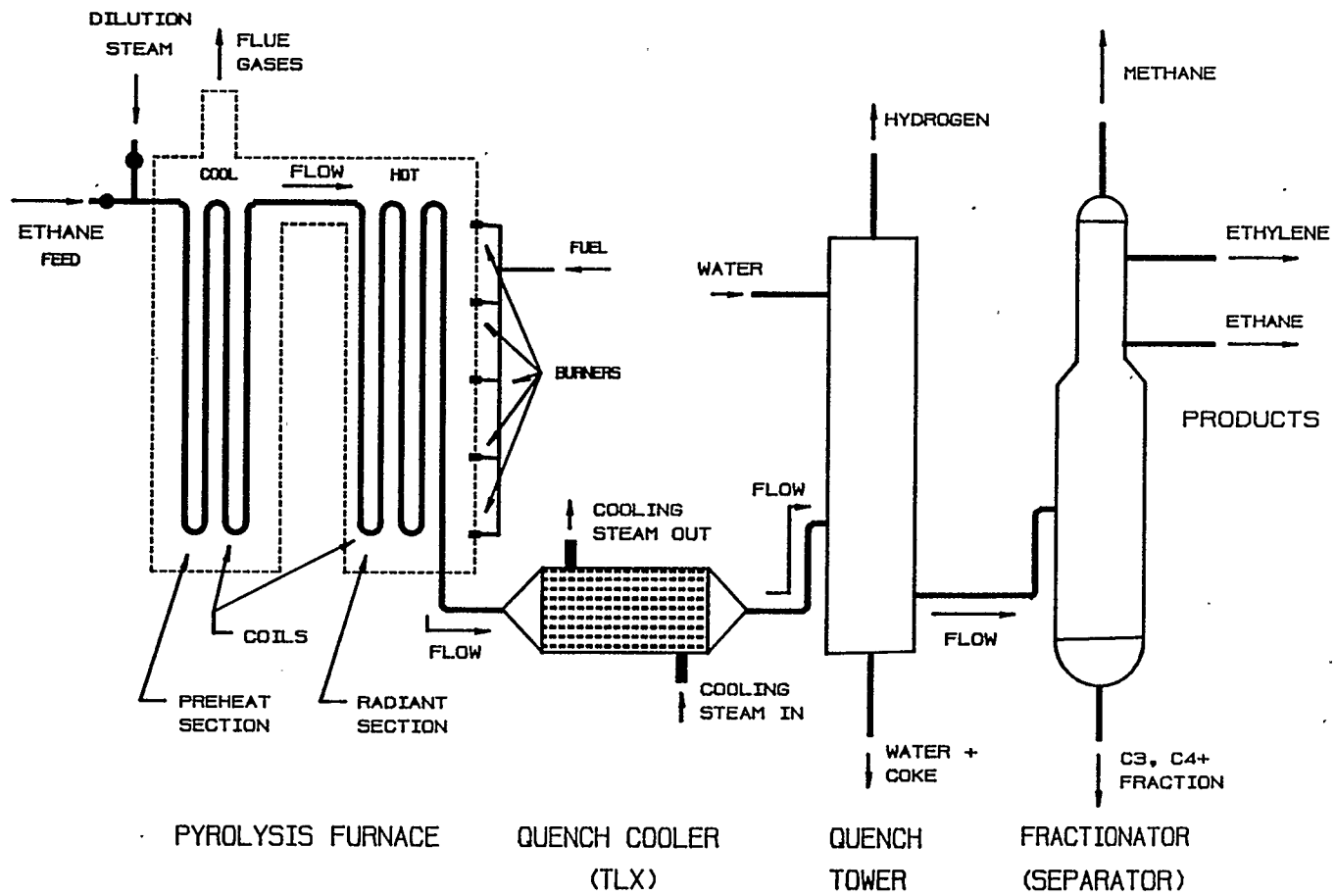


Figure 2.2 Schematic Diagram of a Typical Ethane Pyrolysis Process

2.3 Feedstock Chosen for Study

For this work, ethane is the feedstock used. Of all known reaction schemes for producing Ethylene, the Ethane pyrolysis reaction scheme is the simplest and thus perhaps the best understood. Rate data for this scheme has been available for about 10 years now, and other computer studies have been done using this data. The number of secondary reactions is minimized by using ethane, and fewer components need to be followed when performing parametric simulation studies. Fewer secondary reactions also simplifies the coke formation mechanism. Since coke laydown is one of the primary concerns of this work, and since the complete mechanism of coke formation and deposition is still not fully described, the simple model allows better investigation of some of the factors influencing coke laydown. Finally, the Alberta Gas Ethylene plant in Alberta uses ethane as its feedstock. By building the model using ethane, it is possible to simulate the Alberta Gas Ethylene plant directly.

3.0 Quench Cooler Applications

3.1 Quench Cooler Process Description

The quench cooler (TLX) is located immediately downstream from the pyrolysis furnace. The purpose of quench cooling is to stop all further reaction of the pyrolysis furnace exit gases as quickly as possible to prevent the ethylene from decomposing into significant amounts of highly undesirable side products (especially coke). This is done by rapidly cooling the product stream. Originally, cooling was accomplished by direct contact with a cold fluid such as oil or water (direct quench). Modern plants accomplish this cooling by indirect quench using heat exchangers which employ steam as the cooling fluid.

3.2 Quench Cooler Types and Requirements

There are several ways to cool the process stream rapidly. The original method of cooling the process stream involved the injection of a liquid directly into the process stream. The rapid vaporization of this liquid would cool the process to quench temperature. This was called the direct quench. The fluid injected was often either water or oil. As energy conservation became more important to the

overall plant economics, indirect methods of cooling were employed to cool the process stream and efficiently transfer the energy gained from cooling the process. Heat exchangers are most often employed in the indirect quench, although contacting the process stream with a cold wall has occasionally been used. Common types of heat exchangers are shell and tube exchangers, double pipe exchangers, and fluid bed exchangers. Heat exchange fluids can be steam, hot oils or molten metals.

The method of quench cooling currently in greatest industrial use is the shell and tube or the double pipe heat exchanger, in either a horizontal or vertical orientation, employing high pressure steam in the jacket or shell.

3.3 Direct Quench versus Indirect Quench

Direct quench cooling has the advantage of rapid cooling of the reaction products, as the vaporization of the injected cooling liquid will rapidly absorb most of the thermal energy of the stream. The disadvantage of direct quench cooling is the energy gained by the coolant is very difficult to economically recover, and is often lost. Further, the added fluid must be extracted from the product stream, adding a burden to the downstream separation facilities.

Indirect quench cooling has the advantage of allowing

the recovery of a large portion of the thermal energy which was added to the product stream in the furnace to drive the pyrolysis reactions. This recovered energy can be used in the rest of the plant for electricity generation, or further process heating as required. Further, indirect cooling adds no mass to the process stream, and so product separation is easier to accomplish. The disadvantage of indirect cooling is that cooling takes longer due to the thermal heat transfer barriers introduced by this type of quench cooler. Therefore, efficient design of the cooler becomes important. Rapid cooling must be weighed against pipe diameter, cooling fluid type, and general process specifications (length, size, pressure of steam produced, etc.). Additionally, the indirect cooler will augment problems already existing in the process (coking), and may introduce new problems or new wrinkles to the existing problems (coking of cooler inlet manifold). Figure 3.1 shows a typical industrial shell and tube quench cooler or transfer line exchanger (TLX). Note that for this type of TLX, typical tube lengths (z) are from 6 m to 10 m, typical tube diameters (d_i) are from 20.0 mm to 40.0 mm, and it will contain 80 to 150 tubes.

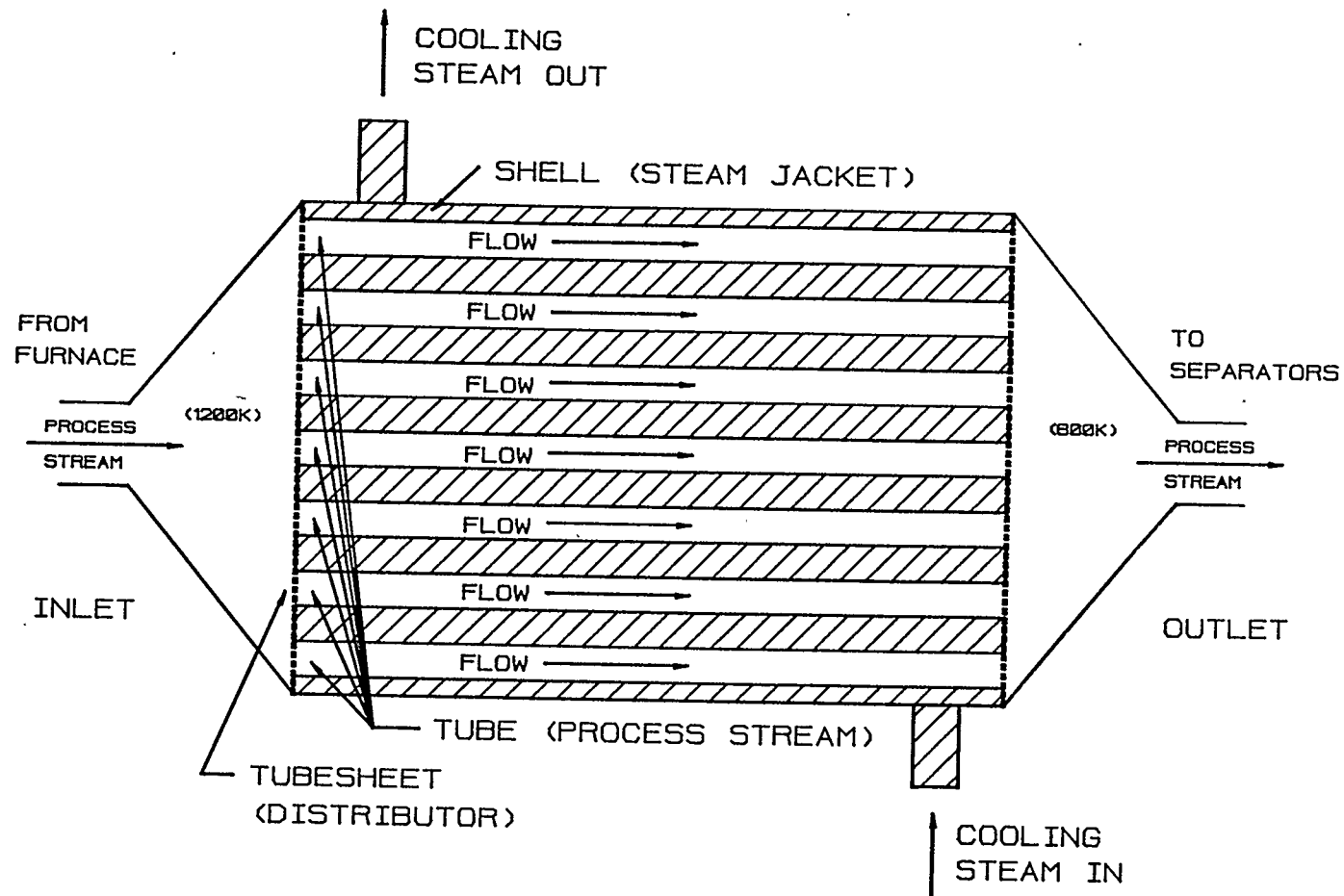


Figure 3.1 Schematic Diagram of a Typical Shell
 and Tube Quench Cooler (TLX)

3.4 Additional Considerations

In the current economy, recovering process stream energy is an important part of overall plant design. Heat lost by direct quench, and the added separation duty placed on downstream separation units by a direct quench can no longer be allowed in a modern ethylene pyrolysis plant. Current plant designs employ heat exchangers in many areas of the plant such as furnace burner exhaust stacks, to recover as much energy as possible. Since the indirect quench cooler can play a fundamental role in energy conservation in such plants, it has now become the quench cooling method of choice in all large industrial pyrolysis plants used for ethylene production.

4.0 Ethane Pyrolysis Model Development

In order to develop a computer simulator for a quench cooler, a method of describing the chemical, physical, and thermal processes must be produced. Most important is the description of the chemical reactions which occur in a form which can be readily used in the model. This requires equations which can rigorously predict the disappearance and formation of every important chemical species in the process as a function of the amounts of species present, the reaction temperature, and other variables important to the accurate simulation of the process.

Models for pressure drop and temperature change are fairly common in engineering literature, and have been well proven. The choice of the equations will depend primarily on the type of process modelled, and the physical description of the quench cooler.

Models for the accurate simulation of the chemical reactions involved in pyrolysis processes are much less common, and are far more difficult to generate. In recent engineering literature, three types of chemical models have been proposed and used in the mathematical simulation of the pyrolysis processes.

4.1 Reaction Schemes

Sundaram and Froment (1977) pioneered much of the work on ethane and propane pyrolysis kinetics. Prior to their work, the predominant reaction scheme used in pyrolysis reactor design and modelling was a scheme using a single reactant to product equation with rate data being obtained from overall pilot plant conversion data of the two components. Rice and Herzfeld (1934) pioneered detailed kinetics work and proposed a set of free radical reactions which could be used to describe the hydrocarbon reactions occurring during pyrolysis. The reaction schemes resulting from such treatments required hundreds of free radical reactions and an equal number of kinetic rate expressions to describe even the simplest of the ethylene producing pyrolysis systems. Sundaram and Froment (1977) proposed a reaction scheme intermediate in detail and complexity between the two, allowing them to model the processes far more rigorously than had been done previously without the need for such exhaustive kinetic data. The three model schemes are described in more detail in the following sections.

4.2 Simple Reaction Scheme

Prior to the advent of powerful computers, plant design had to be undertaken using simplified models in order for the work to be completed. These models usually followed the disappearance of the feedstock and formation of the primary product with a simple equation. The rate expression was evaluated using simple kinetics, and tested against pilot plant data. Usually, first order kinetic models were used, and the activation energy and temperature dependence of the rate expression was calculated using the data from the pilot plant. The change in reactor gas volume was handled in the equation by the use of an empirically determined volume correction term. Table 4.1 shows a typical simple reaction scheme as proposed by Rase (1977a). The pressure drop equation and heat transfer equations were correspondingly simple. Models of this type were used extensively during the 60's and 70's to model pilot plants and assist in plant scale-up. The biggest failing of such models was that the kinetic data was inaccurate outside of the specific conditions of the pilot plant used to obtain the data, and the inability of these models to predict or monitor any other components in the system led to the need for more rigorous models.

Table 4.1 Simple Ethane Reaction Scheme (Rase 1977b)

Reaction: Ethane --> Ethylene + by-products

Empirical plant data for product distribution versus ethane conversion is plotted and used to estimate yields of reaction products for a given ethane conversion. A typical product distribution is given below. The overall conversion of ethane to products employs a first order reaction rate equation, with the rate constant being evaluated from a numerical analysis of the plant data.

$$\begin{aligned} \text{moles ethylene} &= 16.7 m_1 + 35 m_2 + 52 m_3 + 64 m_4 \\ \text{moles methane} &= 1.0 m_1 + 3.7 m_2 + 6 m_3 + 9 m_4 \\ \text{moles } C_3 \text{'s} &= 2.143 X_a \\ \text{moles } C_4 \text{'s} &= 16 m_1 + 37 m_2 + 56 m_3 + 75 m_4 \end{aligned}$$

where X_a is the conversion of ethane (usually chosen before the design. A typical value is 60 %) and the values of m are defined as:

$$\begin{aligned} m_1 &= -104.17 X_a (X_a - 0.4) (X_a - 0.6) (X_a - 0.8) \\ m_2 &= 156.25 X_a^2 (X_a - 0.2) (X_a - 0.6) (X_a - 0.8) \\ m_3 &= -104.17 X_a^3 (X_a - 0.2) (X_a - 0.4) (X_a - 0.8) \\ m_4 &= 26.04 X_a^4 (X_a - 0.2) (X_a - 0.4) (X_a - 0.6) \end{aligned}$$

4.3 Free-Radical Based Reaction Scheme

The free radical model has been around since the 1930's when Rice and Herzfeld (1934) proposed a set of free radical equations which would allow the modelling of complex hydrocarbon processes. The free radical model for ethylene from ethane is shown in Table 4.2. The reactions can be broken down into four basic types of reactions.

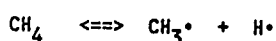
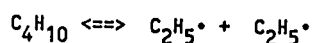
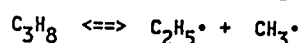
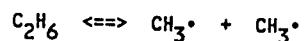
1) Scission and Coupling. Scission is a free radical reaction producing a pair of free radicals by breaking a carbon - hydrogen or a carbon - carbon molecular bond. This is also called initiation, since this step is the beginning of all free radical reactions. The reverse reaction is called coupling. A pair of free radicals is removed from the system when two free radicals combine to form a new molecular bond. The forward reaction (scission) is characterized by a high activation energy. Since this is the dominating reaction of the pyrolysis process from an energy point of view, the overall process is endothermic.



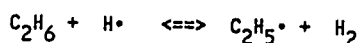
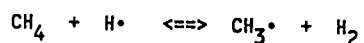
2) Hydrogen Abstraction. A free radical abstracts a hydrogen atom from a molecule, leaving the molecule with the free radical. This is a free radical reaction producing no

Table 4.2 Free Radical Ethane Reaction Scheme (Albright, Crynes and Corcoran, 1983; Rase, 1977b)

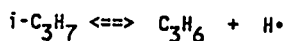
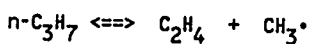
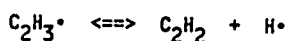
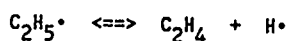
1. Scission / Coupling Reactions



2. Hydrogen Abstraction Reactions

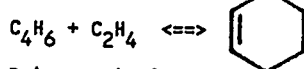


3. Decomposition / Addition Reactions

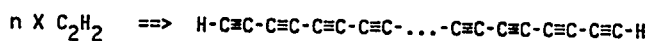


4. Molecular Reactions

Diels-Alder

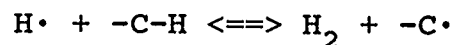


Polyacetylation



NOTE: This is only a partial list of the free radical reactions proposed for ethane pyrolysis. Rase (1977a) lists a complete set of reactions consisting of 11 scission reactions, 36 hydrogen abstraction reactions, 35 addition, 36 decomposition and 4 isomerization reactions (similar to the addition and decomposition reactions), 4 coupling reactions, and 18 molecular reactions.

net change in the number of free radicals in the system. These reactions are characterized by a low, but not zero activation energy.



3) Decomposition and Addition. This is the unimolecular decomposition of a free radical into an olefin and a smaller free radical. No net change in the number of free radicals in the system occurs. These reactions are characterized by activation energies in the 125 to 170 kJ/mol range. Addition is the reverse reaction, in which a small free radical is added to an olefin, producing a larger free radical. Addition is also termed inhibition.

4) Molecular Reactions. These are purely molecular reactions involving no free radicals, such as the Diels-Alder reaction. The primary effect of these reactions is to change the length of molecular chains and to produce ringed compounds from straight chain molecules. These reactions are most common with heavier feedstocks, where larger chain olefins are common. They are also important in the processes which produce the tars and polymers which then dehydrogenate to form coke.

In Table 4.2, the various free radical reactions in the pyrolysis of ethane to ethylene have been labelled as to the type of free radical reaction occurring. Table 4.2 is not

an exhaustive list of every reaction in this process, but rather contains the key reactions.

The problems associated with models using the free radical approach are numerous, and have hampered their use in computer simulations of pyrolysis processes until very recently (Albright, Crynes and Corcoran, 1983; Pacey and Purnell, 1972; Ranzi, Dente, Pierucci, Barendregt and Cronin, 1985; Rase, 1977a). The problems include:

- 1) The free radical reactions required to describe even a simple pyrolysis system are numerous. Rase (1977b), in his free radical based simulation model (Case 102C) uses over 100 reactions with an equal number of rate expressions. This model does not follow coke formation rigorously, even though 51 tar component reactions are employed.

- 2) Obtaining kinetic rate data for all these reactions is difficult. The difficulty in measuring amounts of formed free radicals requires very accurate apparatus, operating at low conversions on small amounts of material. The data obtained is valid for only a very small range of conditions, usually those of the laboratory apparatus used to obtain the rate data. When this data is used to model industrial applications, inaccuracies can result due to the great difference in conditions used. For example, Rase (1977b), in Case 102C uses rate data from reactions studied at very low conversion rates. This is often required to obtain some of the data for short lived free radical species. At higher

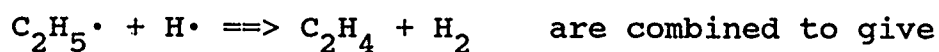
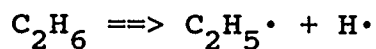
conversions typical of industrial reactors, a model using this rate data performs much poorer than simpler models where the kinetic data was obtained at conditions closer to those of the actual plant. Very little good kinetic data exists for the free radical models, and the data which does exist tends to suffer from the problems described above. Finally, very little of this data has been published.

The conclusion to be drawn from this is that making a model from free radical reaction chemistry, while more consistent with the basic mechanism, does not perform as well as the simpler models under industrial conditions when the available kinetic rate data is applied to the model equations. Given the large increase in computational effort required to simulate this type of model, it is not at present appropriate to use it. Recent work by Ranzi and others (Albright, Crynes and Corcoran, 1983; Ranzi, Dente, Pierucci, Barendregt and Cronin, 1985) has been done using detailed kinetic models. While these recent models match industrial data much better than before, the computer programs developed to solve such models are extremely complex, involving the simultaneous solution of hundreds of coupled differential equations to fully describe the reaction system. Also, the kinetic data used in these models has not been published.

4.4 Component Based Reaction Scheme

A compromise between the simple single species balance and the detailed free radical model is the component model. In this model, the free radical reactions are joined into larger reactions in which the free radicals cancel out.

For example,



This leaves fewer reactions to describe the processes. These reactions contain no free radicals, only whole molecular species. The reactions used to model the ethane conversion to ethylene are shown in Table 4.3. There are two benefits to using this approach. First, there are fewer overall equations to solve in such a reaction scheme; typically less than 10 as opposed to hundreds for a free radical scheme. A computer model produced from such a scheme will take less time to develop, and the reduced equation set is easier to understand and simpler to solve. The second advantage to this model is that the kinetic studies

Table 4.3 Component Based Ethane Reaction Scheme(Sundaram and Froment, 1977)

Ethane reacts reversibly to form ethylene and hydrogen.



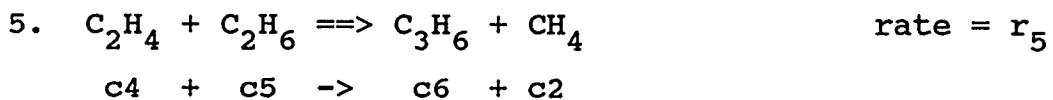
Ethane reacts to form propane and methane.



Propylene reversibly reacts to form acetylene and methane.



Acetylene and ethylene combine to form 1,3-butadiene.



Ethylene and ethane combine to form propylene and methane.



1,3-butadiene dehydrogenates to form coke and hydrogen.

required to obtain accurate rate data are simpler, as only molecular species have to be traced. This can be performed in the laboratory, in the pilot plant, or with industrial reactors. The resulting kinetic data therefore has a wider range of applicability, and better accuracy in the operating range of a typical pyrolysis plant.

Sundaram and Froment (1977) used pilot plant data to determine the rate expressions for three proposed molecular reaction models for the pyrolysis of ethane. The data was examined by numerical methods, and the reaction scheme of Table 4.3 was chosen as the best description of the processes. It is this model which I have chosen to use in my work. It must be noted, however, that kinetic data obtained for such molecular reaction schemes is an approximation, not true kinetic data. For pyrolysis reaction systems, true kinetic data will only be obtained by using detailed reaction schemes employing free radical mechanisms.

4.5 Discussion - Reaction Scheme Chosen

In this work, I have chosen to use the component based reaction scheme. Using this type of model in a computer simulation of the pyrolysis reactions has the following advantages:

- 1) fewer equations to solve means faster simulation times and a much less complex overall model,

2) by following molecules rather than radicals, every species in every equation has direct bearing on the results in a way that can be measured experimentally,

3) industry accepted values for molecular rate constants can be obtained from the literature (Sundaram and Froment, 1977), while values for free radical rate constants are not easy to obtain, and are not always appropriate for industrial simulation work,

4) the model is still complex enough to allow rigorous solution to pressure drop equations and heat transfer equations and,

5) currently available coking models are very crude. The complete coking model is not yet at the level of numerical accuracy of a molecular reaction scheme. The accuracy of a free radical model would therefore be greatly reduced by the current coking models.

5.0 Coke Production in Ethane Pyrolysis

The formation of coke in pyrolysis reactions is of extreme importance to industry. Although the rate of coke formation is low, coke is deposited on furnace and TLX surfaces. This steady buildup of coke leads to decreased thermal efficiency of the process, increased pressure drops, and eventually the process must be halted so the coke can be removed.

Coke deposits on the walls of the furnace tubes, in the elbows of the furnace pipes, in the transfer line between the furnace coils and the quench cooler or transfer line exchanger (TLX), on the inlet manifold of shell and tube type quench coolers, and on the walls of the quench cooler pipe. In ethane pyrolysis, deposits of coke on a shell and tube type quench cooler inlet manifold are extremely heavy. Most ethylene plants using ethane as a feedstock must shut down every 20 to 60 days for decoking, and often it is fouling of the cooler inlet manifold or the transfer line pipe which causes the shutdown.

5.1 Theories of Coke Formation

Coke is now thought to be formed by two primary mechanisms, and the types of coke formed are quite

different. Actual coke deposits in the pyrolysis furnace and TLX are a combination of these coke types.

5.1.1 Surface Reactions

The first mechanism of coke formation consists of surface reactions between pyrolysis formed carbon and the walls of the pipe to produce a filamentous coke containing metal particles. A number of researchers (Cooper and Trimm, 1980; Rostrup-Nielsen and Trimm, 1977; Trimm, 1977) have studied this type of coke formation in detail. This type of coke is produced at high temperatures (such as near the exit of the pyrolysis furnace or the first portion of the quench cooler. Electron microscopy and Xray analysis indicates this coke consists of a carbon fibre attached to the tube wall, with a particle of metal at the end of the fibre furthest from the tube wall (the fibre growth tip). This coke is produced by a surface reaction which begins with carbon depositing on the metal. The carbon then diffuses into the metal wall of the tube and collects at the grain boundaries of the metal. As more carbon collects, the particle of metal above the carbon is pushed out towards the center of the reactor tube, forming the tip of the growing carbon fibre. As more carbon is deposited near this metal tip of the fibre, the fibre grows.

The reaction is catalysed by the metal wall of the tube

(Albright and McGill, 1987; Cooper and Trimm, 1980; Rostrup-Nielsen and Trimm, 1977; Trimm, 1977). Nickel in the tube alloy appears to be the most active catalyst, although iron is also a catalyst. This reaction has been observed both in laboratory studies and by examining plant tubes during decoking. Tubes which are freshly decoked react more rapidly with the gases to produce coke than tubes which have been in service for some time. When oxidizing agents such as steam or hydrogen are introduced into the reaction gases, the amount of coke formed by this type of surface reaction is reduced, possibly due to oxidation of the active metal sites by the hydrogen or steam. Studies with gaseous sulphur compounds show similar results.

Coating the furnace and TLX tubes or using alternate alloys lower in nickel has also been shown to reduce surface coking rates. Recently, Albright and McGill (1987) have shown how furnace tubes coated with aluminum experience significantly less coke production than normal tubes, and survive repeated reaction and decoking cycles with far less carburization or pitting. Carburization of the furnace or TLX tubes occurs because the surface coke removes small amounts of metal as the coke fibre is formed. When the furnace and TLX is decoked, the metal is also removed. The metal removed is significant over the life of the tubes, with the tubes losing up to 20% of their original wall thickness over a three year period.

5.1.2 Bulk Gas Reactions

Not all of the coke is formed by surface reaction with the metal pipe walls. A large portion of the coke is formed by the undesirable secondary reactions occurring in the product gases of ethylene pyrolysis (Albright, Crynes and Corcoran, 1983). Feedstocks which produce more secondary reaction products will produce more coke through this mechanism than those which have a lower yield of secondary products, such as an ethane feedstock.

This type of coke is formed through an extremely complicated series of reactions in which large chain carbon molecules are produced from smaller component molecules by reactions such as the Diels-Alder reaction. This is shown in Figure 5.1. As more of these large molecules are produced, polymerization reactions occur, and eventually large chain polymers and tars are formed in the gas stream. These tars and polymers can condense in the gas stream into droplets of liquid tar. Although most pyrolysis processes operate above the dew point of the majority of the process stream components, some of the heavier tars and polymers will still condense in the gas stream and on the walls of the pipe. The coke resulting from these tars depends on how and where the tar is reduced to coke. The droplets may deposit onto the tube walls and react to produce coke

or they can react to produce coke in the gas stream which then may or may not deposit on the tube walls. In terms of tube wall deposits, two types of coke are formed from these tar droplets.

The coke formed by tar/polymer condensation on tube walls followed by dehydrogenation is a very smooth, hard coke with high thermal conductivity. The coke is smooth because the droplets are "smeared" on the tube walls while still liquid by the high flow rate of the gas stream. Dehydrogenation of this thin film produces a coke very much like graphite. Tube walls with this type of coke appear shiny with many small cracks, formed as the tar dehydrogenated and shrank. This type of coke is a very high temperature coke, usually only found in the hottest portion of the furnace.

Coke formed by gas phase dehydrogenation followed by deposition is much more amorphous in form, since the droplets tend to remain roughly spherical as they "dry". As the tar is reduced to coke, the particle becomes quite porous. At some point during this reduction, the coke may deposit on the wall leaving an amorphous deposit of coke which has a very low thermal conductivity and gives the tube an irregular, bumpy inner wall surface. This type of coke is formed during the high temperature reactions, but may be found throughout the process as the tar particles are carried by the gas stream.

Deposits of this type of coke are found in greatest abundance in places where turbulent backmixing occurs (elbows and bends) and wherever the flow of gases is radically altered. The massive deposits of coke on the quench cooler inlet manifold (tube sheet) of shell and tube quench coolers are composed almost entirely of this type of coke.

The transition between these types of coke is not always sharp, and one type of coke can interact with another to produce combinations. For example, high temperature graphitic coke will tend to coat the tube walls, reducing the amount of surface reaction by shielding the active sites of the tube walls from surface catalysed reactions. Needle coke (surface reactions) presents a filamentous surface to the process flow, which traps the gas carried amorphous coke, leading to a mixture of coke on the walls in those regions. Because the three types of coke have very different properties of roughness and thermal conductivity, the amount and type of coke deposited can have a dramatic effect on the furnace and quench operation. Thermal conductivity between the different types of coke has been found to vary by two orders of magnitude. Knowing what type of coke is deposited makes a dramatic difference when modelling a reactor.

5.2 Coking Problems in Pyrolysis Systems

The problem of coke buildup is one of fundamental con-

cern in industrial pyrolysis. If coke were not formed, pyrolysis reactors could stay on line for years with only minimal service requirements. Instead, reactors must be decoked every 20 to 60 days, often requiring much energy in the form of heat and steam. Additionally, coke deposits on shell and tube exchanger inlet manifolds often requires the disassembly of the exchanger and manual removal (scraping) of the coke.

Although the mechanisms of coke formation are fairly well understood, methods of coke buildup control are not yet known. There are as yet no complete solutions to the total control of coke buildup.

Reducing the partial pressure of secondary pyrolysis products by adding an inert gas will shift the reaction equilibria away from coke forming reactions. However, there is an economic limit to the allowable steam dilution. The overall yield of ethylene must be maintained, so adding more steam will require higher flow rates of hydrocarbon. This may lead to unacceptable pressure drops in the process units. Using steam as a diluent has the additional effect of partially decoking the reactor during pyrolysis via the water gas reaction, although Dente and Ranzi (Albright, Crynes and Corcoran, 1983) indicate this is not significant at industrial conditions.

Coatings and feed additives are available to try to reduce surface catalysed coke formation, and preliminary indi-

cations are that these do work (Albright and McGill, 1987), however further research is needed.

Problems caused by amorphous coke are more severe, especially with lighter feedstocks. The only way to reduce the coke buildup problem in these cases is to radically alter reactor configurations. Novel reactors are currently being tested, such as high severity, short length furnaces with no pipe bends at all, large diameter furnaces and quench coolers with no tube sheets or manifolds. In these cases, the gas phase coke must still be removed at a later stage in the overall process, often during a direct contact quench with water in a water tower downstream from the quench cooler. The coke is then separated from the water. However, for conventional pyrolysis coolers the problem remains, and no real solution to the manifold coke deposition problem exists at this time.

In summary, the problems associated with the formation of coke on the walls of the furnace and cooler tubes are several.

1. Coke deposits on the walls of the furnace and TLX tubes through mechanisms discussed earlier. These deposits decrease the inner diameter of the tubes. This leads to an increased gas velocity and an increase in the overall pressure drop through the system. Eventually, the process must be shut down for decoking.

2. Coke has a finite thermal conductivity. This presents

a barrier to heat transfer which is magnified as the thickness of the coke layer increases. In the furnace more heat is required to continue the reaction. This is provided by increasing the temperature in the furnace firebox. Eventually, the furnace tube outside temperature will exceed the maximum temperature allowed by the tube material, and the furnace must be shut down for cleaning. In the quench cooler or TLX, the stream is cooled less efficiently as coke builds up. The result is an increase of secondary reaction products as the speed of reaction quenching decreases with coke buildup.

5.3 Simulation Problems with Coke Formation

Since the mechanisms of coke buildup presented above are very complex, putting them into a numerical form to allow their simulation is difficult at best. It is not currently possible to quantitatively model all of the coke producing processes. It is also not possible with current laboratory or industrial data to determine the amount of tar, polymer or coke deposited from the gas stream or captured by filamentous coke, nor is it possible to accurately describe the surface reactions which occur.

Simulation of coke formation therefore uses empirical approximations to evaluate coke buildup. Rate data generated from pilot plant studies or laboratory work can be

employed in bulk coking reactions to allow fairly accurate estimates of coke rates. Finally, the judicious use of tuning parameters such as a coke laydown factor can allow the simulator to adjust the rates of coke buildup, and will provide a mechanism for industrial pyrolysis history matching.

6.0 Computer Simulation of the Quench Cooler

6.1 Computer Model

In my project, I have chosen the molecular model shown in Table 4.3. The set of reactions used is supplied by Sundaram and Froment (1977; 1979), and Sundaram, Van Damme, and Froment (1981) in a series of papers which discuss probable reaction schemes, simulation methods, and coking reactions. The basic molecular species recommended by Sundaram and Froment (1977) are shown in Table 6.1, with the reaction scheme they chose shown in Table 4.3. The chosen scheme requires 6 reactions involving 9 molecular species (10, including the inert diluent steam) to describe the pyrolysis of ethane.

Table E.1 in Appendix E gives the rate equations reported by Sundaram and Froment (1977), with the associated reaction rate constants and equilibrium constants provided in Table E.2. Discussion of these equations is found in Appendix E. This set of equations and constants is the one Sundaram and Froment (1977) determined would provide the best model of an industrial reactor. It should be noted these reactions were designed for an ethane pyrolysis furnace, not a quench cooler. However, analysis of the system shows the two models to be equivalent in every respect

Table 6.1 Ethane Reaction Molecular Species

<u>Symbol</u>	<u>Name</u>	<u>Formula</u>
c1	Hydrogen	H ₂
c2	Methane	CH ₄
c3	Acetylene	C ₂ H ₂
c4	Ethylene	C ₂ H ₄
c5	Ethane	C ₂ H ₆
c6	Propylene	C ₃ H ₆
c7	Propane	C ₃ H ₈
c8	1,3-Butadiene	C ₄ H ₆
ck	Coke	C
st	Steam	H ₂ O

except for differences in the heat equation with respect to the direction of the heat flux.

Figure 3.1 shows a diagram of the quench cooler (TLX) I have modelled, and Figure A.1 shows a differential element of the TLX. The equations used in this model are given and discussed in Appendices A through F. The flowchart of the computer program is provided in Appendix G, and computer listings of the models are presented in Appendix J.

The computer program based on this reaction model has been written in the Advanced Continuous Simulation Language (ACSL), which is a superset of FORTRAN. The computer model rigorously solves the heat, mass, and momentum balance equations throughout the cooler (TLX tube). Quench cooler (TLX) operational time is modelled by repeating the TLX solution at constant time intervals. The model employs detailed reaction rate calculations, and uses standard mixing rules and temperature corrections to evaluate all relevant component and bulk fluid properties as required. ACSL is used to code the model because it simplifies the solution of the differential equations. By providing powerful solution techniques and a simplified method of coding differential equations, ACSL allows the model builder to concentrate on the model rather than on the solution techniques. ACSL is specifically designed to solve large numbers of coupled non-linear ordinary differential equations.

6.2 Computer Model Assumptions

The following assumptions have been made to facilitate numerical simulation of the model. Correctness of these assumptions, where they can be tested by parametric modelling with the simulator, will be discussed in the appropriate section of the simulation results.

6.2.1 Assumption of Plug Flow

A tubular plug flow reactor is a very convenient reactor model to use when simulating gas phase reactions in pipes. The ideal tubular plug flow model assumes one dimensional axial flow of the fluids, no radial gradients, and no axial dispersion of the fluids. Rase (1977a) and Albright, Crynes and Corcoran (1983) indicate this type of model is valid for fluids experiencing turbulent flow, where the Reynolds number is above 4000 and the length to diameter ratio (L/D) of the pipe is greater than 50. Under these conditions, radial concentration gradients, radial temperature gradients and axial dispersion are all negligible. This assumption, used in my model, will be tested by observing the Reynolds number for each set of simulation runs, and commenting on the L/D ratio where appropriate.

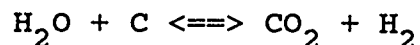
6.2.2 Assumption of Constant Steam Temperature at the Tube Wall

The heat exchanger is much simpler to simulate if the shell side (or outer pipe side) of the quench cooler does not have to be simulated. By assuming a constant steam temperature (equivalent to the shell side tube wall temperature, T_{wall}), this condition can be met. The condition of constant T_{wall} will in fact occur according to Rase (1977a) if the cooling liquid is saturated (condensing) steam. The phase change occurring at the outside wall of the cooler (liquid water changing to vapor in the saturated steam) will remove heat from the process stream without the temperature of the steam increasing (steam quality increases). Rase (1977a) and Albright, Crynes and Corcoran (1983) both indicate this is a common mode of operation for industrial pyrolysis quench coolers. There is no direct means of testing this assumption with this numerical model. Only actual experimental work with industrial coolers would prove this assumption correct or not. Data from Alberta Gas Ethylene indicates confirmation of this assumption.

6.2.3 Assumption of Steam Inertness

The model I am using does not incorporate the water

shift reaction:



The water shift reaction is thought to reduce the overall coke content in the reactor by removing some of the coke during the pyrolysis reactions. However, Dente and Ranzi (Albright, Crynes and Corcoran, 1983) indicate the effect of this reaction is negligible at industrial conditions.

As with coke deposition, coke removal via the water shift reaction is believed to be a surface catalysed reaction. An additional surface oxidizing reaction between steam and "bare" (clean tube or freshly decoked tube) walls is thought to inhibit coke formation. Current understanding of pyrolysis coking reactions is such that the overall effect of this reaction cannot be quantitatively evaluated, nor is there any kinetic data for coke removal during pyrolysis.

This assumption cannot be tested with the current numerical model. Further basic research is required before these assumptions can be replaced with equations which can be incorporated into a numerical model. However, since the effect is negligible at industrial conditions, such work would have a low priority.

6.2.4 Assumption of Horizontal Flow

Quench coolers in industrial use are generally of two physical configurations. Vertical quench coolers are used to cool product streams which exit the pyrolysis furnace at the top of the firebox, or where plant layout space is at a premium. Horizontal quench coolers, especially of the shell and tube type, are often used when the process stream exits the firebox at the bottom, or when plant layout space is not at a premium.

Both to remove the added complexity of modelling the quench cooler under the effects of gravity, and to allow simulation of the Alberta Gas Ethylene quench cooler in Joffre, Alberta (which is horizontal), I have chosen to model a horizontal quench cooler. This is a design consideration, rather than an assumption.

6.2.5 Assumption of Smooth Pipe

Although standard friction factors for steel pipe have been incorporated into the model pressure drop equations, no special considerations have been given to the modelling of deviations from smoothness in the pipe caused by coke deposits on the tube walls. This is because such deviations are not possible to quantitatively describe at this time. As

discussed in the sections on coke formation, three types of coke can be deposited separately or in combination (although the graphitic coke is not likely to be found in the relatively cooler environment of the quench cooler).

The two types of coke found in the quench cooler have very different degrees of roughness (amorphous versus filamentous) and so can be expected to change the roughness of the pipe wall. At this time, as with the entire coke laydown picture, nothing but qualitative information exists on this phenomenon.

The inability to model these roughness changes will introduce some inaccuracies into the model, but these should not be significant (less than a 10% change in the pressure drop for a TLX tube).

At this time no method exists for describing or estimating numerically the increase in roughness attributable to the coke deposits. Basic research needs to be conducted in this area using industrial reactors as well as laboratory models to try to characterize and quantitatively describe the coke deposits formed on the walls of the tubes.

6.2.6 Assumption of Pseudo Steady State

The system is modelled using a pseudo steady state approach assuming the initial flow, temperature and pressure profiles are fully developed prior to the simulations "time

0", (i.e. I do not start with a cold empty cooler). The transient "start-up" time for the TLX represents a small fraction of the total TLX "on stream" time. Testing this assumption is beyond the scope of this numerical model, however, the work done by Nighswander, Mehrotra and Behie (1988) indicates these effects are not significant, especially under current industrial conditions (20 ms or greater quench times).

6.2.7 Assumption of Constant Changes Between Simulation Time Steps

The only time dependent equation in the fully developed flow system of this model is the coke laydown equation. The solution of the temperature and pressure equations are assumed constant during a time step. A time step solution of the model is appropriate if the assumption is made that reaction rates will not vary greatly from time step to time step. The effects of the coke rate expression (coke thickness) are updated explicitly at the end of each time step. This portion of the assumption can be tested by observing reaction rate changes between time steps.

6.3 Treatments of Coke Formation

The two coke models used in this study are described in

Appendix F. Both models have a common derivation of the basic coke rate equation. The differences between the two models occurs in the way the rate equation is integrated to obtain coke thickness.

The first coke model performs the integration assuming the coke rate will not change significantly as a function of TLX operational time. Consequently, the coke thickness equation is one which calculates the total coke thickness for any given total elapsed time.

The second coke model performs the integration assuming the coke rate will change as a function of TLX operational time, but the rate of change between time steps will not be significant. Consequently, the coke thickness equation is one which calculates the change in coke thickness during the time step. This change in coke thickness must be added to the accumulated coke thickness stored by the model from time step to time step.

The two models will be run in parallel in the parametric simulation studies to observe the effects of the coke equation dependent parameters on the behavior of the two coke models. The goal is to recommend one of the two coke buildup schemes for further simulation work.

6.4 Discussion - Computer Simulation

Simulation of the chosen quench cooler model is an in-

volved process. The model must be assembled from the various equations describing the physical processes occurring. The assembled model must then be coded into the computer language chosen, compiled and tested. Parametric cases are run using the model to test the effects of changing input parameters on the model. Results of these runs are processed by the user into a form to allow discussion of the model response to the runs.

The model developed for this work involves the solution of 11 coupled ordinary differential equations (ODEs) rigorously solving the mass, momentum and temperature balance equations of a single tube of the quench cooler (TLX). Supporting these ODEs are a large number of equations for the rigorous calculation of all relevant component properties, mixing rules to calculate bulk fluid properties, and equations to correct properties to reflect current TLX conditions.

The Advanced Continuous Simulation Language (ACSL) simplifies the overall process by allowing the model designer to concentrate on the equations and physical processes occurring rather than on the details of numerical integration. ACSL contains language provisions to perform numerical integration of the differential equations along the quench cooler length, and is specifically designed to solve large numbers of non-linear coupled ordinary differential equations. ACSL also has provisions for varying model input pa-

rameters and output variables without recompiling the model. Professor Behie and his colleagues at the University of Calgary (Eng, McRae, Behie and Luker, 1987) have recently presented key methodological issues relative to the use of simulation languages to solve complex differential equations in a University environment.

7.0 Computer Simulation Input and Results

7.1 Design Conditions and Input Variables

The quench cooler modelled is a 6.1 m shell and tube horizontal heat exchanger with feed supplied by the exit coil of an ethane pyrolysis furnace. Data for this quench cooler is taken from Case Study 102B and 103 (Rase, 1977b).

The temperature of the inlet process stream is 1133.7 K with an inlet pressure of 214.8 kPa (2.12 atm). The feed mass flux is $50.0 \text{ kg/m}^2 \cdot \text{s}$. The shell side steam is 10.284 MPa (101.5 atm) saturated steam at 586 K. The inner tube diameter is 24.6 mm, giving an L/D ratio of 248, which is greater than the value of 50 required by Rase (1977a) for the plug flow assumption to be valid. The steam dilution ratio upon exit from the furnace is 0.2819 (0.25 kg steam per kg hydrocarbon in the original furnace feed).

Details of the default (base) case are presented in Table 7.1. Details of the parametric simulation cases in which various parameters are varied from the base case values are presented in Table H.1 of Appendix H.

Table 7.1 Parametric Simulation Base Case (Rase, 1977b)

Inlet Temperature:	1133.7 K
Inlet Pressure:	214.809 kPa (2.12 atm)
Feed Mass Flux:	50.0 kg/m ² ·s
Steam Dilution Ratio	0.2819
TLX Length:	6.1 m
TLX Tube Inner Diameter:	24.638 mm
Steam Temperature:	586.48 K
Steam Heat Transfer Coefficient:	11584.0 W/m ² ·K
Coke Deposition Ratio:	1.0
Coke Thermal Conductivity:	5.5 W/m·K
TLX inlet feed composition (mole %):	
Hydrogen:	30.04
Methane:	3.81
Acetylene:	0.17
Ethylene:	23.99
Ethane:	17.02
Propylene:	1.29
Propane:	1.41
1,3-Butadiene:	0.28

7.2 Parametric Simulation - General Discussion

Parametric modelling is accomplished by varying one parameter in the model system while keeping all others constant to observe the effects of the chosen parameter on the system. Parametric modelling was used in this work to exercise the model by testing various model assumptions, background theories, and to observe the sensitivity of the model to some of the design parameters which could affect the quench coolers actual performance.

7.2.1 Model Assumptions

The assumptions tested by parametric modelling using the numerical model were

- 1) Plug Flow - tested by varying mass flux and tube diameter while observing fluid velocity and Reynolds number,
- 2) Constant Steam Temperature at the Tube Wall (T_{wall}) - not tested directly, but by varying T_{wall} , the effect of steam temperature and therefore the effect of a non-constant steam temperature can be observed, and
- 3) Constant Changes Between Simulation Time Steps - by observing reaction rate changes during time steps (the smoothness of the rate profile plots), the validity of this assumption, and appropriateness of the chosen time step size

can be tested.

7.2.2 Model Theories

The method of modelling coke laydown is discussed in Appendix F. Both methods were modelled, and the differences between the predicted coke laydown of each model under various conditions can be observed and commented upon.

7.2.3 Sensitivity

Each set of model runs tested the response of the numerical model to changes in one of the input parameters. The goal is to find those parameters which affect most significantly the output of the model; those which produce the largest change in output for least change in input. Having found those input parameters, one can concentrate on optimizing them when making changes to the model such as for obtaining optimum efficiency, or modelling industrial quench coolers.

7.3 Effect of Total Elapsed Operational Time

The simulation model was allowed to run, as initially described in the input variables section, for a total elapsed operational time of 24 days or less, depending on

coke thickness (12 days for coke model 2). Six day time steps were used in the simulation. Changes in all fundamental variables were noted, especially the changes in tube wall diameter due to coke thickness.

7.4 Effect of Feed Mass Flux

The mass flux of the feed stream was varied in four runs using rates of $10.0 \text{ kg/m}^2\cdot\text{s}$, $50.0 \text{ kg/m}^2\cdot\text{s}$, $100.0 \text{ kg/m}^2\cdot\text{s}$, and $200.0 \text{ kg/m}^2\cdot\text{s}$. The first three rates are reasonable values provided by Rase (1977a) and other design literature. The fourth is a doubling of the last rate to test the effect of excessive mass flux on the system. These cases are used to study the effect of changing mass flux on the cooling behavior of the system, the pressure drop of the system, and the overall conversion attained. Theory predicts one of the parameters affected by changes to molar flow rates (a function of mass flux and diameter) will be the pressure drop. It is the large pressure drop associated with high mass fluxes which should determine the upper limit of acceptable mass fluxes. Rase (1977a) also states that flow velocities should not exceed 304.8 m/s or severe corrosion will result in system elbows and bends. Flow velocity values from 3.048 m/s to 30.48 m/s are more common.

7.5 Effect of Tube Inside Diameter

Tube inside diameter was increased from the initial value of 24.6 mm diameter to 50.0 mm and 100.0 mm. The 100.0 mm diameter pipe is the size of a typical double pipe exchanger which has been used in some commercial ethane pyrolysis installations. This diameter pipe should be able to operate longer due to the larger diameter available for flow, but should suffer from longer quench times. A careful check of output results in the large tube case must be made to determine if the turbulent flow assumption is still valid, or if the system is operating in the laminar flow regime. Calculations show the L/D ratio to be 248.0 for the 24.6 mm tube, 122.0 for the 50.0 mm tube, and 61.0 for the 100.0 mm tube. The latter value falls just within the criteria proposed by Rase (1977a) (L/D must exceed 50.0), and so the plug flow assumption is valid for all cases.

7.6 Effect of Steam Dilution

Because the dilution steam is essentially inert (Albright, Crynes and Corcoran, 1983), the only effect which this steam will have on this model will be in changing the hydrocarbon partial pressure, and consequently the concentration of hydrocarbon available for reaction. This effect

should be significant, however, as the hydrocarbon partial pressure will effect the equilibrium shift of the overall reaction system. For the same total pressure, more steam should produce higher conversion of ethane to ethylene, less conversion of ethylene to secondary reaction products, and therefore less coke laydown. However, this will come at the expense of lower total ethylene production due to the lower hydrocarbon molar flow rate. Lower steam dilution ratios should have the opposite effect. The steam dilutions used in this test are both lower than the original input value (no steam at all) and substantially higher (almost four times the original value).

It should also be noted in industrial reactors, the mass flux of the hydrocarbon and the steam dilution ratio are not independent. The total molar flow is composed of both hydrocarbon and steam component. Changing the steam dilution ratio will change the overall mass flux, and thus the hydrocarbon molar flow rates. Industrial reactors compensate for this effect by adjusting both mass fluxes to achieve an overall mass flux for a given steam dilution. In the parametric simulation runs, I have separated the two effects into a total mass flux and a steam dilution ratio in order to observe the effect of each independently.

7.7 Effect of Steam Temperature

The steam temperature was changed from the default value of 586.0 K (10.3 MPa saturated steam) to 700.0 K (55 K superheated at 22.0 MPa) and finally to 273.15 K (0.101 MPa saturated steam). High temperature steam is a more valuable process stream, and so the higher the steam temperature, the more work can be done with the produced steam. The temperature chosen exceeds the maximum saturated steam temperature allowed, but will show the effects of a limiting steam temperature on reaction quench times. The low temperature run is carried out to observe the effect of these temperatures in the cooler walls. Although 273.15 K is above ambient temperature, the low temperature run will indicate the type of behavior to expect from the system in sections of pipe exposed to low temperatures. Such sections occur industrially during the transfer of the process stream from the furnace to the quench cooler, where it is common to find up to 2 metre lengths of uninsulated, large diameter (200.0 mm) pipe connecting the two process units. Results from this case may be helpful in providing recommendations to the industry when dealing with such transfer sections.

7.8 Effect of Steam Heat Transfer Coefficient

The steam heat transfer coefficient was varied between values reported in Perry and Chilton (1973) for various heat exchanger configurations. Since these reported values are often inexact and are situation dependent, bracketing an acceptable range of coefficients was done to determine the sensitivity of the quench cooler to this parameter.

7.9 Effect of Coke Laydown Parameter

Because of the various coking mechanisms involved in the amount of coke which is deposited on the walls, a coke laydown parameter (α), was incorporated into the overall coke thickness equations for the model. There is evidence to suggest that much of the coke formed in the process stream does not deposit on the walls of the furnace or quench cooler but rather is carried in the turbulent process stream until the stream is interrupted by a change in direction or a barrier, or until zones of less turbulence are reached, at which time the coke may be deposited on the surfaces at that point. By varying the value of α from 0.1 to 1.0, the effect of this parameter can be studied. In practice, no method of determining this parameter beforehand currently exists, so it is of limited predictive use, but it

should help in actual industrial quench cooler matching. Results of these cases were studied after 12 days of simulation to observe system changes after coke had been allowed to build up.

7.10 Effect of Coke Thermal Conductivity

The value of the coke thermal conductivity (k_{ck}) varies greatly depending on the type of coke being used as discussed in Section 5. The difference between graphitic coke (average $k_{ck} = 76.0$ W/m·K), needle coke (average $k_{ck} = 5.5$ W/m·K) and amorphous coke (average $k_{ck} = 0.55$ W/m·K) provides sufficient reason to test the response of the model to these three values of k_{ck} . In industrial practice, some sort of average value would have to be chosen, since the actual value could be expected to change with time as different cokes accumulate), and current theory is not able to predict this change numerically.

7.11 Comparison of Different Coke Formation Models

Section 6.3 discussed treatments of coke formation with respect to the computer model used in the simulation studies. By running parallel cases for both coke models, differences in the parallel case results will be due to differences in the coke buildup models used. The effect of the

total elapsed operational time, the effect of the coke laydown parameter, and the effect of coke thermal conductivity should be the parametric cases best able to display the differences in the coke models.

7.12 Comparison with Experimental Results

Very little actual quench cooler data for ethane pyrolysis is provided in the literature. Rase (1977b), in his simulation work (Case 102 and 103) provides an indication of how his model performed compared to the pilot plant data which produced his model, but the actual data is not presented. Although others (Albright and McGill, 1987; Lichtenstein, 1964; Petryschuk and Johnson, 1968; Plehiers and Froment, 1987; Ranzi, Dente, Pierucci, Barendregt and Cronin, 1985; Snow, 1957; Sundaram and Froment, 1977; Sundaram, Van Damme and Froment, 1981) worked with ethane pyrolysis systems, only the furnace was investigated, not the quench cooler. The data provided in these papers was insufficient to allow simulation of a quench cooler (TLX).

Simulation of the Alberta Gas Ethylene quench cooler in their Joffre, Alberta plant (136000 tonnes of Ethylene produced per year) will be a much better test of the ability of the computer model to match actual plant results.

7.13 Comparison with Other Simulators

As with the experimental data, few actual ethane pyrolysis simulation results have been published in the literature. A number of researchers (Albright and McGill, 1987; Lichtenstein, 1964; Petryschuk and Johnson, 1968; Plehiers and Froment, 1987; Ranzi, Dente, Pierucci, Barendregt and Cronin, 1985; Snow, 1957; Sundaram and Froment, 1977; Sundaram, Van Damme and Froment, 1981) have all employed computer simulations in their work, but as discussed previously, these simulations were of the pyrolysis furnace only. Data sufficient to allow simulation of a quench cooler was not available from these papers.

The only simulation data complete enough to allow comparison with my model is the TLX simulation done by Rase (1977b) reported as Case 103.

8.0 Discussion of Computer Simulation Results

The various test cases described in the previous sections have been executed using the ACSL computer simulator described previously. A description of the cases studied showing the basic variables and the variables changed for each case is presented in Table 7.1 (the base case) and Table H.1 in Appendix H (the parametric cases). Table H.2 in Appendix H shows a summary of the results produced for each case. Appendix I contains an example computer printout from one of the computer runs (base case, coke model 2, time = zero days). Graphical output of the simulation results are presented with the discussion of each case in this section.

The cases which show the effect of total elapsed operational time, the effect of coke laydown, and the effect of coke thermal conductivity were run for 24 days or less, depending on overall coke thickness. The cases showing the effect of total elapsed operational time were plotted for all time steps simulated. Comparison of results and plots for the other two time dependent cases was done at 12 days total elapsed operational time. This allows the effect of increasing coke thickness to be observed after some coke has been allowed to accumulate. All other cases were run and plotted at 0 days, since the effects studied were indepen-

dent of simulation time.

8.1 Effect of Total Elapsed Operational Time

The series of plots for this case is found in Figures 8.1.1 to 8.1.5 for coke model 1, and Figures 8.1.6 to 8.1.10 for coke model 2. These plots show clearly the effect of coke deposition on the cooler walls and the secondary effect this coke deposit has on the other variables of the reaction. Figures 8.1.11 to 8.1.15 are the same basic plots as Figures 8.1.6 to 8.1.10, except the independent axis is residence time instead of TLX length.

Initially, a clean TLX will cool the pyrolysis exit gases to a full quench within the first 2 metres of the quench cooler (Figures 8.1.1 and 8.1.6). This represents a residence time of 0.022 s or 22.0 ms (Figure 8.1.11). A full quench has occurred when the slope of the ethane conversion curve (Figures 8.1.3, 8.1.8 and 8.1.13) has dropped to zero, indicating no further reaction is occurring. Within 3 metres (residence time = 36.0 ms) the process gases have been cooled from their initial temperature of 1133.7 K to below 800 K. The rest of the quench cooler length simply provides additional cooling of the process stream. The quench cooler exit temperature is 644 K.

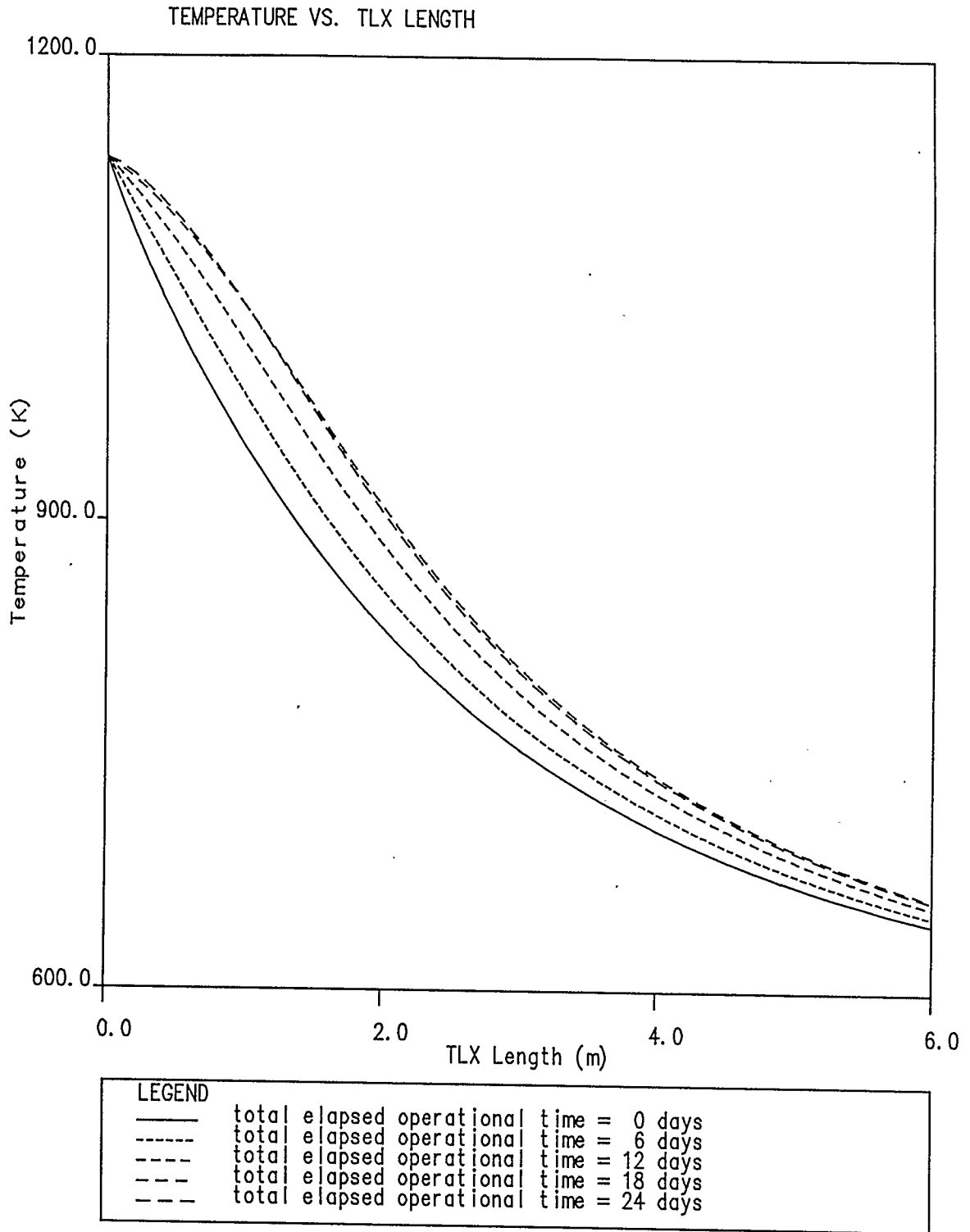


Figure 8.1.1 TLX Temperature profiles at different total elapsed operational times using coke model 1 (base case)

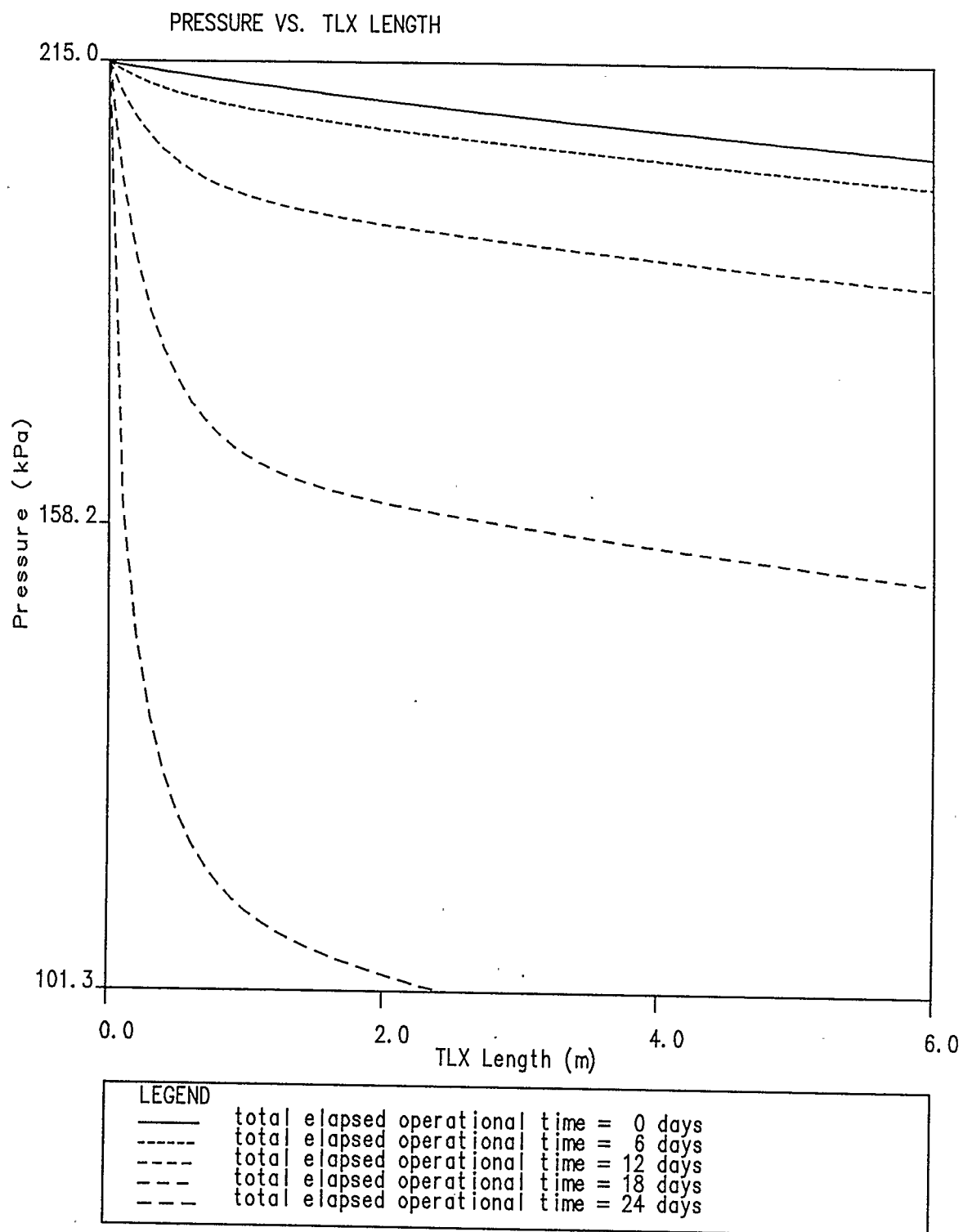


Figure 8.1.2 TLX Pressure profiles at different total elapsed operational times using coke model 1 (base case)

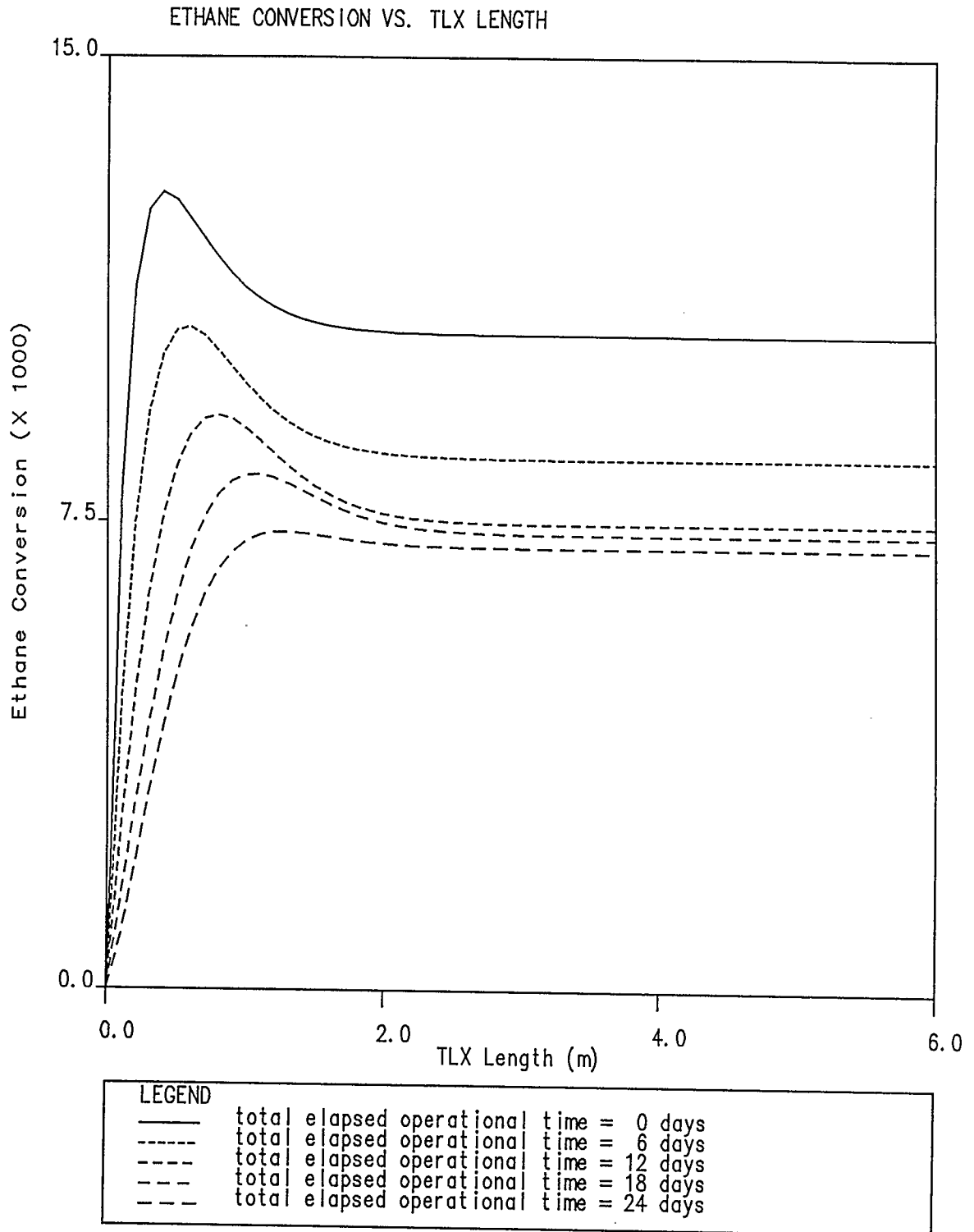


Figure 8.1.3 TLX Ethane conversion profiles at different total elapsed operational times using coke model 1 (base case)

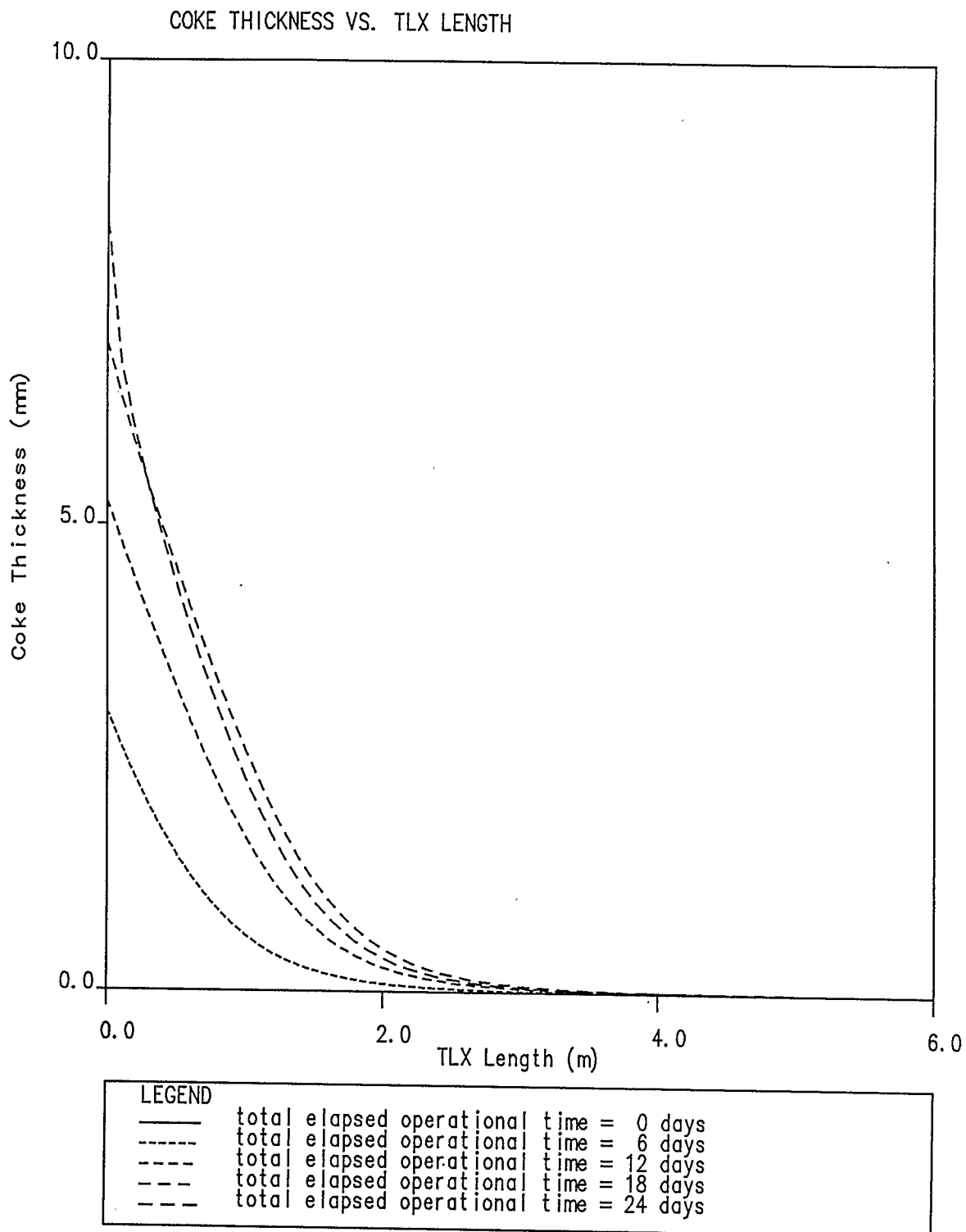


Figure 8.1.4 TLX Coke thickness profiles at different total elapsed operational times using coke model 1 (base case)

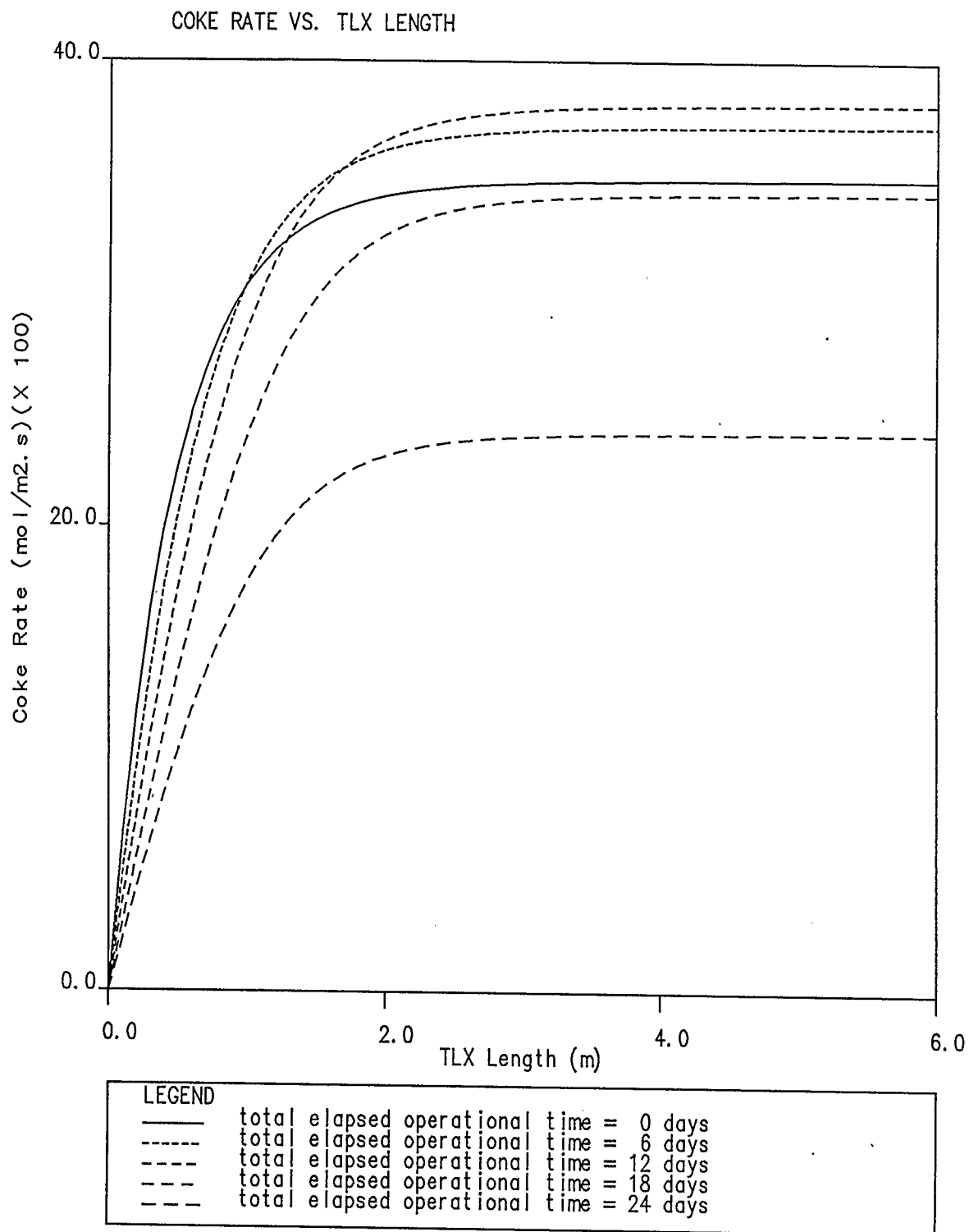


Figure 8.1.5 TLX Coke rate profiles
at different total elapsed operational times
using coke model 1 (base case)

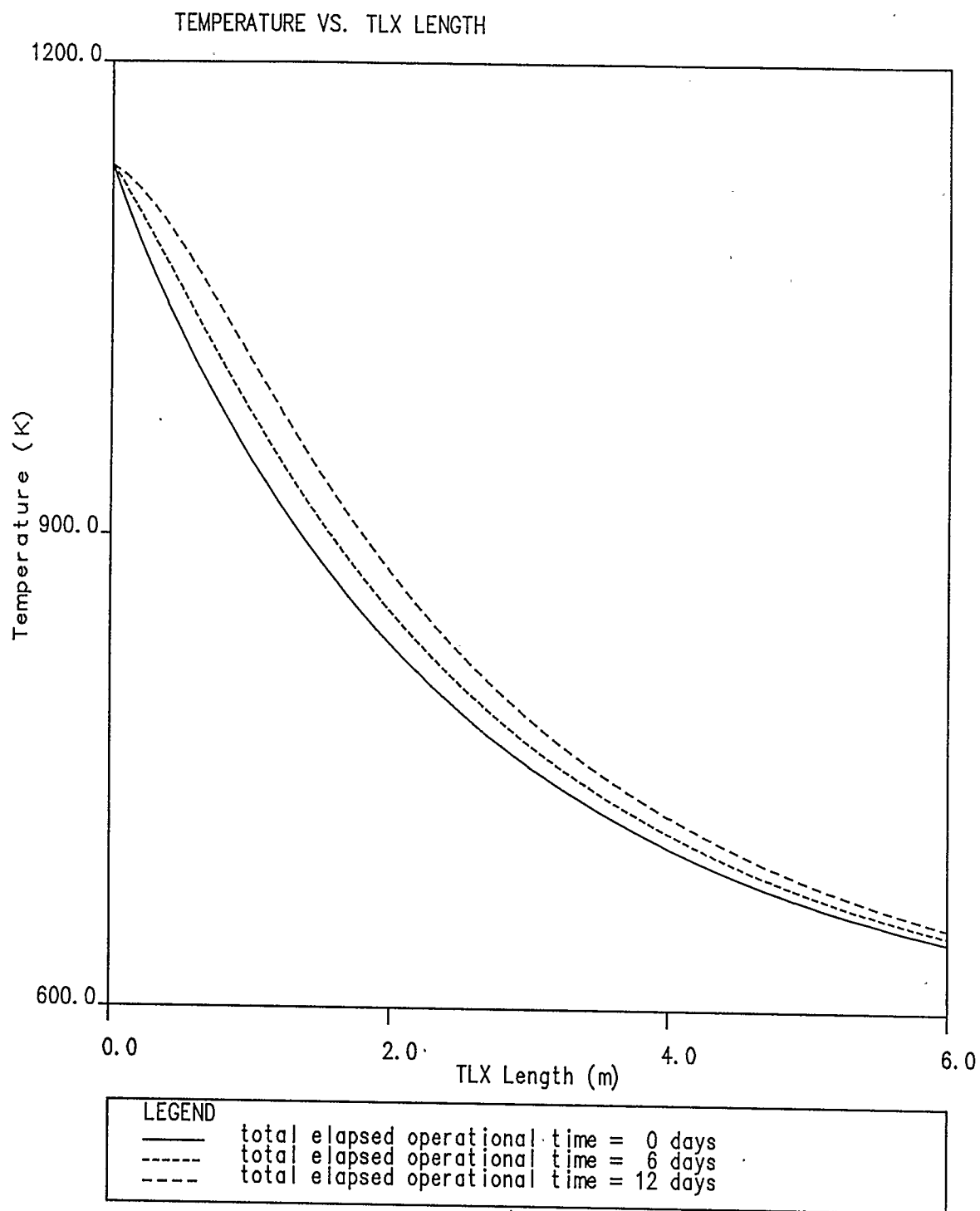


Figure 8.1.6 TLX Temperature profiles
at different total elapsed operational times
using coke model 2 (base case)

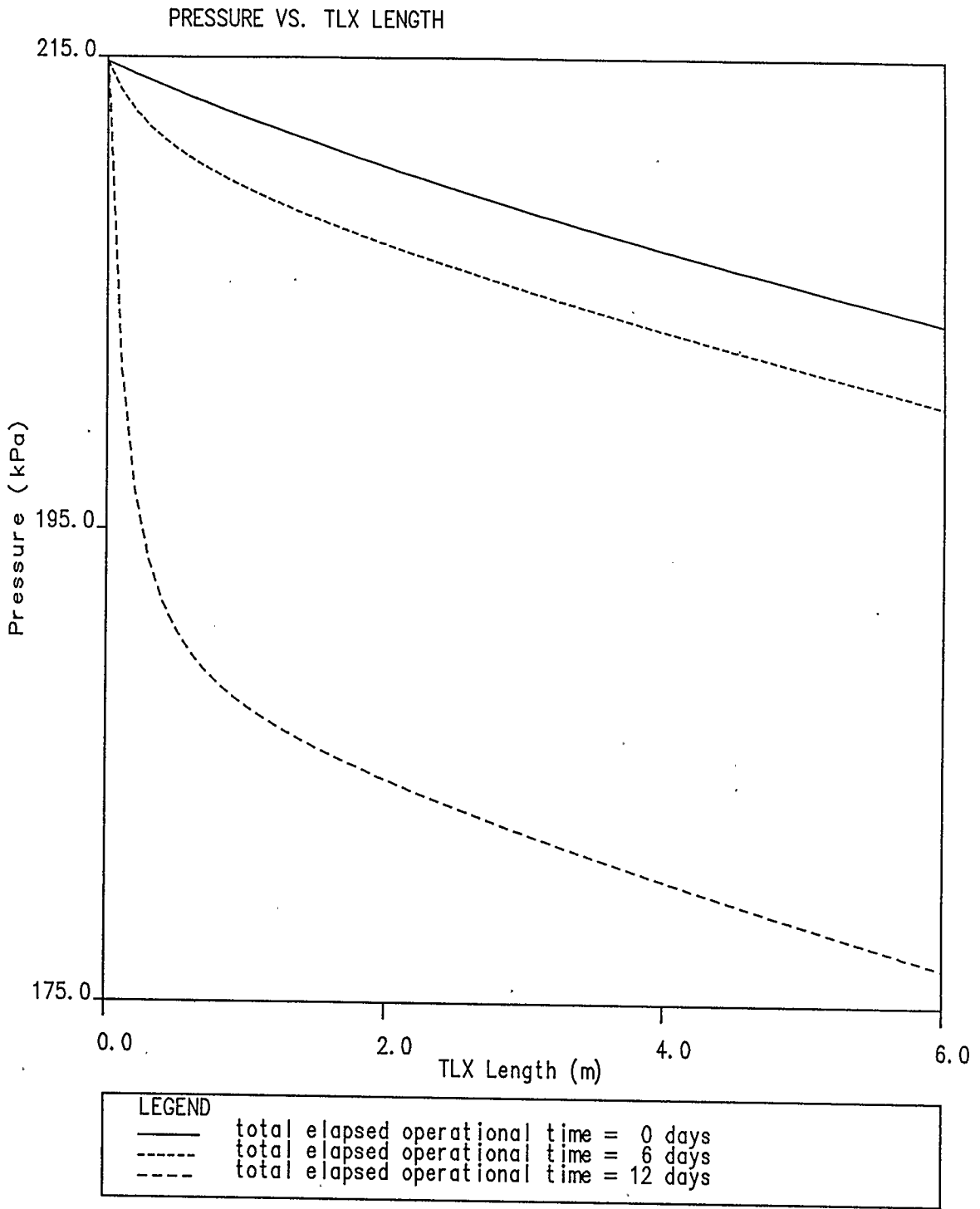


Figure 8.1.7 TLX Pressure profiles at different total elapsed operational times using coke model 2 (base case)

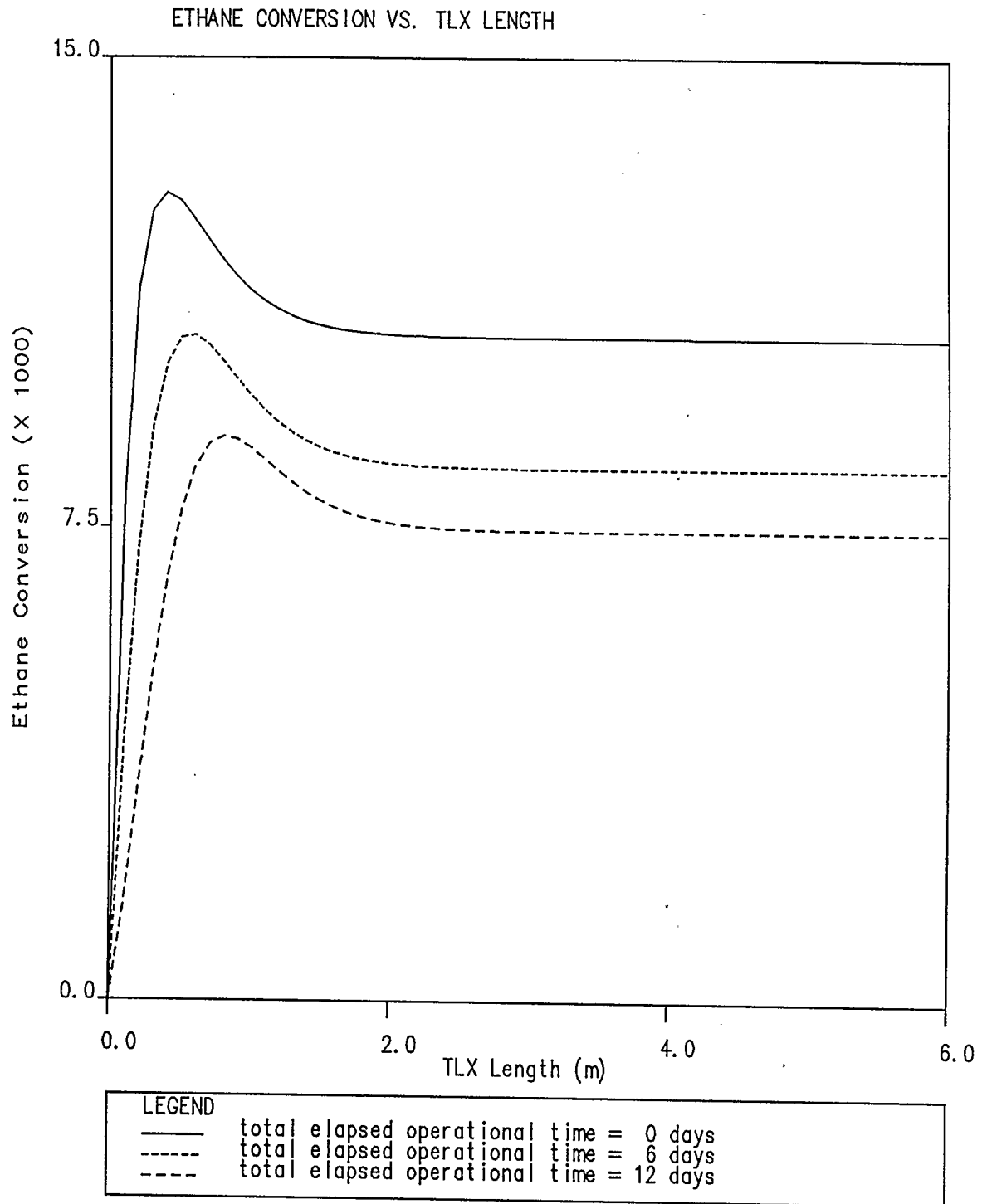


Figure 8.1.8 TLX Ethane conversion profiles at different total elapsed operational times using coke model 2 (base case)

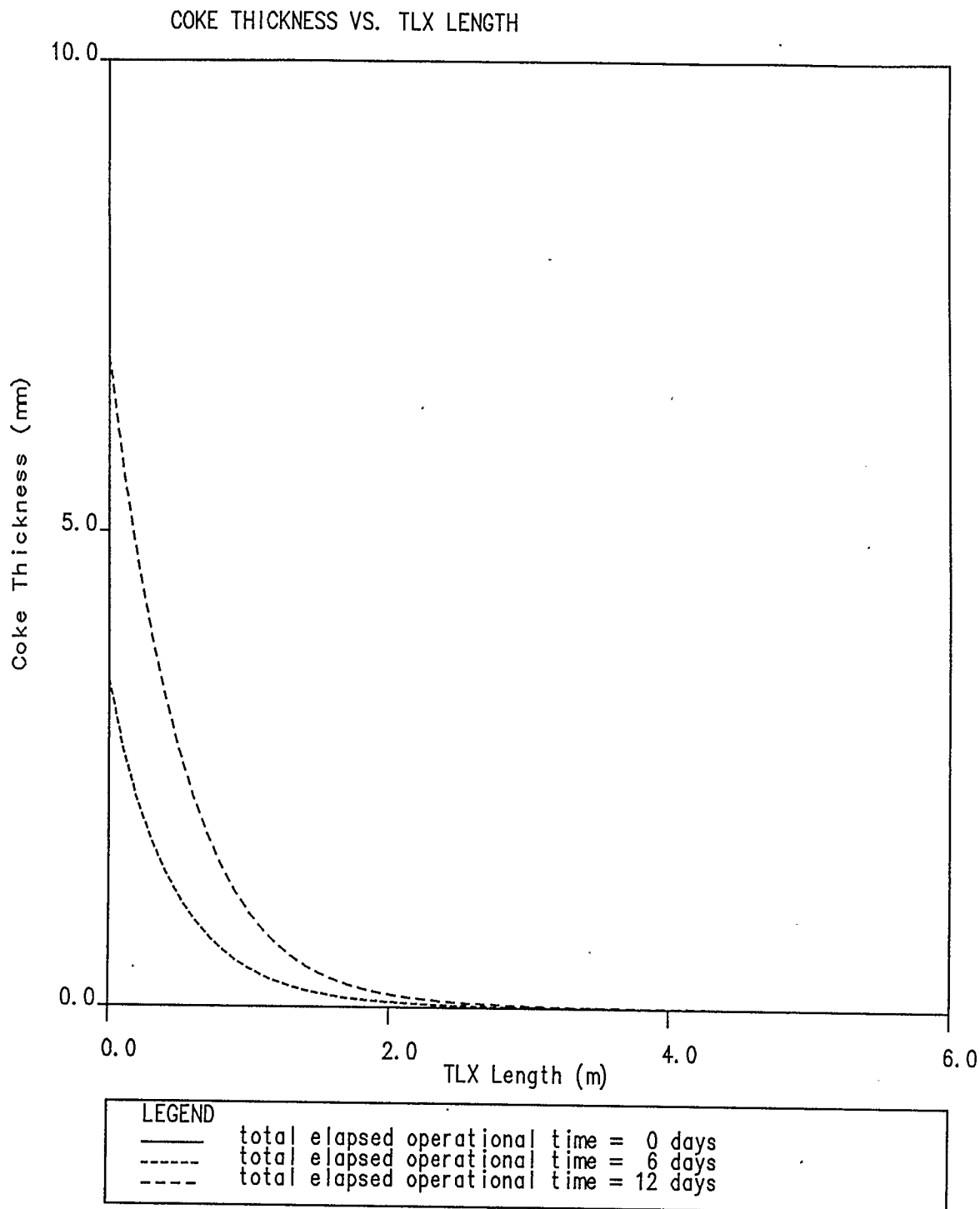


Figure 8.1.9 TLX Coke thickness profiles
at different total elapsed operational times
using coke model 2 (base case)

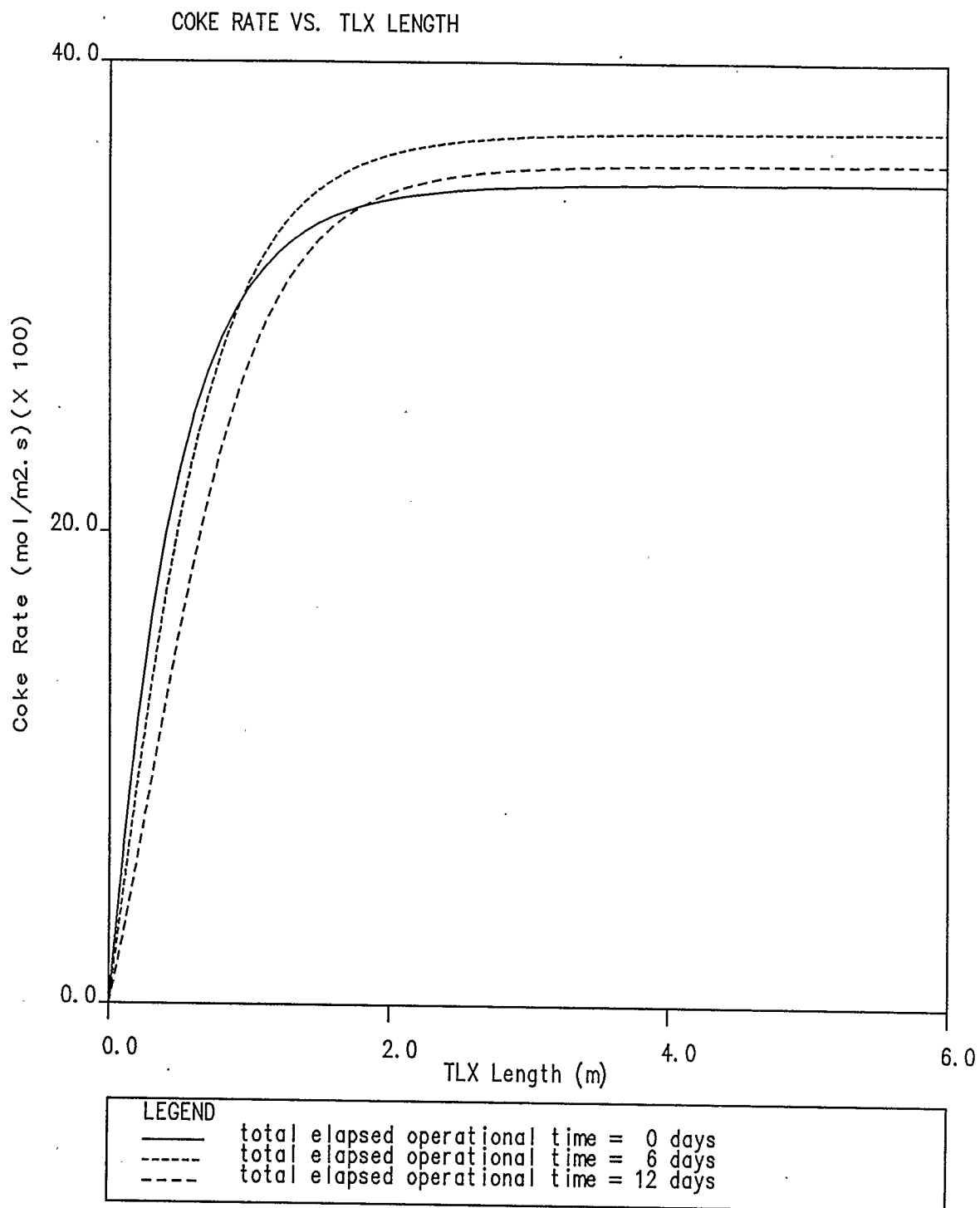


Figure 8.1.10 TLX Coke rate profiles
at different total elapsed operational times
using coke model 2 (base case)

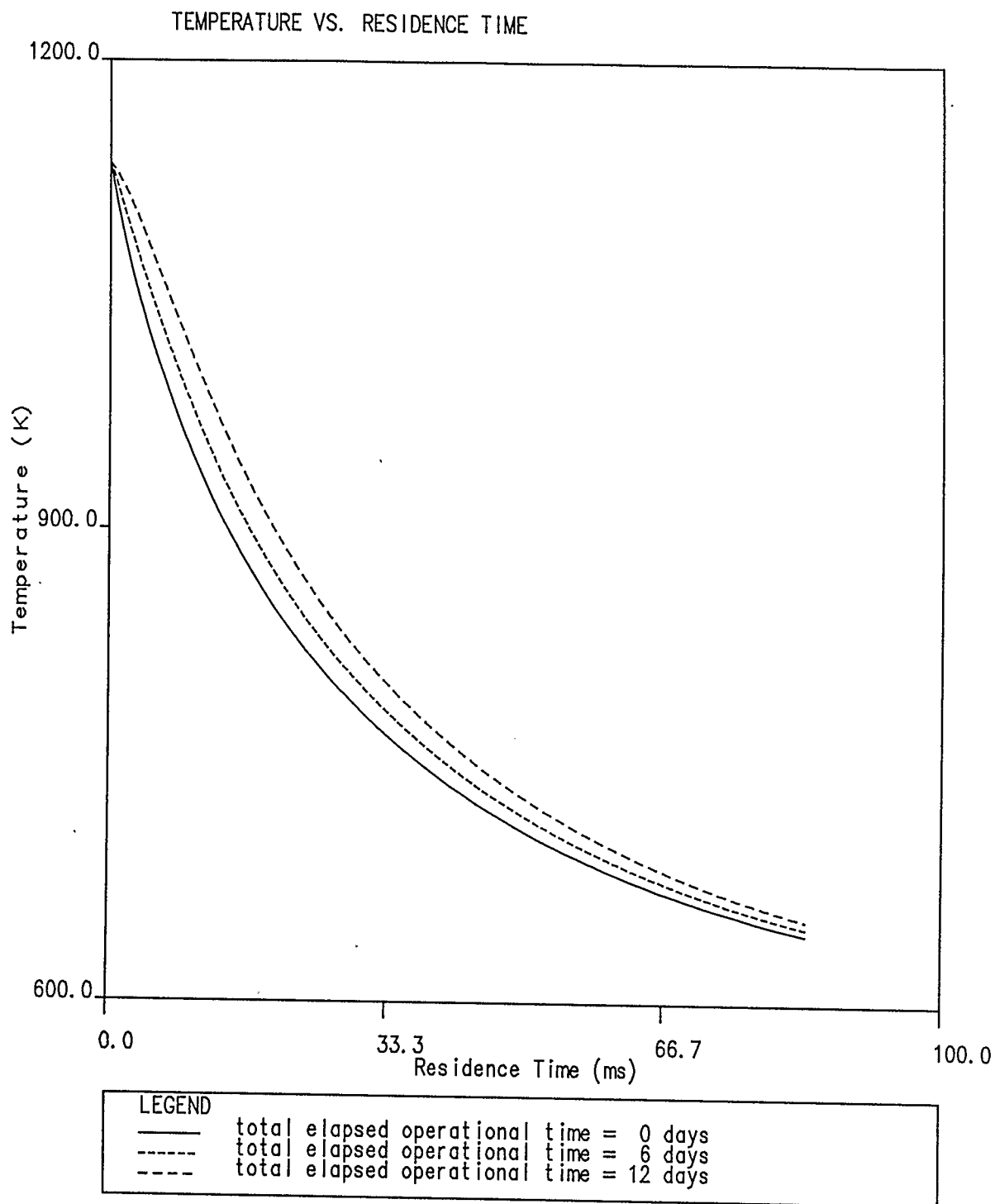


Figure 8.1.11 TLX Temperature profiles at different total elapsed operational times using coke model 2 (base case)

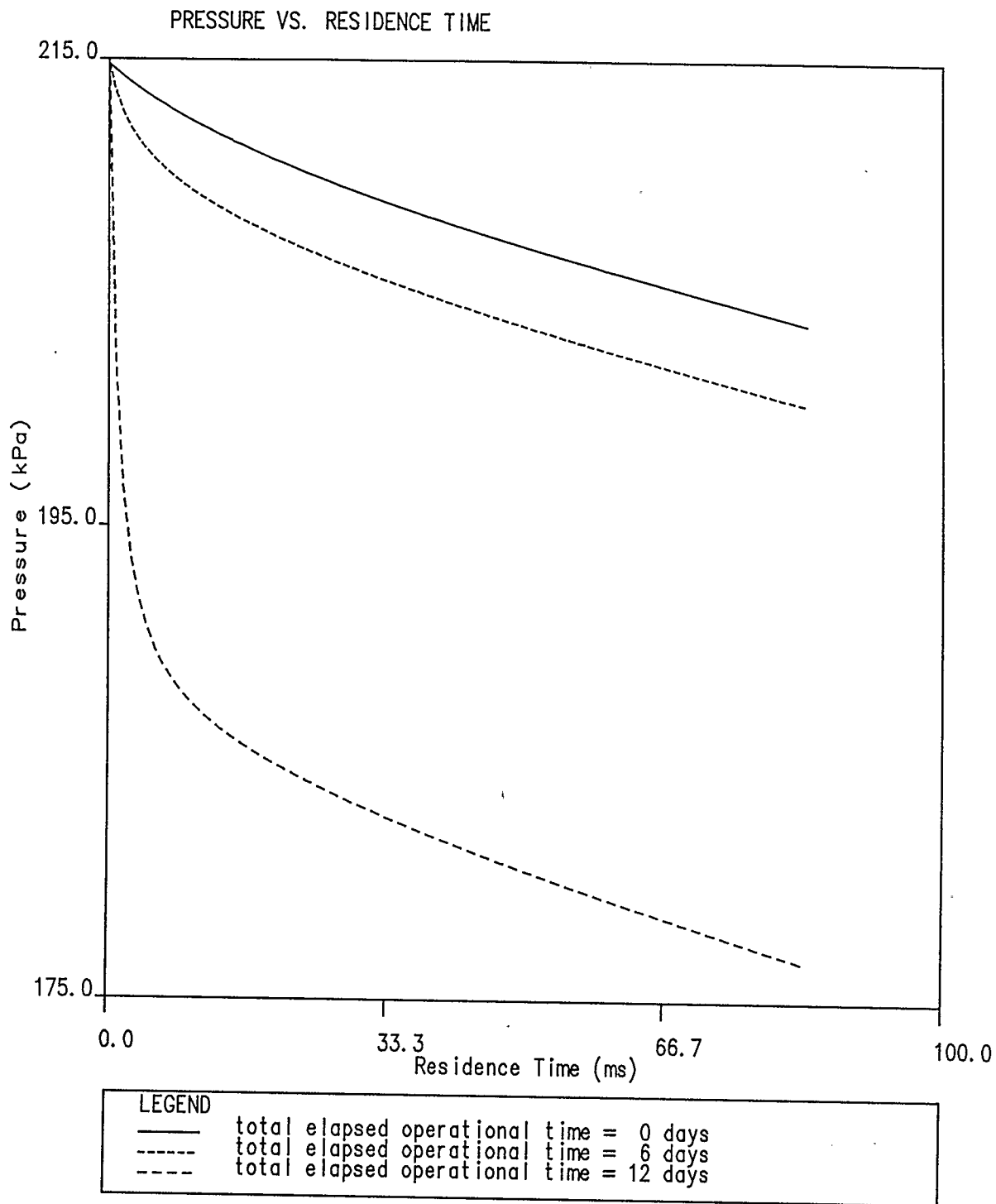


Figure 8.1.12 TLX Pressure profiles
at different total elapsed operational times
using coke model 2 (base case)

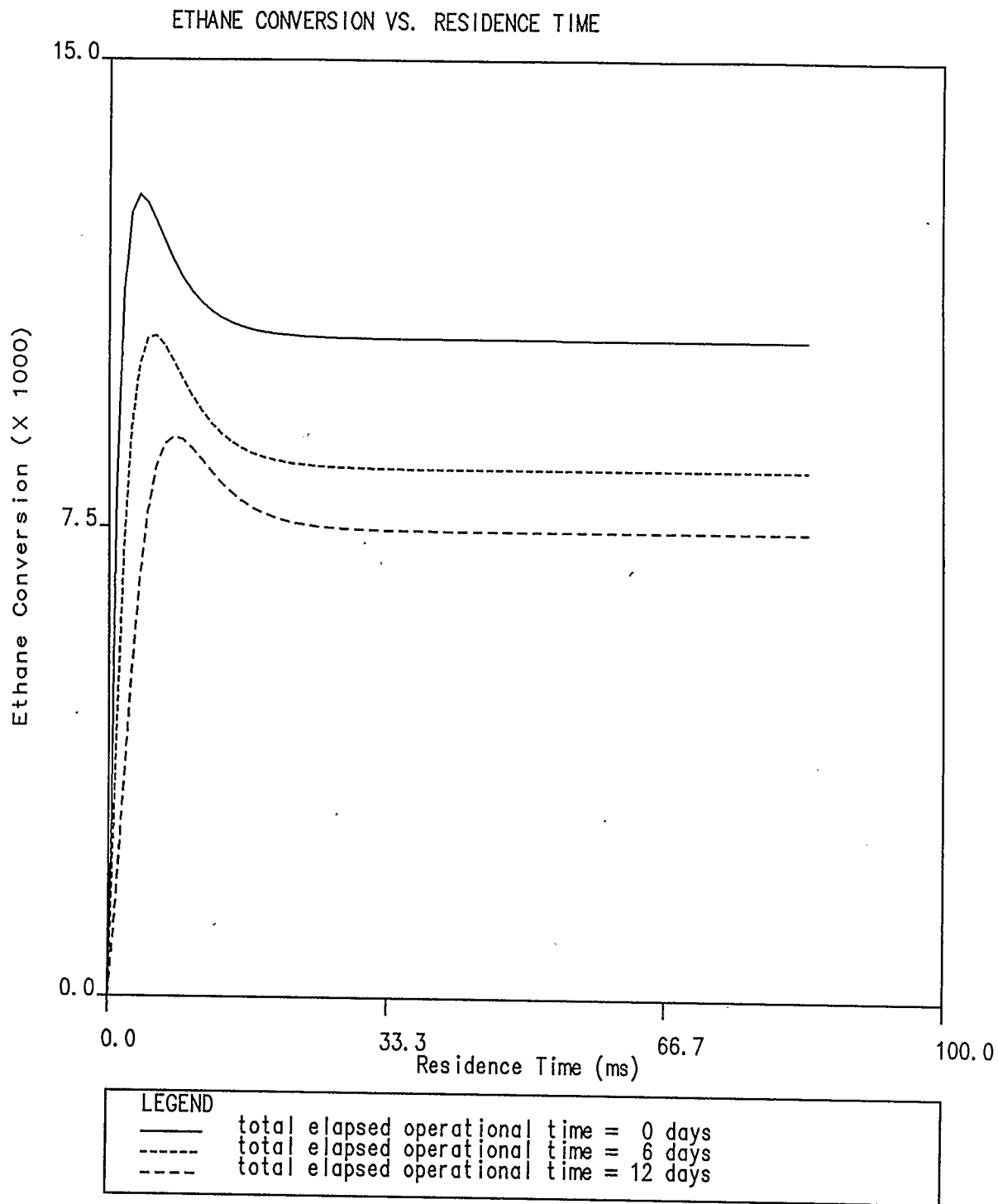


Figure 8.1.13 TLX Ethane conversion profiles at different total elapsed operational times using coke model 2 (base case)

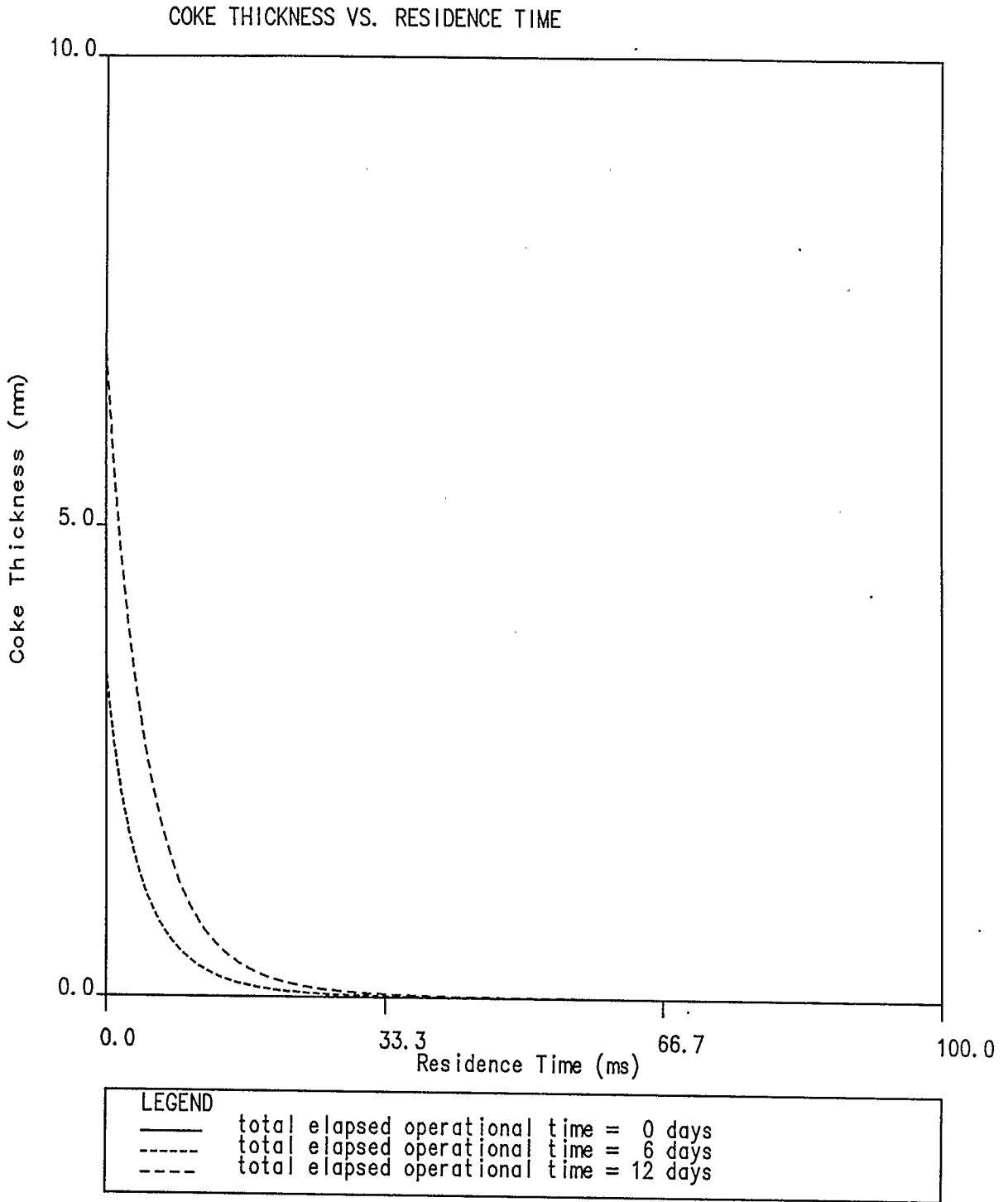


Figure 8.1.14 TLX Coke thickness profiles at different total elapsed operational times using coke model 2 (base case)

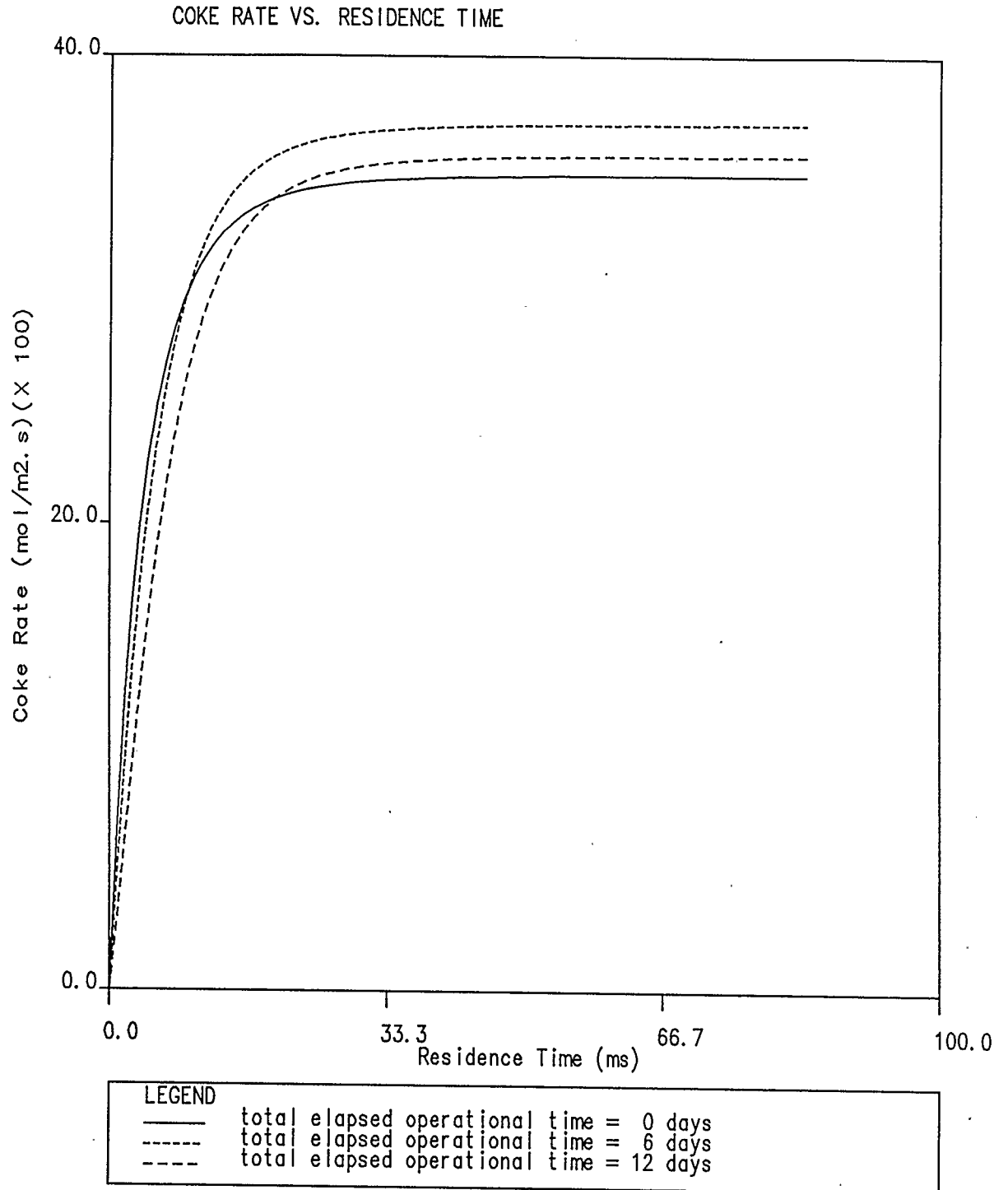


Figure 8.1.15 TLX Coke rate profiles
at different total elapsed operational times
using coke model 2 (base case)

Although the additional TLX length is not necessary for reaction quench, the additional heat extracted from the process stream in this portion of the exchanger is very valuable in terms of both the cooling provided to the process stream (which must be cooled prior to downstream separation) and in the value of the additional steam produced in this section.

As time proceeds, the temperature drops less rapidly near the cooler inlet, due to the decreased TLX diameter caused by coke deposition. However, even after 24 days for coke model 1 or 12 days for coke model 2, full quench is still achieved within 3 metres (residence time = 36.0 ms) of the inlet. Based on this observation, the quench cooler appears quite capable of continued quenching for a considerable period of time. It is the other effects of coke deposition such as severe pressure drop and tube blockage which require the TLX to be periodically shutdown for decoking. These simulation runs were terminated because the total coke thickness at the inlet would exceed the total inner diameter of the pipe on a subsequent time step. Since the coke lay-down parameter (α) was 1.0 for these runs, this represents a worst case for coke buildup.

The pressure drop in the simulation (Figures 8.1.2, 8.1.7 and 8.1.12) is affected much more by the coke deposits. This is expected, since the coke changes the diameter of the TLX significantly (Figures 8.1.4, 8.1.9 and 8.1.14).

Change in diameter translates into a change in area available for fluid flow, and the same fluid mass flux through a smaller pipe will result in an increased fluid velocity, and consequently a much larger pressure drop. The pressure drop in the quench cooler is greatest in the first 0.5 m, corresponding to the region of greatest coke buildup. Appendix D shows the pressure drop equation, and the relationship between flow rate (or mass flux), diameter and pressure drop can be seen from the equation.

The pressure drop changes are not linear with time, although the other curves appear to change in a linear manner with time. This is because the diameter change with time is essentially linear, and the pressure drop depends on the area change, which is quadratic (Appendix D).

The ethane conversion (Figures 8.1.3, 8.1.8 and 8.1.13) decreases quickly as the coke builds up due to the decreased cooling rate caused by the coke, and also due to the increased velocity of the process stream in the smaller tube. The coke buildup does not appreciably effect the ethane or ethylene molar flow rate. Rather, the pipe diameter restrictions are translated into increased fluid velocities and therefore higher pressure drops.

The final variable observed in this case is the coke formation rate (Figures 8.1.5, 8.1.10 and 8.1.15). This is an unusual series of curves, as the curves appear to increase, then decrease again with time. This response is

due primarily to the fact that the coke affects only the initial 0.5 m of the TLX to a great degree. After the initial 0.5 m of cooler, the cooler conditions become much closer to those of a clean tube TLX. Since effectively only the first 0.5 m of the TLX is changing with time, looking at the initial portion of the coke rate curve shows the response of the rate in this region. It can be seen that in this region, the rate of coke formation decreases steadily with time, similar to the way the ethane conversion decreases with time. As the process stream leaves this initial coked portion of the quench cooler, conditions approach clean tube conditions, and quenching proceeds more normally. This causes a change in the shape of the coke rate curve. This rate change, not found in a clean TLX, is seen as the crossing of the curves at 6 days. The same shaped curves exist at increased times, but initial rates are now lower due to further coke buildup, the curves do not cross.

8.2 Effect of Feed Mass Flux

The effects caused by changing the mass flux of the feed to the quench cooler are seen in Figures 8.2.1 to 8.2.4. The feed flux controls the fluid velocity, and this affects both the rate of temperature change as well as the pressure drop. The temperature profile (Figure 8.2.1) is much lower for the low feed mass flux case, and higher for

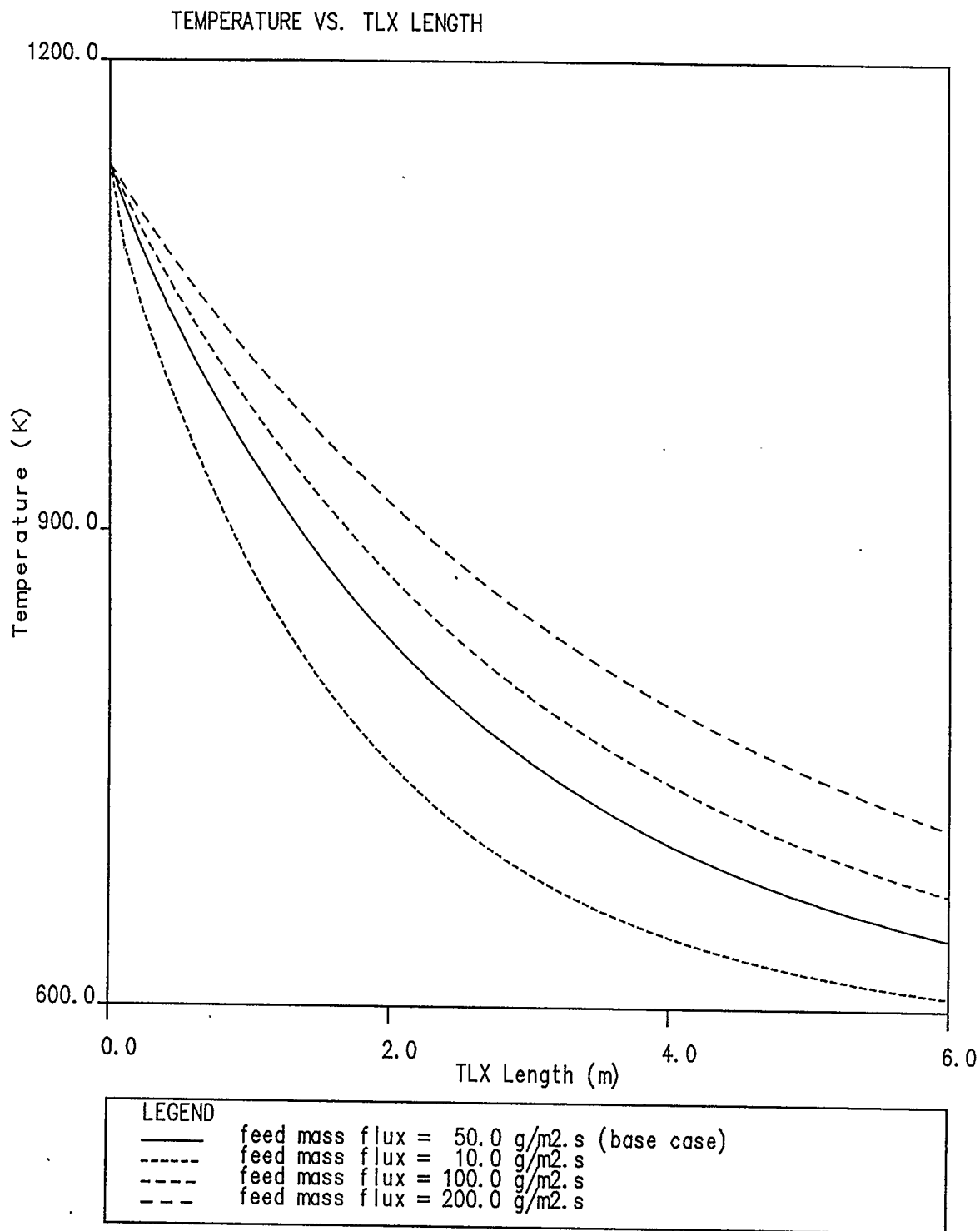


Figure 8.2.1 TLX Temperature profiles for different feed mass fluxes at clean tube conditions using either coke model

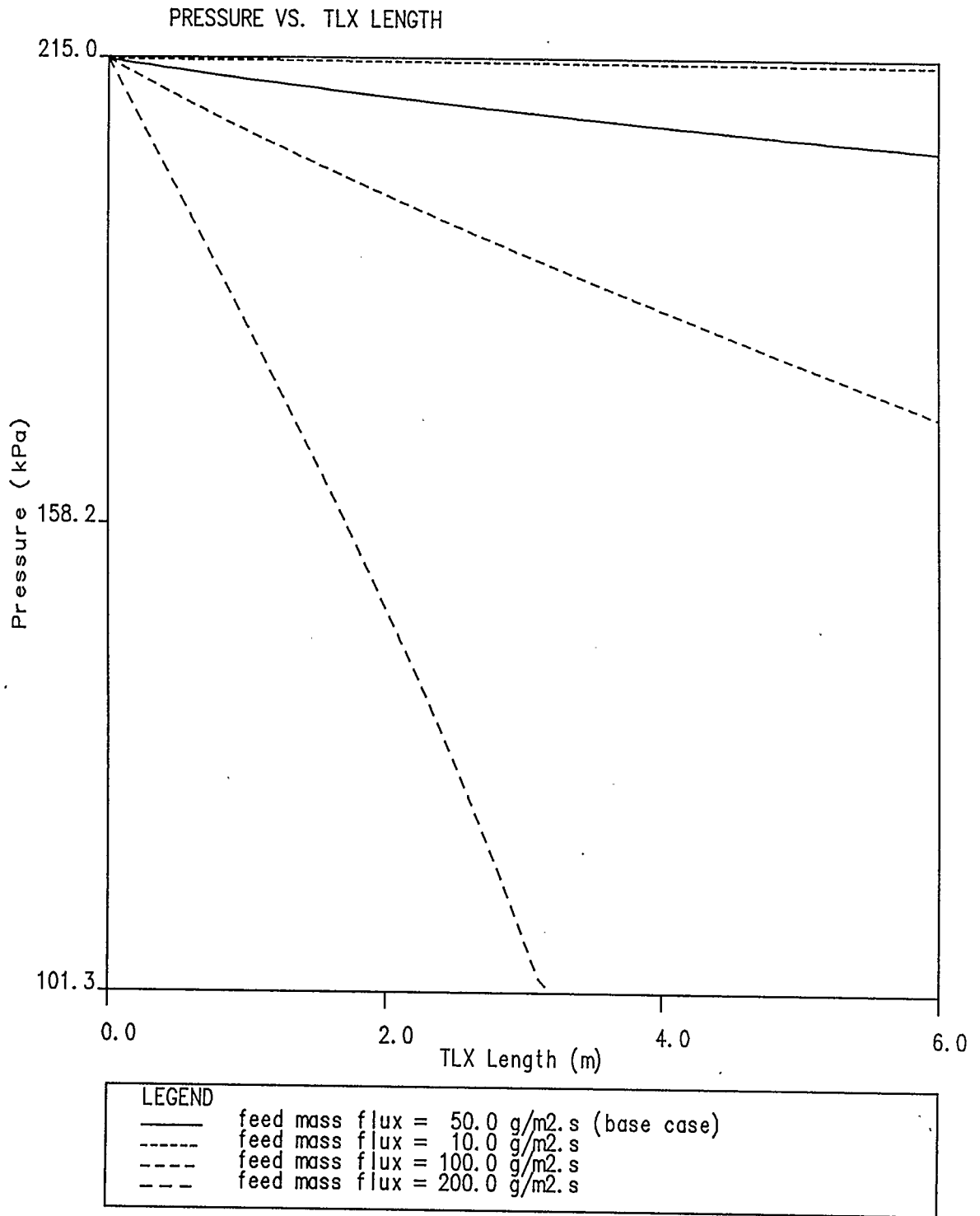


Figure 8.2.2 TLX Pressure profiles for different feed mass fluxes at clean tube conditions using either coke model

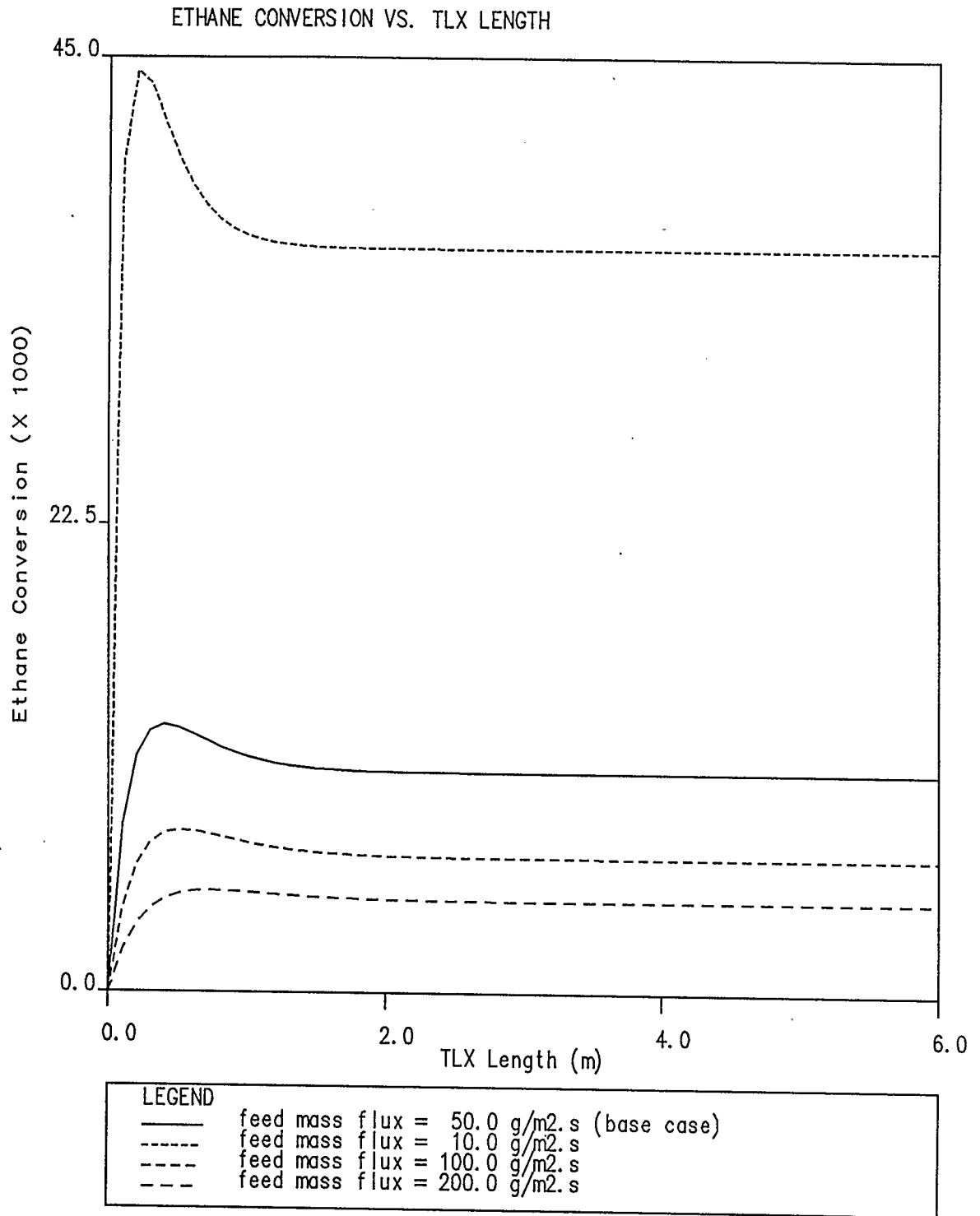


Figure 8.2.3 TLX Ethane conversion profiles for different feed mass fluxes at clean tube conditions using either coke model

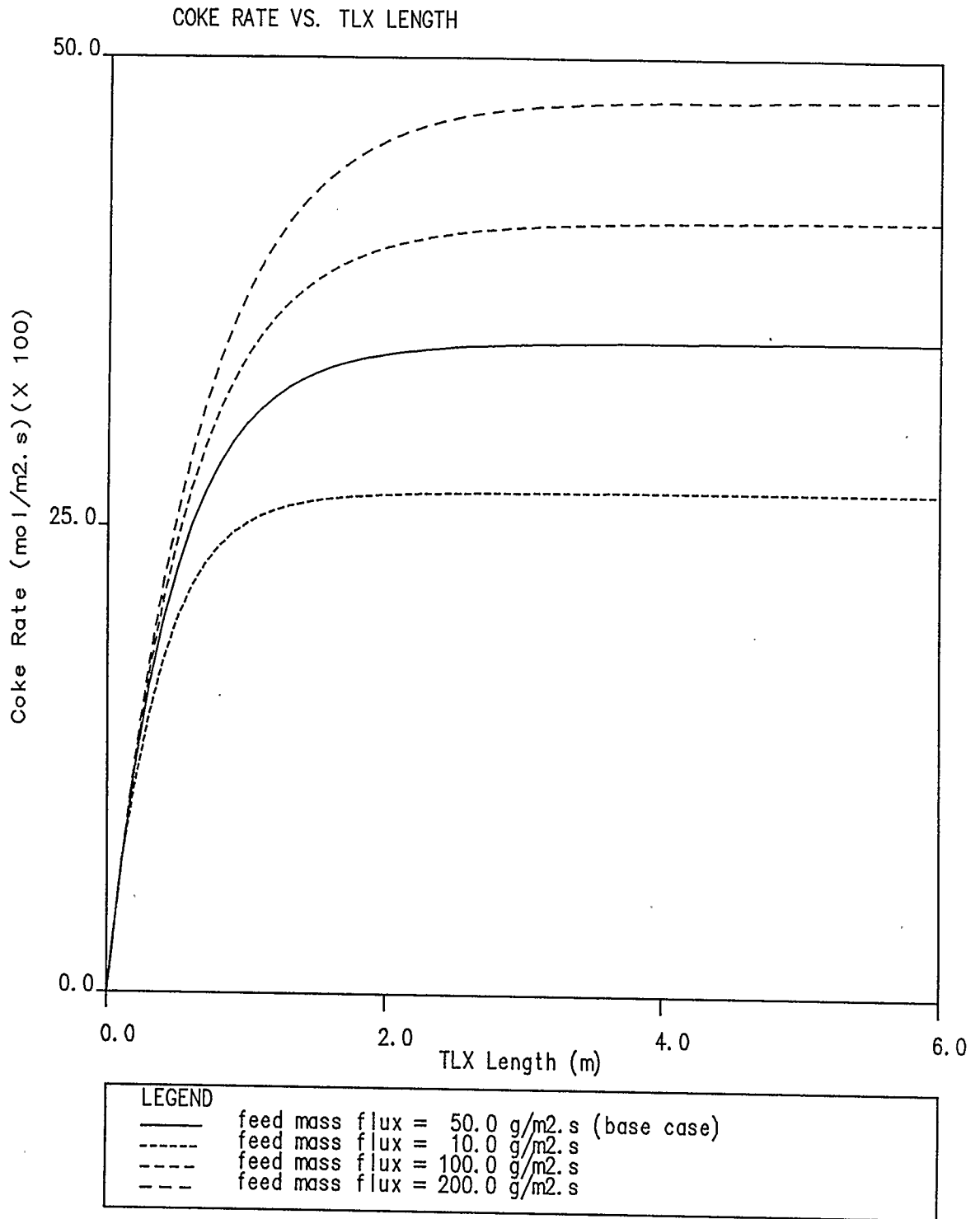


Figure 8.2.4 TLX Coke rate profiles for different feed mass fluxes at clean tube conditions using either coke model

the high mass flux case. These changes do not appear to be linear. The pressure drop (Figure 8.2.2) is less for lower mass fluxes, and very much higher for the larger fluxes. At $200.0 \text{ kg/m}^2 \cdot \text{s}$, the pressure drop is larger than the system is capable of handling, and the pressure inside the TLX drops to 0.0 kPa at 4.2 m . The fluid velocity at each mass flux is 13.0 m/s for $10.0 \text{ kg/m}^2 \cdot \text{s}$, 71.7 m/s for $50.0 \text{ kg/m}^2 \cdot \text{s}$, 177.7 m/s for $100.0 \text{ kg/m}^2 \cdot \text{s}$, and 585.2 m/s for $200.0 \text{ kg/m}^2 \cdot \text{s}$. Since the fluid velocity at this last mass flux exceeds the maximum velocity of 304.8 m/s recommended by Rase (1977a), the mass flux should not realistically exceed $150.0 \text{ kg/m}^2 \cdot \text{s}$ for this diameter pipe. Note that for the cases showing the effect of total elapsed operational time, a smaller quench cooler diameter at later times had the same effect as the changed mass flux in these cases. This will also be discussed in Section 8.3 where TLX diameter is changed.

At low mass flux, the conversion of ethane (Figure 8.2.3) is higher than the conversion at high mass flux. This is because the low mass flux shifts the equilibrium reaction towards ethylene formation.

8.3 Effect of Tube Inside Diameter

The effects of changing TLX tube diameter are plotted in Figures 8.3.1 to 8.3.4. Changing the diameter of the tube should have similar effects on the model as changing the mass flux. This conclusion was obtained initially by observing the effect of total elapsed operational time on the TLX, Section 8.1, where coke deposits changed reactor diameter, compared to observing the effect of changing mass flux, Section 8.2. This set of runs confirms that conclusion.

Enlarging the TLX tube increases the area available for flow, and so reduces the fluid velocity and molar flow rates, while also decreasing the overall pressure drop (Figure 8.3.2). The thermal efficiency is also reduced as the walls must cool more material in a given element of the TLX. As a result, the overall cooling rate drops and the temperature profile flattens out as TLX tube size increases (Figure 8.3.1).

The ethane conversion curve (Figure 8.3.3) does not flatten out for the largest diameter pipe, showing the reaction is not quenched for the 100.0 mm diameter pipe. This can also be seen by observing the temperature profile, as the exit temperature of the 100.0 mm diameter pipe is 900 K, which is above the quench temperature of 800 K observed in

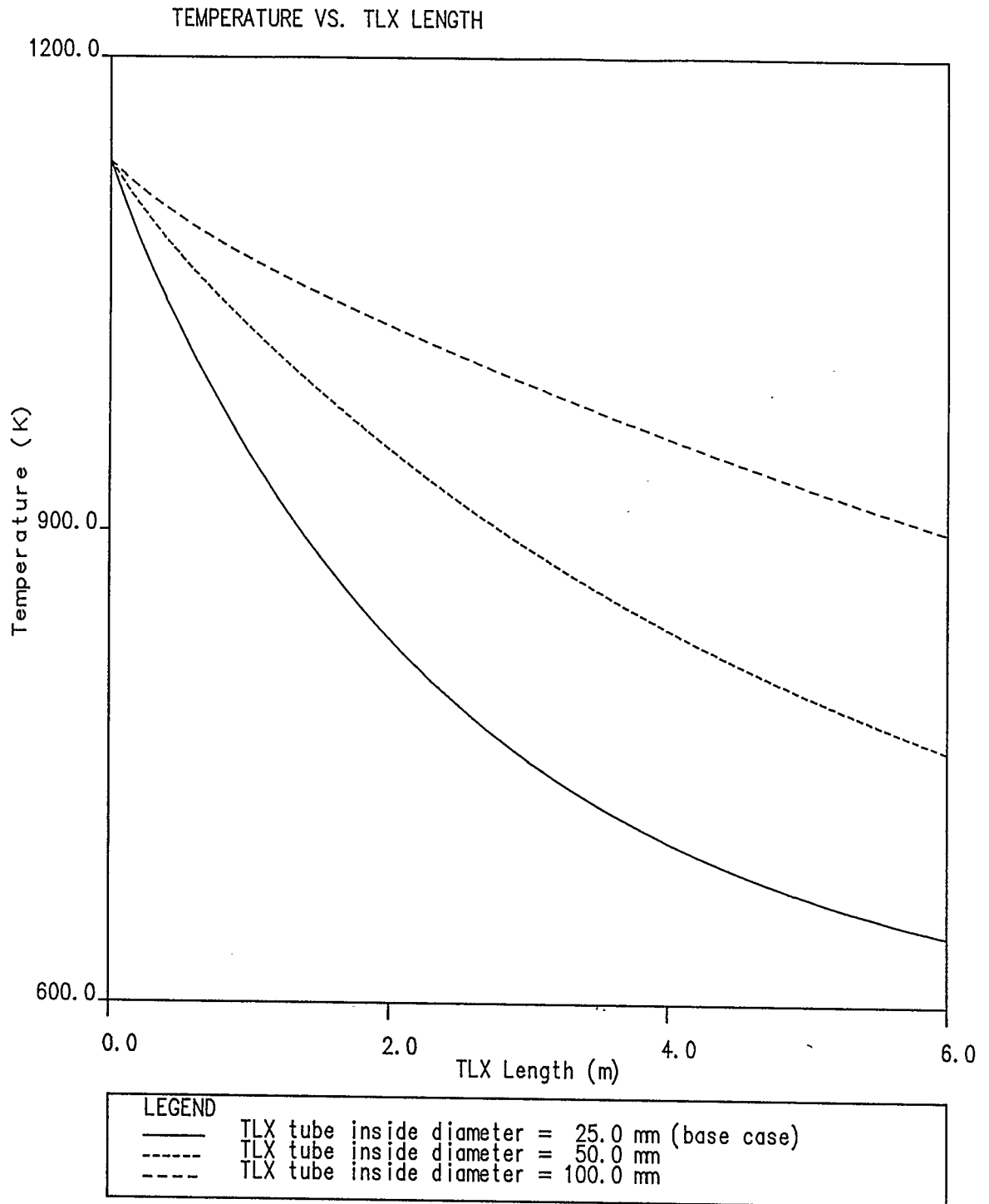


Figure 8.3.1 TLX Temperature profiles for various TLX tube inside diameters at clean tube conditions using either coke model

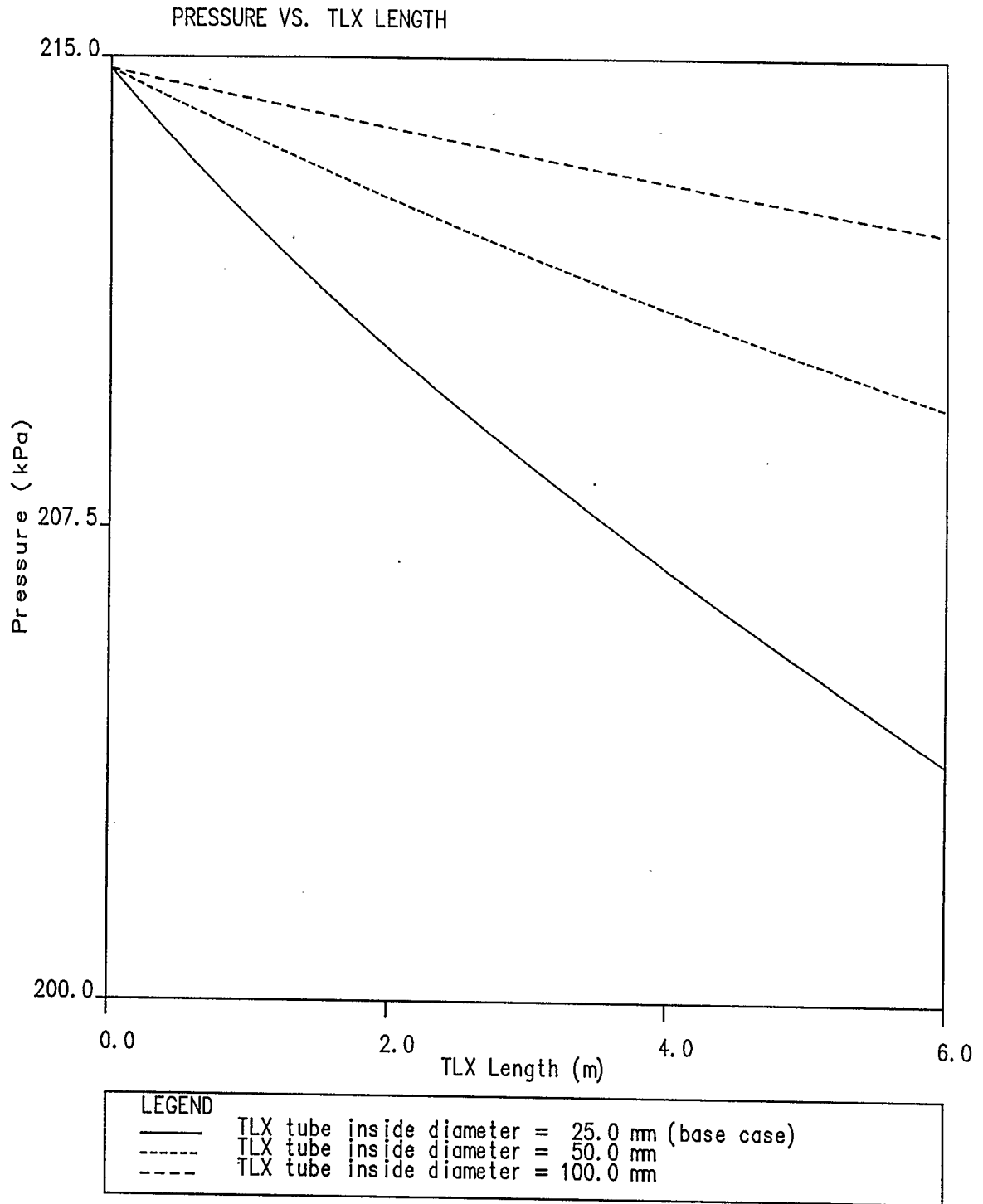


Figure 8.3.2 TLX Pressure profiles
for various TLX tube inside diameters
at clean tube conditions using either coke model

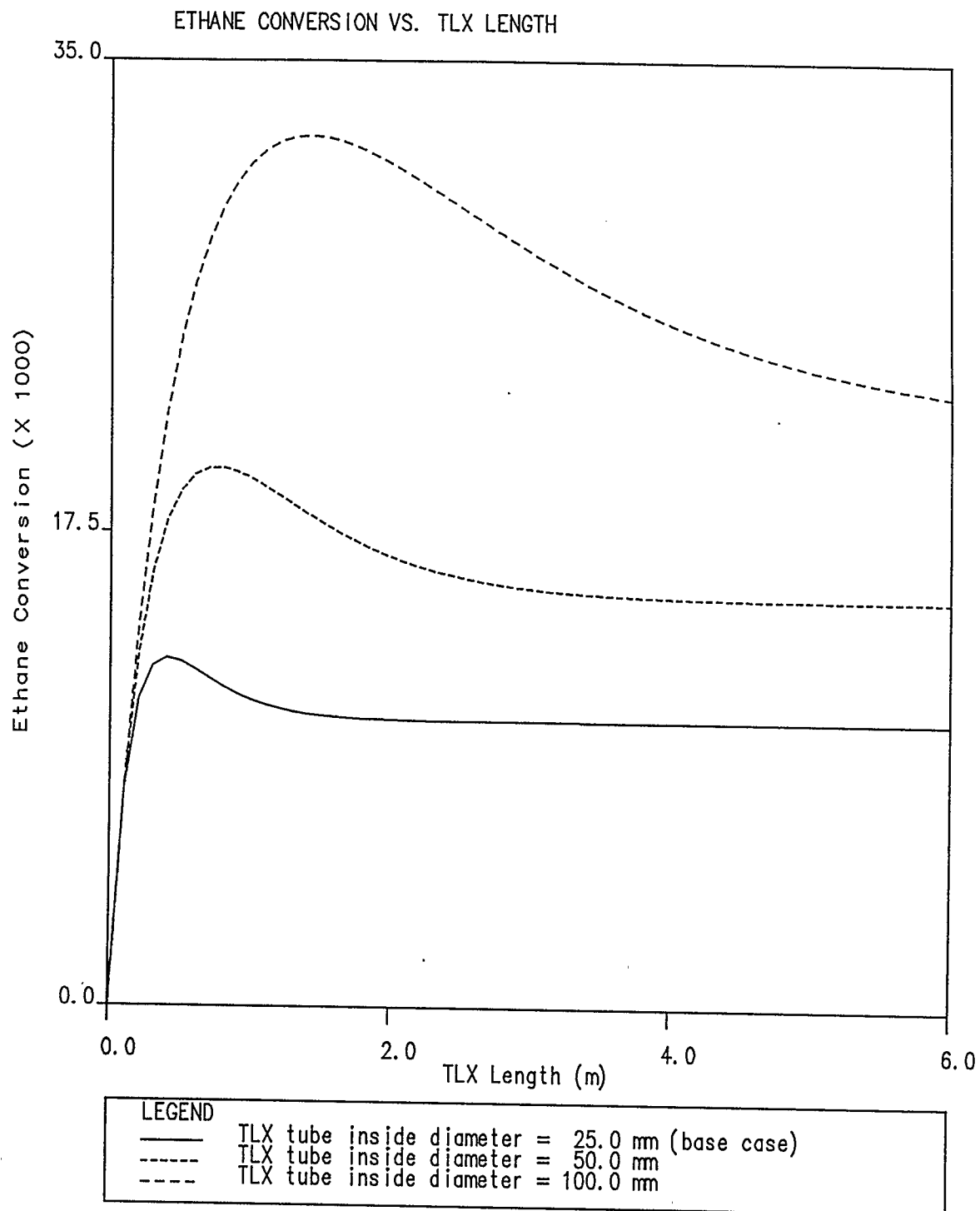


Figure 8.3.3 TLX Ethane conversion profiles for various TLX tube inside diameters at clean tube conditions using either coke model

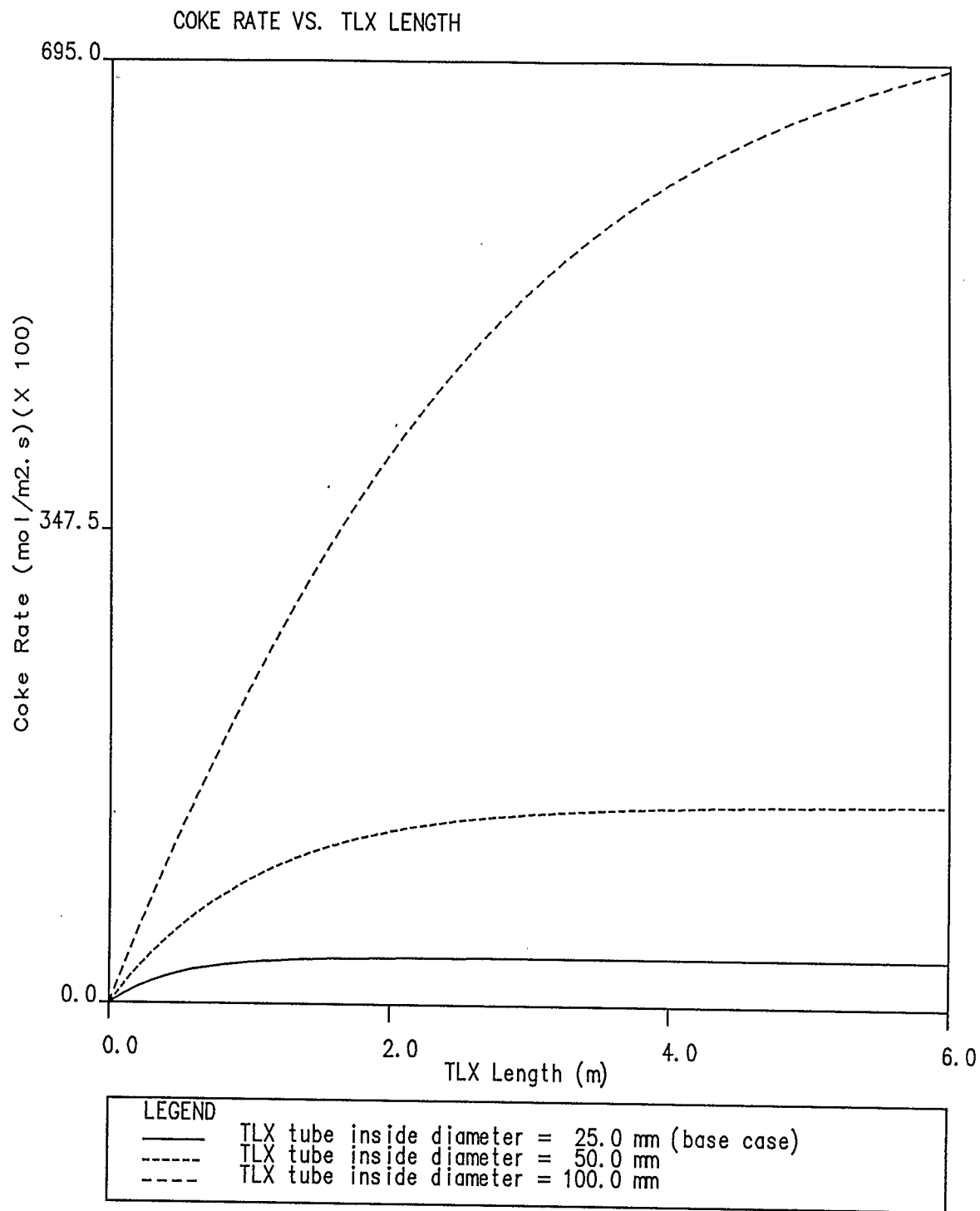


Figure 8.3.4 TLX Coke rate profiles
for various TLX tube inside diameters
at clean tube conditions using either coke model

Section 8.1. Because the reaction is not quenched, the ethane conversion curve shows a large local maximum. This is caused by the significant formation of by-products from secondary reactions. As ethylene is converted to the undesirable by-products, the ethane reaction equilibrium shifts towards the production of more ethylene, and the corresponding disappearance of ethane. This is also observed in the greater rate of coke production for the large diameter case. Molar flow rates respond to the diameter changes by increasing for small diameters and decreasing for large diameters. This is because the same mass flux through a larger area will reduce the molar flow rate, which is area dependent.

8.4 Effect of Steam Dilution

The effects of changing the steam dilution ratio changes are plotted in Figures 8.4.1 to 8.4.4. Since steam is inert in this model, the only effect studied is reduction in hydrocarbon concentration or partial pressure and the resulting reduction of the hydrocarbon molar flow rates. Since total pressure does not change significantly, changing steam dilution should not affect temperature or pressure profiles for a given amount of coke deposited, and this is seen in these two curves (Figures 8.4.1 and 8.4.2).

The variable most affected by changing steam dilution ratio is the ethane conversion (Figure 8.4.3), which shows

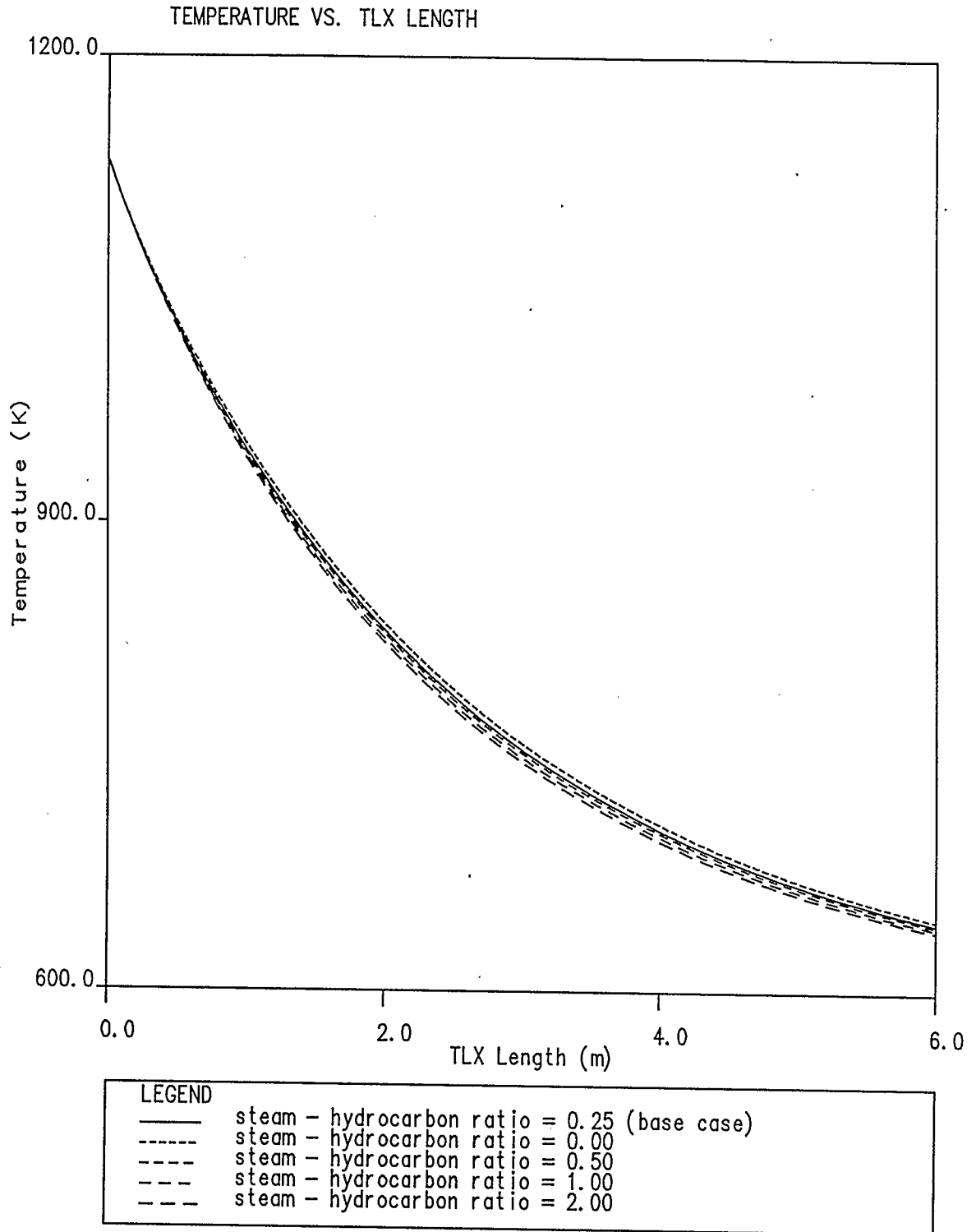


Figure 8.4.1 TLX Temperature profiles
for different steam - hydrocarbon ratios
at clean tube conditions using either coke model

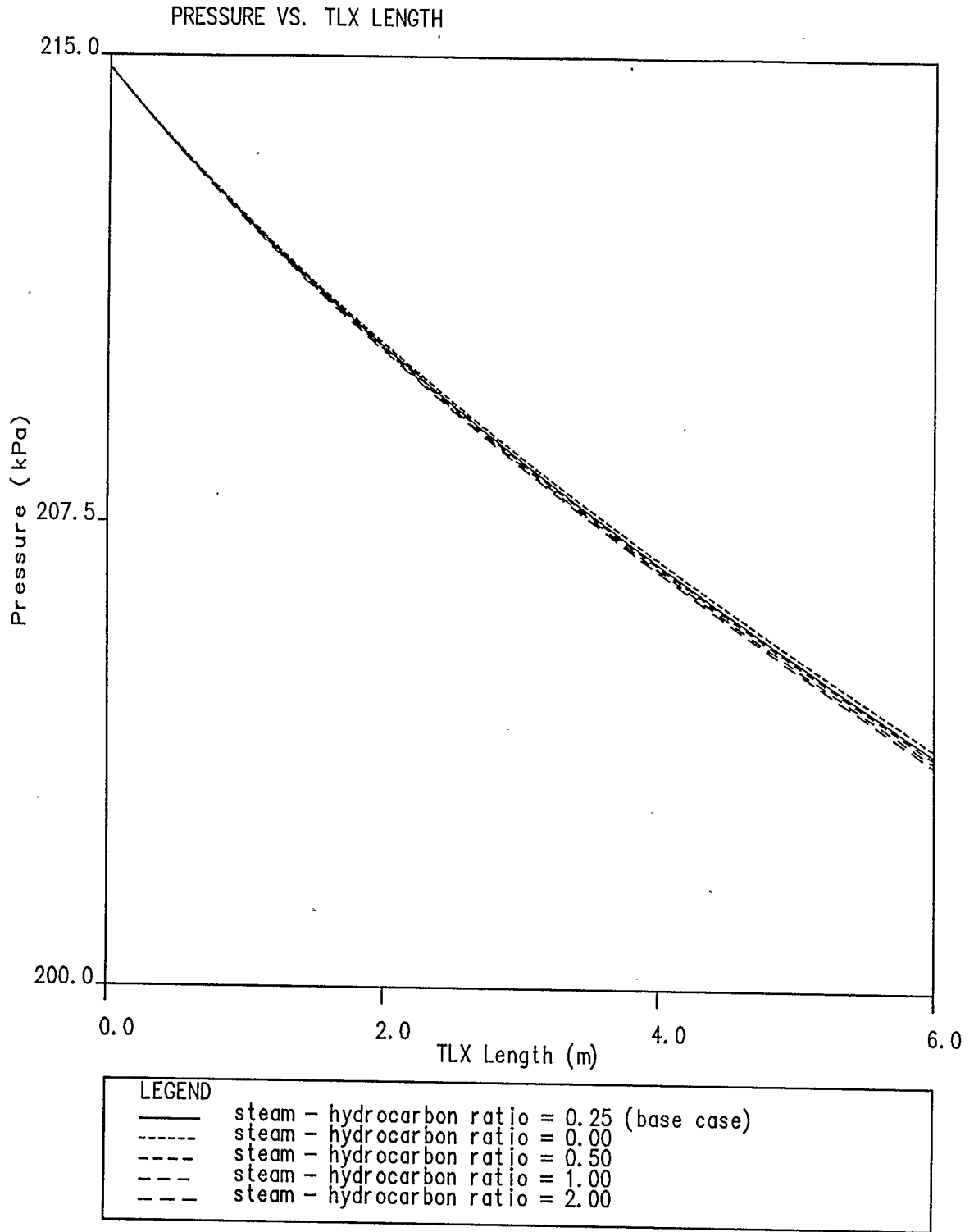


Figure 8.4.2 TLX Pressure profiles for different steam - hydrocarbon ratios at clean tube conditions using either coke model

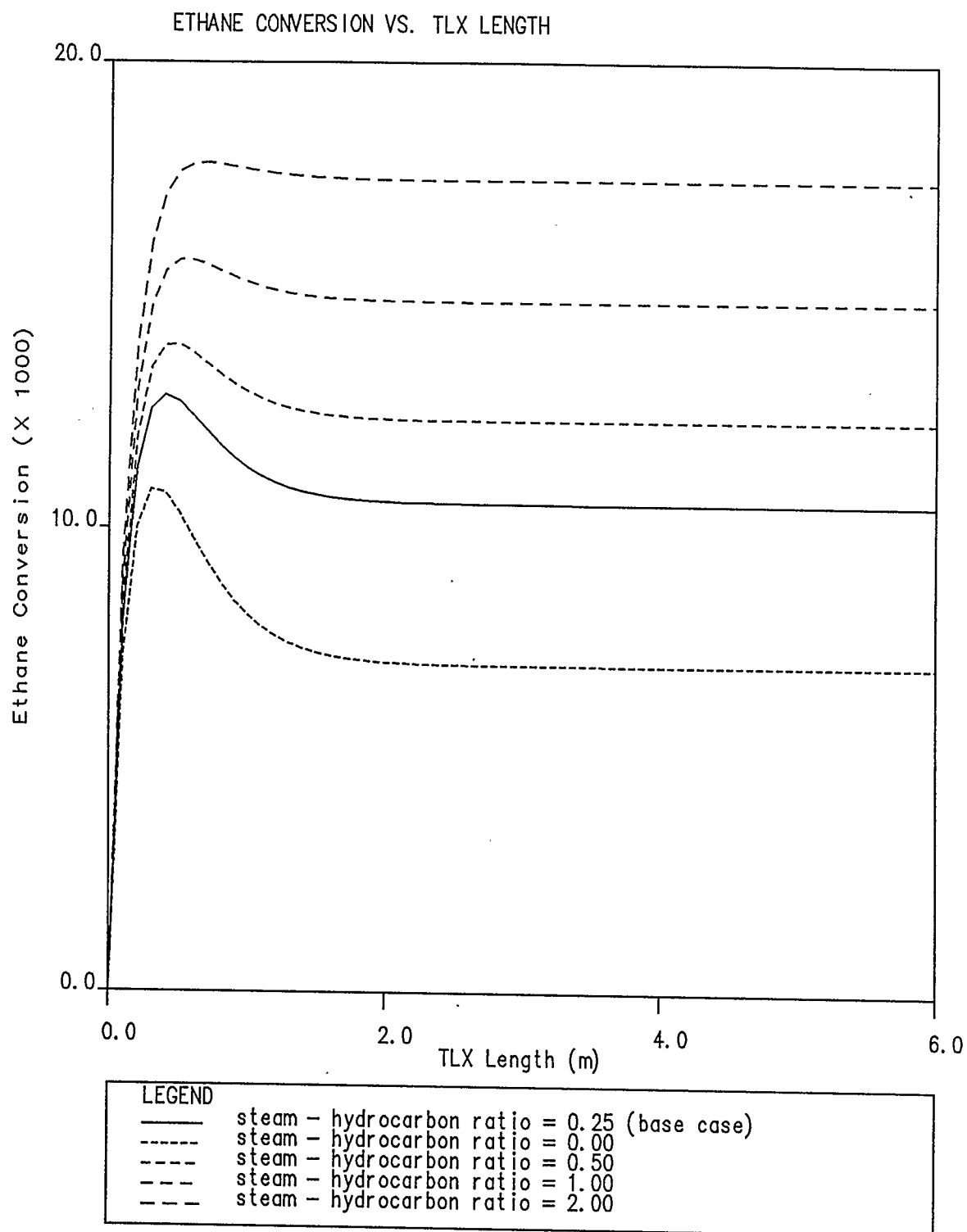


Figure 8.4.3 TLX Ethane conversion profiles for different steam - hydrocarbon ratios at clean tube conditions using either coke model

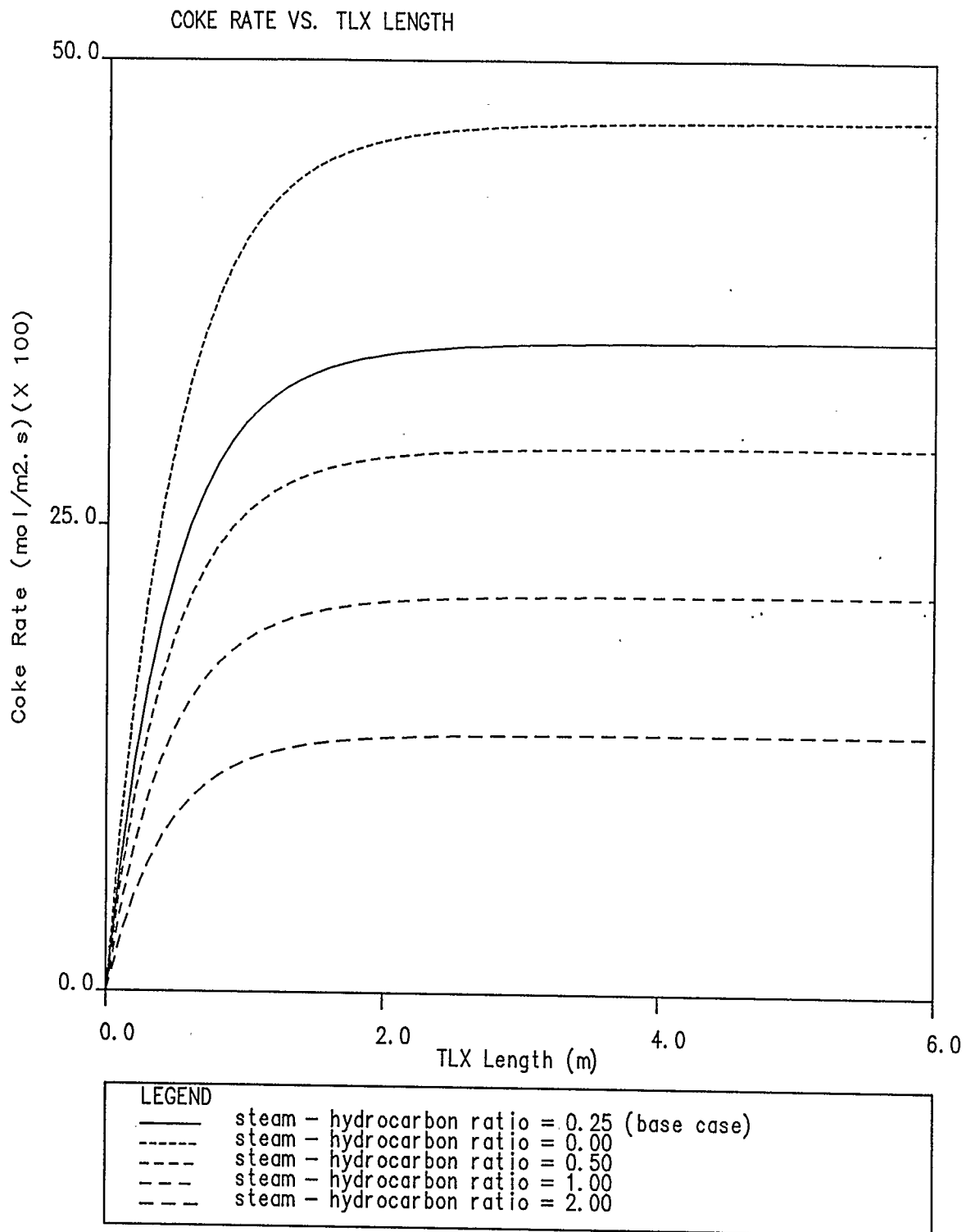


Figure 8.4.4 TLX Coke rate profiles for different steam - hydrocarbon ratios at clean tube conditions using either coke model

strong response to the changes in hydrocarbon partial pressure produced by adding steam. As hydrocarbon partial pressure decreases, ethane conversion increases. Production of by-products also decreases, as seen by the reduced size of the local maximum in the ethane conversion curve. Molar flow rates mirror this dilution effect, since fewer moles of ethane and ethylene are flowing for the same mass flux as more steam is added. Coke rate (Figure 8.4.4) also responds to the reduced presence of hydrocarbon, forming the most coke when pure hydrocarbon is present (steam ratio 0.0), and the least when the steam ratio is 2.0. These results are predicted by the model development theory behind the model equations, as the partial pressure of each component in the reaction is the primary variable in the rate equations and molar flow rates are a key variable in the mass balance equations (Appendices B and E).

8.5 Effect of Steam Temperature

Steam temperature was varied from a base value of 586.0 K (10.3 MPa saturated steam). Values of 373.15 K (0.101 MPa saturated steam) and 700.0 K (55 K superheat at 22.0 MPa) were used. Plots of these runs are shown in Figures 8.5.1 to 8.5.4.

As expected by varying the shell side temperature, the temperature profiles (Figure 8.5.1) of the product stream

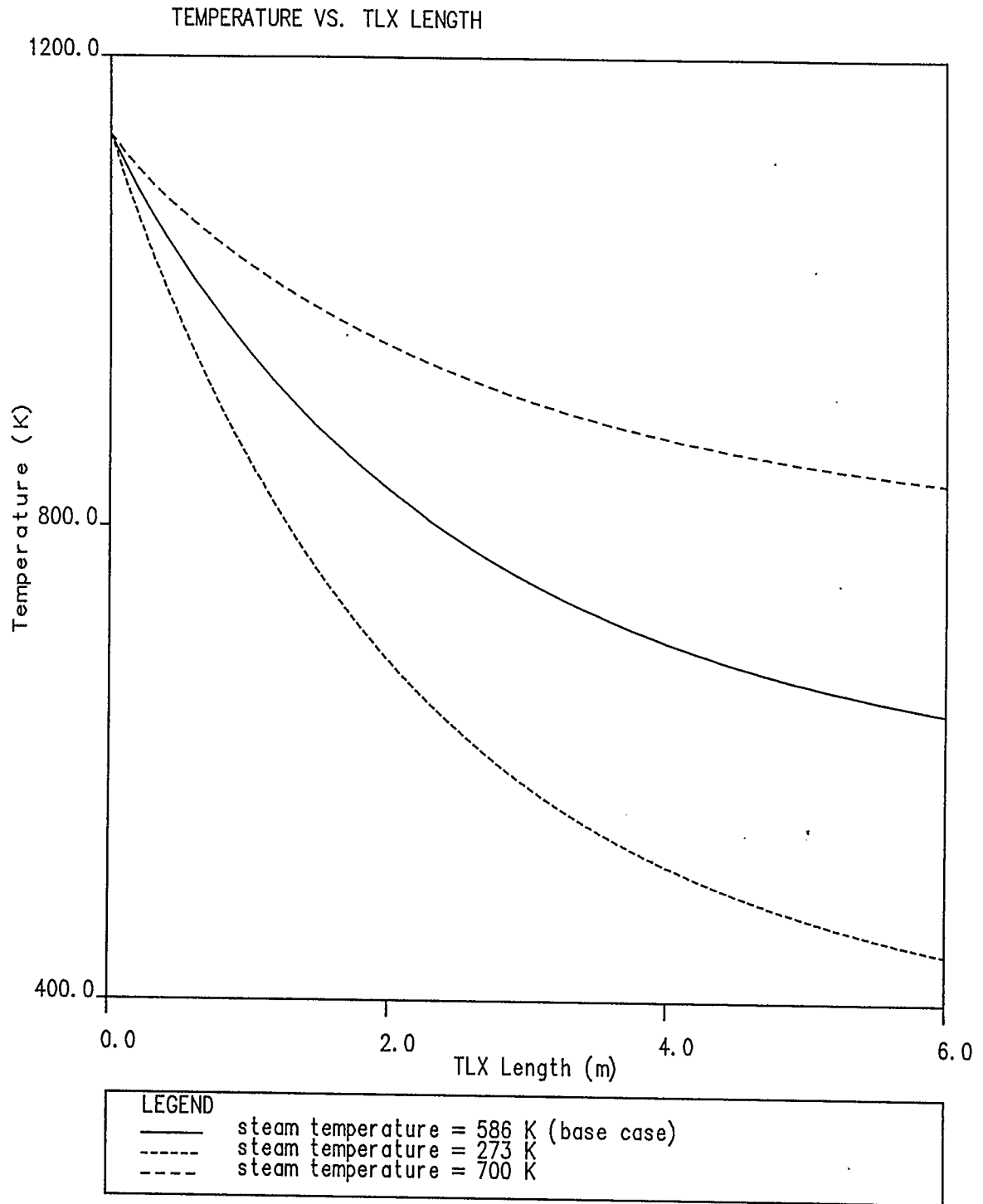


Figure 8.5.1 TLX Temperature profiles
for different shell side steam temperatures
at clean tube conditions using either coke model

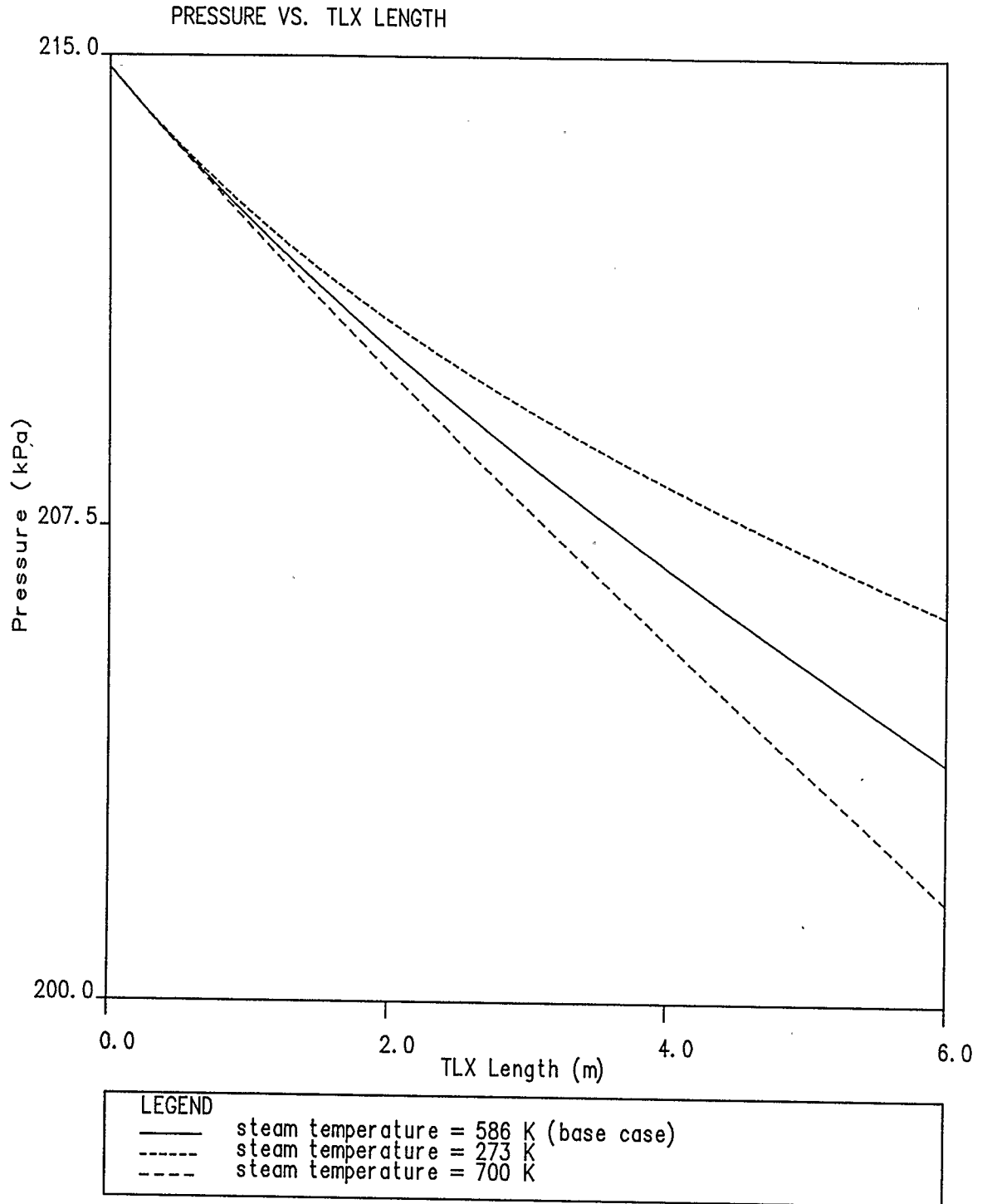


Figure 8.5.2 TLX Pressure profiles
for different shell side steam temperatures
at clean tube conditions using either coke model

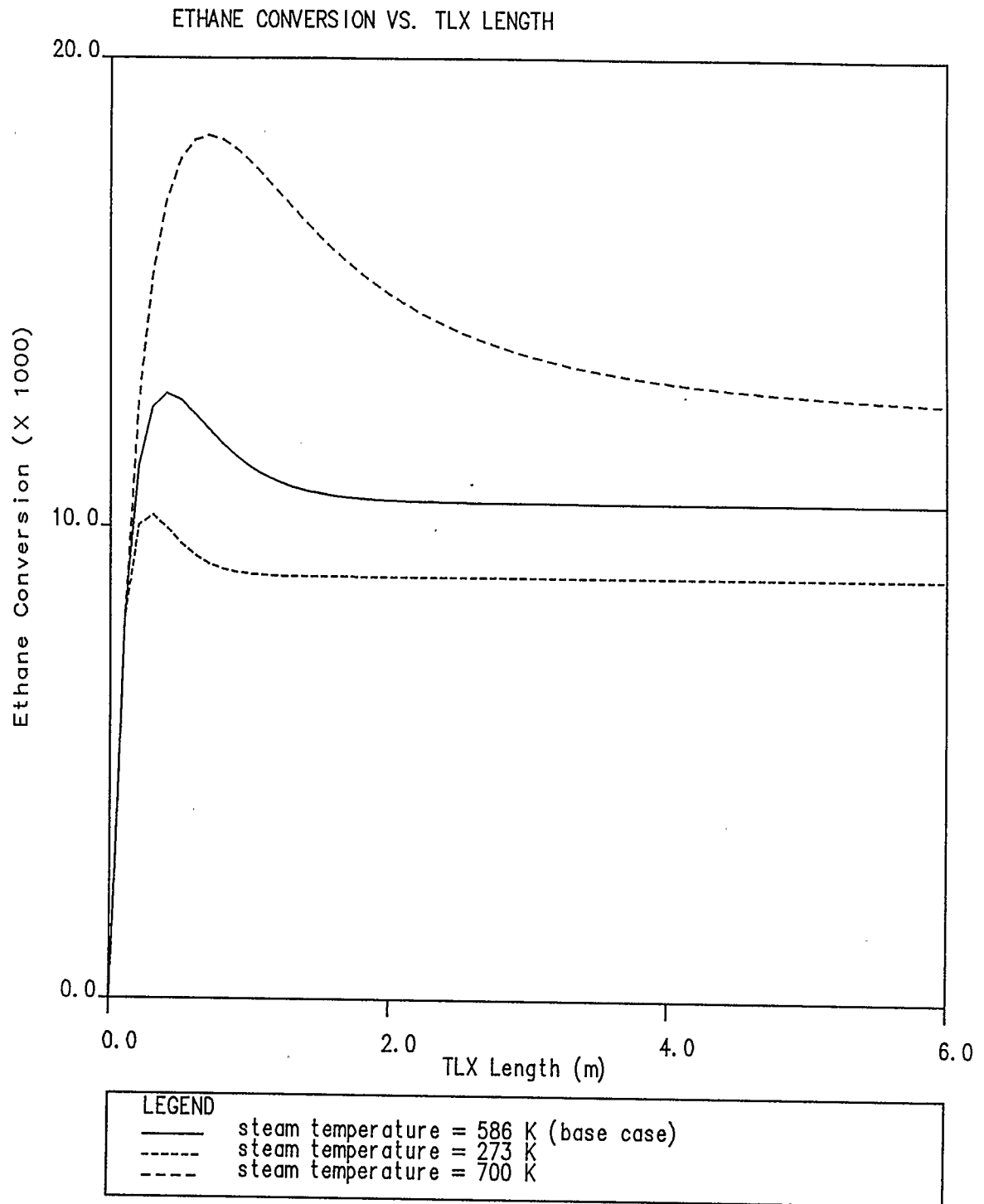


Figure 8.5.3 TLX Ethane conversion profiles for different shell side steam temperatures at clean tube conditions using either coke model

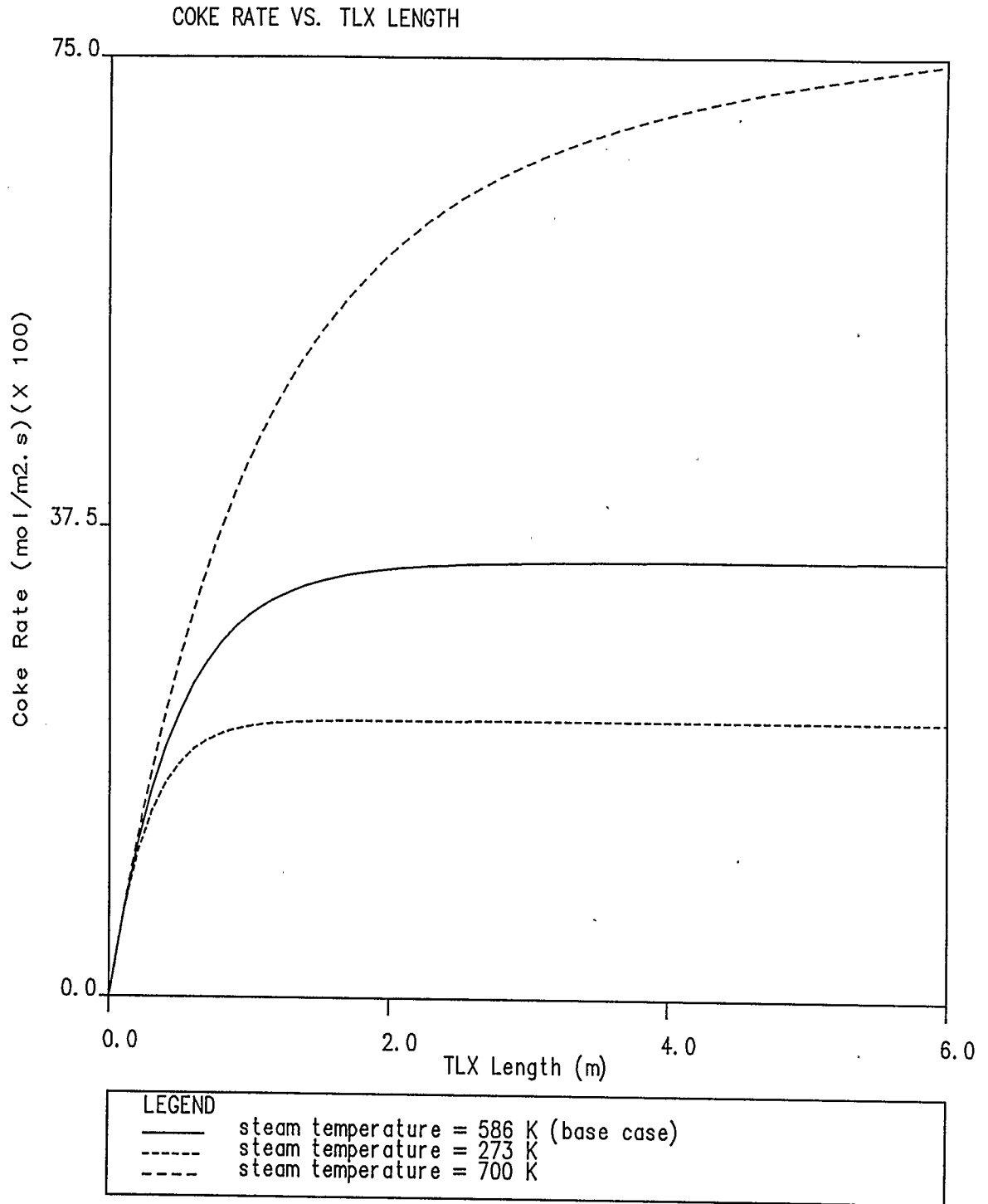


Figure 8.5.4 TLX Coke rate profiles
for different shell side steam temperatures
at clean tube conditions using either coke model

showed a strong response to the changing steam temperature. At the high end of the scale, the 700.0 K steam did not quench the reaction, as seen by the ethane conversion curve (Figure 8.5.3), which does not flatten out. With TLX outlet temperature at 838.0 K, lack of quench is expected since a process temperature below 800.0 K is required for total quench. At the other end of the scale, the low temperature steam quenched the reaction very quickly, in less than 2 metres. The final process stream temperature was also very low, 414.0 K. As in the other cases studied, conversion of ethylene and production of by-products such as coke all responded as expected (discussed in previous sections), given the temperature profiles.

The selection of steam temperature therefore will directly affect the thermal efficiency of the process, but this is offset by the lower value of the steam produced.

8.6 Effect of Steam Heat Transfer Coefficient

The steam heat transfer coefficient (h_o) cases are plotted in Figures 8.6.1 to 8.6.4. The plots show little temperature effects (Figure 8.6.1), and almost no pressure effects (Figure 8.6.2). The pressure response is expected because the pressure drop depends on mass transfer terms such as mass flux, velocities and tube diameter, not on the heat transfer terms. Only when the heat transfer effects

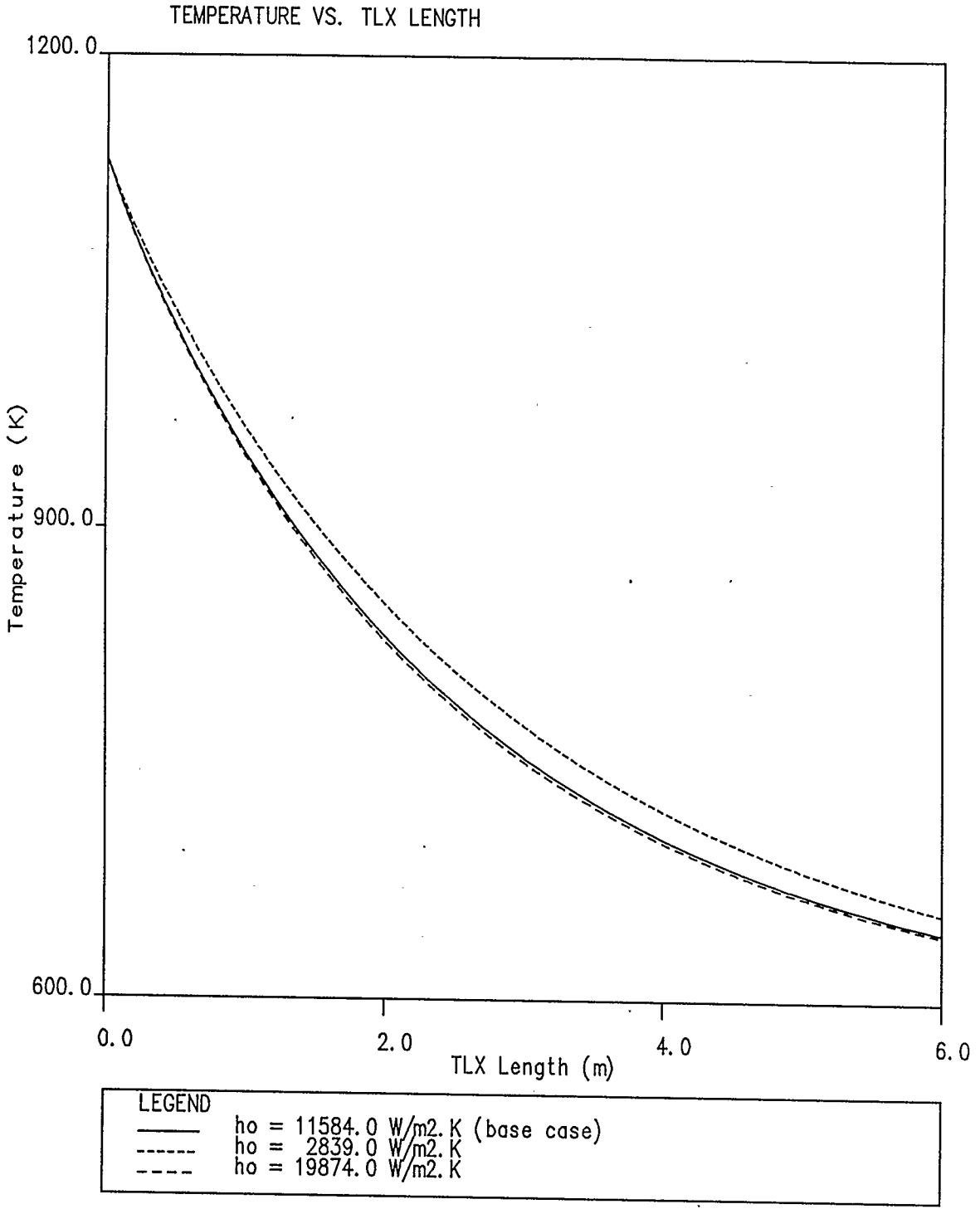


Figure 8.6.1 TLX Temperature profiles for different steam heat transfer coefficients at clean tube conditions using either coke model

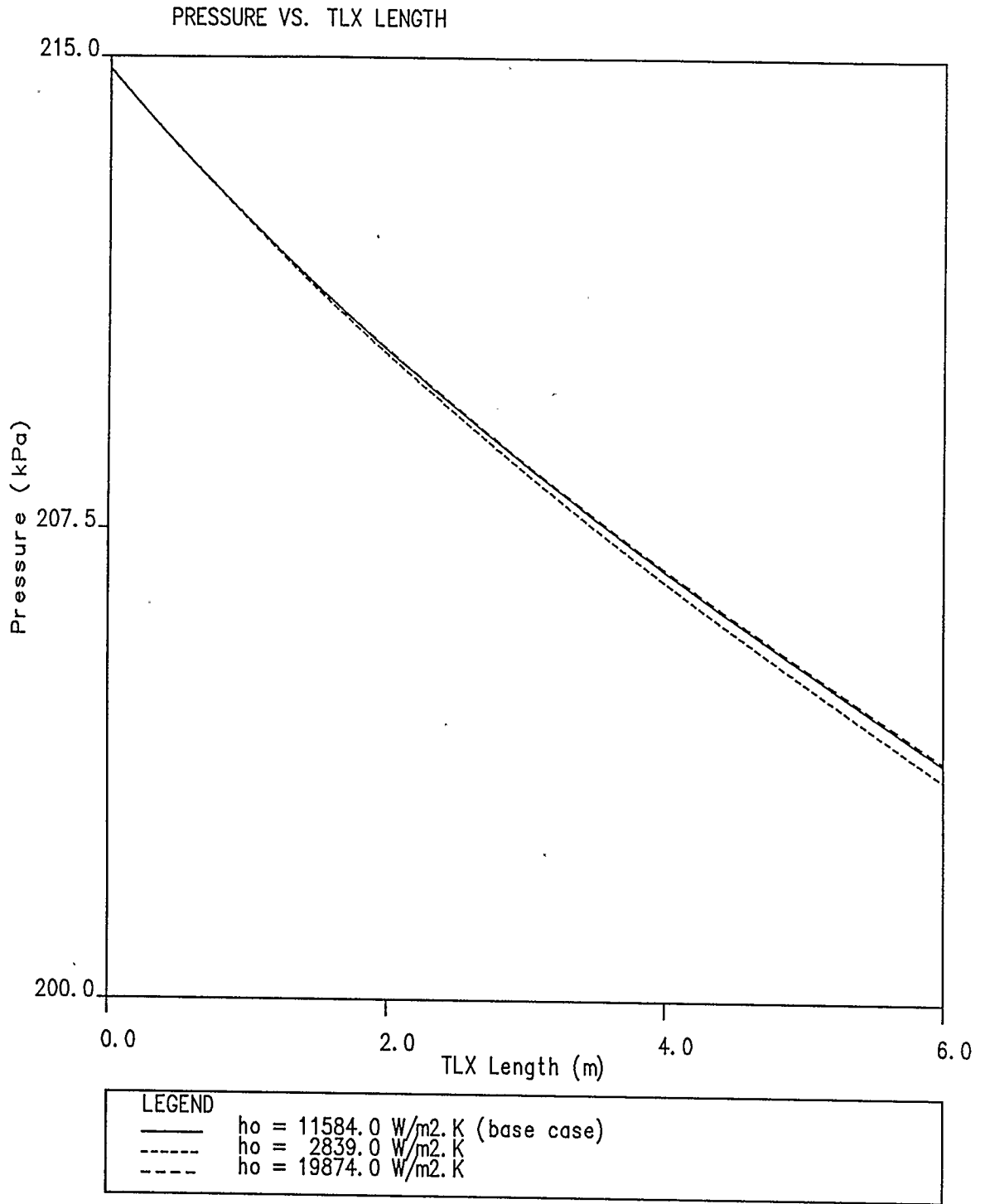


Figure 8.6.2 TLX Pressure profiles for different steam heat transfer coefficients at clean tube conditions using either coke model

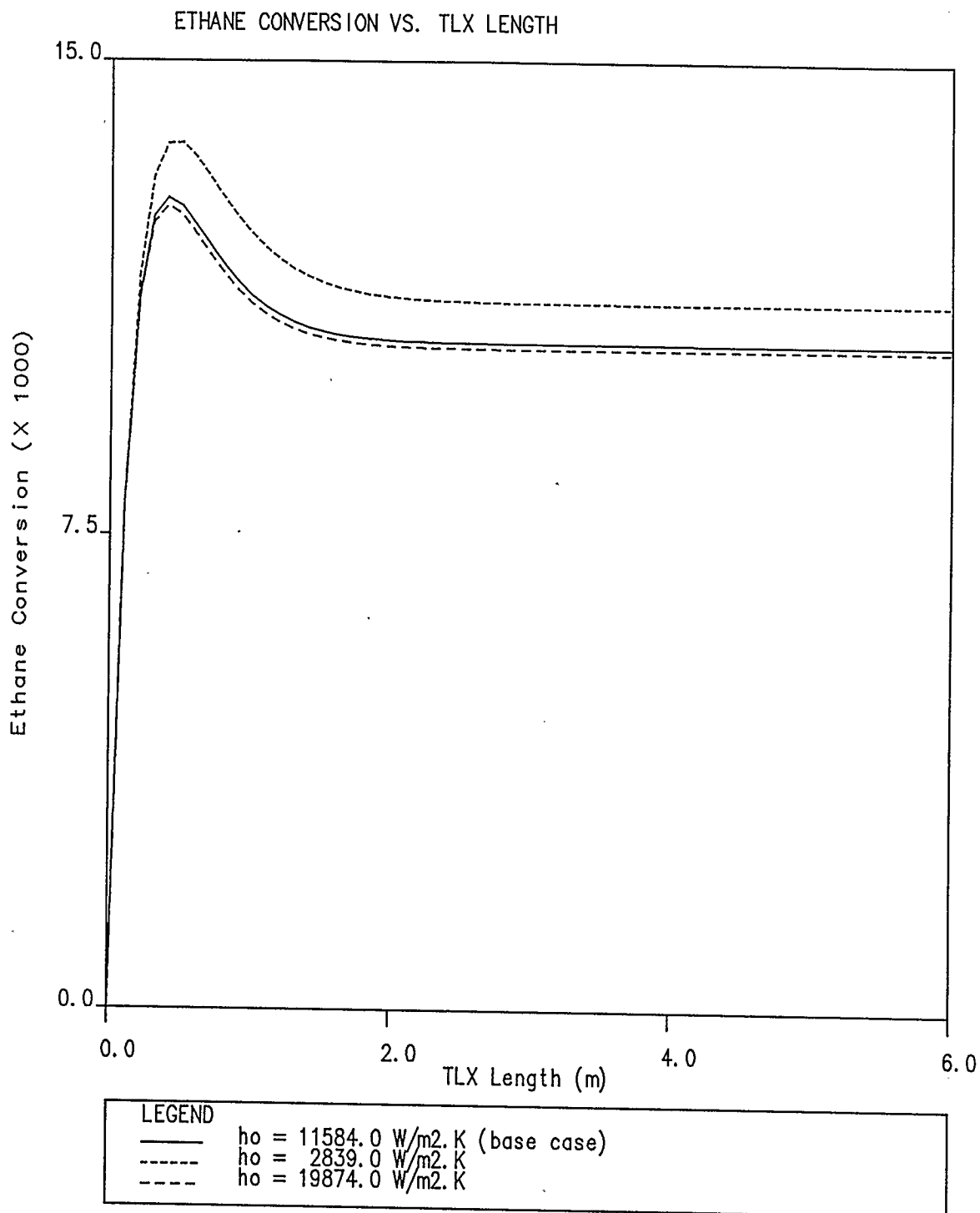


Figure 8.6.3 TLX Ethane conversion profiles for different steam heat transfer coefficients at clean tube conditions using either coke model

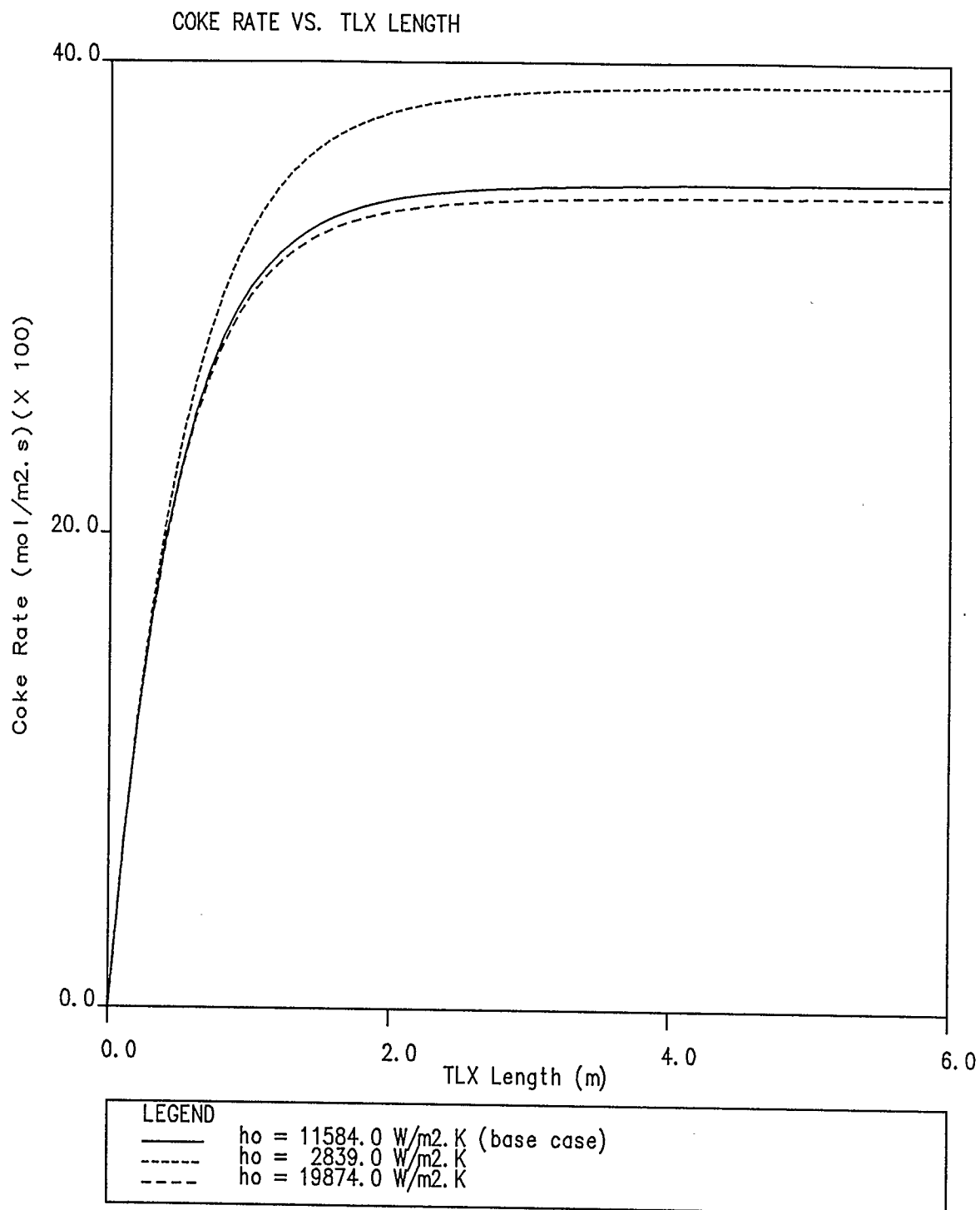


Figure 8.6.4 TLX Coke rate profiles for different steam heat transfer coefficients at clean tube conditions using either coke model

are translated into coke rate changes do they impact on the mass transfer side of the model equations. Similarly, molar flow rates are unaffected.

Ethane conversion (Figure 8.6.3) raises for lower values of the steam heat transfer coefficient and drops for higher values of steam heat transfer coefficient, but the effect is the smallest of all those studied in these parametric simulations. The coke rate curve (Figure 8.6.4) changes as the value of steam heat transfer coefficient is changed but the effect is small. These rate and conversion effects are due to the increased or decreased rate of heat exchange from the steam to the TLX tube walls produced by varying the heat transfer coefficient.

It is striking that the effect of this parameter on the temperature profile of the cooler is so low. The steam heat transfer coefficient appears to be a non sensitive parameter in this model. Because the steam heat transfer coefficient (h_o) is one of several resistance terms in the heat transfer equation, its effect on the system must be measured against other terms in the equation (Appendix C). Since the value of h_o is large compared to other heat transfer coefficients in the equation, and since the reciprocal of the coefficient is used, the effect of a large value of h_o will be overshadowed by the smaller heat transfer coefficients, such as the coke thermal conductivity.

8.7 Effect of Coke Laydown Parameter

Plots of the effects of changing the coke deposition ratio (α) are shown in Figures 8.7.1 to 8.7.5 for coke model 1 and 8.7.6 to 8.7.10 for coke model 2. This parameter is an empirical parameter introduced to the equations for coke buildup to allow the TLX designer to model the formation of gaseous coke, not all of which will deposit on the TLX tube walls. The parameter does not directly enter into any model equation except the coke thickness calculation (Appendix F), so any effects produced by varying the value of the coke deposition ratio (except coke thickness) are secondary, resulting as a consequence of the changing coke thickness on the walls of the TLX. In this sense, the coke deposition ratio can be viewed as a modification to the effect of operational time on the cooler. Changes in the system caused by a certain value of coke thickness will be the same, but will occur at later values of the total operational time as the value of α is reduced.

The plots clearly show this effect. The changes in pressure, temperature, coke rate, and ethane conversion all vary much as they did in Section 8.1, but at different rates depending on the deposition ratio used. The end result is that lower values of α would allow the TLX to be run for a much longer period of time than with the default α of 1.0

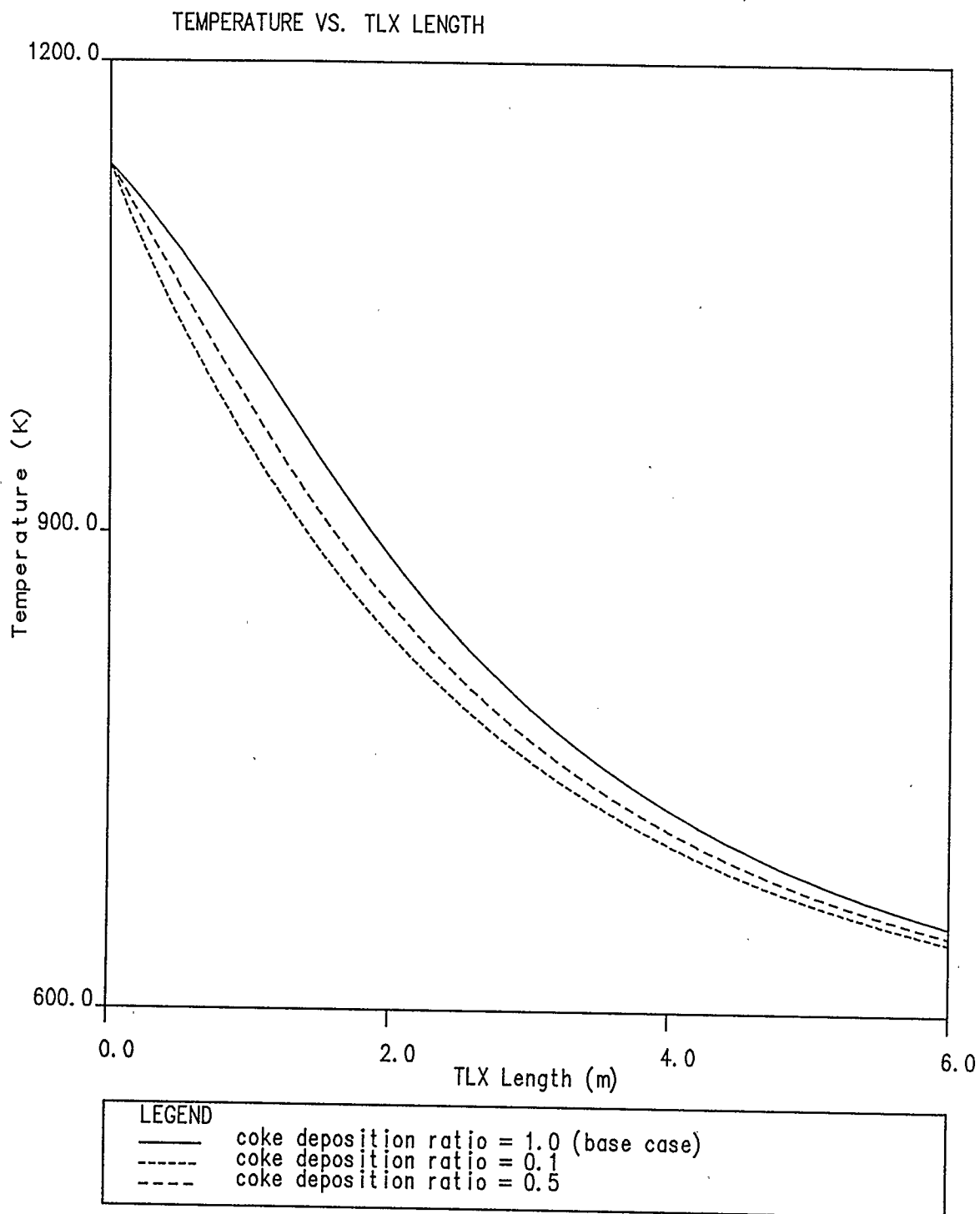


Figure 8.7.1 TLX Temperature profiles
for different coke deposition ratios at 12 days
total elapsed operational time using coke model 1

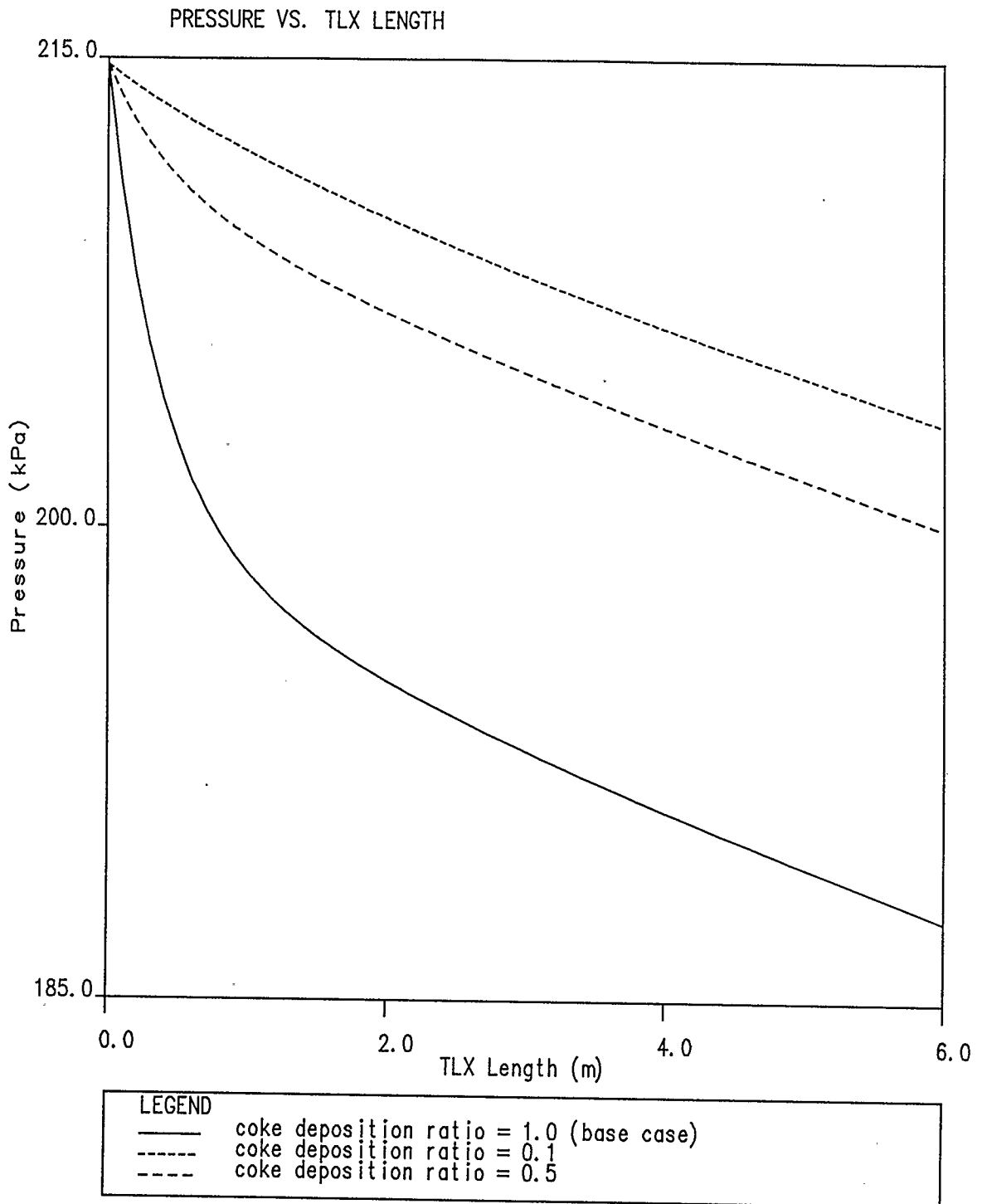


Figure 8.7.2 TLX Pressure profiles
for different coke deposition ratios at 12 days
total elapsed operational time using coke model 1

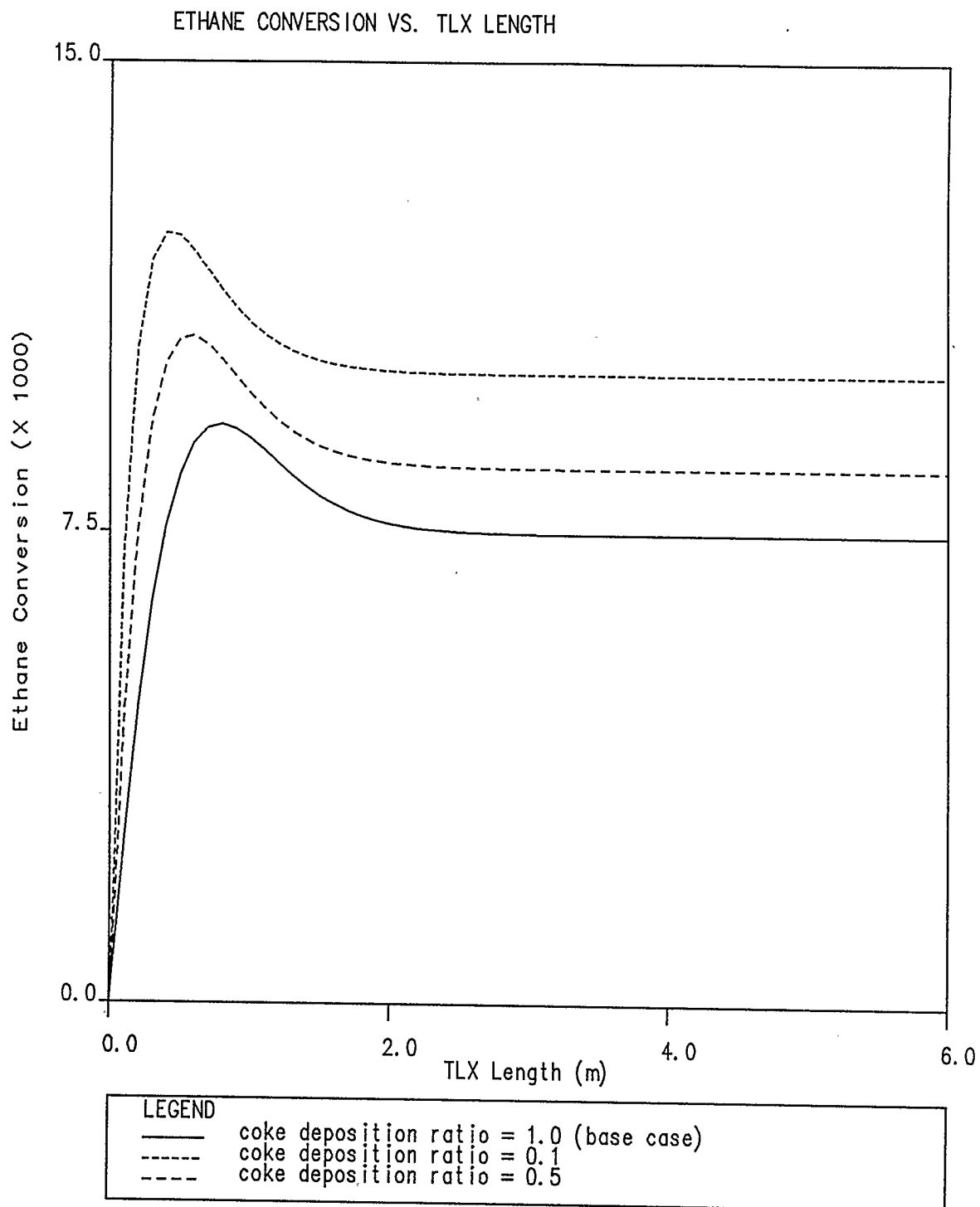


Figure 8.7.3 TLX Ethane conversion profiles for different coke deposition ratios at 12 days total elapsed operational time using coke model 1

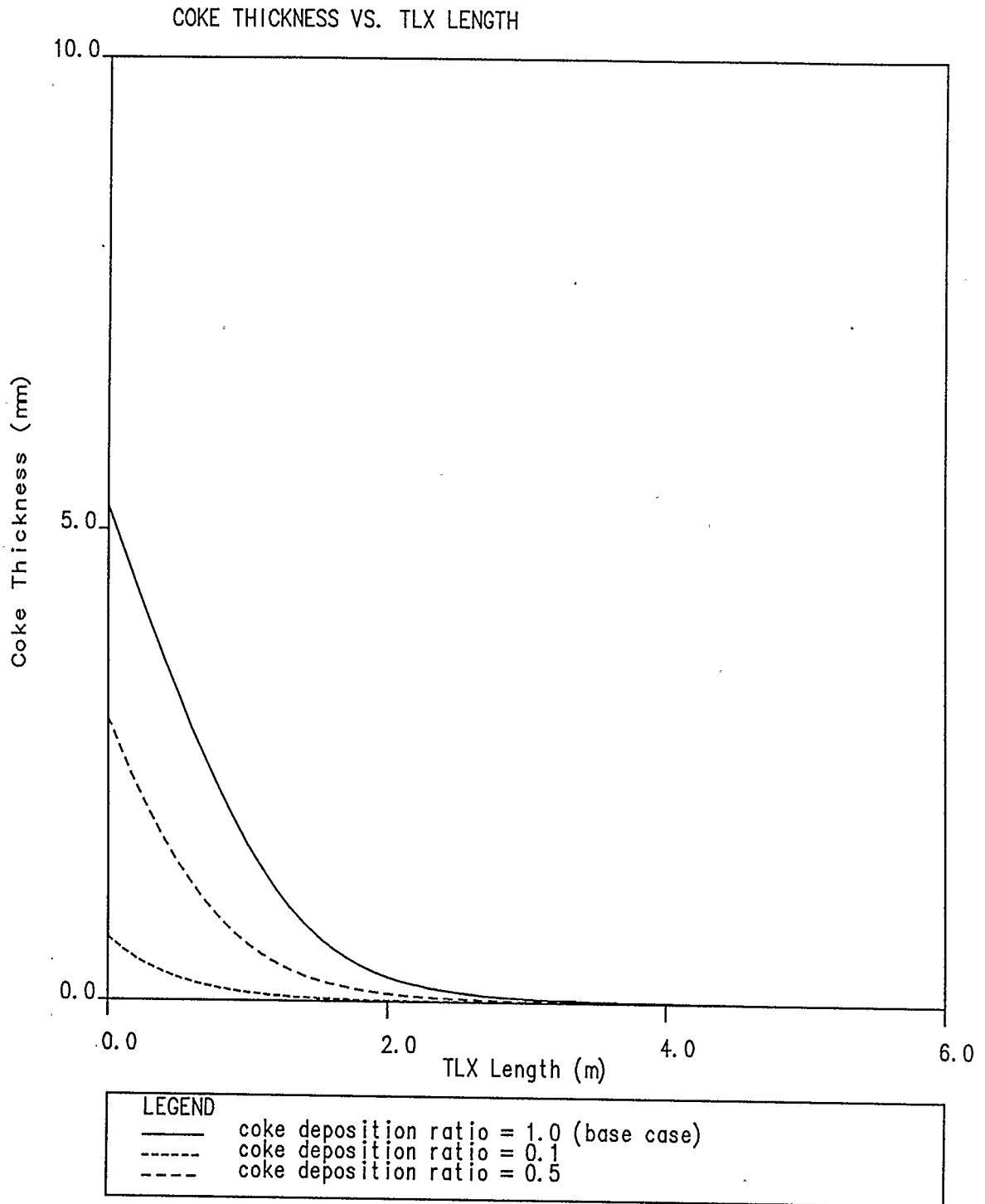


Figure 8.7.4 TLX Coke thickness profiles for different coke deposition ratios at 12 days total elapsed operational time using coke model 1

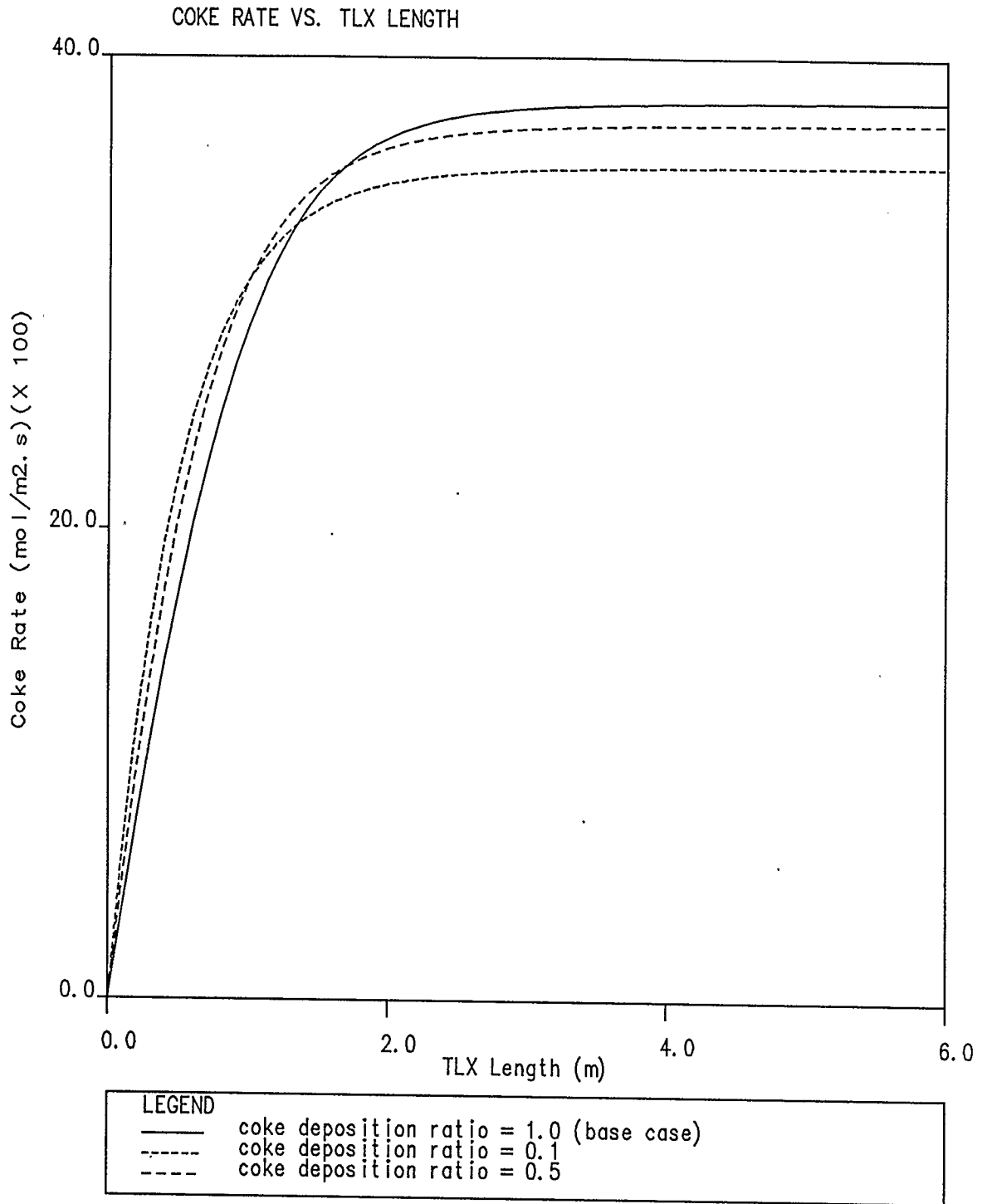


Figure 8.7.5 TLX Coke rate profiles for different coke deposition ratios at 12 days total elapsed operational time using coke model 1

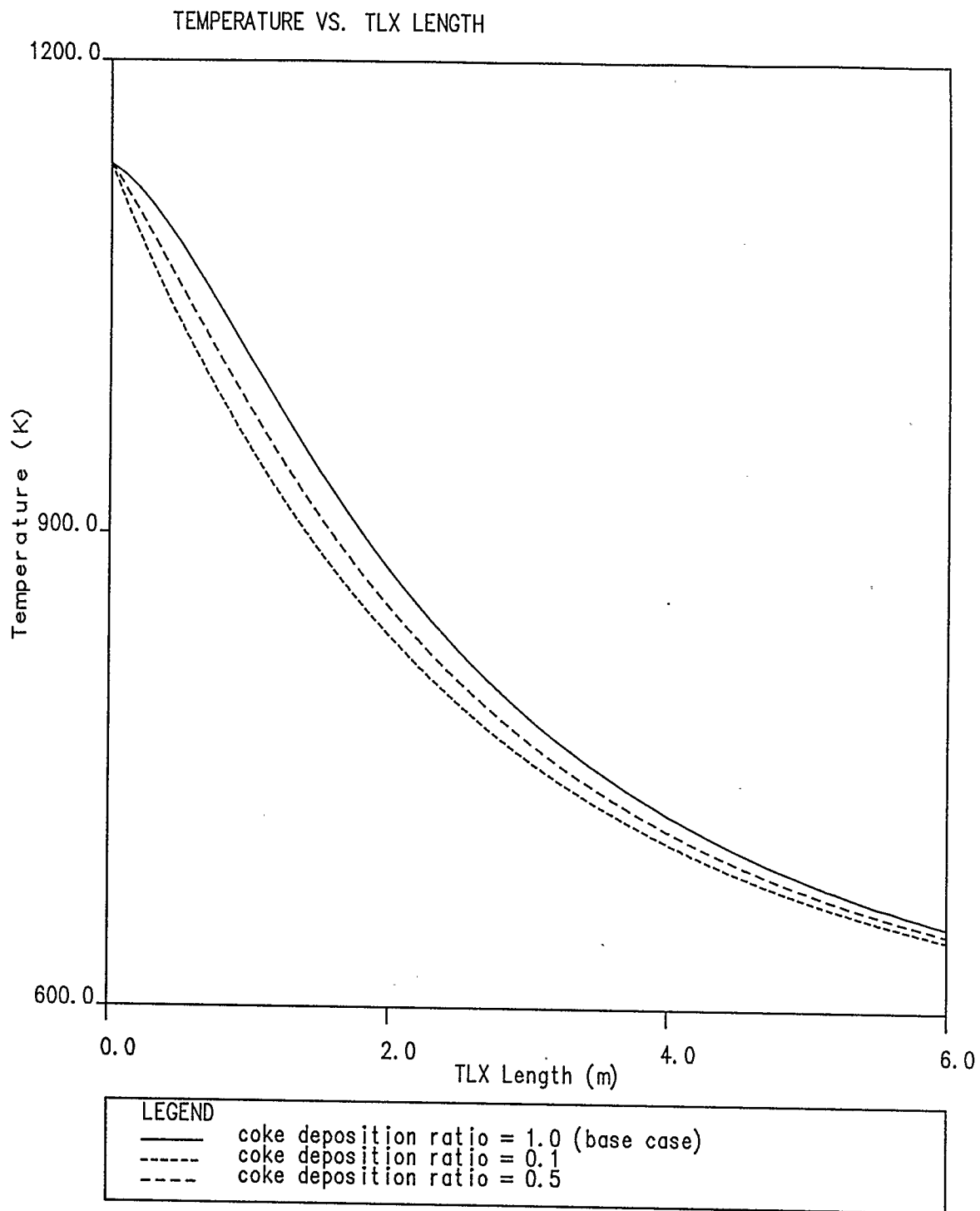


Figure 8.7.6 TLX Temperature profiles
for different coke deposition ratios at 12 days
total elapsed operational time using coke model 2

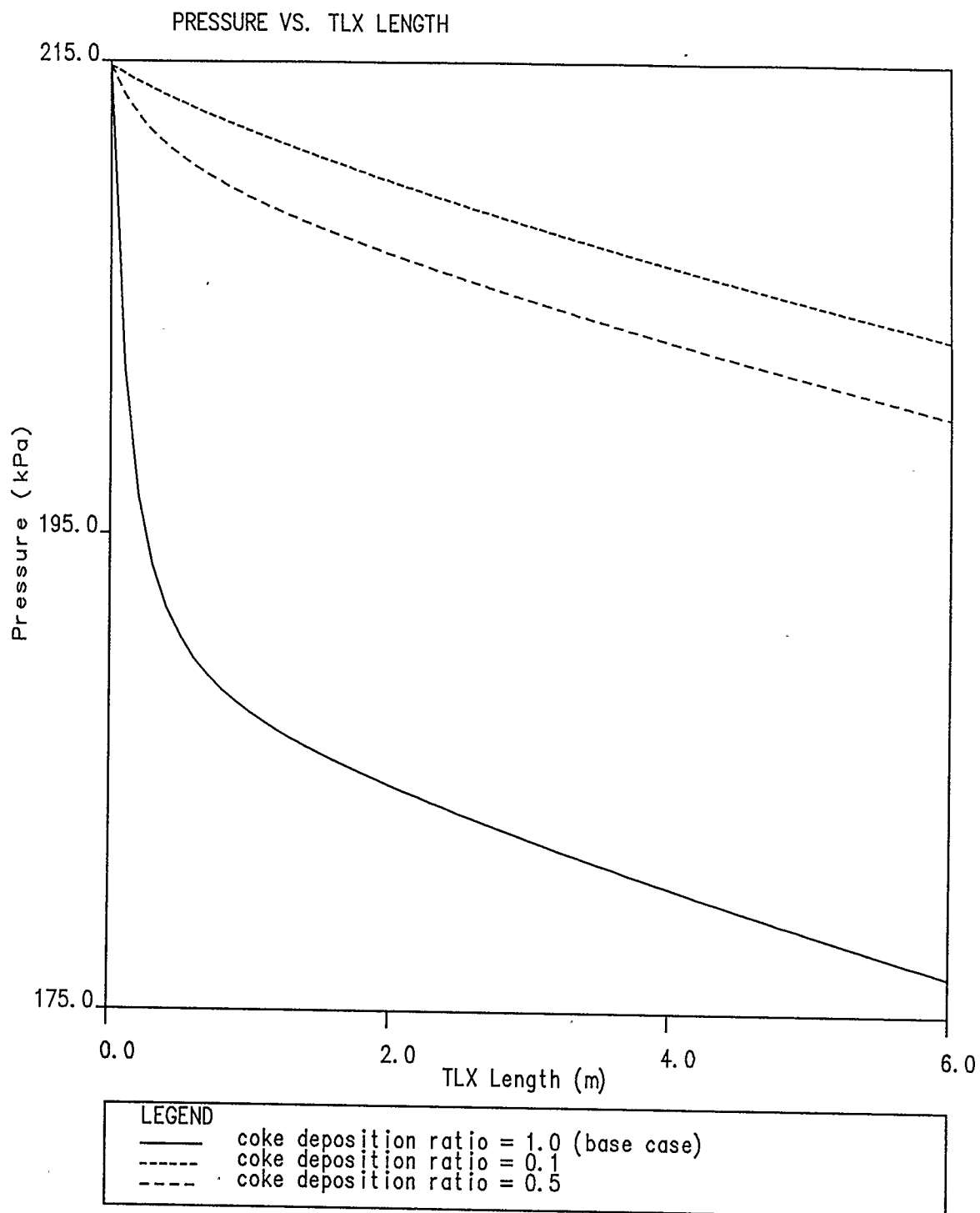


Figure 8.7.7 TLX Pressure profiles
for different coke deposition ratios at 12 days
total elapsed operational time using coke model 2

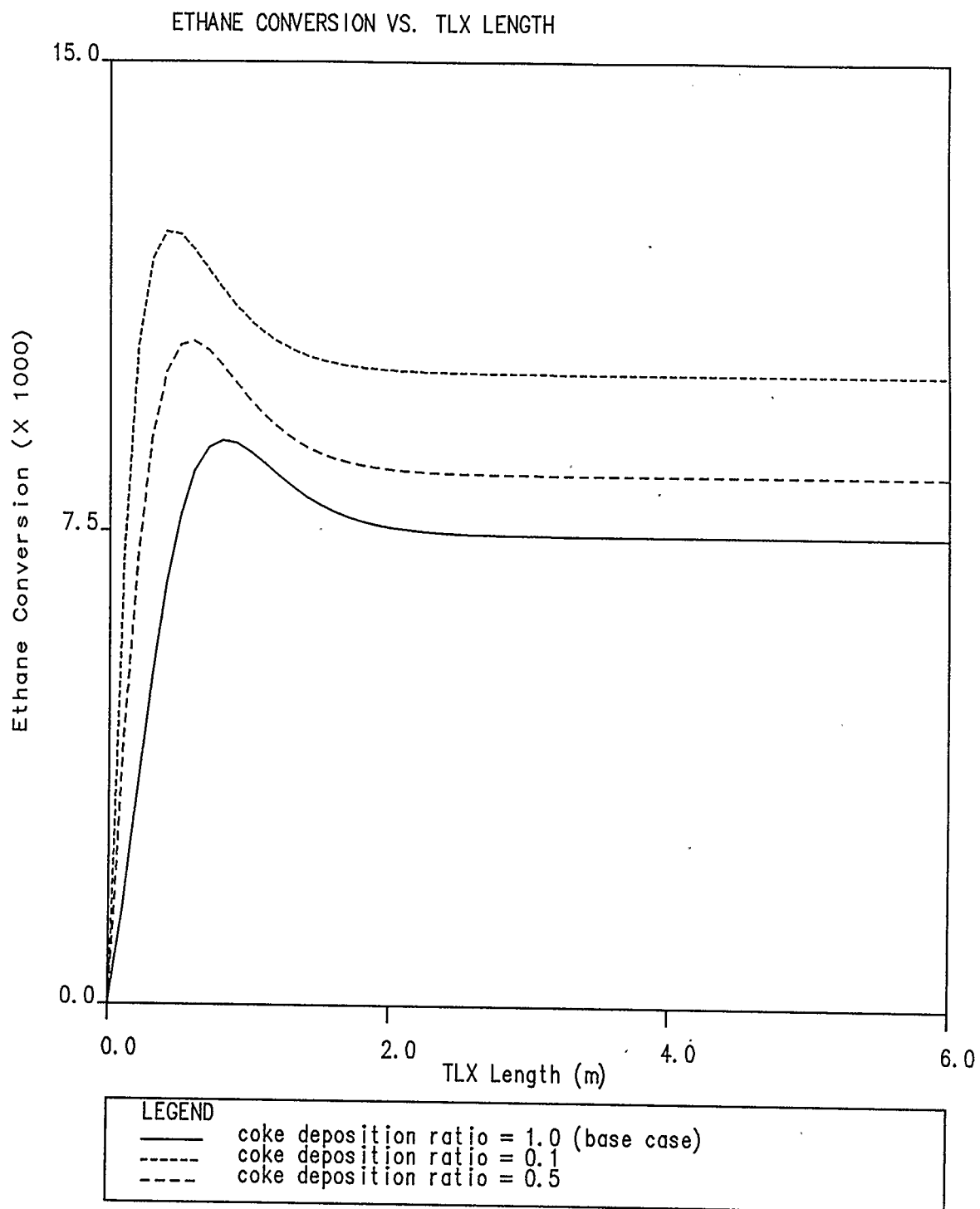


Figure 8.7.8 TLX Ethane conversion profiles for different coke deposition ratios at 12 days total elapsed operational time using coke model 2

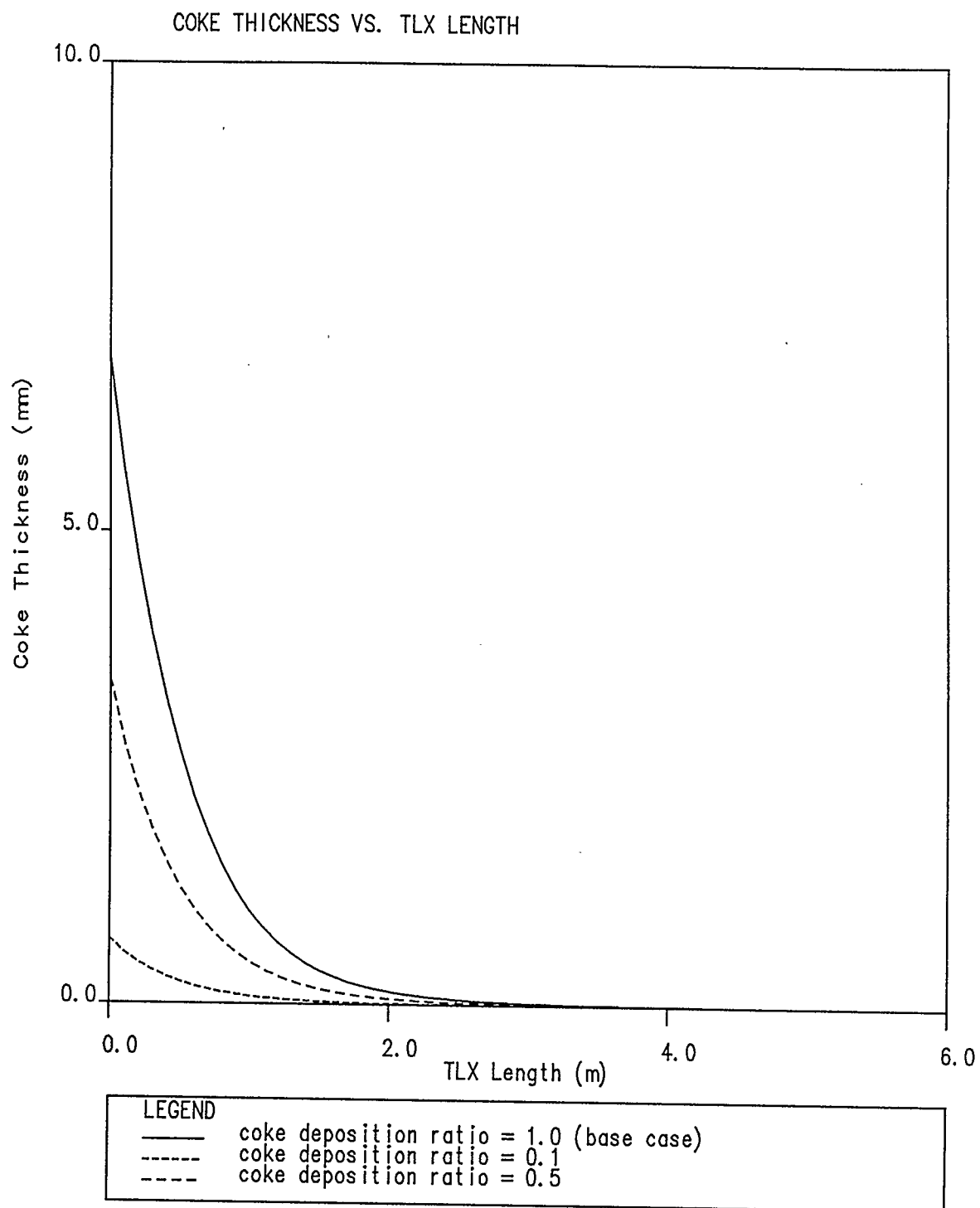


Figure 8.7.9 TLX Coke thickness profiles for different coke deposition ratios at 12 days total elapsed operational time using coke model 2

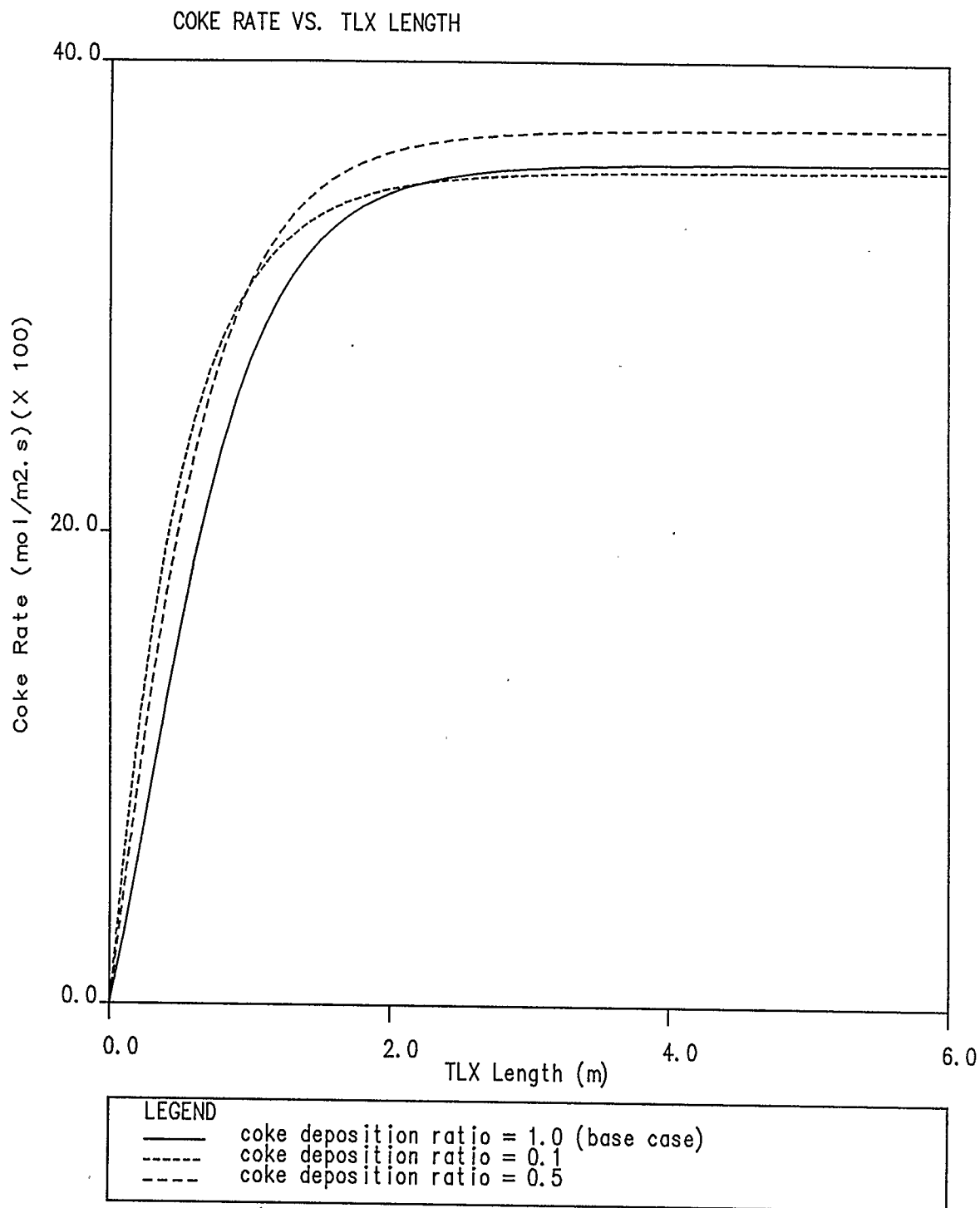


Figure 8.7.10 TLX Coke rate profiles
for different coke deposition ratios at 12 days
total elapsed operational time using coke model 2

(all coke formed will deposit on the walls).

The relationship between all of the variables and the coke deposition ratio shows a linear variation, except for the pressure drop, which is quadratic, as has been discussed in Section 8.1. Thus it is possible to estimate the total possible run time of a TLX for any value of the deposition ratio given the total run time of a run using a different value of α .

8.8 Effect of Coke Thermal Conductivity

Plots showing the effect of varying the thermal conductivity of coke (k_{ck}) are presented in Figures 8.8.1 to 8.8.5 for coke model 1 and Figures 8.8.6 to 8.8.10 for coke model 2. Changing the coke thermal conductivity by an order of magnitude has a considerable effect on the other variables, especially after coke is allowed to build on the walls for some days.

Increasing the value of k_{ck} has a small effect on the simulation results, while decreasing the value of k_{ck} has a much larger effect. This is because the normal value of k_{ck} represents a small resistance in the heat transfer equation compared to all of the resistance terms except the steam heat transfer coefficient, h_o (Section 8.6). Increasing k_{ck} reduces this thermal resistance and so decreases its effect further. Decreasing the value of k_{ck} has a larger effect on

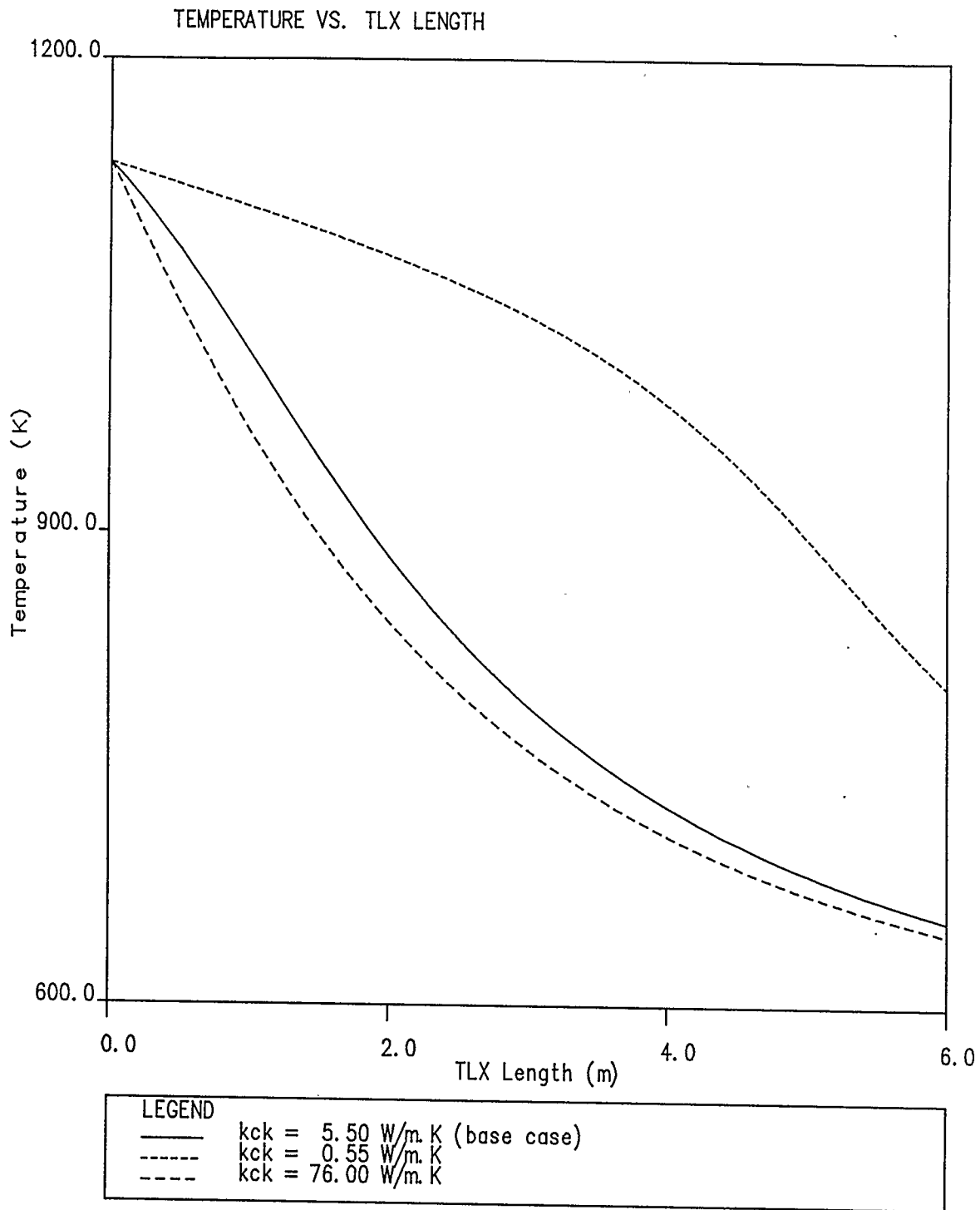


Figure 8.8.1 TLX Temperature profiles for different coke thermal conductivities at 12 days total elapsed time using coke model 1

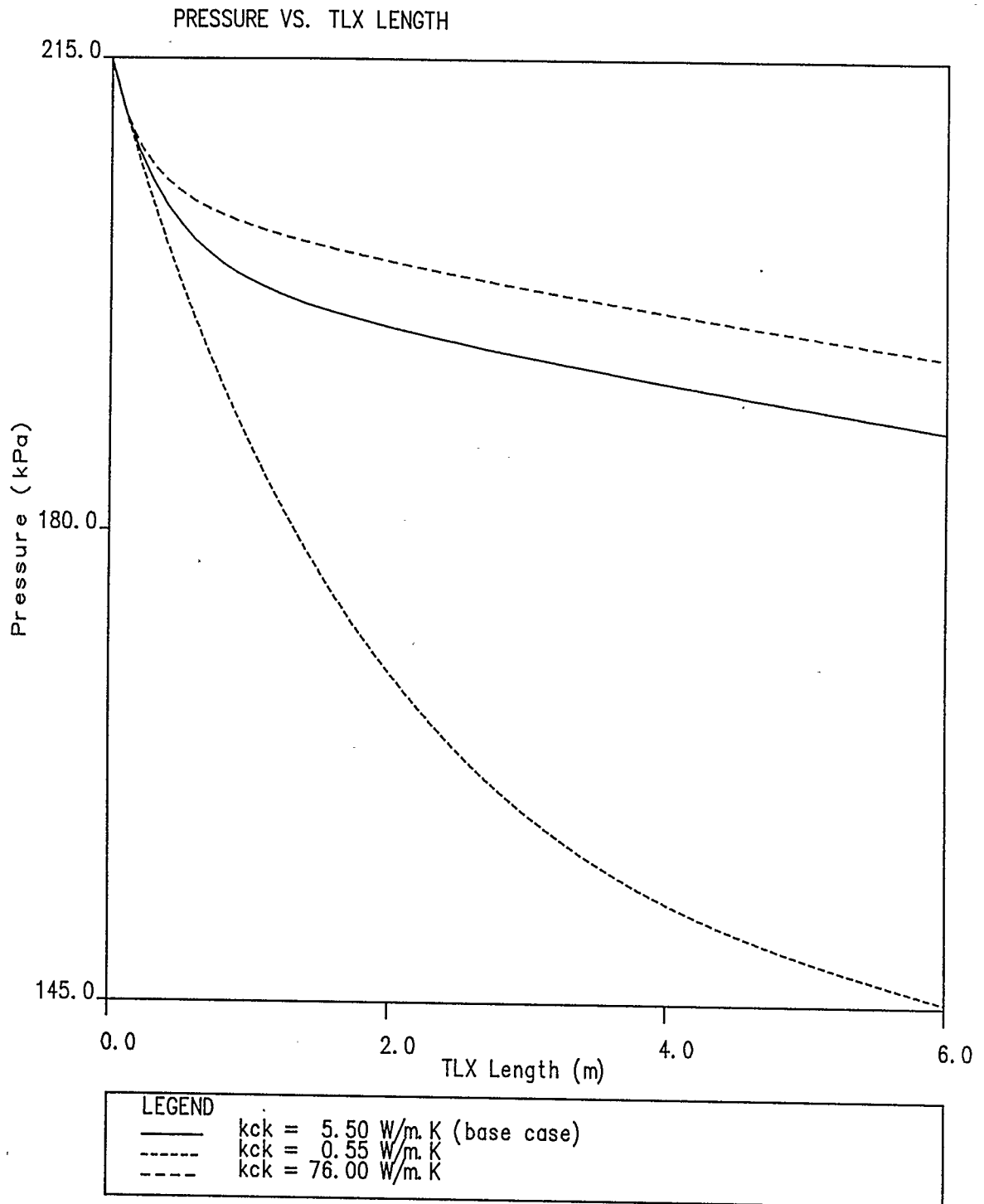


Figure 8.8.2 TLX Pressure profiles
for different coke thermal conductivities at
12 days total elapsed time using coke model 1

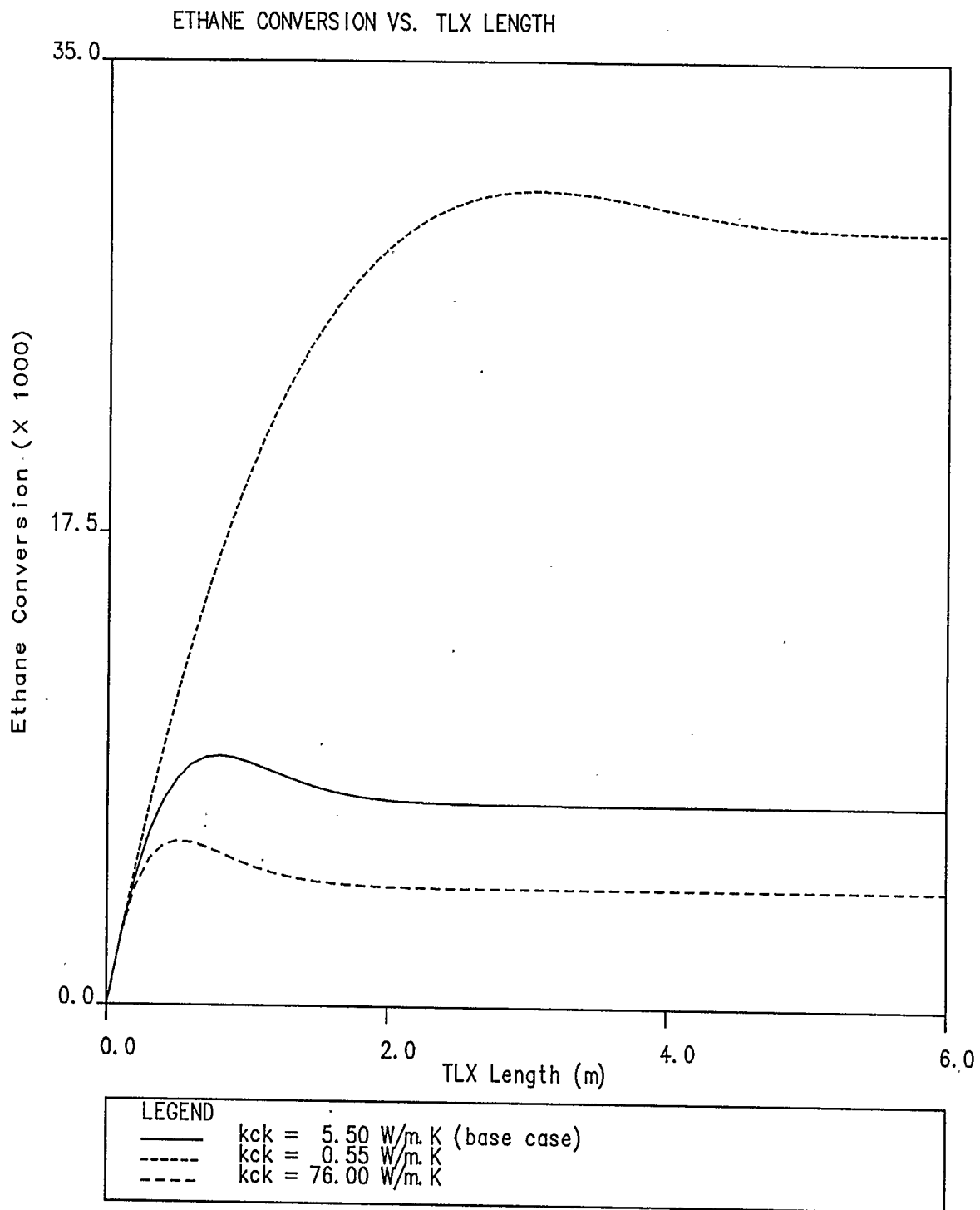


Figure 8.8.3 TLX Ethane conversion profiles for different coke thermal conductivities at 12 days total elapsed time using coke model 1

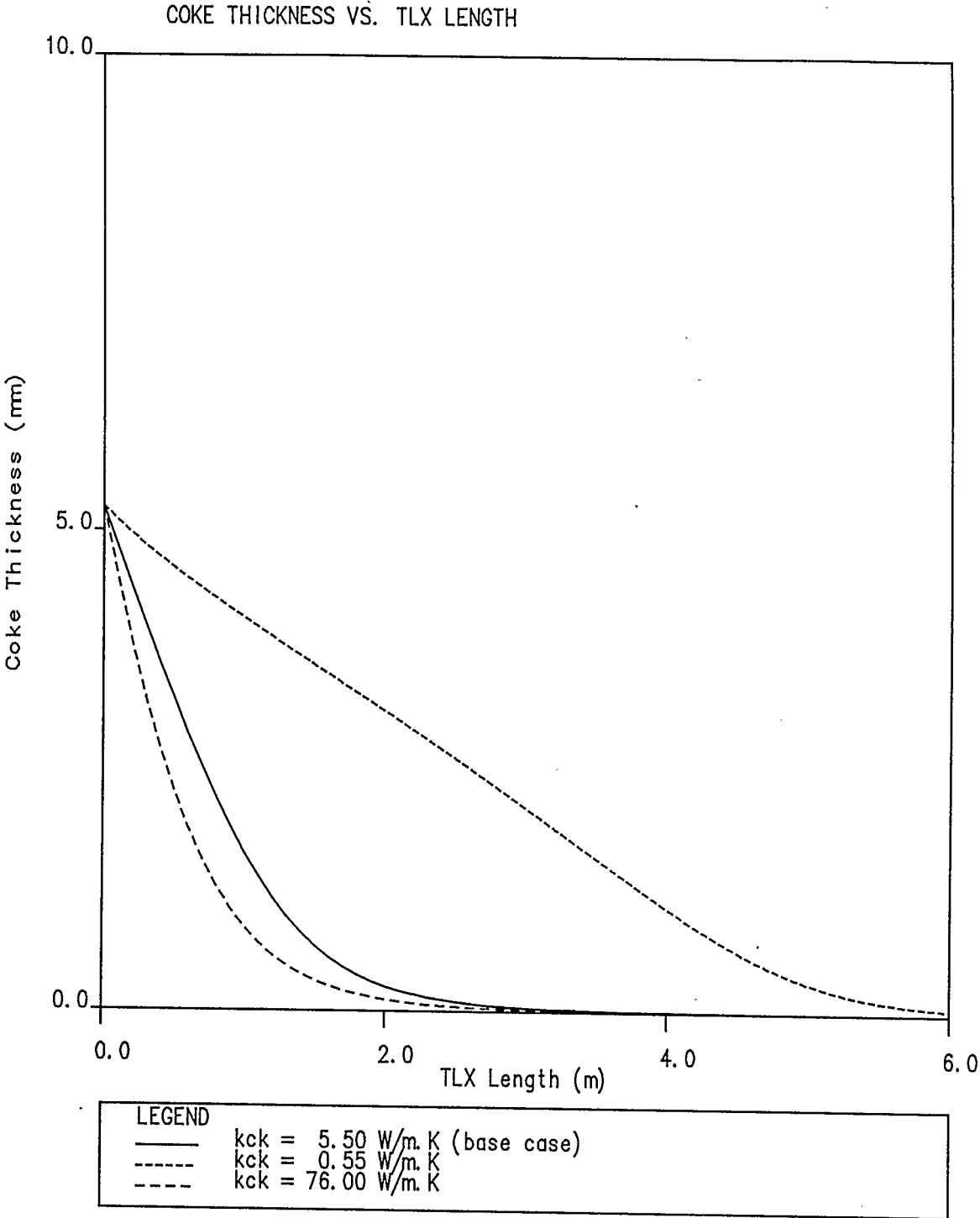


Figure 8.8.4 TLX Coke thickness profiles for different coke thermal conductivities at 12 days total elapsed time using coke model 1

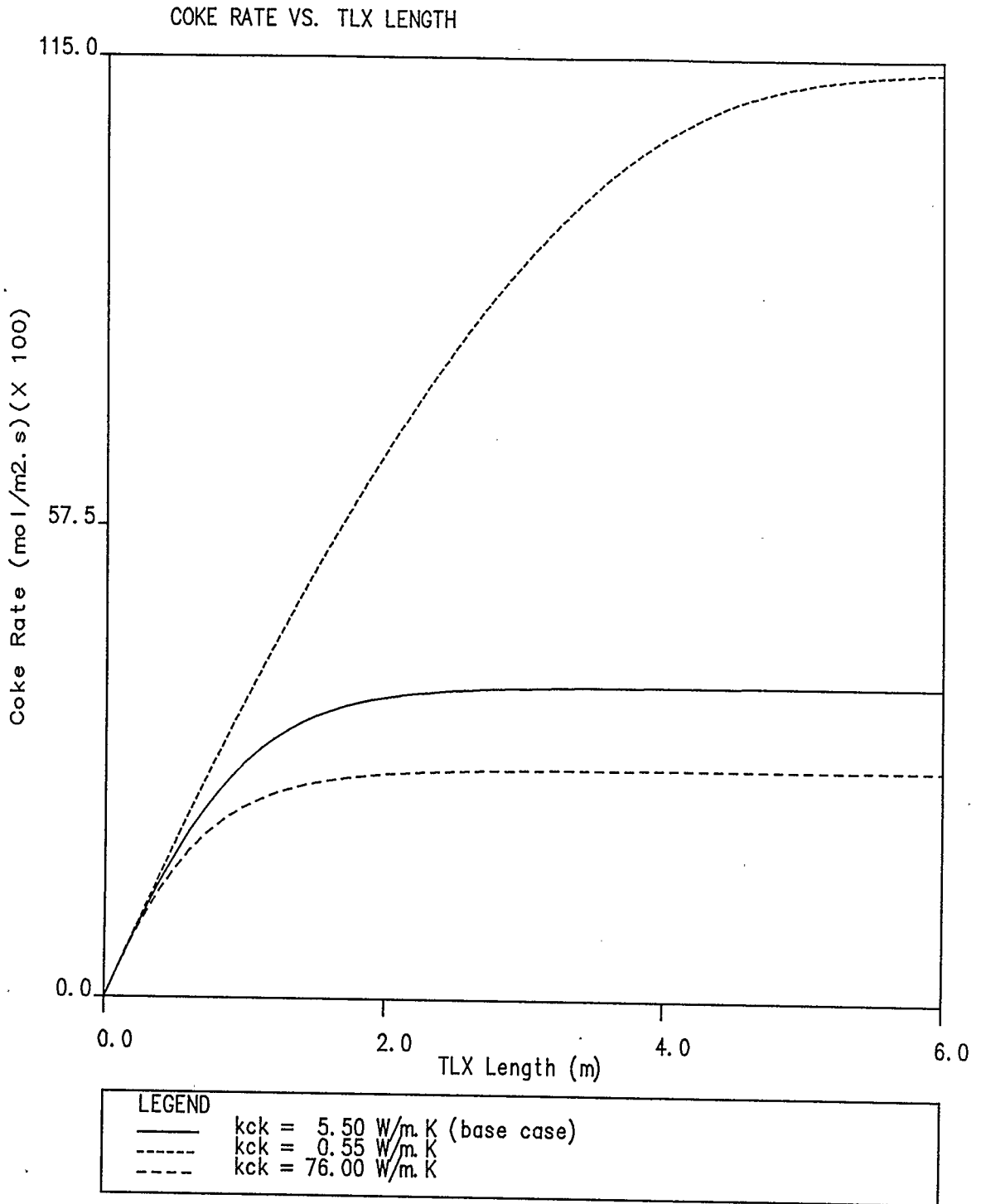


Figure 8.8.5 TLX Coke rate profiles for different coke thermal conductivities at 12 days total elapsed time using coke model 1

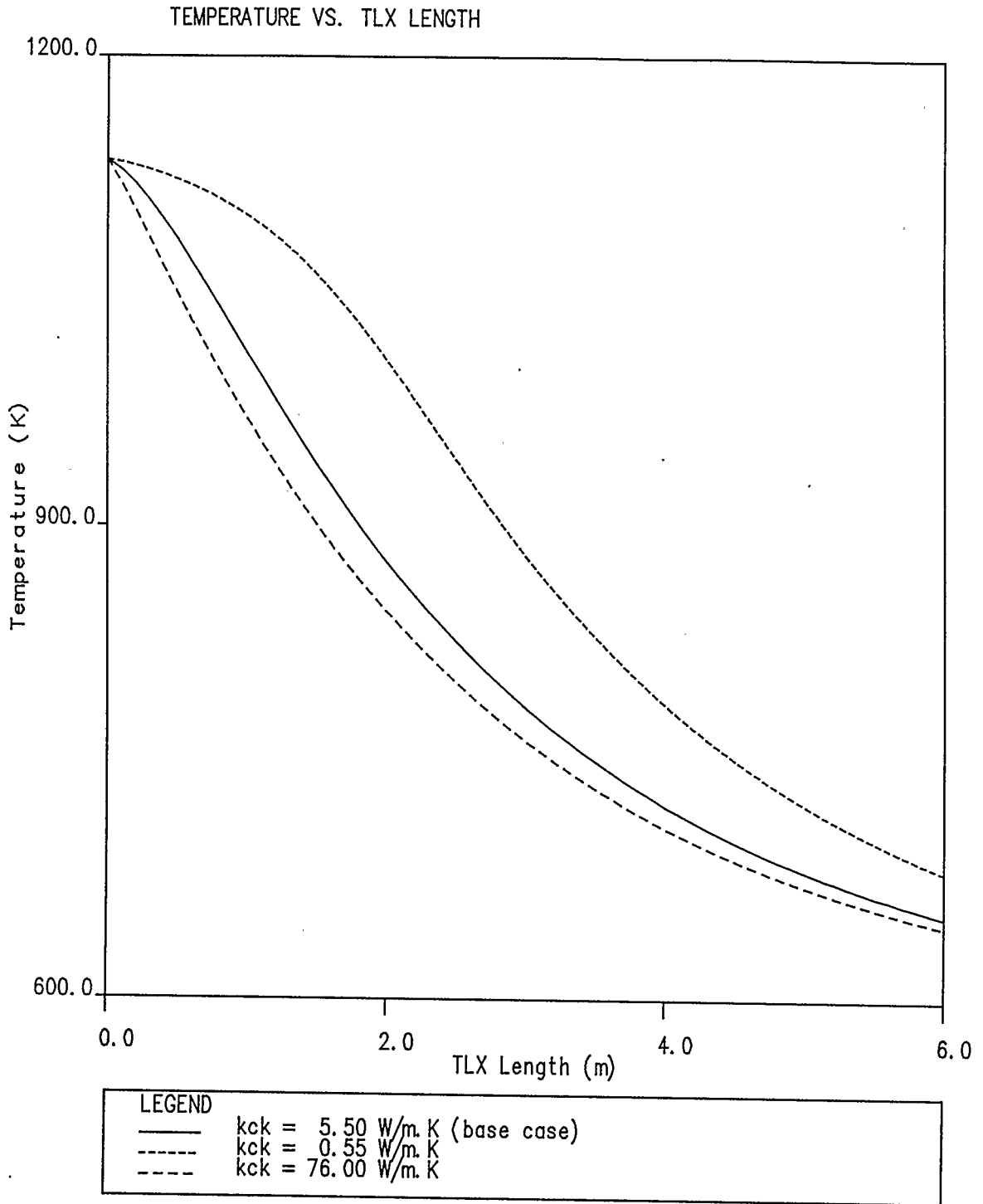


Figure 8.8.6 TLX Temperature profiles for different coke thermal conductivities at 12 days total elapsed time using coke model 2

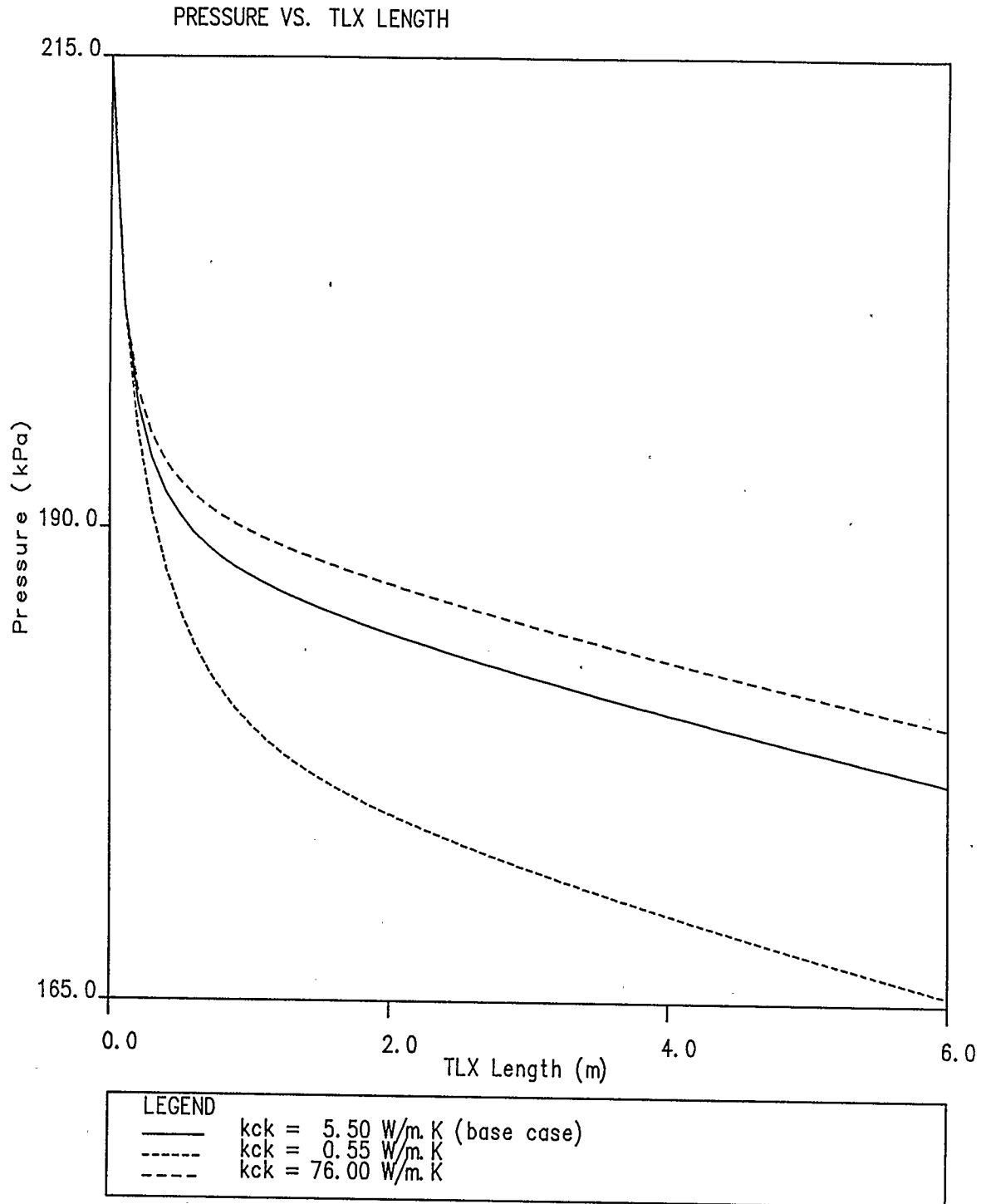


Figure 8.8.7 TLX Pressure profiles
for different coke thermal conductivities at
12 days total elapsed time using coke model 2

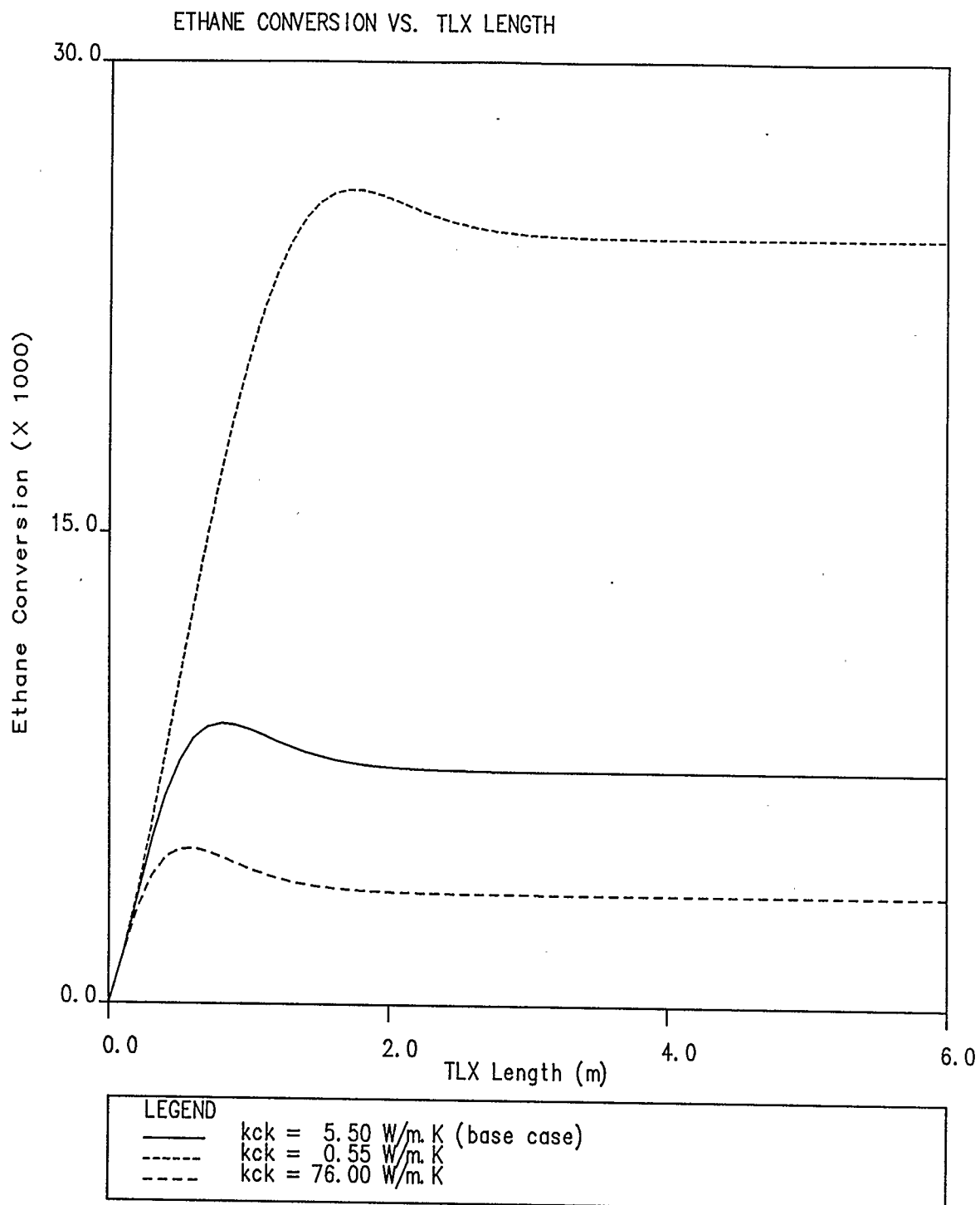


Figure 8.8.8 TLX Ethane conversion profiles for different coke thermal conductivities at 12 days total elapsed time using coke model 2

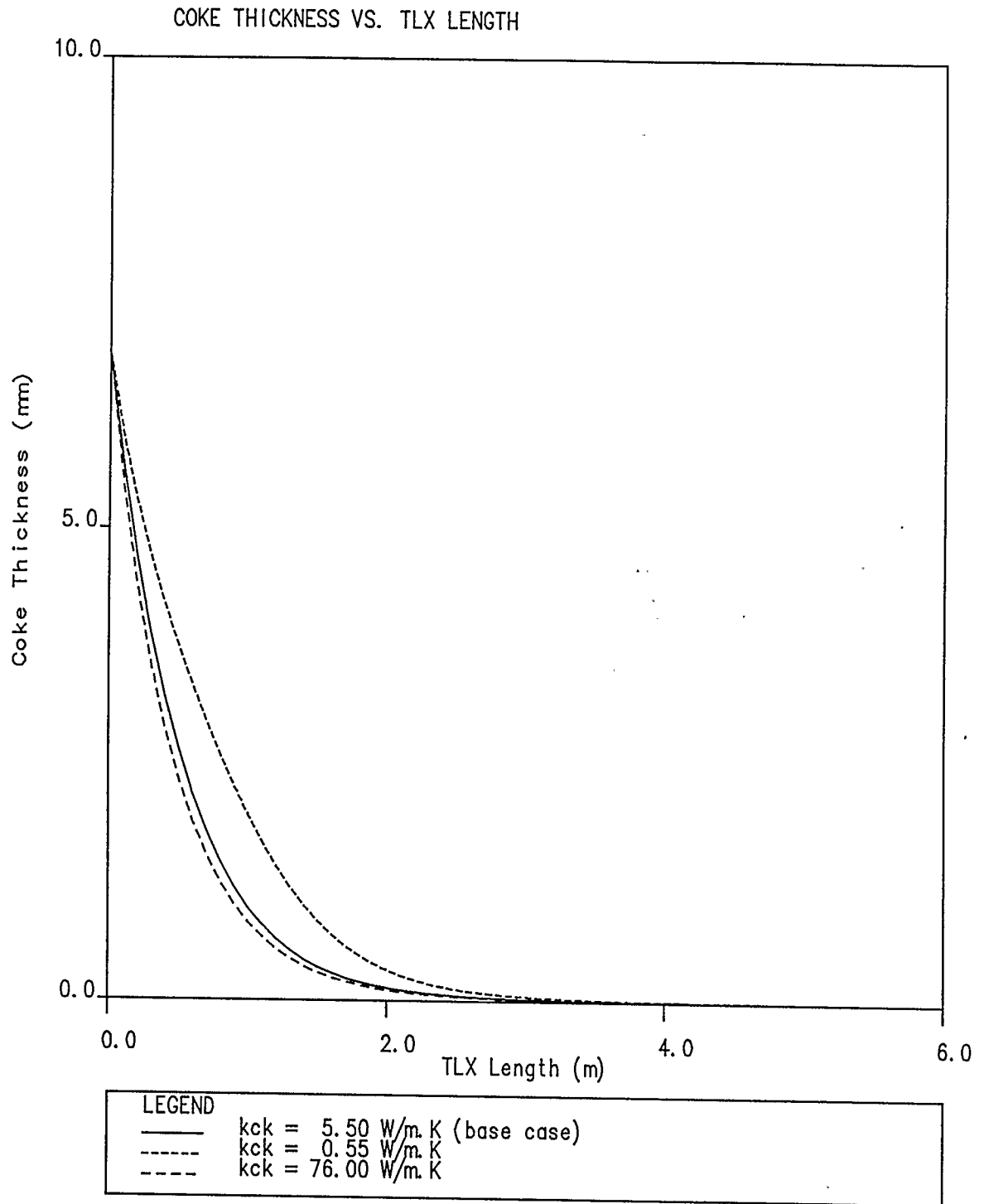


Figure 8.8.9 TLX Coke thickness profiles for different coke thermal conductivities at 12 days total elapsed time using coke model 2

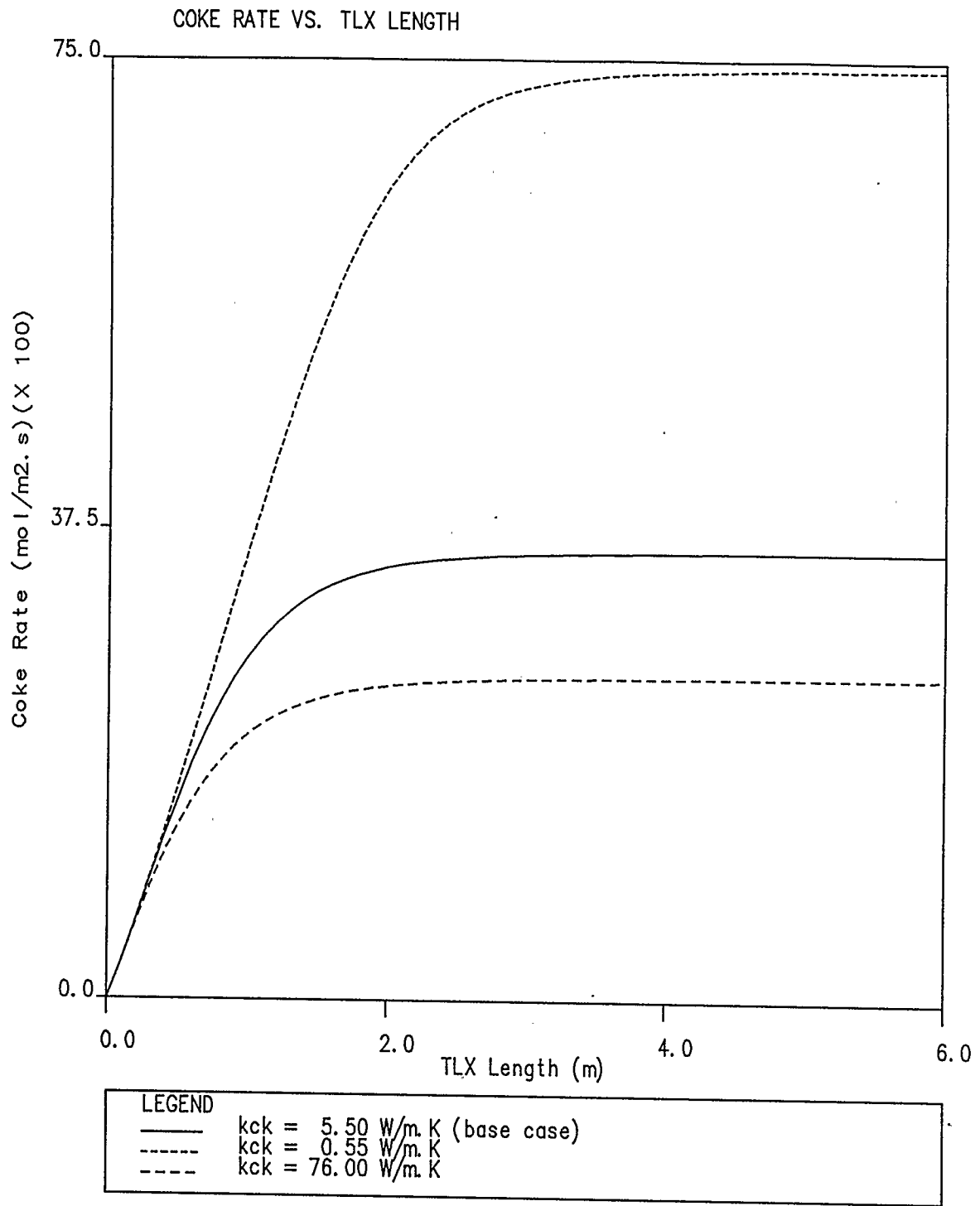


Figure 8.8.10 TLX Coke rate profiles for different coke thermal conductivities at 12 days total elapsed time using coke model 2

the system for the same reason. Decreasing k_{ck} increases the coke thermal resistance, making it the dominant resistance in the equation, reducing the transfer of heat from the process gases to the steam. The heat balance showing these thermal resistances is presented in Appendix C.

When k_{ck} is reduced by a factor of ten, corresponding to a very good insulating coke such as the amorphous coke, the reaction is not quenched until the very end of the TLX (final exit temperature = 800.0 K) for coke model 1 (Figure 8.8.1). As a result, ethane conversion is higher (Figures 8.8.3 and 8.8.6), but so is by-product formation as evidenced by the larger local maximum in the ethane conversion curves. The formation of coke is also greater (Figures 8.8.4 and 8.8.9). With increased coke formation (and deposition due to the default $\alpha = 1.0$) comes a larger pressure drop (Figures 8.8.2 and 8.8.7).

This case shows the importance of correct characterization of the coke, as a quench cooler producing more amorphous coke (lower k_{ck}) would have a lower thermal efficiency than a quench cooler with less amorphous coke.

8.9 Discussion - Coke Parameters

The coke parameters changed in this work are the coke thermal conductivity (k_{ck}) and the coke deposition ratio (α). Although the theory underlying the quantitative

selection of both parameters is still rudimentary, both can be used to effectively model an existing TLX, whether in a pilot plant, laboratory, or industrial setting. Having adjusted the values of k_{ck} and α to successfully match the performance of an existing model, the parameters can be very useful in describing what must be occurring in the TLX to produce the match. In such an application, these parameters become very valuable to a designer, both for further case studies on an existing cooler, and for discussions pertaining to the apparent mechanisms of coke production working in that particular TLX. While this information will not help greatly in the design of a new quench cooler (unless it conforms closely to a working, modelled TLX), the information is useful if ways are being sought to reduce the formation of coke in the currently operating TLX.

The value of α tells the simulation user how much of the coke appears to be produced in the gas stream and not deposited on the tube walls, and how much is produced or deposited on the tube walls. The parameter α cannot be used to determine the amount of coke produced by surface catalysed reaction, because the surface reactions were not modelled in this simulator, and because coke found on the tube walls of industrial reactors is a mixture of both surface formed coke and coke deposited from the gas phase.

The value of k_{ck} required to match a working TLX can be used to give an indication of the representative

fractions of the coke deposited on the tube walls which is high thermal conductivity (graphitic), medium thermal conductivity (filamentous) and low thermal conductivity (amorphous). This gives some indication to the operator as to the coking mechanisms at work in the both the furnace and the quench cooler.

The drawback to this concept is that there are two unknowns and one overall equation which leads to multiple solutions to a given set of operating conditions. One solution to this dilemma is to measure these coke parameters for the actual furnace or TLX after a period of operation. By measuring actual coke deposited on the tube walls and the k_{ck} of that coke, these values can then be better characterized.

Until a better quantitative understanding of the mechanisms of coke deposition is found and better numerical models are produced from the fundamental research, the current model is sufficient for further simulation work.

8.10 Comparison of Different Coke Formation Models

The effect of employing two different models for the accumulation of coke in the TLX appears only after a finite simulation time, since both models use the same coke rate expression. Both models were run in parallel for the cases showing the effect of total elapsed operation time (Section

8.1), the effect of coke thermal conductivity (k_{ck}) (Section 8.7), and the effect of coke deposition ratio (α) (Section 8.8). Plots showing the behavior of both coke models for these cases are shown in Figures 8.1.1 to 8.1.10 (time), 8.7.1 to 8.7.10 (k_{ck}), and 8.8.1 to 8.8.10 (α). In each set, plots 1 to 5 are for coke model 1, and plots 6 to 10 are for coke model 2.

With the effect of total elapsed operational time study, the temperature profiles (Figures 8.1.1 and 8.1.6), conversion profiles (Figures 8.1.3 and 8.1.8), and coke rate profiles (Figures 8.1.5 and 8.1.10) are all very similar for both models. The primary difference between the two coke models is in the rate at which the coke builds up on the tube walls (Figures 8.1.4 and 8.1.9).

Coke thickness builds much more rapidly in model 2 than in model 1, terminating the model 2 run at 12 days, while model 1 is able to run for 24 days. The rapid buildup of coke in model 2 also effects the pressure drop for a given time step (Figures 8.1.2 and 8.1.7), again with model 2 having the more severe response. Divergence of coke buildup in the two coke models, and consequently differences in pressure drop at 12 days is significant, especially in the first metre of the cooler.

An important difference between the two coking models can be seen Figures 8.1.4 and 8.1.9, the plots of coke thickness. For model 1 at 24 days, the coke thickness is

less than it was at 18 days. This is caused by the assumption used to develop this model, and will be discussed below. For model 2, the coke thickness always increases with total elapsed operational time.

The effect of coke thermal conductivity (k_{ck}) on the two coking models shows the most significant difference between the two models. All curves (Figures 8.8.1 to 8.8.10) are almost identical for the standard value of k_{ck} , and for the large value of k_{ck} . This is not unexpected, as was discussed in Section 8.8, the effect of coke thermal conductivity. Divergence between model results, however, is large for the low k_{ck} case. Temperature, conversion, coke formation, and coke rate are all significantly different for the two models. The coke buildup profile (Figure 8.8.4) for the first model is almost linear, while all other profiles are much more curved.

Because the effect of coke deposition ratio (α) is primarily on the rate of buildup of coke on the tube walls, both models respond to varying α in the same way they responded to different simulation times, except at a slower rate as α is decreased from 1.0.

My conclusion is that model 2 is the better model, and should be used in future work because of its more rigorous derivation of the coke buildup equation. Model 1 is rejected because a basic assumption in the derivation of its coke buildup equation is false, as discussed below.

Model 1 is an integration of the coke rate expression with respect to total elapsed operational time from time 0 to the time calculated, and assumes a constant rate of coke formation for the calculation (Appendix F). The coke formation rate is in fact not constant, but decreases with total elapsed operational time as shown in Figure 8.1.5. As the coke rate decreases, the model 1 coke buildup equation produces a total coke thickness less than that calculated at an earlier time step, when the coke rate was larger (Figure 8.1.4). This is because the integration results in an equation which always calculates the total coke thickness, not an incremental coke thickness. Thus, model 1 produces a result which is not correct (coke thickness cannot decrease since there is no mechanism in this model to allow it to decrease) and should be rejected.

Model 2 shows coke buildup at a faster rate than model 1. This is due to the way the rate equation is incorporated into the models. Model 2 calculates a change in coke thickness at each time step using the current coke rate and adds it to the coke already present. As the coke rate decreases with total elapsed operational time, model 2 calculates the new change in coke thickness with this reduced rate, but adds it to the accumulated coke which was previously calculated, using the correct rate for each previous time step. Thus, model 2 correctly accounts for the change in coke rate at each time step.

8.11 Discussion - Cases Studied

The second coke model is the more correct model (since a basic assumption underlying model one is false) and will be used in all further simulation work with this ethane pyrolysis simulation model. The second coke model will be used to simulate the Alberta Gas Ethylene quench cooler in the next section of this work. Careful choice of the coke deposition ratio and the coke thermal conductivity are required to try and best reflect the actual coke produced in an industrial quench cooler. In the absence of good coke production and deposition data, varying the coke deposition ratio to model actual run times, pressure and temperature profiles, followed by varying thermal conductivity to model ethane conversion appears the best method to match these parameters.

The value of the steam heat transfer coefficient used is not critical to this model as shown by the negligible response to changing its value (Section 8.6). The default value obtained from Rase (1977b) will be used in the simulation of the Alberta Gas Ethylene plant quench cooler (TLX).

Steam temperature, although critical for proper quenching of the process stream, is quite easy to determine for an actual TLX. In design work, choice of steam temperature depends on balancing quench time and overall quench cooler

thermal efficiency against the quality of steam produced (Fanaritis and Streich 1973; Mol 1978). Fast quench and high thermal efficiency in the quench cooler requires low temperature steam, which is less valuable as an energy source for the rest of the plant. High quality steam reduces the thermal efficiency of the cooler, and lengthens the quench times, with more by-product produced. The value used in this study represents a good compromise between these two extremes.

A more complex design decision is the selection of tube diameter, mass flux and steam dilution. All three are strongly interdependent; the selection of all three requires a careful optimization of the overall pyrolysis process. Fundamental design criteria affecting the choices are the targeted ethylene production capacity, the amount and cost of steam available for dilution, the size of pumps and pipe available and the type of materials available to construct the furnace and TLX, and the severity of the pyrolysis system. Steam dilution will affect the overall mass flux which cannot exceed maximum values specified by tube diameter and material. Although higher steam dilution ratios favor ethylene production and minimize by-product formation, they also increase mass flux for given ethylene production target capacities, require more steam (which may be costly), and increase the separation requirements for downstream process units.

A discussion of the detailed design of a pyrolysis furnace and cooler combination is beyond the scope of this work, however, the iterative processes involved lend themselves nicely to the inclusion of a computer simulation tool such as this in the overall design process.

8.12 Discussion - Assumptions

The model always maintained Reynolds numbers in excess of 4000 (Appendix H), and the length to diameter ratio always exceeded 50. Consequently, the assumption of plug flow was valid for all model runs.

The assumption of pseudo steady state with respect to the coke model was valid, as observed model variables responded in a well behaved manner to the stepwise addition of coke to the tube walls. This is seen in the behavior of the various plots (Figures 8.1.1 to 8.1.10) for the case dependent on total elapsed operational time (Section 8.1).

8.13 Comparison with Experimental Results

As discussed in Section 7.12, Rase (1977b) provided no experimental results for his quench cooler study (Case 103), so a detailed comparison cannot be performed. Using the same model for a furnace study (Case 102), he indicated good agreement between his model and the experimental pilot plant

data used to construct the model. By comparing my model to his computer results, some small indication of the potential experimental agreement obtainable with my model may be shown.

The lack of detailed descriptions of experimental data in the literature hampers comparative simulation efforts. Simulation of the Alberta Gas Ethylene TLX will provide a much better actual test of the computer model.

8.14 Comparison with Other Simulators

The quench cooler simulation performed by Rase (1977b) (Case 103) provides simulation results for comparison with my model. The base case data for my simulation runs (Table 7.1) is the same as that used by Rase in his simulation runs (except for some of the component thermal property data). Rase provides TLX exit temperatures, pressure drops and ethane conversions for three mass fluxes, which are comparable to the cases discussed in Section 8.2. A number of cases were run with my model using a values of the feed mass flux between $10 \text{ kg/m}^2 \cdot \text{s}$ and $100 \text{ kg/m}^2 \cdot \text{s}$ to provide additional data for the plots. Figures 8.14.1 to 8.14.3 display the results of both model simulations.

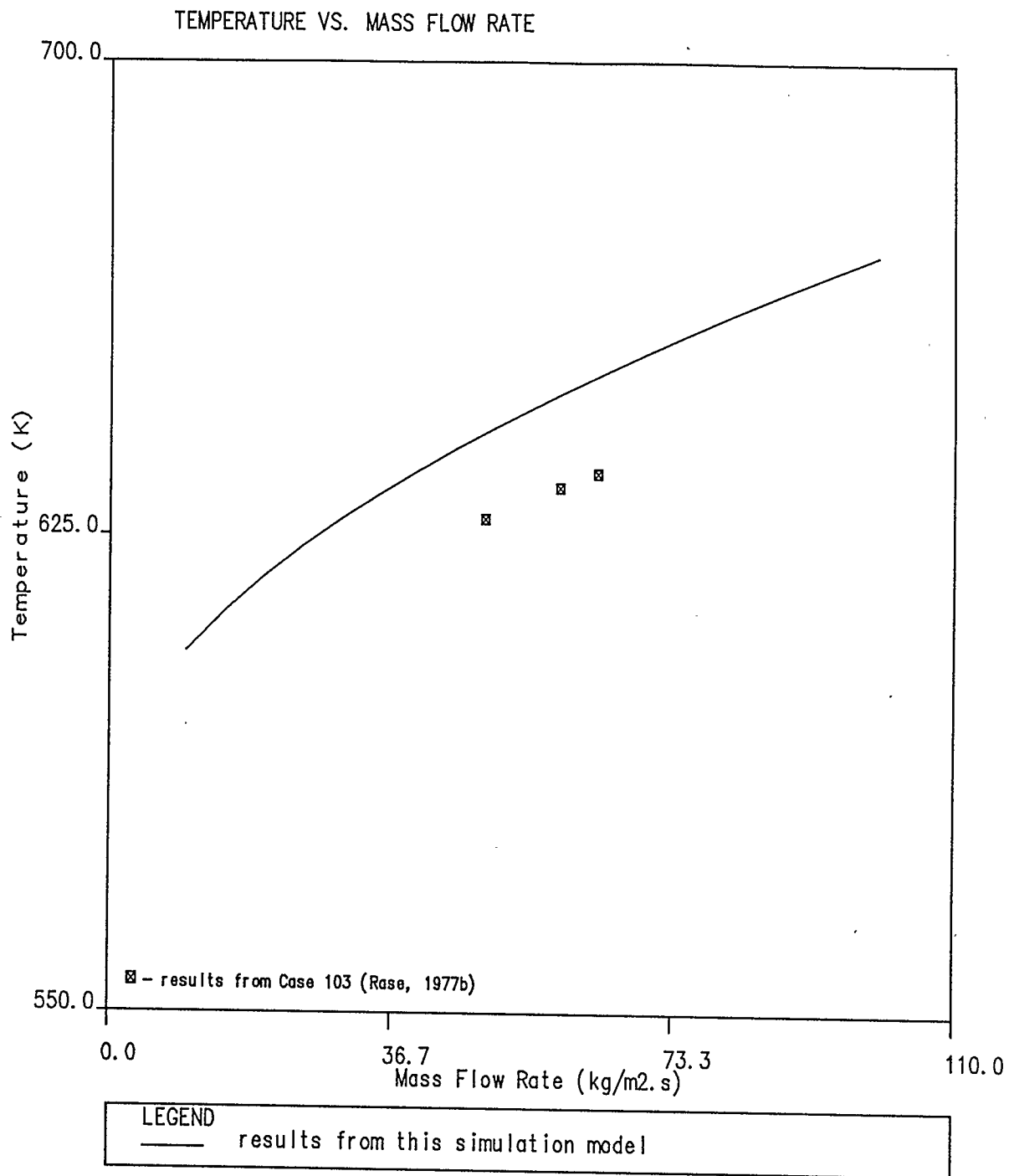


Figure 8.14.1 TLX Outlet Temperatures at different mass flow rates comparing this simulation model to the simulation of Rase (1977b)

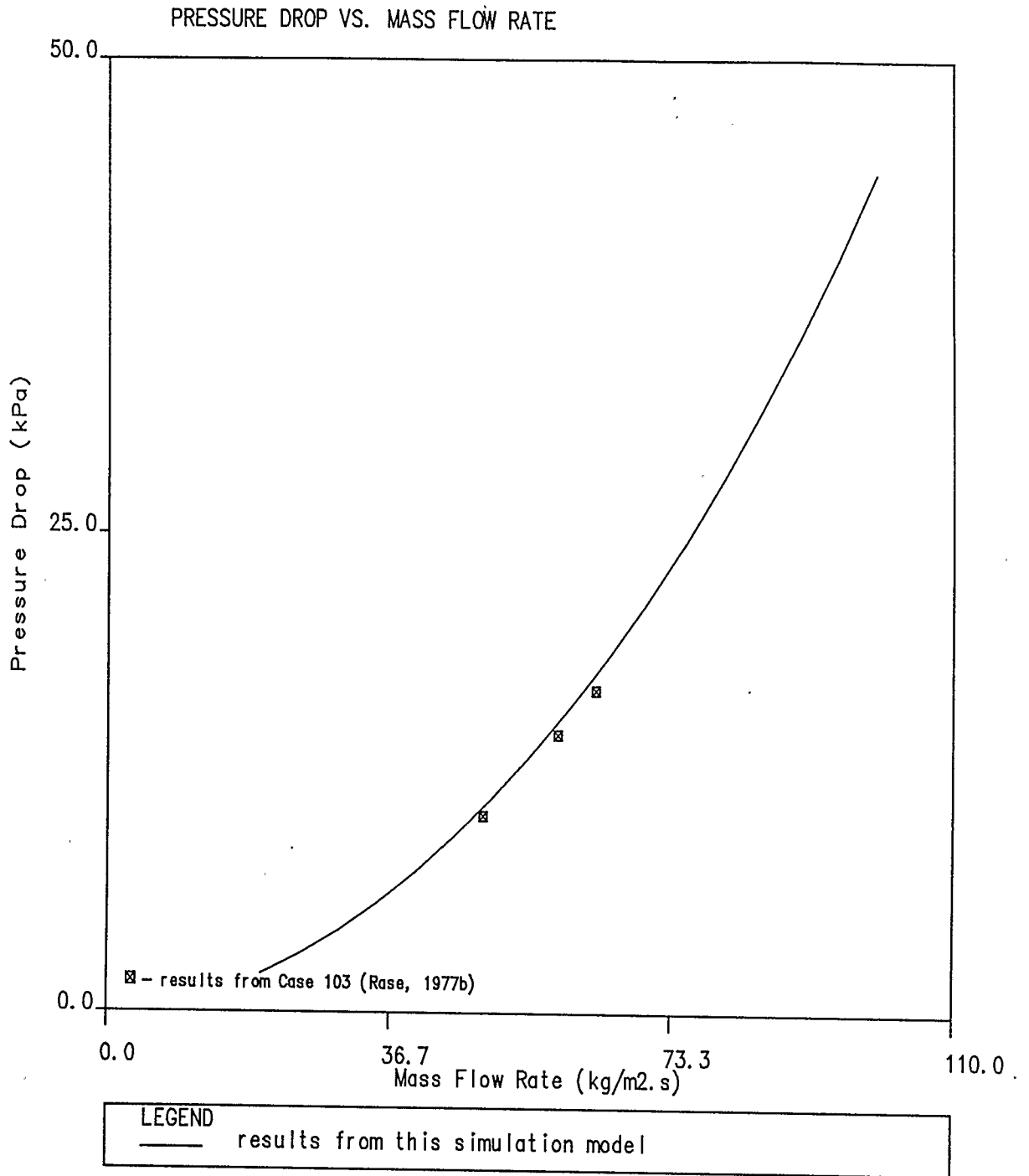


Figure 8.14.2 TLX Outlet Pressure Drops at different mass flow rates comparing this simulation model to the simulation of Rase (1977b)

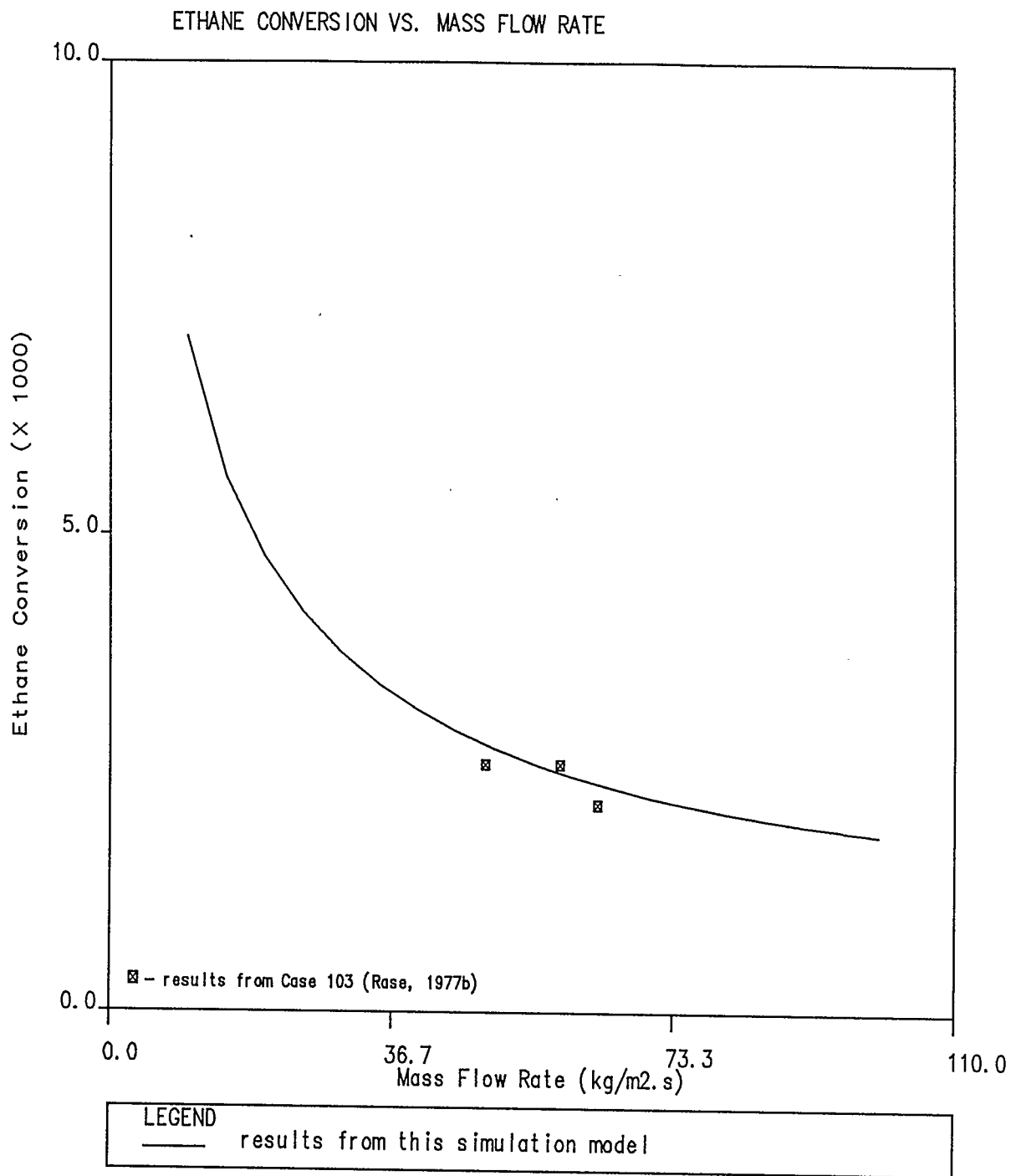


Figure 8.14.3 TLX Outlet Conversions at different mass flow rates comparing this simulation model to the simulation of Rase (1977b)

The agreement in results between my model and Rase's (1977b) is due to the similarity of the models. The only significant difference between models is in the values of the component thermal properties used. The result of these differences can be seen in Figure 8.14.1, the plot of exit temperature for various feed mass fluxes. Figure 8.14.1 shows some difference in the outlet temperatures (less than 10%), although the trend is the same. The pressure and conversion plots (Figures 8.14.2 and 8.14.3) show excellent agreement with Rase's simulation work.

Even with the different thermal data, the agreement between simulation models is excellent. Both models use the molecular kinetic data of Sundaram and Froment (1977), and both solve the same set of rigorous differential equations.

In conclusion, in spite of the small differences between the two models, an excellent match was achieved. The ability of my model to match previously published simulation results provides excellent verification of this model.

9.0 Simulation of the Alberta Gas Ethylene Plant

The Alberta Gas Ethylene Company operates a very large, world scale ethylene production facility in Joffre, near Red Deer, Alberta. This work will simulate a single tube in the quench cooler from one of the ethylene pyrolysis process streams using the computer model developed for this work.

9.1 Description of the Alberta Gas Ethylene Plant

The Alberta Gas Ethylene plant in Joffre, Alberta is a five furnace plant capable of producing 136000 tonnes (3 billion pounds) of ethylene per year (Table 1.1) from ethane feedstock. Each furnace in the plant houses 4 pyrolysis coils, each coil having 11 tubes of 13.7 m for a total coil length of 150.7 m. The pyrolysis coils have an inside diameter of 14.0 mm. Each furnace is served by two quench coolers. The process gas stream from the coils is combined at the furnace outlet at the bottom of the furnace into a single 200.0 mm diameter uninsulated transfer pipe 1.8 m long. This transfer section makes a 90 degree bend coming out of the furnace to enter the quench cooler or transfer line exchanger (TLX).

The quench coolers for the Alberta Gas Ethylene plant

are horizontal shell and tube heat exchangers with a tube length of 8.4 m. There are 108 tubes in each exchanger each with an internal diameter of 30.0 mm, fed by the production of the two combined furnace coils. The shell side of the quench cooler contains 4.4 MPa saturated steam and Alberta Gas Ethylene indicates the TLX has a constant shell side tube temperature.

A schematic diagram of the major process units is presented in Figure 2.2. A schematic diagram of a typical horizontal shell and tube quench cooler (TLX) is presented in Figure 3.1.

9.2 Modifications to the Computer Model

In order to simulate the Alberta Gas Ethylene pyrolysis quench cooler (TLX) with the model produced for this work, a few modifications to the original computer program were made.

The first modification to the model was the replacement of the manner in which feed mass flux was established. The original model had mass flux and steam dilution ratio as input parameters. The model then calculated the molar flow rate for each component. This is a good method of isolating the effects of steam dilution and mass flux for parametric simulation. For the Alberta Gas Ethylene model, the supplied data was kg hydrocarbon and kg steam per unit time per

furnace coil. This was manually converted into kg/s/coil, and then using the flow geometry initially supplied by Alberta Gas Ethylene into $\text{kg/m}^2 \cdot \text{s}$ hydrocarbon and $\text{kg/m}^2 \cdot \text{s}$ steam (hydrocarbon and steam mass flux) for the single cooling tube simulated. The initial geometry was 2 furnace coils combining into one transfer line and then dividing into 108 TLX tubes (2 to 1 to 108 for an overall flow geometry 2/108). The simulation computer model was modified to accept these two mass fluxes as the primary feed flow input data. The computer program then combines these numbers with the feed mole fractions to produce the component molar flow rates required by the mass balance equations.

The second change to the computer model for simulation of the Alberta Gas Ethylene cooler was the addition of code to calculate and print out the normalized mole fractions of hydrocarbon. This modification was done to allow comparison of the quench cooler outlet hydrocarbon mole fractions provided in the Alberta Gas Ethylene plant data with those produced by the computer simulation.

Otherwise the computer model was computationally the same as the model employing coke model 2, used in the parametric simulation study previously discussed.

9.3 Simulation Input Variables

Based on data provided by Alberta Gas Ethylene for their ethane pyrolysis plant in Joffre Alberta, the input of the computer model was appropriately modified. The input variables changed to reflect the Alberta Gas Ethylene data are:

1) Feed parameters: hydrocarbon mass flux, steam mass flux, feed inlet temperature, feed inlet pressure, hydrocarbon feed component mole fractions.

2) Physical parameters: tube inner diameter, tube thickness, TLX length, number of coke accumulation grid blocks (a function of TLX length).

3) Cooling Steam Parameters: steam temperature.

All other input parameters for the model were unchanged from the model used in the parametric studies.

Details of the input data used to model the Alberta Gas Ethylene quench cooler are provided in Table 9.1. Two cases were studied for this work, based on the data provided by Alberta Gas Ethylene. The cases are labelled H143 and HAVG. Clean tube data was provided for a TLX labelled H143. Initial history matching runs were done with this data. A second set of data was provided for four similar quench coolers (H142, H144, H146 and H150) at total elapsed operational times greater than zero. Because this data was very

Table 9.1 Alberta Gas Ethylene Plant Data

<u>TLX Identity</u>	H143	H142	H144	H146	H150	HAVG *
Days on Line	0	4	2	44	34	3 / 39
<u>Feed Mass Flux</u> (kg/m ² ·s):						
Hydrocarbon Feed	29.41323	32.91481	32.91481	32.91481	32.91481	32.91481
Steam Feed	9.13211	10.09854	10.16857	10.16157	10.11955	10.13706
Total Feed	38.54534	43.01335	43.08338	43.07638	43.03436	43.05187
<u>Pressure</u> (kPa):						
TLX Inlet Press.	205.175	228.775	225.225	226.525	239.979	230.125
TLX Outlet Press.	————— (** see note) —————					
<u>Temperature</u> (K):						
TLX Inlet Temp.	1109.200	1108.300	1110.900	1107.700	1107.600	1108.625
TLX Outlet Temp.	557.650	564.950	563.150	571.150	573.700	564.238/ 572.425
<u>Inlet Composition</u> (mole fraction):						
Hydrogen	0.354107	0.345970	0.345139	0.344551	0.344828	0.345122
Methane	0.061365	0.063268	0.062205	0.067805	0.066050	0.064832
Acetylene	0.001811	0.002310	0.002308	0.001607	0.001810	0.002009
Ethylene	0.320909	0.325885	0.324571	0.321949	0.323213	0.323905
Ethane	0.250490	0.250064	0.253336	0.251632	0.252840	0.251968
Propane (est.)	0.003244	0.003741	0.003712	0.003767	0.003443	0.003666
Propylene (est.)	0.003244	0.003741	0.003712	0.003767	0.003443	0.003666
C ₄ +	0.004829	0.005021	0.005017	0.004922	0.004373	0.004833
<u>Additional Data</u> (common to all the TLX's):						
Reactor Length:						8.4 m
Tube Inner Diameter:						30.6 mm
Tube Wall Thickness:						3.76 mm
Steam Temperature:						493.4 K
Steam Heat Transfer Coefficient:						11584.0 W/m ² ·K
Coke Deposition Ratio:						0.33 (final)
Coke Thermal Conductivity:						5.5 W/m·K

* **NOTE:** The data for HAVG is the arithmetic average of the data for TLX H142, H144, H146 and H150. The data from the four TLXs is averaged to obtain all values except for the TLX outlet temperature. Two values for the TLX outlet temperature are provided to reflect the two different sets of "days on line" values.

** **NOTE:** The supplied outlet pressure is an estimate of 171.34 kPa to 181.37 kPa for H143 and 196.27 kPa to 206.30 kPa for H142, H144, H146, and H150 (HAVG).

similar, it was averaged to produce a dataset for a hypothetical TLX called HAVG which could be used for history match runs both at clean tube conditions and also after 42 days total elapsed operational time.

9.4 Simulation Results

The results of the simulation of the Alberta Gas Ethylene quench cooler are presented in Figures 9.1 to 9.10. Where actual data from Alberta Gas Ethylene are available, they are plotted with the results.

Initial simulation runs were done at zero days to allow matching of output data provided by Alberta Gas Ethylene for both cases. Mass fluxes were varied to match the reported outlet temperatures and pressures. Figures 9.7 and 9.8 show the effect of mass flux on the outlet temperature and pressure drop for both TLX cases.

After a clean tube (0 days total elapsed operational time) match was achieved, a 60 day run was done for the HAVG TLX to observe the effect of coke accumulation on the quench cooler. The coke deposition ratio (α) was varied to produce a history match with the HAVG data. Figures 9.9 and 9.10 show the effect of the coke deposition ratio (α) on the outlet temperature and pressure drop of the HAVG TLX at 42 days total elapsed operational time.

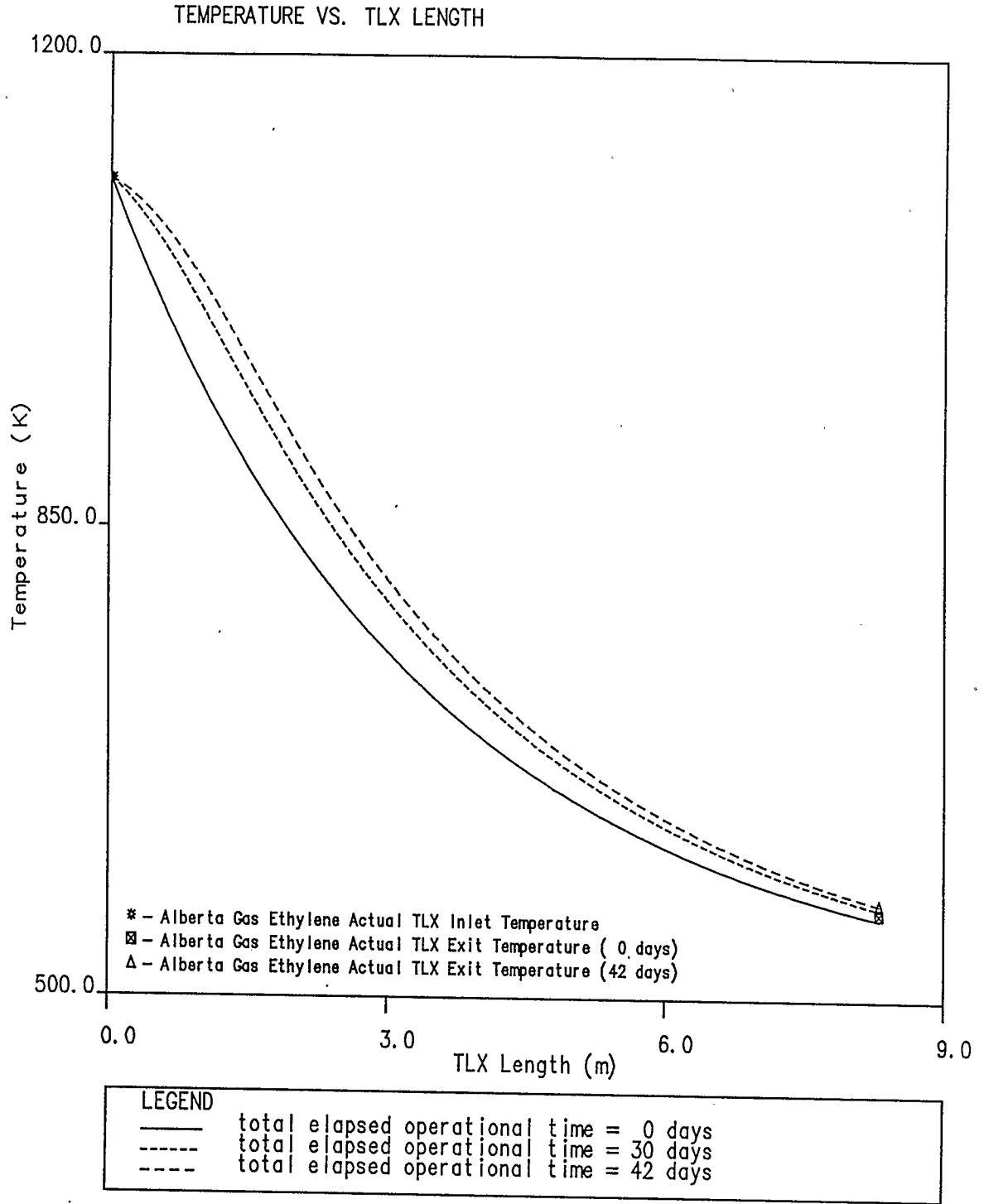


Figure 9.1 TLX Temperature profiles at different total elapsed operational times for the Alberta Gas Ethylene TLX simulation

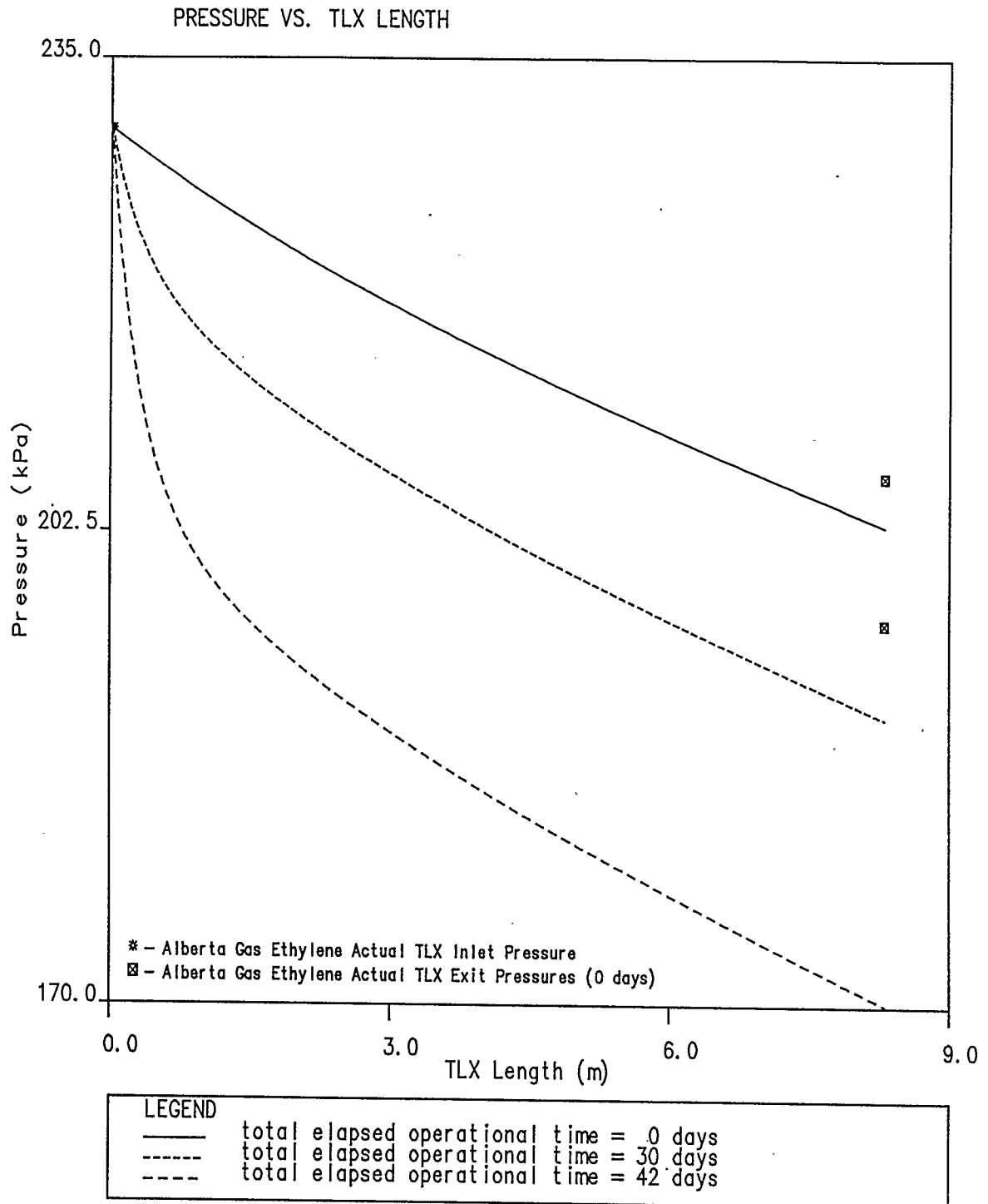


Figure 9.2 TLX Pressure profiles
 at different total elapsed operational times
 for the Alberta Gas Ethylene TLX simulation

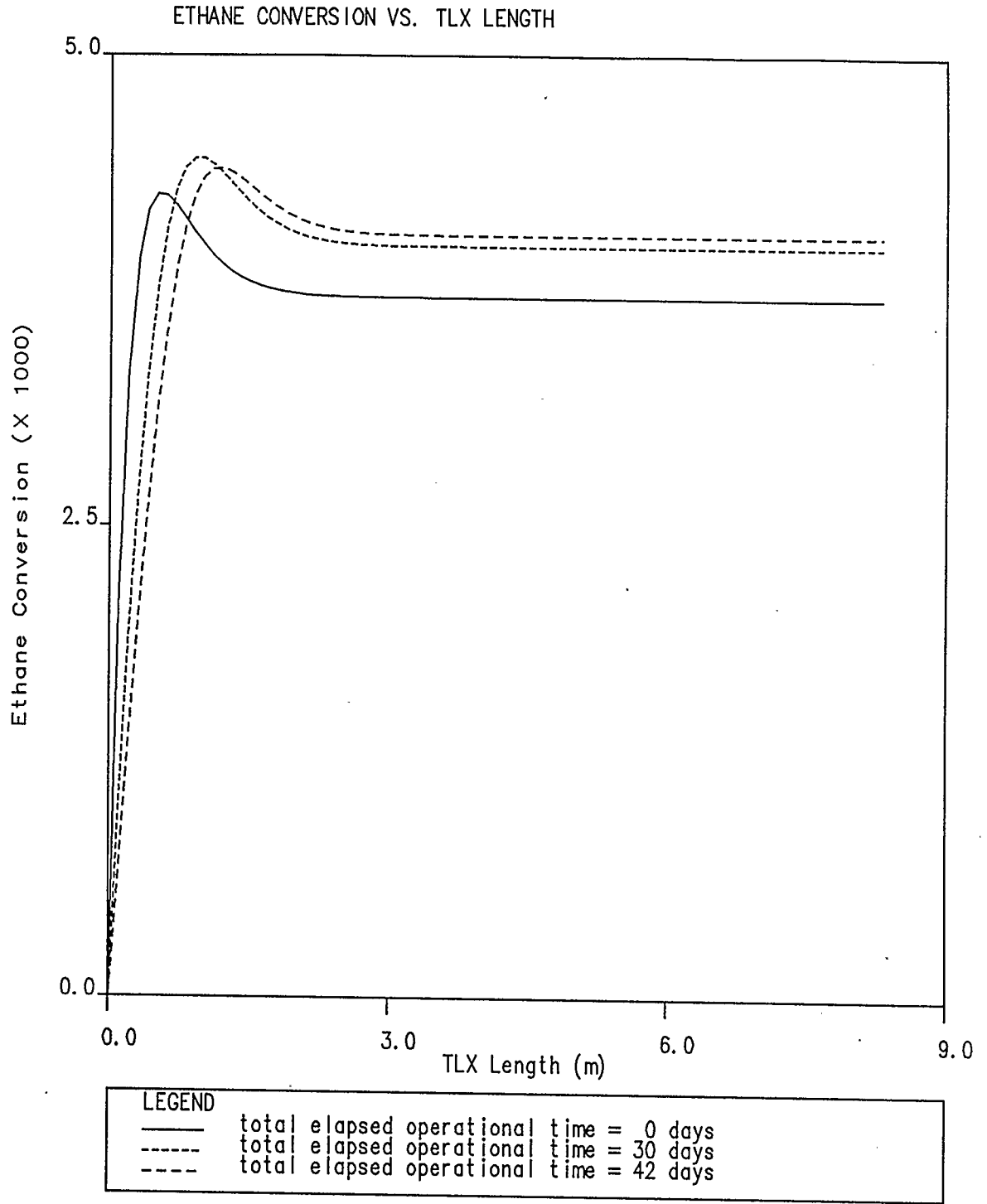


Figure 9.3 TLX Ethane conversion profiles at different total elapsed operational times for the Alberta Gas Ethylene TLX simulation

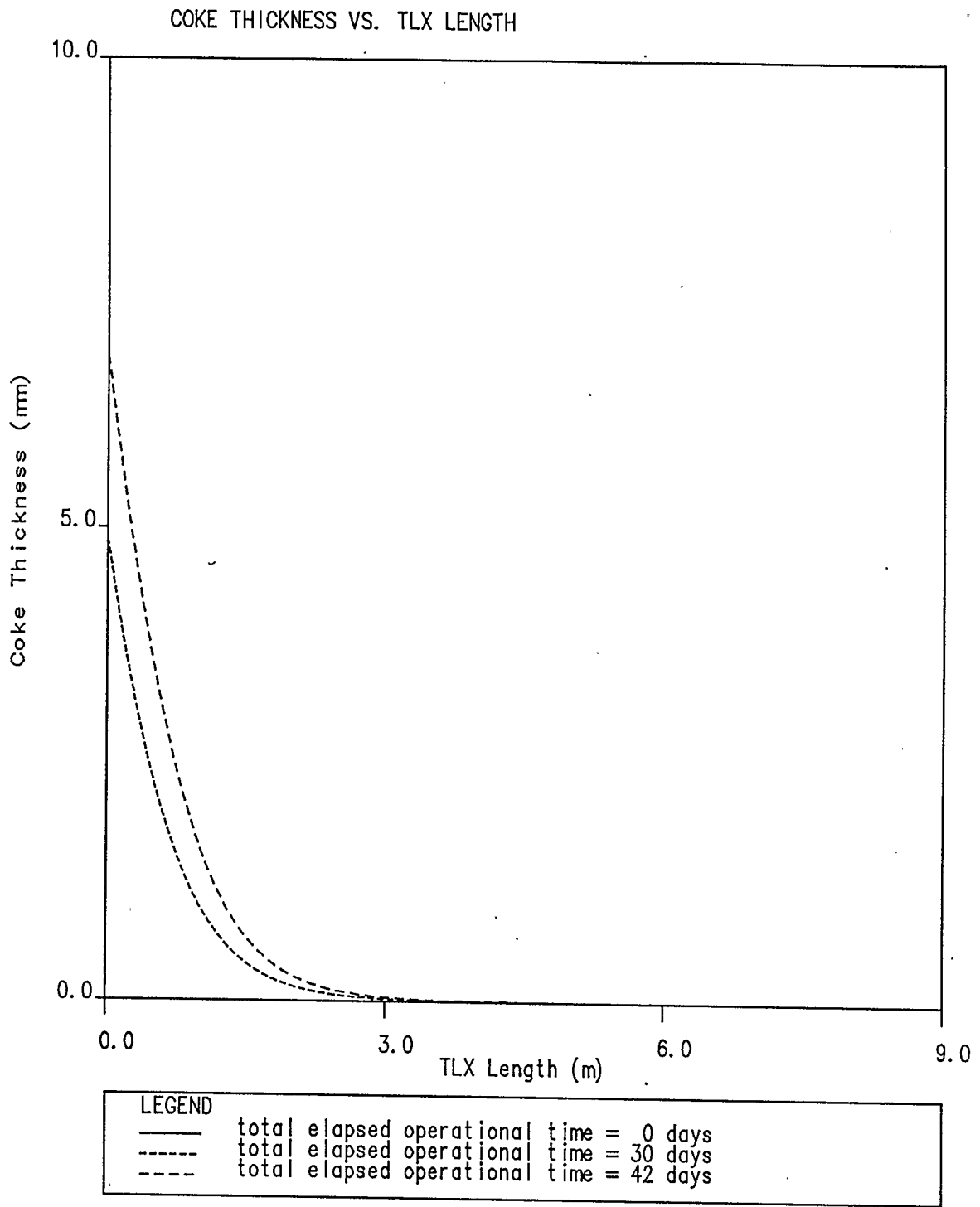


Figure 9.4 TLX Coke thickness profiles at different total elapsed operational times for the Alberta Gas Ethylene TLX simulation

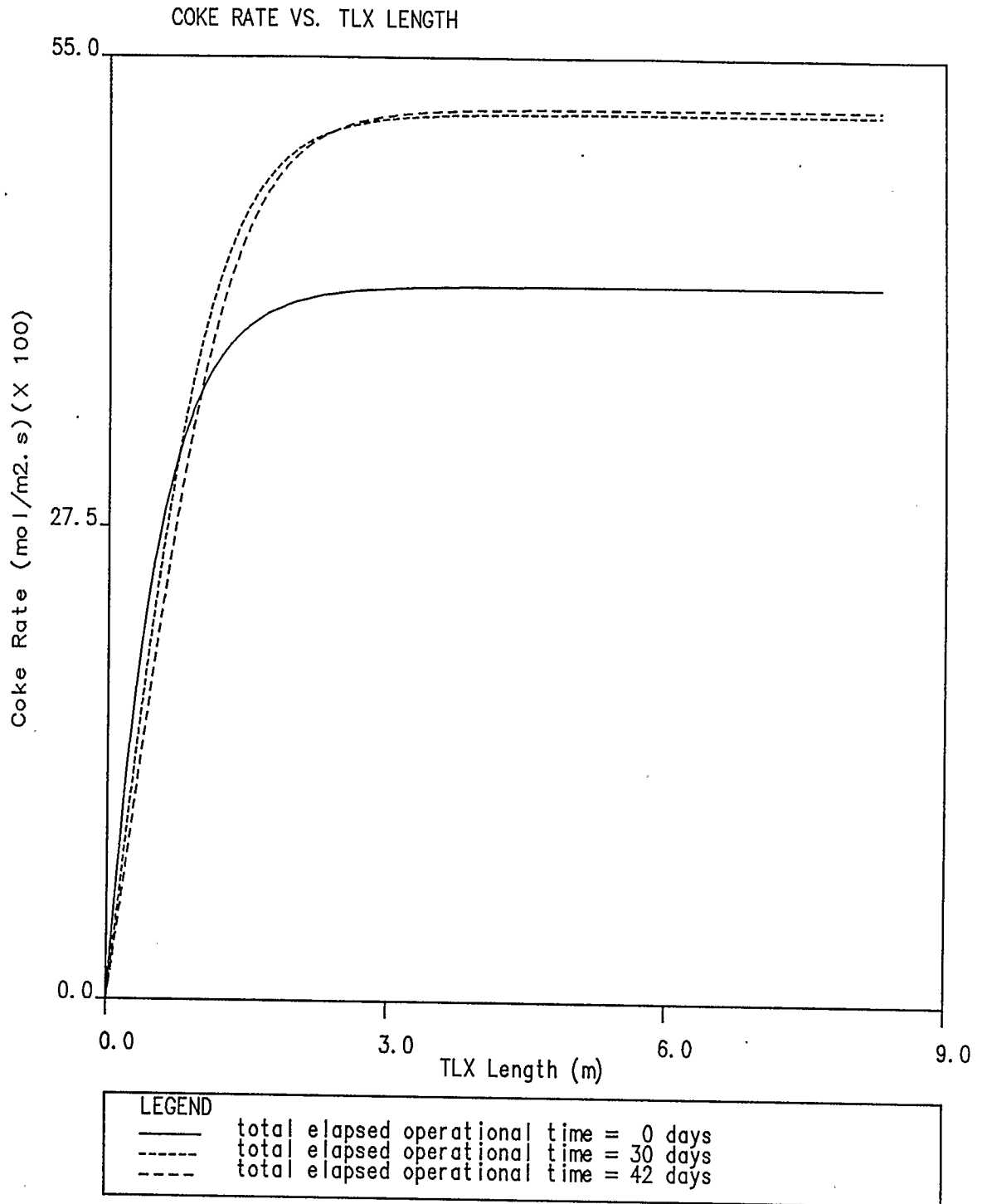


Figure 9.5 TLX Coke rate profiles at different total elapsed operational times for the Alberta Gas Ethylene TLX simulation

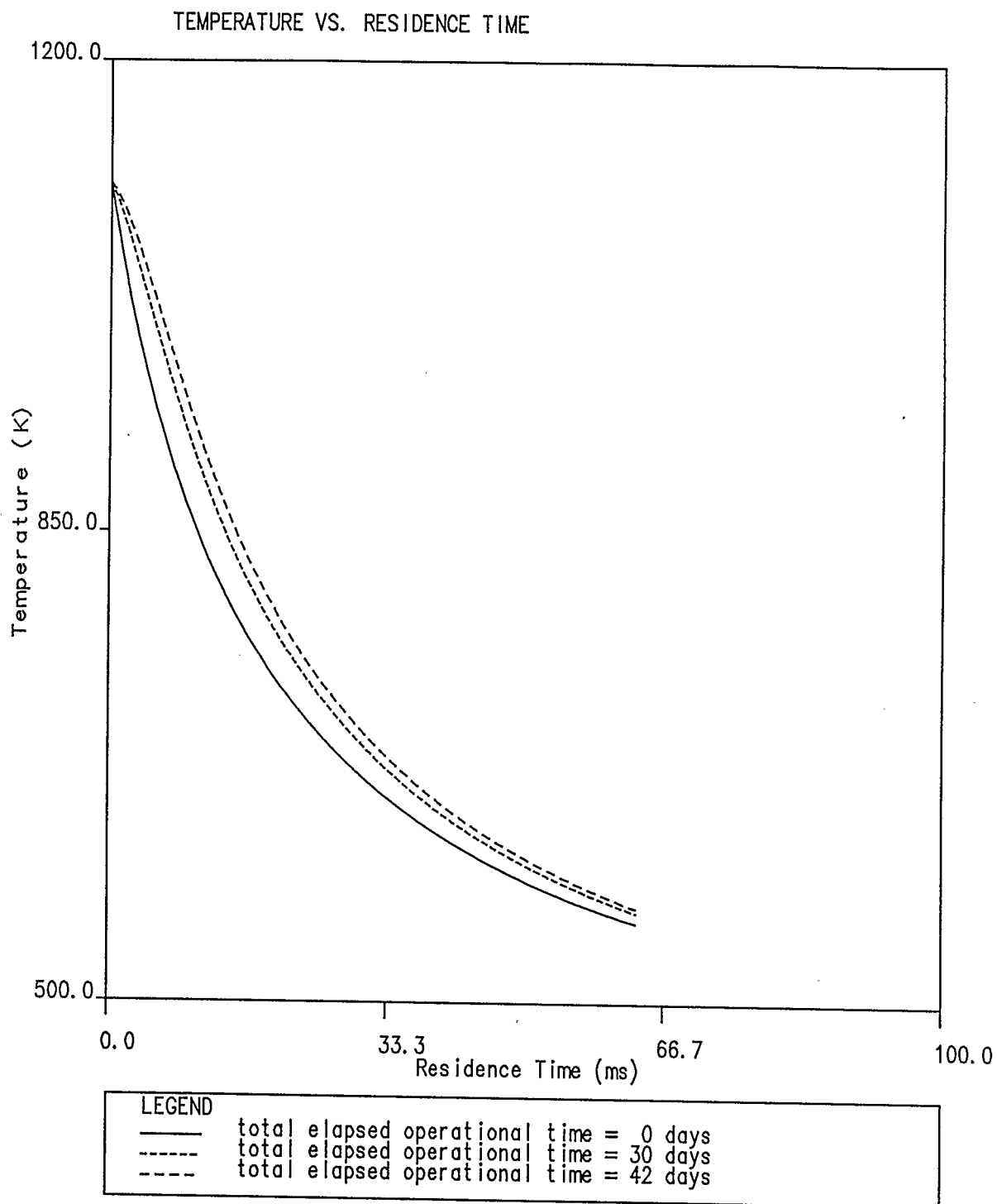


Figure 9.6 TLX Temperature profiles at different total elapsed operational times for the Alberta Gas Ethylene TLX simulation

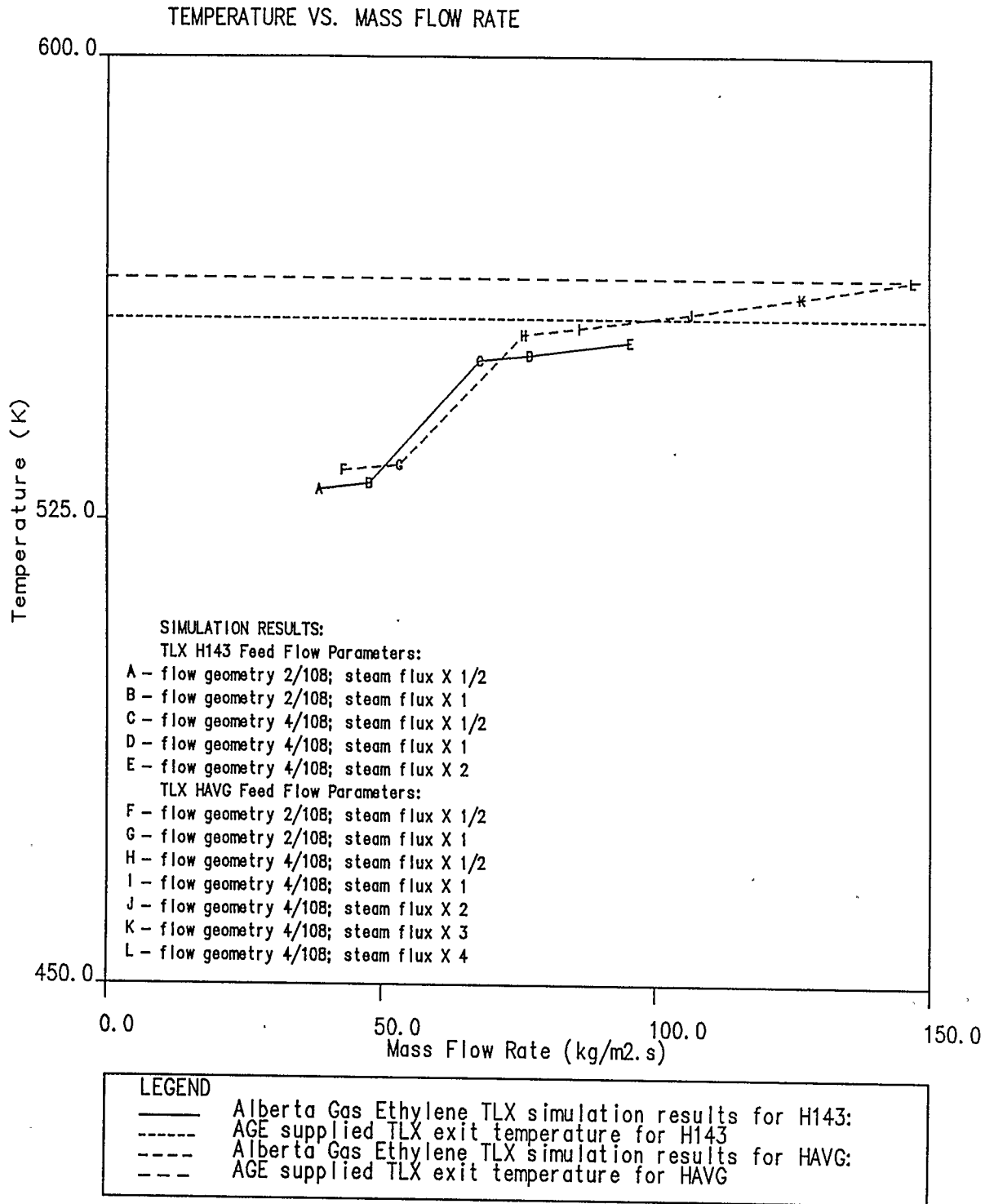


Figure 9.7 TLX Outlet Temperatures at different feed mass fluxes for the Alberta Gas Ethylene Simulation

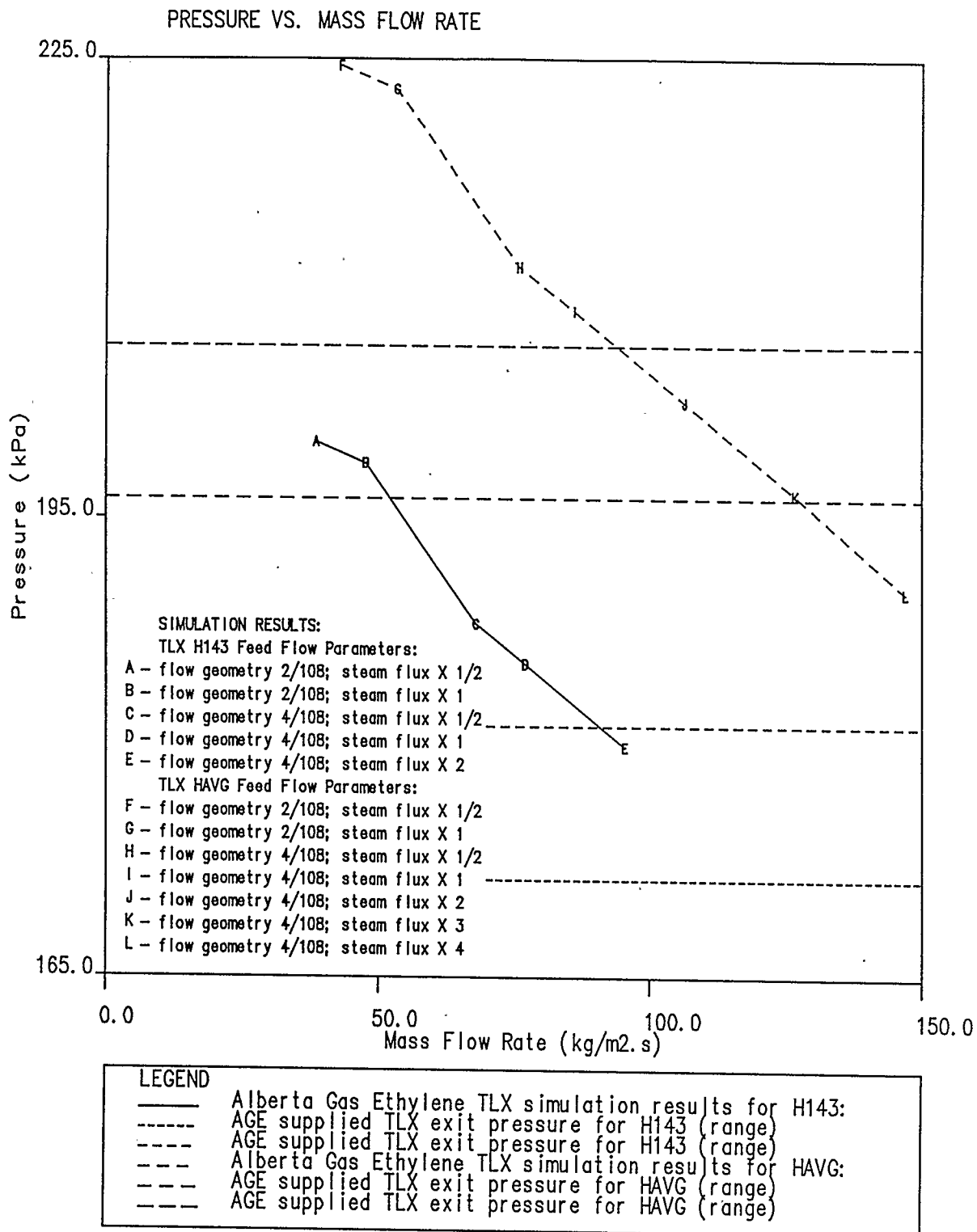


Figure 9.8 TLX Outlet Pressures
at different feed mass fluxes for
the Alberta Gas Ethylene Simulation

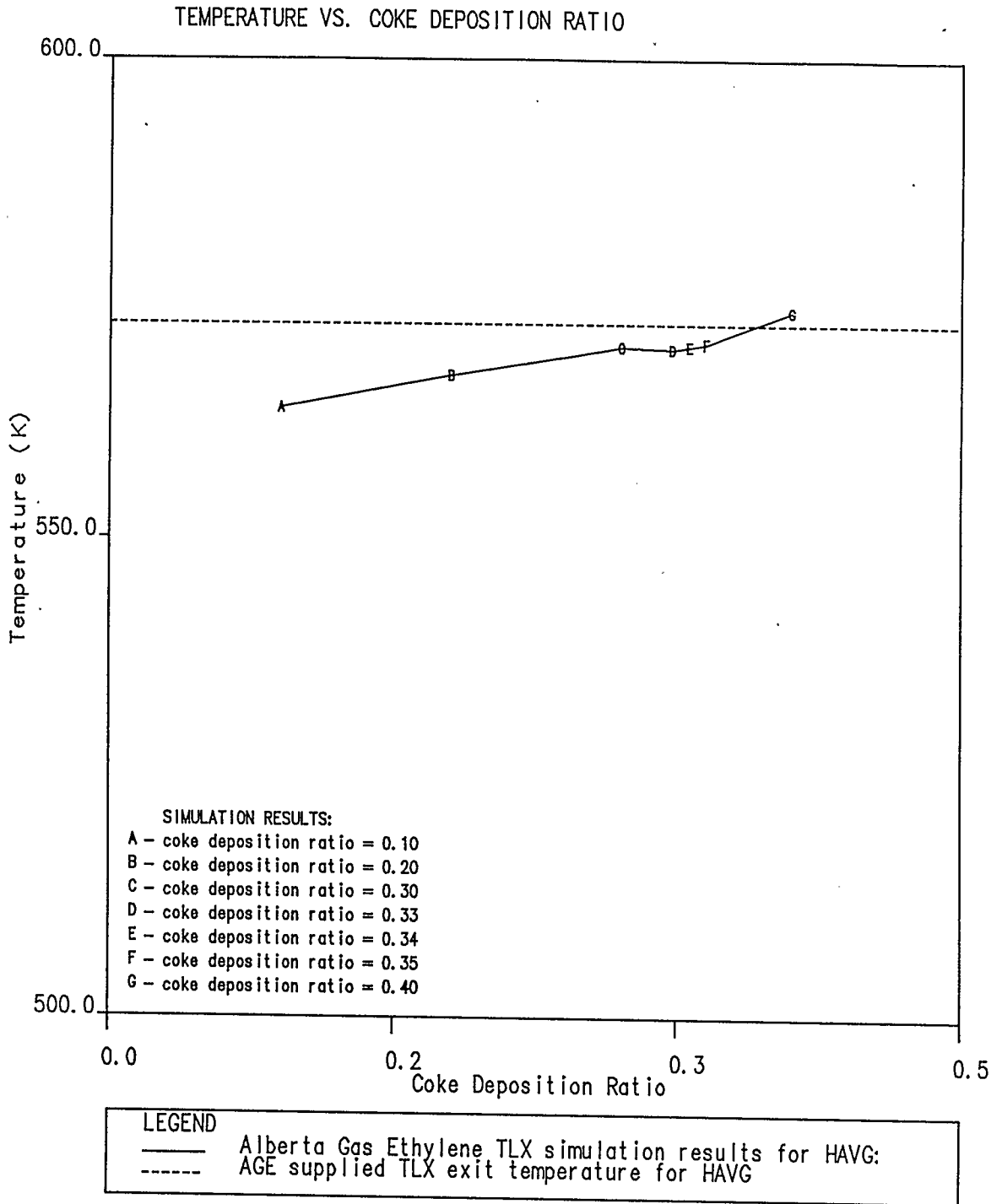


Figure 9.9 TLX Outlet Temperatures at different coke deposition ratios for the Alberta Gas Ethylene Simulation

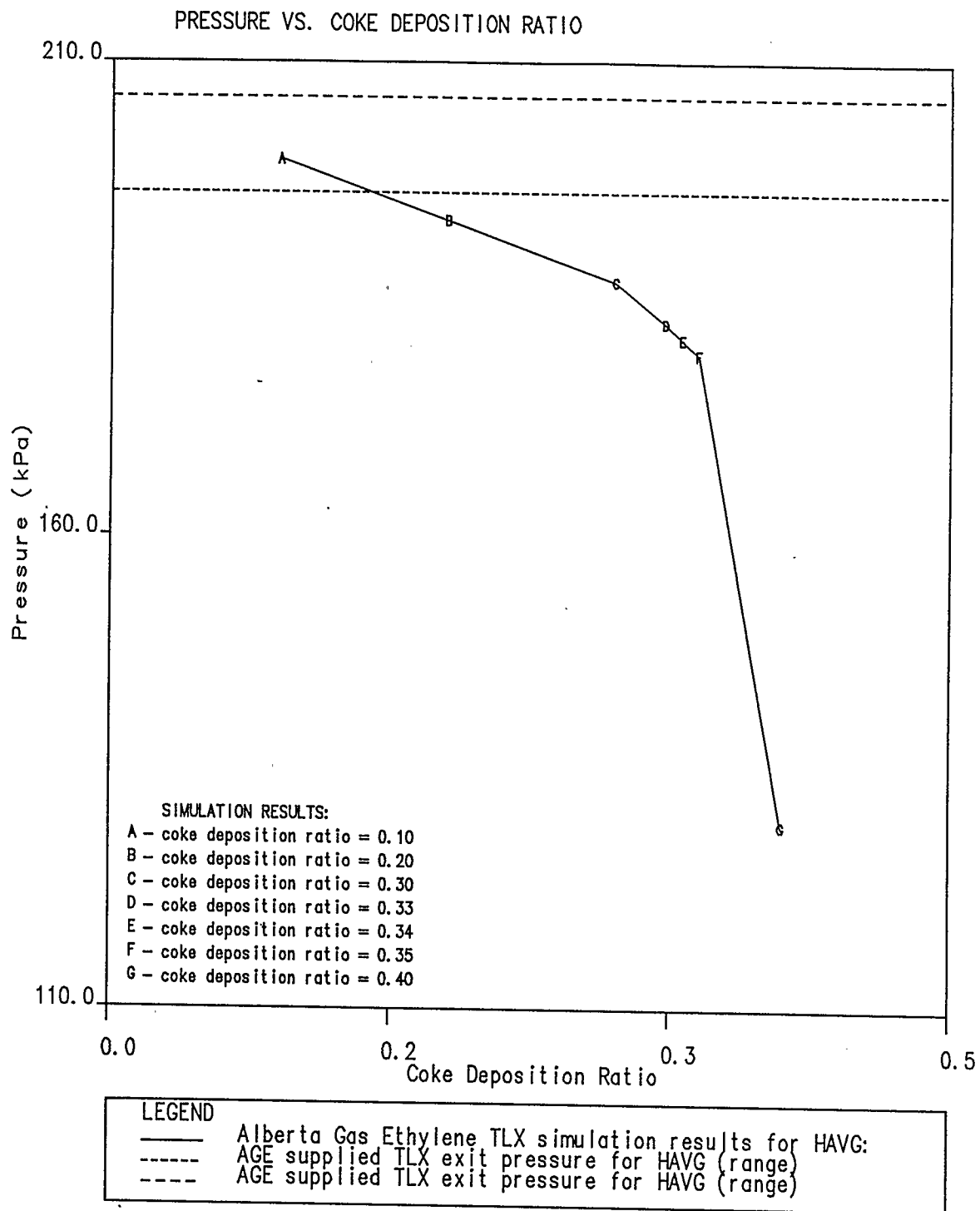


Figure 9.10 TLX Outlet Pressures
at different coke deposition ratios
for the Alberta Gas Ethylene Simulation

9.5 Discussion of Results

Simulation of the Alberta Gas Ethylene quench cooler (TLX) was made more complicated because Alberta Gas Ethylene could not supply TLX feed composition data (mole fractions of hydrocarbon components at the TLX inlet). Due to the location and type of sampling ports on the furnace and TLX, Alberta Gas Ethylene is capable of providing only the furnace inlet composition, temperature and pressure, the quench cooler (TLX) outlet composition and temperature, and the TLX inlet temperature and pressure. The process stream composition at the inlet to the quench cooler (or the exit to the furnace) is not available as there is no sampling mechanism at that point.

As a result, an iterative modelling technique was used to estimate the inlet composition. An initial run was made with the quench cooler outlet composition (provided by Alberta Gas Ethylene) used as the inlet composition (the initial guess). The results of this run were then used to update the inlet composition (the difference between the simulator outlet composition and the supplied outlet composition would be used to refine the inlet composition guess), and the simulation was rerun. This was done until the outlet composition matched the values reported by Alberta Gas Ethylene. In practice, the reaction quench was so rapid

that changes in mole fractions between the TLX inlet and outlet were less than the variations in the original outlet mole fraction data provided by Alberta Gas Ethylene (Table 9.1). Consequently, only one iteration was required to establish the feed composition.

9.5.1 History Match for Clean Tube Conditions

An exact match of the outlet pressure of the quench cooler was not possible, since Alberta Gas Ethylene did not supply exact outlet pressure data for the TLX. Alberta Gas Ethylene provided a range of TLX outlet pressures for the two sets of TLX data. For TLX H143, the outlet pressure range was from 171.0 kPa to 181.0 kPa at clean tube conditions. For TLX HAVG, the outlet pressure range was from 196 kPa to 206 kPa at clean tube conditions.

An match of the outlet temperature was possible since this data was supplied by Alberta Gas Ethylene. For H143, the outlet temperature was 558 K at clean tube conditions. For HAVG, the outlet temperature was 564 K at clean tube conditions.

The pressure and temperature profiles in the TLX are strong functions of both mass flux and tube diameter. Since the diameter of the TLX tubes was fixed by the value supplied by Alberta Gas Ethylene, the mass flux was adjusted to obtain a pressure and temperature history match for both of

the TLX data sets.

There are two reasons the feed mass flux adjusted to obtain a history match. First, there was some doubt as to the flow geometry of the furnace and TLX supplied by Alberta Gas Ethylene. It was not entirely certain whether 2 furnace coils or 4 furnace coils combined into one transfer pipe which then was distributed to the 108 TLX tubes. This represents two possible flow geometries, either 2/108 or 4/108. Since the feed flow data is provided as kg/hr/furnace coil, the flow geometry is required to convert the supplied feed data to TLX feed mass fluxes (as described in Section 9.2). The uncertainty in supplied flow geometries represents a potential factor of two difference in the calculated TLX feed mass flux. This would affect the clean tube conditions history match. Second, information from Alberta Gas Ethylene indicates coke buildup at the TLX inlet distributor manifold is a significant problem and may lead to plugging of TLX tubes at the inlet. This tube plugging will changing of the feed mass flux since less tubes open to flow means greater flow through the remaining tubes. It is not a factor at clean tube conditions, but would increase in effect at later values of the total elapsed operational time.

Steam feed mass flux was also varied independently of the hydrocarbon feed mass flux to determine whether or not any error exists in the reported steam feed mass flux. Various values of the steam feed mass flux were used to ob-

serve the effect of changing steam dilution, and to determine if there might be an error in the supplied steam rate.

Figures 9.7 and 9.8 (and Figures 9.1 and 9.2) show the outlet temperatures and pressures for various feed mass fluxes using both sets of TLX data (H143 and HAVG). An excellent history match for both quench coolers (represented by points "E" and "J" on the curves) was obtained using the flow geometry of 4/108 (to calculate TLX mass flux from the supplied furnace feed rates) with double the supplied steam feed mass flux. This indicates the preferred flow geometry has four furnace coils combining into the single transfer pipe, then dividing into the 108 TLX tubes in the quench cooler. Also, this result indicates a possible error in the measured steam mass flux as supplied by Alberta Gas Ethylene.

9.5.2 History Match for Coked Tube Conditions

The Alberta Gas Ethylene plant remains on line for at least 44 days (total elapsed operational time), according to the supplied data. Since the initial parametric time study with coke model 2 only operated for 12 days before coke deposition plugged the tube, a value of α less than 1.0 was required to match the Alberta Gas Ethylene TLX at 42 days (total elapsed operational time). Figures 9.9 and 9.10 show the effect of varying α on the outlet temperature and the

pressure drop at 42 days total operational time. Because no data on manifold coke plugging of the TLX tubes was provided by Alberta Gas Ethylene, feed mass fluxes were not varied in these simulation runs. The optimum history match was obtained using a value of α of 0.33. Using this value, the maximum on-stream time for the simulated cooler was between 48 and 54 days (Table H.3 in Appendix H). The simulation was terminated when the TLX pressure at any point in the cooler dropped below atmospheric pressure. This was due to coke buildup in the initial 1.5 m of the TLX tube (Figure 9.4). Since the TLX would not operate under this condition, the actual shutdown time would be between that value and the previous value of the total elapsed operational time.

9.6 Simulation Conclusions

The simulation of two Alberta Gas Ethylene quench coolers (TLXs) produced excellent history matches. A feed flow geometry of 4/108 (used to determine the TLX feed mass flux from supplied furnace feed flow rates) with double the supplied steam feed mass flux was required to obtain this history match for both sets of quench cooler data (H143 and HAVG). It appears an error in measuring the steam mass flux at the Alberta Gas Ethylene plant may be occurring.

This simulation shows that the Alberta Gas Ethylene quench cooler is very efficient, quenching the reaction in

1.8 m for a residence time of 20.0 ms (Figure 9.6). The remainder of the TLX acts as a large heat exchanger extracting additional energy from the process stream. The rapid quench is due to the use of 4.4 MPa saturated steam (493.4 K), which would be considered a low temperature steam. If Alberta Gas Ethylene were to switch to a higher temperature steam in the quench cooler, quenching time and by-product formation would increase.

Figure 9.4 shows the significant buildup of coke in the TLX tubes at 42 days total elapsed operational time. Although Alberta Gas Ethylene did not provide exact on-stream times for the quench coolers (verbally estimating them to be between 2 to 3 months), the simulation predicted that the quench cooler would have to be shut down for cleaning at a total elapsed operational time between 48 days and 54 days (Table H.3, Appendix H). Only the simulation of the TLX tube is considered in this prediction.

9.7 Special Considerations - Recommendations

One aspect of the Alberta Gas Ethylene plant not simulated in this work is the fouling of the transfer section between the furnace and the quench cooler inlet with coke, and the similar fouling of the quench cooler inlet tubesheet. This is because equations to handle such coking mechanisms do not yet exist, as discussed in Section 5. As

discussed previously, this coke fouling could have a significant effect on the feed mass flux to the TLX should the TLX tubes become plugged at the inlet manifold. Further investigation of this fouling needs to be done, both to determine the extent of fouling, and the effect the mass flux changes will have on the overall operation of the TLX.

Based on the coking models studied and discussed earlier in this work, a mechanism for coke fouling of these areas can be proposed. A large portion of the coke in ethane pyrolysis is produced by the gas phase secondary reactions in the hottest portion of the furnace (Albright, Crynes and Corcoran, 1983; Rase, 1977a). Since not all the coke formed in the gas phase will deposit on the walls, this coke is carried along in the process stream. Rase (1977a) indicated that any portion of the flow system which contains flow obstructions or surfaces which induce turbulent backmixing such as pipe bends and elbows or cooler inlet manifolds will provide an environment for coke deposition and buildup. Accumulations will be quite heavy on large obstructions such as the quench cooler inlet manifold.

Although the process has been designed to exceed the coke dewpoint throughout, the Alberta Gas Ethylene plant has a long section (1.8 m) of large diameter (200.0 mm) uninsulated pipe connecting the furnace coils to the quench cooler. This transfer section exits the furnace at the bottom, bends 90 degrees, and enters the TLX. The mixing of the furnace

coil streams may produce some turbulent backmixing as will the 90 degree bend. Any coke or tar near the walls of this pipe will be cooled rapidly by contact with the uninsulated pipe wall, which will have a lower temperature than any other portion of the process flow stream due to contact with the atmosphere. The pipe wall temperature at this point will probably be below the dewpoint of the heavier hydrocarbons which produce coke. The combined effects of a low temperature section of pipe, the turbulent eddies of the pipe bend and the mixing of the two coil process streams could lead to conditions ideal for the rapid buildup of coke. Having the shell and tube quench cooler's inlet manifold immediately downstream of this transfer pipe does not improve the situation.

Alberta Gas Ethylene's difficulty with coke production in the transfer line section and the quench cooler inlet is caused in part by the large obstructions to flow these areas provide, as well as the cooling provided by the uninsulated pipe. Insulating the transfer line section would not slow the quench process appreciably. This study did not simulate the transfer section at all, and still produced a quench in the first 1.8 m of the cooler (20.0 ms residence time). Insulating this pipe would keep the tube walls above the dewpoint for tar precursors, and therefore could lessen coke production at this point and could reduce the amount of coke in the process gas stream available for accumulation on the

quench cooler inlet tubesheet. Altering the design of the process to eliminate the bend in the transfer line pipe, or replacing the shell and tube exchanger with a double pipe exchanger would also lengthen overall run times, but no detailed simulation work could be done with this model to determine how much effect either of these suggestions would have on run times.

Another possibility available to Alberta Gas Ethylene to reduce the coke problems is to redesign the overall flow path of the furnace - TLX system. By using more, smaller quench coolers (i.e. one smaller TLX per furnace coil), the turbulence related problems caused by combining the process flow streams at the furnace outlet as discussed above, are eliminated. Additionally, less total coke must be handled by any one TLX (the same mass is now passing through 2 to 4 times as many quench coolers). Using smaller quench coolers is possible in this scheme since the model predicts total quench in less than 2 metres (of the 8 metre TLX). Also, since the same mass is now flowing through more total TLX tubes, the individual tube mass flux is lower, increasing the heat transfer efficiency, lowering the pressure drop, and making the quench coolers more efficient overall.

10.0 Conclusions and Further Study

The model appears to be a good balance between current theory and industrial practice. Although not all reactions and parameters can be quantitatively modelled using the current theories (i.e. coke deposition), the simulation model was able to achieve an excellent history match of an actual industrial quench cooler operated by Alberta Gas Ethylene in Joffre, Alberta.

The parametric modelling study showed the most important input parameters for the quench cooler model were the temperature of the cooling steam, the mass flux of the hydrocarbon feed, the steam dilution ratio, the coke laydown parameter, and the coke thermal conductivity.

The simulation of two coking models proved the coke model employing an analytical integration of the coke thickness equation, currently employed in some other simulators, is incorrect and should be discarded. A second form of the coke thickness calculation was proposed, which solves the equation using numerical integration of the equation over small time steps. The coke thickness calculated at each time step is added to the accumulated coke thickness of all previous time steps. This second form was shown to be more correct, and should be adopted in subsequent simulation work of this type.

The model obtained an excellent match with the simulation study Case 103 of Rase (1977b).

To achieve the history match of the Alberta Gas Ethylene quench coolers, a feed flow geometry of 4 furnace coils combining into one transfer line and then dividing into 108 TLX tubes was used to convert supplied furnace feed data into TLX feed mass fluxes (a flow geometry of 4/108). The supplied steam feed mass flux was doubled. Since two independent sets of supplied TLX data (H143 and HAVG) required the same flow changes to obtain their excellent history matches, I conclude that these flow changes are probably accurate reflections of the actual feed mass fluxes occurring in the Alberta Gas Ethylene plant. It is therefore possible that an error in steam mass flux measurement has been made, and this possibility should be investigated. Should investigation confirm this error in the reported steam feed mass flux, then these model results provide an excellent example of how process simulation modelling can be an extremely useful design tool.

10.1 Areas not Covered in Simulation

The simulation model presented in this work is designed to work with an industrial shell and tube quench cooler or transfer line exchanger (TLX). Double pipe quench coolers were not directly studied (although a rough indication of

the performance of a larger diameter TLX can be obtained by viewing the results of Section 8.3). Other types of reaction quench, such as fluid bed exchangers or direct quenching were also not studied.

Coking in the TLX was not simulated in minute detail due to the lack of rigorous mathematical models to describe important theoretical aspects of the coking process such as surface catalysed reactions and gas phase coke deposition, to name two examples.

The portions of the Alberta Gas Ethylene process most prone to coke problems were not simulated due to lack of rigorous coke models and flow profiles. These included the transfer pipe between the furnace and the quench cooler, and the inlet to the quench cooler, where the single feed divides at the inlet manifold into 108 process streams. Coke plugging of the TLX tubes at the inlet manifold may be a significant problem in the Alberta Gas Ethylene plant, and deserves further investigation.

10.2 Design Considerations

The design of a quench cooler is a delicate balance of a number of critical interdependent parameters. The computer model alone will not provide answers to the best choice of these parameters. However, the computer model is a tool designed to augment the normal design process by providing the designer with a fairly accurate method of quickly testing various design alternatives to see the interaction of various design elements, and the changes they produce in the final model. The computer model can also indicate areas where design calculations may be in error, requiring detailed analysis of the process at that point. Computer models will become increasingly more valuable as the complexity of the design increases. For example, design of newer millisecond cracking processes, in which the process is run at a much greater severity requires more rigorous modelling in order to optimize the overall process, and minimize the production of unwanted by-products (Nighswander, Mehrotra and Behie, 1988).

10.3 Experimental Work

Some of the important input parameters studied in this work are not well understood in a fundamental sense. The

coke laydown parameter and the coke thermal conductivity are critical parameters in the time dependent simulation of the quench cooler. Neither parameter has been studied extensively in relation to the rigorous modelling of actual coke buildup or coke types deposited.

The coke laydown parameter is an empirical attempt to model the incomplete deposition of coke. The current status of coke theory is not much beyond the qualitative stage. Much more detailed experimental work needs to be done to understand the details of coke formation in terms of the amounts or ratios of each type of coke produced, and the actual portion of the produced gas phase coke which is deposited on reaction surfaces. Initially, the best approach might be to obtain a better empirical data for values of the coke laydown parameter under various quench cooler conditions. If an equation for estimating this parameter could be found, then this would allow for more accurate simulation.

Similarly, the actual ratios of coke types produced under a given set of quench cooler (or furnace) conditions, and the resulting properties of that coke would be very useful in better defining the values of coke thermal conductivity to be used in simulations.

More research is needed at all levels (laboratory, pilot plant, and in operating industrial plants) to better understand these variables and provide a mechanism for the de-

sign of improved physical and mathematical descriptions of the processes, leading ultimately to better computer simulation models and much more accurate design work.

11.0 References

Albright, L.F., "Survey of Propane Pyrolysis Literature", Industrial Engineering Chemistry, Process Design Development, 17 (3), 377, (1978)

Albright, L.F., Crynes, B.L. and Corcoran, W.H. (editors), Pyrolysis Theory and Industrial Practice, Academic Press, (1983)

Albright, L.F. and McGill, W.A., "Aluminized Ethylene Furnace Tubes Extend Operating Life", Oil and Gas Journal, August 31, 46, (1987)

Chambers, L.E. and Potter, W.S., "Design Ethylene Furnaces: Part 1: Maximum Ethylene", Hydrocarbon Processing, 53 (1), 121, (1974)

Cooper, B.J. and Trimm, D.L., "Carbon Deposition from Propylene on Polycrystalline and Single Crystal Iron", Journal Catalysis, 62, 35, (1980)

Eng, J.H., McRae, J.R., Behie, L.A., and Luker, P.A., "CSSL's Revisited: Benchmark Models from Chemical and Petroleum Engineering", Proceedings of the 1987 Summer Computer Simulation Conference, Montreal, July 27-30, The Society for Computer Simulation, La Jolla, (1987)

Fanaritis, J.P. and Streich, H.J., "Heat Recovery in Process Plants", Chemical Engineering, May 28, 80, (1973)

Farrow, J.F., "User Guide to Steam Turbines", Hydrocarbon Processing, 50 (3), 71, (1971)

Kumar, P. and Kunzru, D., "Coke Formation During Naphtha Pyrolysis in a Tubular Reactor", Canadian Journal of Chemical Engineering, 65 (4), 280, (1987)

Lichtenstein, I., "Design Cracking Furnaces by Computer", Chemical Engineering Progress, 60 (12), 64, (1964)

Maddock, M.J., "Today's Technology Helps Keep Ethylene Plants Competitive", Oil and Gas Journal, September 3, 60, (1984)

McCabe, W.L. and Smith, J.C., Unit Operations of Chemical Engineering, third edition, McGraw-Hill, (1967)

Mol, A., "Why Revamp Older Steam Crackers?", Hydrocarbon Processing, 57 (7), 179, (1978)

Newsome, D.S. and Leftin, H.P., "Coking Rates in a Laboratory Pyrolysis Furnace", Chemical Engineering Progress, 76, (5), 76, (1980)

Nighswander, J.A., Mehrotra, A.K. and Behie, L.A., "Quench Time Modelling in Propane Ultrapyrolysis", submitted to the Canadian Journal of Chemical Engineering, July, (1988)

Pacey, P.D. and Purnell, J.H., "Propylene from Paraffin Pyrolysis", Industrial Engineering Chemistry, Fundamentals, 11 (2), 233, (1972)

Perry, R.H. and Chilton, C.H., Chemical Engineer's Handbook, fifth edition, McGraw-Hill, (1973)

Petryschuk, W.F. and Johnson, A.I., "The Simulation of an Existing Ethane-Dehydrogenation Reactor", The Canadian Journal of Chemical Engineering, 46 (6), 172, (1968)

Plehiars, P.M. and Froment, G.F., "Reversed Split Coil Improves Ethylene Yields", Oil and Gas Journal, August 17, 41, (1987)

Ranzi, E., Dente, M., Pierucci, S., Barendregt, S. and Cronin, P., "Coking Simulation Aids On-Stream Time", Oil and Gas Journal, September 2, 49, (1985)

Rase, H.F., Chemical Reactor Design for Process Plants, Volume One: Principals and Techniques, John Wiley and Sons, Inc., (1977a)

Rase, H.F., Chemical Reactor Design for Process Plants, Volume Two: Case Studies and Design Data, John Wiley and Sons, Inc., (1977b)

Rice, F.O. and Herzfeld, K.F., "The Thermal Decomposition of Organic Compounds from the Standpoint of Free Radicals. VI. The Mechanism of Some Chain Reactions", Journal of the American Chemical Society, 56 (2), 284, (1934)

Ried, R.C., Prausnitz, J.M. and Sherwood, T.K., The Properties of Gases and Liquids, third edition, McGraw-Hill, (1977)

Rostrup-Nielsen, J. and Trimm, D.L., "Mechanisms of Carbon Formation on Nickel-Containing Catalysts", Journal Catalysis, 48, 155, (1977)

Schutt, H.C., "Light Hydrocarbon Pyrolysis ... The Effects of Pressure and Equilibrium Approach", *Chemical Engineering Progress*, 55 (1), 68, (1959)

Slotboom, H.W. and Penninger, J.M.L., "The Role of the Reactor Wall in the Thermal Hydrocracking of Polyaromatic Compounds", *Industrial Engineering Chemistry, Process Design Development*, 13 (3), 296, (1974)

Smith, J.M., Chemical Engineering Kinetics, third edition, McGraw-Hill, (1981)

Snow, R.H. and Schutt, H.C., "Design of an Ethane Pyrolysis Reactor", *Chemical Engineering Progress*, 53 (3), 133-M, (1957)

Sundaram, K.M. and Froment, G.F., "Modelling of Thermal Cracking Kinetics - 1. Thermal Cracking of Ethane, Propane and Their Mixtures", *Chemical Engineering Science*, 32, 601 (1977)

Sundaram, K.M. and Froment, G.F., "Kinetics of Coke Deposition in the Thermal Cracking of Propane", *Chemical Engineering Science*, 34, 635, (1979)

Sundaram, K.M., Van Damme, P.S. and Froment, G.F., "Coke Deposition in the Thermal Cracking of Ethane", *AIChE Journal*, 27 (6), 946, (1981)

Sundstrom, D.W. and DeMichiell, R.L., "Quenching Processes for High Temperature Chemical Reactions", *Industrial Engineering Chemistry, Process Design Development*, 10 (1), 114, (1971)

Trimm, D.L., "The Formation and Removal of Coke from Nickel Catalyst", *Catalyst Review - Science Engineering*, 16 (2), 155, (1977)

Unauthored, "Refinery and Petrochemical Report", *Oilweek*, June 20, 12, (1988)

Van Camp, C.E., Van Damme, P.S., Willems, P.A., Clymans, P.J. and Froment, G.F., "Severity in the Pyrolysis of Petroleum Fractions. Fundamentals and Industrial Application", *Industrial Engineering Chemistry, Process Design Development*, 24 (3), 561, (1985)

Van Damme, P.S., Willems, P.A. and Froment, G.F., "Temperature, Not Time, Controls Steam Cracking Yields", *Oil and Gas Journal*, September 3, 68, (1984)

Weast, R.C., Handbook of Chemistry and Physics, 60th edition, Chemical Rubber Company, (1972)

Zdonik, S.B., Green, E.J. and Hallee, L.P., Manufacturing Ethylene, The Petroleum Publishing Company, (1970)

12.0 Appendices

- Appendix A. General Equations
- Appendix B. Continuity Equation
- Appendix C. Heat Transfer Equation
- Appendix D. Momentum Equation
- Appendix E. Reaction Rates
- Appendix F. Coke Thickness
- Appendix G. Quench Cooler Computer Program
Flowchart
- Appendix H. Summary of Computer Runs and Results
- Appendix I. Typical Computer Run Output
Listing - Run 6
- Appendix J. Quench Cooler ACSL Program Listings
- Appendix K. Program Run Post Processing

Appendix A. General Equations

A differential element of the tubular plug flow reactor modelled is shown in Figure A.1. All equations were derived for this differential element of quench cooler pipe.

A.1 Pipe Diameters

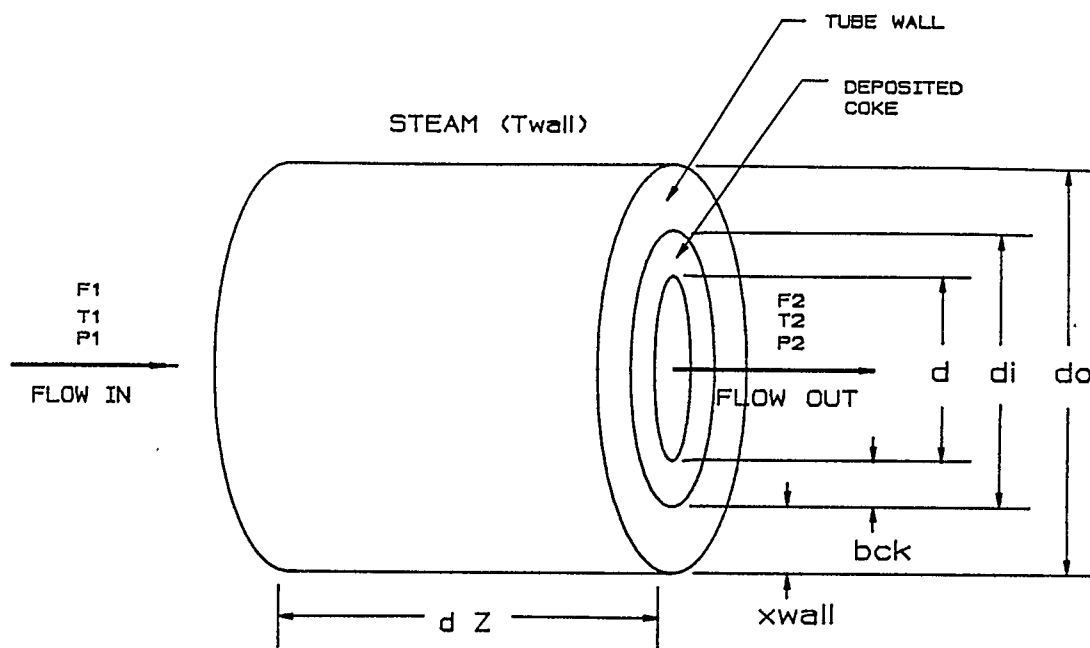
The inside diameter of the pipe, d_i , is the diameter of the pipe as specified at clean tube conditions. The diameter of the pipe available for flow of pyrolysis process stream is d . Both d_i and d can be calculated from the outside pipe diameter, d_o . The value of d may also be calculated from the original (clean) pipe inner diameter, d_i .

$$d_i = d_o - 2 (x_{\text{wall}})$$

$$d = d_o - 2 (x_{\text{wall}}) - 2 (b_{\text{ck}})$$

$$d = d_i - 2 (b_{\text{ck}})$$

where x_{wall} is the pipe wall thickness, and b_{ck} is the thickness of coke.



DIFFERENTIAL ELEMENT OF A QUENCH COOLER (TLX) PIPE

Figure A.1 Differential Element of a Plug Flow Reactor
Showing Pertinent Calculation Variables

Additional diameters required in the calculations are based on these diameters, and are:

$$D_{ck} = d - b_{ck}$$

$$D = d + x_{wall}$$

A.2 Cross Sectional Area of Pipe

The area of the pipe open to flow in the system is calculated as

$$A = \pi \left[\frac{d_i}{2} \right]^2$$

where d_i is the inside diameter of the pipe

A.3 Inside Perimeter of the Pipe

The inside perimeter of the pipe is required in the coke rate expression. It is calculated as

$$S = \pi d_i$$

A.4 Reynolds Number

The Reynolds number is required in the heat transfer equations and in the pressure drop equations. A standard form of the Reynolds number is used:

$$\text{Re} = \frac{G d}{\mu_m}$$

where G is the mass flux of the process stream, and μ_m is the mixed process stream viscosity.

A.5 Prandtl Number

The Prandtl number is required in the heat transfer calculations, and is given as

$$\text{Pr} = \frac{C_{pm} \mu_m}{k_{fm}}$$

where C_{pm} is the process stream average heat capacity, μ_m is the mixed process stream viscosity, and k_{fm} is the heat transfer coefficient for the process stream.

A.6 Fluid Heat Capacity

The overall heat capacity of the process stream is calculated using standard component based mixing rules:

$$C_{pm} = \sum_i Y_i C_{pi} \quad ; \quad (i = 1 \text{ to number of components, } nc)$$

The component heat capacities are calculated from a polynomial expression provided by the CRC handbook (Weast, 1972):

$$C_{pi} = C_{pA} + C_{pB} T + C_{pC} T^2 + C_{pD} T^3$$

The values for the coefficients in this heat capacity polynomial are given in Table A.1. Temperature is in degrees Kelvin.

Table A.1 Component Thermal Properties

COMPONENT	MW	T _c	P _c	C _{pA}	C _{pB}	C _{pC}	C _{pD}	H _f
HYDROGEN	2.016	33.2	12.8	6.483	2.215e-3	-3.298e-6	1.826e-9	0.0
METHANE	16.043	190.6	45.4	4.598	1.245e-2	2.860e-6	-2.703e-9	-17890.0
ACETYLENE	26.038	308.3	60.6	6.406	1.810e-2	-1.196e-5	3.363e-9	54190.0
ETHYLENE	28.054	282.4	49.7	0.909	3.740e-2	-1.994e-5	4.192e-9	12500.0
ETHANE	30.070	305.4	48.2	1.292	4.254e-2	-1.657e-5	2.081e-9	-20240.0
PROPYLENE	42.081	365.0	45.6	0.886	5.602e-2	-2.771e-5	5.266e-9	4880.0
PROPANE	44.097	369.8	41.9	-1.009	7.315e-2	-3.789e-5	7.678e-9	-24820.0
1,3-BUTADIENE	54.092	425.0	42.7	-0.403	8.165e-2	-5.589e-5	1.513e-8	26330.0
COKE	12.000	-----	-----	2.673	2.617e-3	0.0	0.0	0.0
STEAM	18.015	647.3	217.6	7.701	4.595e-4	2.521e-6	-0.859e-9	

Definition of component data:

H_2 = c1 (hydrogen)"
 CH_4 = c2 (methane)"
 C_2H_2 = c3 (acetylene)"
 C_2H_4 = c4 (ethylene)"
 C_2H_6 = c5 (ethane)"
 C_3H_8 = c6 (propylene)"
 C_3H_8 = c7 (propane)"
 C_4H_8 = c8 (1,3-butadiene)"
 C_4H_6 = c9 (coke)"

Definition of Property Units:

MW - molecular weight - g/g-mol
 T - critical tempereare - K
 P_c - critical pressure - atm
 C - heat capacity coefficient - cal/g-mol·K₂
 C_{pA} - heat capacity coefficient - cal/g-mol·K₂
 C_{pB} - heat capacity coefficient - cal/g-mol·K₃
 C_{pC} - heat capacity coefficient - cal/g-mol·K₄
 C_{pD} - heat capacity coefficient - cal/g-mol·K₄
 H_f - heat of formation - cal/g-mol

A.7 Component Viscosity

The component viscosity for the process stream components is given by Rase (1977a) as:

$$\mu_i = \mu_{ri} \mu_{cri}$$

where

$$\ln (\mu_{ri})^{0.2} = (-0.1208 + 0.1354 \ln (T / T_{ci}))$$

$$\mu_{cri} = 7.70 MW_i^{1/2} P_{ci}^{2/3} T_{ci}^{-1/6}$$

The values of P_{ci} and T_{ci} were obtained from Perry and Chilton (1973) and are given in Table A.1.

A.8 Process Stream Mixed Viscosities

The mixing rule for the process stream viscosity as provided by Rase (1977a) is:

$$\mu_m = \frac{\sum_i Y_i \mu_i (MW_i)^{1/2}}{\sum_i Y_i (MW_i)^{1/2}} \quad ; (i = 1 , nc)$$

A.9 Average Process Stream Molecular Weight

The mixing rule for molecular weight of the process stream is similar to the heat capacity mixing rule:

$$MW_m = \sum_i Y_i MW_i \quad ; (i = 1 , nc)$$

A.10 Total Molar Flow Rate and Mole Fractions

The total molar flow rate is defined as the sum of the individual molar flows:

$$F_{tot} = \sum_i F_i \quad ; (i = 1 , nc)$$

The total hydrocarbon flow rate is the same as the total molar flow rate, except the steam term is not included.

$$F_{\text{tothc}} = \sum_i F_i \quad ; (i = 1, \text{nc})$$

(not including steam)

Given the molar flow rates and the total molar flow rate, the individual component mole fractions may be calculated:

$$Y_i = F_i / F_{\text{tot}}$$

The hydrocarbon mole fractions are calculated in a similar fashion:

$$x_i = F_i / F_{\text{tothc}}$$

A.11 Conversion

The conversion of any component is defined as

$$X_i = (F_i^{\circ} - F_i) / F_i^{\circ}$$

where F_i° is the initial molar flow rate of that component.

A.12 Process Stream Density

The density of the gaseous process stream is given by the equation

$$\rho_f = \frac{P_t \text{ MW}_m}{R T}$$

This equation is based on the ideal gas law, and is accurate enough for the model as it currently exists.

A.13 Fluid Velocity

The fluid velocity of the process stream is a function of the mass flux and the fluid density:

$$U_m = \frac{G}{\rho_f}$$

A.14 Mass Flux

The mass flux of the process stream is calculated at all points in the cooler (excepting the inlet, which is defined in the input data) using the formula:

$$G = F_{\text{tot}} * MW_m / A$$

A.15 Residence Time

Chambers and Potter (1974) define the residence time of the process stream, calculated at any point z in the cooler length L as:

$$t_r = \frac{z}{U_m}$$

The total fluid velocity (U_m) is a function of process stream density and the mass flux. Both of these variables are functions of the component molar flow rates, which are primary variables in the continuity equation. Because the primary variables are solved rigorously for the cooler, these derived variables will also change as a function of the overall reaction. Therefore, this equation represents a rigorous solution to the residence time equation in the context of this simulation model.

Appendix B. Continuity Equation

In general terms, the mass balance equation for a differential volume element in a tubular plug flow reactor is given as

$$\text{Mass in} - \text{Mass out} + \text{Mass generated} = \text{Mass Accumulated}$$

B.1 Flowing Component Mass Balance

The specific form of this equation for fluid flowing in a tubular plug flow tubular reactor is

$$\frac{d F_i}{d z} = A \sum_j s_{ij} r_j$$

where the summation term is a summation of all j reactions with stoichiometric coefficient (s_{ij}) for component i . For a gaseous flowing system, the molar flow rates of species i is used.

The accumulation term is assumed to be zero for all components except coke, which is treated as a special case in a later section.

Figure B.1 shows the overall reactions contributing to

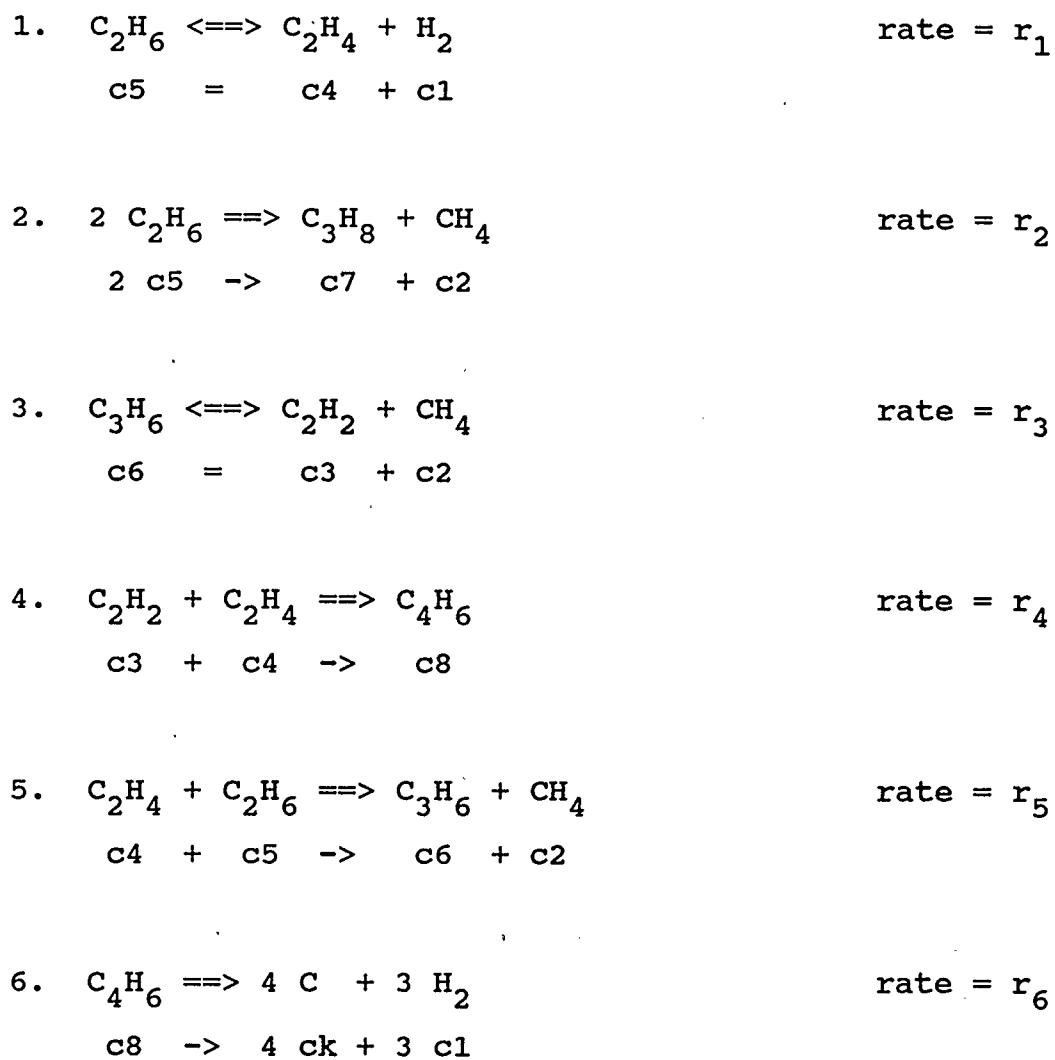


Figure B.1 Ethane Pyrolysis Reactions

(Sundaram and Froment, 1977;

Sundaram, Van Damme and Froment, 1981)

the mass balance.

Taking all components and reactions together, the mass balances on each component are:

1. Hydrogen:

$$\frac{d F_1}{d z} = A (r_1 + 3r_{6*})$$

2. Methane:

$$\frac{d F_2}{d z} = A (r_2 + r_3 + r_5)$$

3. Acetylene:

$$\frac{d F_3}{d z} = A (r_3 - r_4)$$

4. Ethylene:

$$\frac{d F_4}{d z} = A (r_1 - r_4 - r_5)$$

5. Ethane:

$$\frac{d F_5}{d z} = A (-r_1 - 2r_2 - r_5)$$

6. Propylene:

$$\frac{d F_6}{d z} = A (r_5 - r_3)$$

7. Propane:

$$\frac{d F_7}{d z} = A (r_2)$$

8. 1,3 Butadiene:

$$\frac{d F_8}{d z} = A (r_4 - r_{6*})$$

9. Coke:

$$\frac{d F_{ck}}{d z} = S (4r_6)$$

The convention used in the above mass balance equations is that production of a component is positive, while depletion of a component by reaction is negative.

There are three equations which use the coke reaction rate. The first two, equations 1 and 7, use a form of the coke rate expressed (r_{c*}) in units of coke rate per unit volume. The coke rate (r_c) used in equation 8 is expressed in units of coke rate per unit area.

B.2 Units

The units of all of the mass balance equations are mol/s. The reaction rates are in $\text{mol/m}^3 \cdot \text{s}$ (or $\text{mol/cm}^3 \cdot \text{s}$), except for the coke rate which is in $\text{mol/m}^2 \cdot \text{s}$ (or $\text{mol/cm}^2 \cdot \text{s}$). Area is in m^2 (or cm^2) and tube perimeter is in m (or cm).

Appendix C. Heat Transfer Equation

The heat balance on a differential element of the tubular plug flow reactor produces an expression analogous to the mass balance expression:

$$\text{Heat in} - \text{Heat out} + \text{Heat Generated} = \text{Heat Accumulated}$$

A common form of this equation is found in Smith:

$$\frac{dT}{dz} = \frac{1}{\sum_i F_i C_{pi}} \left[S U_o (T_w - T) + A \sum_j r_j (-\Delta H_{rj}) \right]$$

; (i = 1 , nc)

This equation is used to solve for the change in temperature in the gas process stream over a differential volume of the cooler. The driving force of the temperature change is both the heat change due to reaction, and the temperature difference between the shell side steam and the process stream.

C.1 Heat Generated or Removed by Reaction

The heat generated or removed by the chemical reaction in the quench cooler is contained in the above equation in

the term $(-\Delta H_{rj})$. This term expands to become:

$$\Delta H_r = \Delta H_r^\circ + \int_{T_0}^T \Delta C_p \, dT$$

For each reaction this equation can be written

$$\Delta H_{rj} = \sum_i s_{ij} \Delta H_{fi}^\circ + \int_{T_0}^T \left[\sum_i s_{ij} \Delta C_{pi} \right] dT$$

; (i = 1 , nc)

The heat of reaction is a summation of the individual reaction components, multiplied by their stoichiometric coefficient in the reaction. The heat of reaction at standard temperature (298 K) is a summation of the component heats of formation. Temperature correction to process temperature is accomplished by adding the reaction change in heat capacity due to the temperature difference.

C.1.1 Heats of Reaction

The heat of reaction is a stoichiometric sum of all reaction species heats of formation. Table A.1 gives the heat

of formation for each component, as obtained from the CRC handbook. For the ethane pyrolysis reactions, the standard temperature heat of reactions are:

1. $\Delta H_{r1}^{\circ} = \Delta H_{fc4}^{\circ} + \Delta H_{fc1}^{\circ} - \Delta H_{fc5}^{\circ}$
2. $\Delta H_{r2}^{\circ} = \Delta H_{fc7}^{\circ} + \Delta H_{fc2}^{\circ} - 2 \Delta H_{fc5}^{\circ}$
3. $\Delta H_{r3}^{\circ} = \Delta H_{fc3}^{\circ} + \Delta H_{fc2}^{\circ} - \Delta H_{fc6}^{\circ}$
4. $\Delta H_{r4}^{\circ} = \Delta H_{fc8}^{\circ} - \Delta H_{fc3}^{\circ} - \Delta H_{fc4}^{\circ}$
5. $\Delta H_{r5}^{\circ} = \Delta H_{fc6}^{\circ} + \Delta H_{fc2}^{\circ} - \Delta H_{fc4}^{\circ} - \Delta H_{fc5}^{\circ}$
6. $\Delta H_{r6}^{\circ} = 4 \Delta H_{fck}^{\circ} + 3 \Delta H_{fc1}^{\circ} - \Delta H_{fc8}^{\circ}$

C.1.2 Delta Heat Capacities

The heat capacity integral

$$\int_{T_0}^T \left[\sum_i s_{ij} \Delta C_{pi} \right] dT \quad ; (i = 1, nc)$$

can be solved by first expanding the value of C_p to the polynomial form provided in the CRC handbook (Weast, 1972).

$$C_{pi} = C_{pAi} + C_{pBi} T + C_{pCi} T^2 + C_{pDi} T^3$$

Substitution into the integral and integrating gives

$$\left| \sum_i s_{ij} \left[C_{pAi} T + \frac{1}{2} C_{pBi} T^2 + \frac{1}{3} C_{pCi} T^3 + \frac{1}{4} C_{pDi} T^4 \right] \right|_{T_0}^T ; (i = 1, nc)$$

which, when evaluated between T and T_0 , reduces to the form

$$\int_{T_0}^T \left[\sum_i s_{ij} C_{pi} \right] dT = \left[\sum_i s_{ij} C_{pAi} (T - T_0) + \frac{1}{2} \sum_i s_{ij} C_{pBi} (T - T_0)^2 + \frac{1}{3} \sum_i s_{ij} C_{pCi} (T - T_0)^3 + \frac{1}{4} \sum_i s_{ij} C_{pDi} (T - T_0)^4 \right] ; (i = 1, nc)$$

The use of the reaction sums with stoichiometric coefficients will provide values for C_{pA} , C_{pB} , C_{pC} and C_{pD} for each reaction similar in form to those shown for the heat of reaction, Section C.1.1. For each reaction, a general form of the heat capacity coefficient, C_{pN} is

1. $C_{pNr1} = C_{pNc4} + C_{pNc1} - C_{pNc5}$
2. $C_{pNr2} = C_{pNc7} + C_{pNc2} - 2 C_{pNc5}$
3. $C_{pNr3} = C_{pNc3} + C_{pNc2} - C_{pNc6}$
4. $C_{pNr4} = C_{pNc8} - C_{pNc3} - C_{pNc4}$
5. $C_{pNr5} = C_{pNc6} + C_{pNc2} - C_{pNc4} - C_{pNc5}$
6. $C_{pNr6} = 4 C_{pNck} + 3 C_{pNc1} - C_{pNc8}$

C.2 Heat Transfer

The heat transfer term in the heat balance equation is $U_o (T_{wall} - T)$. This represents the transfer of heat from the process stream to the steam in the shell side of the quench cooler. The driving force for this heat transfer is the temperature difference between the steam and the process stream. The term U_o represents the resistance to heat transfer, and is composed of a number of series resistances to heat transfer. These resistances consist of the resistance of the process gas stream, the coke layer, the tube wall, and the shell side steam. The equation used to solve for U_o is provided by Rase (1977a):

$$\frac{1}{U_o} = \frac{1}{h_i} \frac{d_o}{d} + \frac{b_{ck}}{k_{ck}} \frac{d_o}{D_{ck}} + \frac{x_{wall}}{k_{wall}} \frac{d_o}{D} + \frac{1}{h_o}$$

The individual heat transfer terms are determined from empirical equations, also provided by Rase (1977a). These equations use British units. For simplicity, the entire equation is calculated in British units, and then converted to the metric system for integration into the overall quench cooler model.

C.2.1 Inner (Process Stream) Thermal Resistance

The process stream resistance to the heat transfer is

$$\frac{1}{h_i} \frac{d_o}{d}$$

where h_i is defined by the empirical equation of Rase (1977a) as

$$h_i = \frac{0.021 \text{ Re}^{0.8} \text{ Pr}^{0.4} k_{fm}}{(T_{wall} / T)^{(0.29 + 0.0019 z/D)} d}$$

This formula is valid for the range

$$\begin{aligned}
 10 < L/D < 240 \\
 200 < T < 2800 \text{ (R)} \\
 1.1 < T_{\text{wall}} / T < 8.0
 \end{aligned}$$

This formula assumes h_i will change as both the process stream temperature and flow rates change.

C.2.2 Process Stream Heat Transfer Coefficient

The value of k_{fm} is calculated from the empirical formula of Rase (1977a)

$$k_{fm} = \frac{\mu_m C_{vm}}{MW_m} \left[\frac{3.670}{C_{vm}} + 1.272 \right]$$

This equation is valid for the same process flow conditions given in the previous section. The value of C_{vm} is defined as

$$C_{vm} = C_{pm} - 1.99$$

C.2.3 Outer (Shell Side) Thermal Resistance

The thermal resistance due to the steam is given as $1/h_o$. The value of h_o used in normal shell and tube quench

coolers with saturated steam on the shell side of the exchanger is 2040 Btu/hr·ft²·F. This value is assumed constant for all model conditions.

C.2.4 Wall Thermal Resistance

The wall of the quench cooler contributes resistance to the transfer of heat from the process stream to the steam by the term

$$\frac{x_{\text{wall}}}{k_{\text{wall}}} \frac{d_o}{D}$$

The value of k_{wall} is given by Rase (1977a) as

$$k_{\text{wall}} = 14.1 + 0.00433 (T_{\text{far}} - 1300)$$

This is an average value of k_{wall} for steel pipe, and will change if the temperature of the process stream changes.

C.2.5 Coke Thermal Resistance

The thermal resistance to heat flow provided by the coke is given by the expression

$$\frac{b_{ck}}{k_{ck}} \frac{d_o}{D_{ck}}$$

This expression, provided by Rase (1977a) is dependent on the thickness of coke, and on the thermal conductivity of the coke. Values provided in literature for k_{ck} range from a low of 0.32 to a standard value of 3.2 and a high value of 44.0 (Btu/hr·ft²·F)

C.3 Units

The units used in the heat balance for this simulation are primarily British units. This is because the empirical equations employed in the overall heat transfer coefficient calculation are in British units. Heat transfer coefficients are in Btu/hr·ft²·F (SI = W/m²·K). Heat capacities are in cal/g·mol·K (SI = J/mol·K) which is equivalent to the required Btu/lb-mole·R. Viscosity is in lb/hr·ft (SI = Pa·s). This can be converted from the calculated viscosity values of centipoise (cP) by multiplying by 2.42. Once the overall heat transfer coefficient, U_o , is calculated, the value is converted to units of cal/cm²·s·K (SI = W/m²·K) for integration into the rest of the model calculations.

Although SI units are normally used, the empirical nature of the equations and the supplied data requires the use of the units noted above.

Appendix D. Momentum Equation

D.1 Pressure Drop

The Fanning pressure drop equation for turbulent flow in a straight pipe as provided by McCabe and Smith (1967) is used in the model.

$$\frac{dP}{dz} = \frac{\rho_f U_m^2 f}{2 g_c d} = \frac{G^2 f}{2 g_c d \rho_f}$$

The pressure drop in a straight pipe depends on the mass flux, the density of the fluid flowing and the friction factor of the pipe. The density of the fluid will change as the component mixture changes due to reaction.

D.1.1 Friction Factor

The friction factor for smooth pipe as used in this model is given by Rase (1977a):

$$f = 0.184 \text{ Re}^{-0.2}$$

The Reynolds number is defined in Appendix A, Section

A.4.

The friction factor will change as coke deposits change the roughness of the pipe. However, no quantitative means for estimating this change exists. Calculations indicate the change would be less than 10%, and so the effect can be ignored until better data is available.

D.2 Units

The pressure drop equation is calculated in cgs units for compatibility with the units used in the other equations of the model. The actual pressure drop is in absolute atmospheres (atm). The units of mass flux are $\text{g}/\text{cm}^2 \cdot \text{s}$ and the units of velocity are cm/s . SI units for the above equations are kPa for pressure, $\text{kg}/\text{m}^2 \cdot \text{s}$ for mass flux and m/s for velocity.

Appendix E. Reaction Rates

Figure B.1 shows the six reactions which are used as the basis for the reaction equations used in this model.

E.1 Reaction Rate Equations

Sundaram and Froment (1977) and Sundaram, Van Damme and Froment (1981) give the reaction rate equations for each reaction used in this model. These equations are given in Table E.1.

E.2 Reaction Rate Constants

The rate constants for each reaction in Table E.1 are found for a given temperature by solving the Arrhenius equation for each reaction:

$$k_j = A_j e^{(-E_j / R T)}$$

They used laboratory and pilot plant data to determine the values for the reaction constant and the activation energy. By solving for these parameters using a least squares technique, they obtained values for these parameters. These values were then tested in actual plant simulations.

Table E.1 Ethane Pyrolysis Reaction Rates(Sundaram and Froment, 1977;Sundaram, Van Damme and Froment, 1981)

Equation	units of k_j
$r_1 = k_1 (P_5 - P_4 P_1 / Kc_1)$	1/s
$r_2 = k_2 (P_5)$	1/s
$r_3 = k_3 (P_6 - P_3 P_2 / Kc_3)$	1/s
$r_4 = k_4 (P_3 P_4)$	$\text{cm}^3/\text{mol}\cdot\text{s}$
$r_5 = k_5 (P_4 P_5)$	$\text{cm}^3/\text{mol}\cdot\text{s}$
$r_6 = k_6 (P_8) (MW_8 / MW_{ck})$	$\text{g}_{ck}/\text{g}_{C4+}\cdot\text{s}$

where

$$P_i = \frac{F_i P_t}{F_{\text{tot}} R T} \quad (\text{mol}/\text{cm}^3)$$

$$r_j = \text{mol}/\text{cm}^3\cdot\text{s} \quad \text{except for}$$

$$r_6 = \text{mol}/\text{cm}^2\cdot\text{s}$$

$$Kc_j = \text{mol}/\text{cm}^3$$

The values reported by Sundaram and Froment (1977) and Sundaram, Van Damme and Froment (1981) are given in Table E.2.

This data is generally accepted in industry as representing the best currently available rate data for the ethane pyrolysis reaction system.

E.3 Equilibrium Constants

The Kc_j values used in the two reversible reactions shown in Figure B.1 were determined by Sundaram and Froment (1977) in a similar manner to that described above for the main reaction rates. These values were calculated at various temperatures. The raw data as provided by Sundaram and Froment (1977) is given in Table E.2. A plot of these values at different temperatures, shown in Figure E.1, shows a linear relationship between $\ln(Kc)$ and temperature. The resulting formula for the two equilibrium constants is

$$Kc_1 = .001 e^{(-19.496 + .014098 T)}$$

$$Kc_3 = .001 e^{(-18.286 + .013040 T)}$$

Both values of Kc are in units of mol/cm^3 .

Table E.2 Ethane Pyrolysis Rate Constants(Sundaram and Froment, 1977;Sundaram, Van Damme and Froment, 1981)A. Main Rate Constants

$$\text{EQUATION: } k_j = A' e^{(-E / R T)}, T \text{ (K)}$$

k_j	A'	units of A'	E (cal/mol)
1	$4.652 \cdot 10^{13}$	1/s	65200
2	$3.850 \cdot 10^{11}$	1/s	65250
3	$9.814 \cdot 10^8$	1/s	36920
4	$1.026 \cdot 10^{15}$	$\text{cm}^3/\text{mol} \cdot \text{s}$	41260
5	$7.083 \cdot 10^{16}$	$\text{cm}^3/\text{mol} \cdot \text{s}$	60430
6	$8.550 \cdot 10^4$	$\text{g}_{\text{ck}} \cdot \text{cm}/\text{g}_{\text{C4+}} \cdot \text{s}$	28250

B. Equilibrium Constants

$$\text{EQUATION: } Kc_j = e^{(A + B T)}, T \text{ (K)}$$

T (K)	Kc_1 (mol/L)	Kc_3 (mol/L)
1048.15	$8.895 \cdot 10^{-3}$	$9.849 \cdot 10^{-3}$
1073.15	$1.276 \cdot 10^{-2}$	$1.375 \cdot 10^{-2}$
1098.15	$1.800 \cdot 10^{-2}$	$1.890 \cdot 10^{-2}$

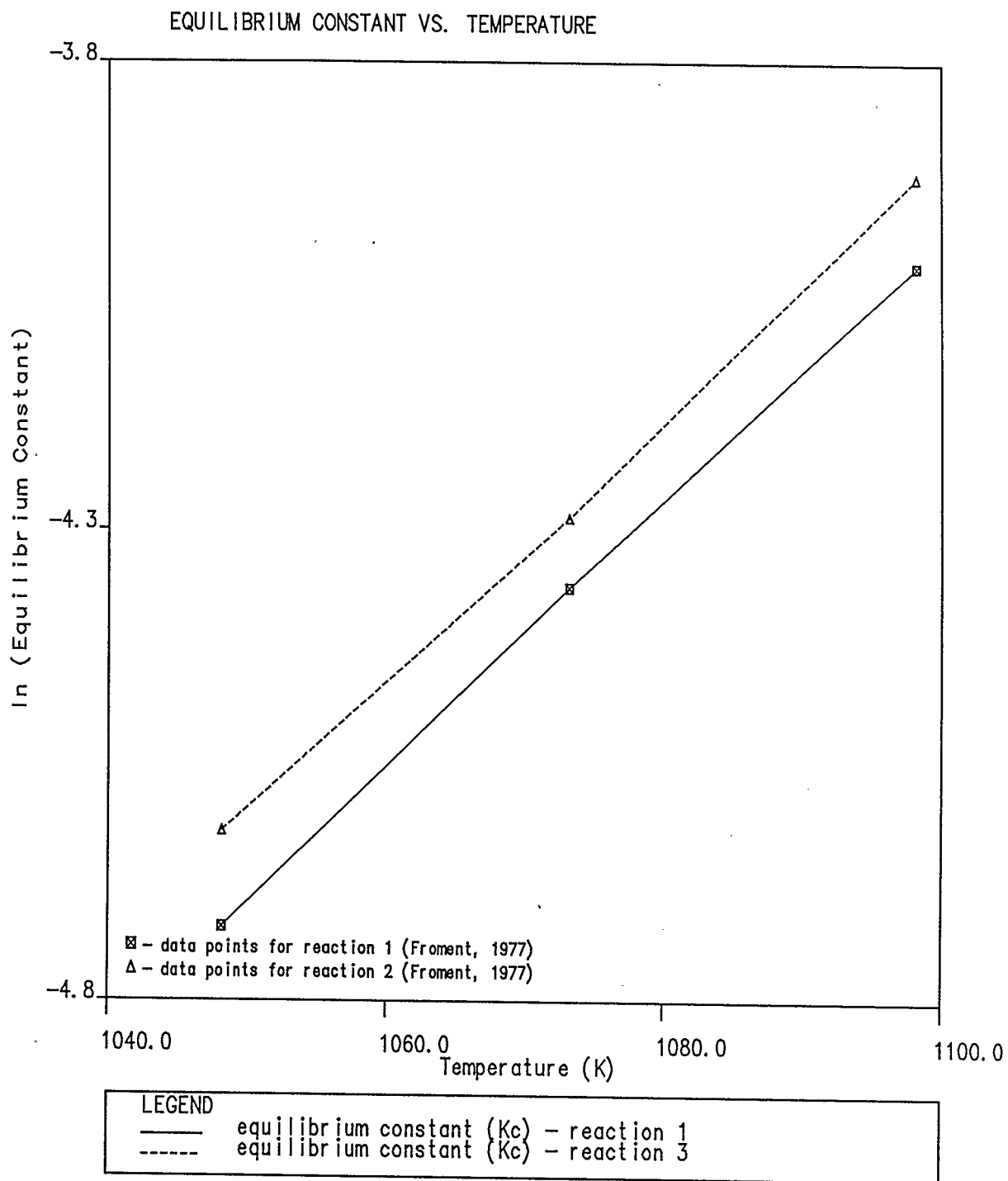


Figure E.1 Plot of Equilibrium Constants for Ethane Pyrolysis Reactions 1 and 3 (Froment, 1977)

Appendix F. Coke Thickness

This model used two forms of the coke thickness calculation. Both forms have a common derivation, but the actual implementation of each form is different.

F.1 Derivation of the Basic Coke Thickness Equation

The calculation of the change in coke thickness with time is based on the mass balance of a differential volume of the quench cooler pipe, as shown in Figure A.1. The mass balance on this element, assuming coke in - out = 0 is

$$\frac{d n_{ck}}{d t} = \alpha r_{ck} \frac{\pi d^2}{4}$$

where d is the diameter of the reaction tube including coke buildup and n_{ck} is the moles of coke produced.

This equation can also be written in terms of the area available for flow:

$$\frac{d n_{ck}}{d t} = \alpha r_{ck} A$$

Either form of this equation describing the change in moles of coke with time can be used in further derivations of the two coke thickness models.

F.2 Integrated Coke Thickness Equation

Starting with the expanded form of the coke rate expression shown above:

$$\frac{d n_{ck}}{d t} = \alpha r_{ck} \frac{\pi d^2}{4}$$

The following derivation is similar to the one used by Lichtenstein (1964).

Defining the moles of coke produced per unit length of the quench cooler:

$$n_{ck} = \frac{\pi (d_i^2 - d^2) \rho_{ck}}{4 MW_{ck}}$$

Take the time derivative of the above equation:

$$\frac{d n_{ck}}{d t} = - \frac{\pi d \rho_{ck}}{2 MW_{ck}} \frac{d d}{d t}$$

Defining the coke thickness as

$$b_{ck} = \frac{1}{2} (d_i - d)$$

and the derivative of the above as

$$d d = - 2 d b_{ck}$$

Substituting this into the time derivative above gives

$$\frac{d n_{ck}}{d t} = \left[\frac{\pi d \rho_{ck}}{MW_{ck}} \right] d \left[\frac{d b_{ck}}{d t} \right]$$

Substituting the above equation for the change in moles of coke in the original coke rate expression produces

$$\frac{d b_{ck}}{d t} = \frac{\alpha r_{ck} MW_{ck} d}{4 \rho_{ck}}$$

Rearranging and substituting for d ; $d = (d_i - 2 b_{ck})$

$$\frac{d b_{ck}}{d_i - 2 b_{ck}} = \frac{\alpha r_{ck} MW_{ck}}{4 \rho_{ck}} d t$$

At this point, the integral form of the coke expression and the differential form of the coke buildup equation are equivalent. The fundamental difference in the two coke mod-

els is in how the next step, integration of the equation, is handled.

The integral of the above equation to solve for coke thickness as a function of time is:

$$\int_0^{b_{ck}} \frac{d b_{ck}}{d_i - 2 b_{ck}} = \int_{t_0}^t \frac{\alpha r_{ck} MW_{ck}}{4 \rho_{ck}} d t$$

The fundamental assumption required for the first coke buildup model (the integrated form of the coke equation) is that the reaction rate of coke does not vary significantly over the time range of interest. If this assumption is allowed, the right hand side of the above equation becomes a simple integral of time:

$$\int_0^{b_{ck}} \frac{d b_{ck}}{d_i - 2 b_{ck}} = \frac{\alpha r_{ck} MW_{ck}}{4 \rho_{ck}} \int_{t_0}^t d t$$

This integral is now solved:

$$\frac{1}{2} \ln \left[\frac{d_i}{d_i - 2 b_{ck}} \right] = \frac{\alpha r_{ck} MW_{ck} t}{4 \rho_{ck}}$$

Taking the antilog of both sides of the above equation and rearranging to solve for the coke thickness gives the

final form of the equation used in coke model one. This is also the coke thickness equation provided by Rase (1977a) and derived by Lichtenstein (1964).

$$b_{ck} = \frac{1}{2} d_i \left[1 - e \left[- \frac{\alpha r_{ck} MW_{ck} t}{2 \rho_{ck}} \right] \right]$$

This form of the coke thickness equation calculated the total coke thickness for any total simulation time t . The expression assumes the coke rate does not change with time. If the rate does change with time, then the overall value of b_{ck} at some later time in the simulation will be different than a value of b_{ck} calculated using the original rate. Since the coke thickness is not accumulated between timesteps, but is rather calculated entirely from this equation at any time, the difference between the coke calculated with an initial coke rate and that calculated with a later coke rate is an error which cannot be corrected.

F.2.1 Units

The only modification made to the above formula for the overall coke thickness is to convert the units of the coke reaction rate from area units to surface units as required by the above expression. This is done by multiplying the

reaction rate by the ratio S / A :

$$r_{ck} \frac{S}{A} = r_{ck} \frac{\frac{d_i^2}{4}}{\frac{d_i^2}{4}} = \frac{4}{d_i^2} r_{ck} S$$

F.3 Differential Coke Thickness Equation

The second form of the coke thickness equation used in the computer model begins with the equation for change in moles of coke with time as shown in Section F.1

$$\frac{d n_{ck}}{d t} = \alpha r_{ck} A$$

Defining the moles of coke produced per unit length of the TLX as was done in section F.1:

$$n_{ck} = \frac{\pi (d_i^2 - d^2) \rho_{ck}}{4 MW_{ck}}$$

The area of the pipe filled with coke for a unit length of the quench cooler pipe is defined as the difference in the original inside area of the pipe less the current area of the pipe open to flow

$$A_{ck} = A_i - A$$

or in terms of the pipe diameters:

$$A_{ck} = \frac{\pi (d_i^2 - d^2)}{4}$$

Substituting this equation into the above definition for the moles of coke gives:

$$n_{ck} = \frac{A_{ck} \rho_{ck}}{MW_{ck}}$$

Combining this equation with the change in moles of coke with time and rearranging gives:

$$\frac{d A_{ck}}{A} = \frac{\alpha r_{ck} MW_{ck}}{\rho_{ck}} dt$$

$$\text{Substituting for } A = \frac{\pi d^2}{4} \text{ and } A_{ck} = \frac{\pi (d_i^2 - d^2)}{4}$$

$$\text{where } d A_{ck} = \frac{\pi}{4} (d_i^2 - d^2) dd$$

and integrating both sides of the equation gives between the limits d to d_i and t to $t + \Delta t$ gives

$$d_i - d = \frac{\alpha r_{ck} MW_{ck}}{\rho_{ck}} \Delta t$$

For any small change in time, if the coke reaction rate and density can be assumed constant, then the above integration for the small time change can be performed. Substituting for the coke thickness gives the final equation for the change in coke thickness for a small time increment:

$$b_{ck} (\Delta t) = \frac{\alpha r_{ck} MW_{ck}}{\rho_{ck}} \Delta t$$

This equation is the same as the equation provided by Sundaram and Froment (1979) in their coking studies.

The equation is solved at each simulation timestep for the change in coke thickness. This change in coke thickness is added to the accumulated coke thickness for use in the tube diameter calculations for the next timestep.

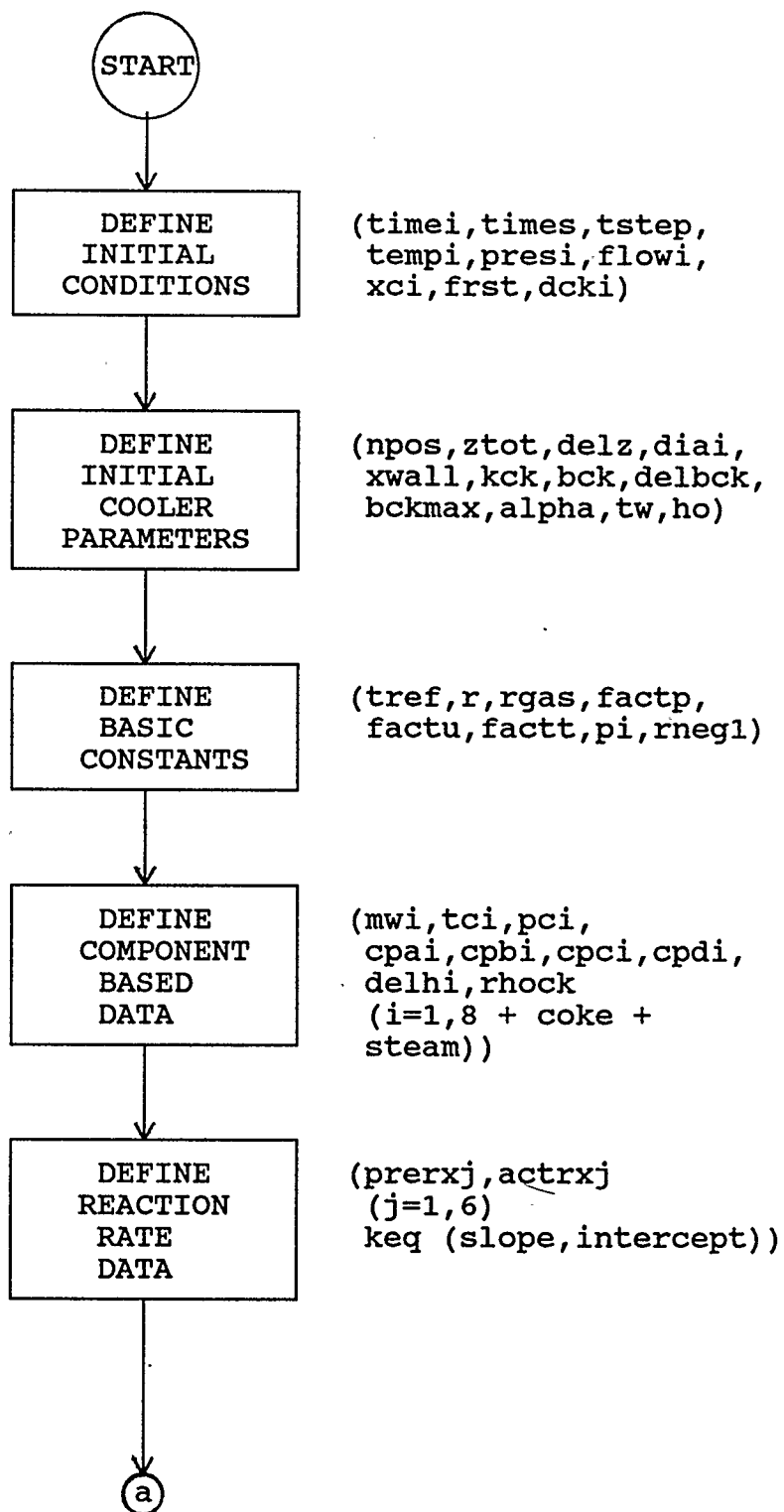
This form of the equation should be more accurate than the integrated form when the rate of coke formation changes with time, as the correct initial rate is used during early timesteps, and the correct rate is used for the additional coke produced during later timesteps.

If the rate of coke formation decreases with time, the coke accumulation predicted by the second equation will be greater than that predicted by the integrated form. This is because the high initial rate will produce more coke than later rates, but the integrated form will only use the lower rate for the later time calculations, while the differential form will accumulate coke at the correct rate for each time-step.

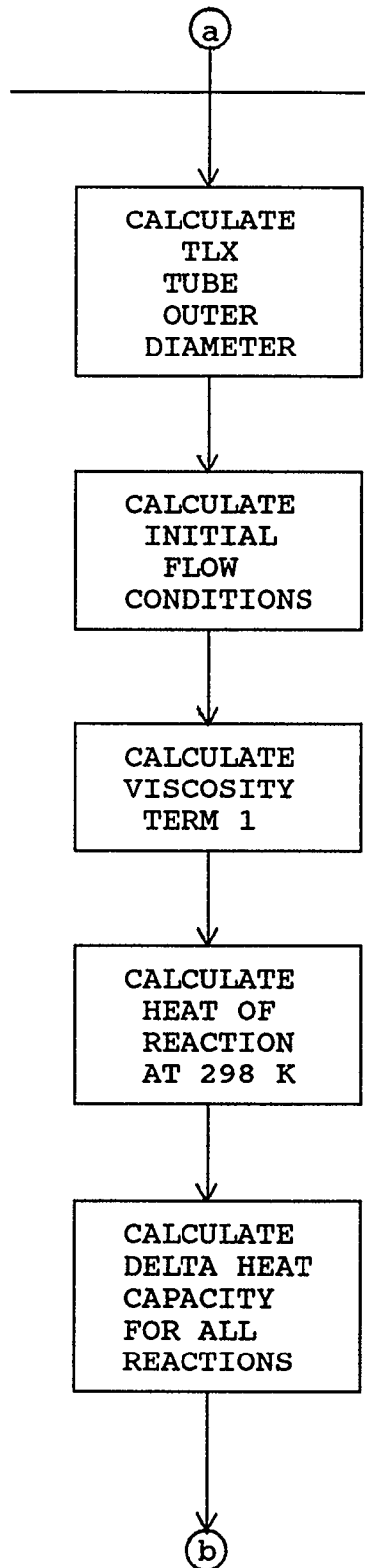
F.3.1 Units

Sundaram and Froment (1979) do not include the molecular weight of the coke in their differential coke thickness equation. This is because they used a form of the coke rate which was calculated in $g_{ck}/cm^2 \cdot s$ (SI = $kg/m^2 \cdot s$). The coke rate used in this model is in units of $g_{ck} \cdot cm/g_{C4+} \cdot s$. This is converted in the computer program to units of $mol/cm^2 \cdot s$ (SI = $mol/m^2 \cdot s$) for use in the overall mass balance equations. The molecular weight of coke in the above equation is used to convert this molar rate back to the mass based weight required by this equation. As with the other equations in this model, cgs units are used to conform to the units of the other equations.

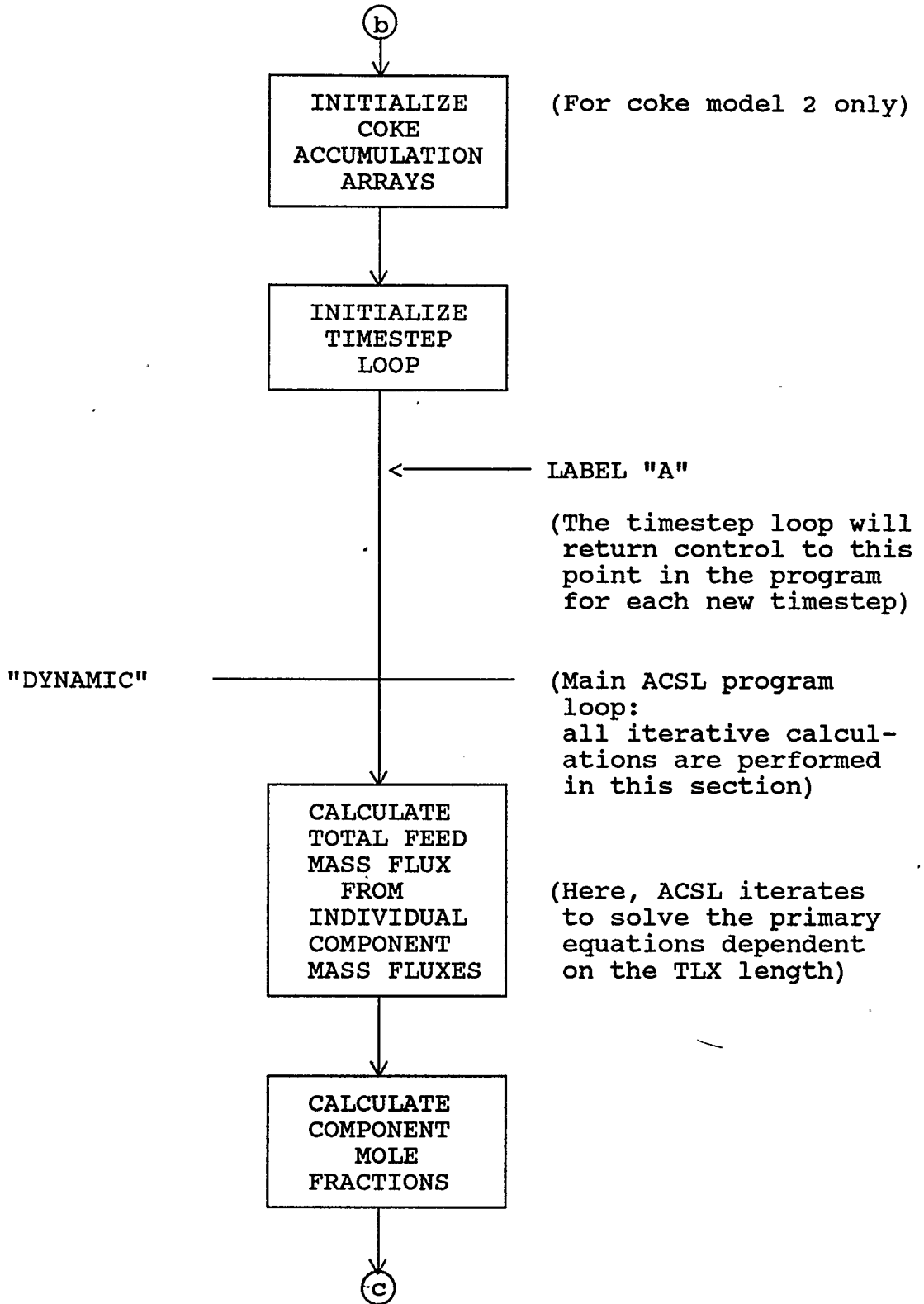
Appendix G. Quench Cooler Computer Program Flowchart

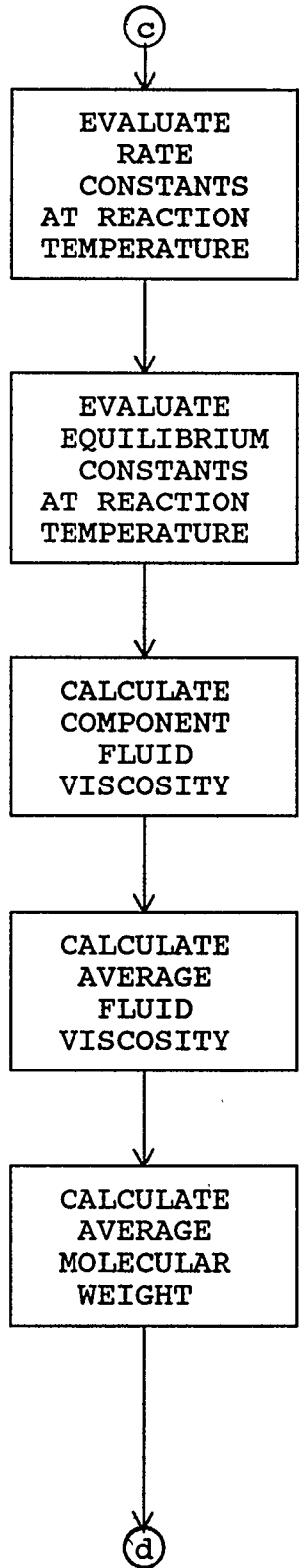
FLOWCHART FOR ACSL PROGRAM TLE.ACS

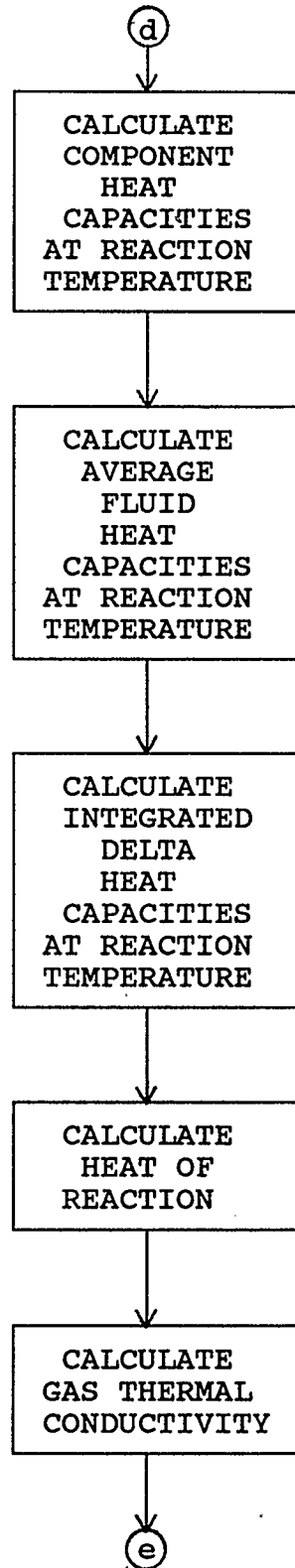
"INITIAL"

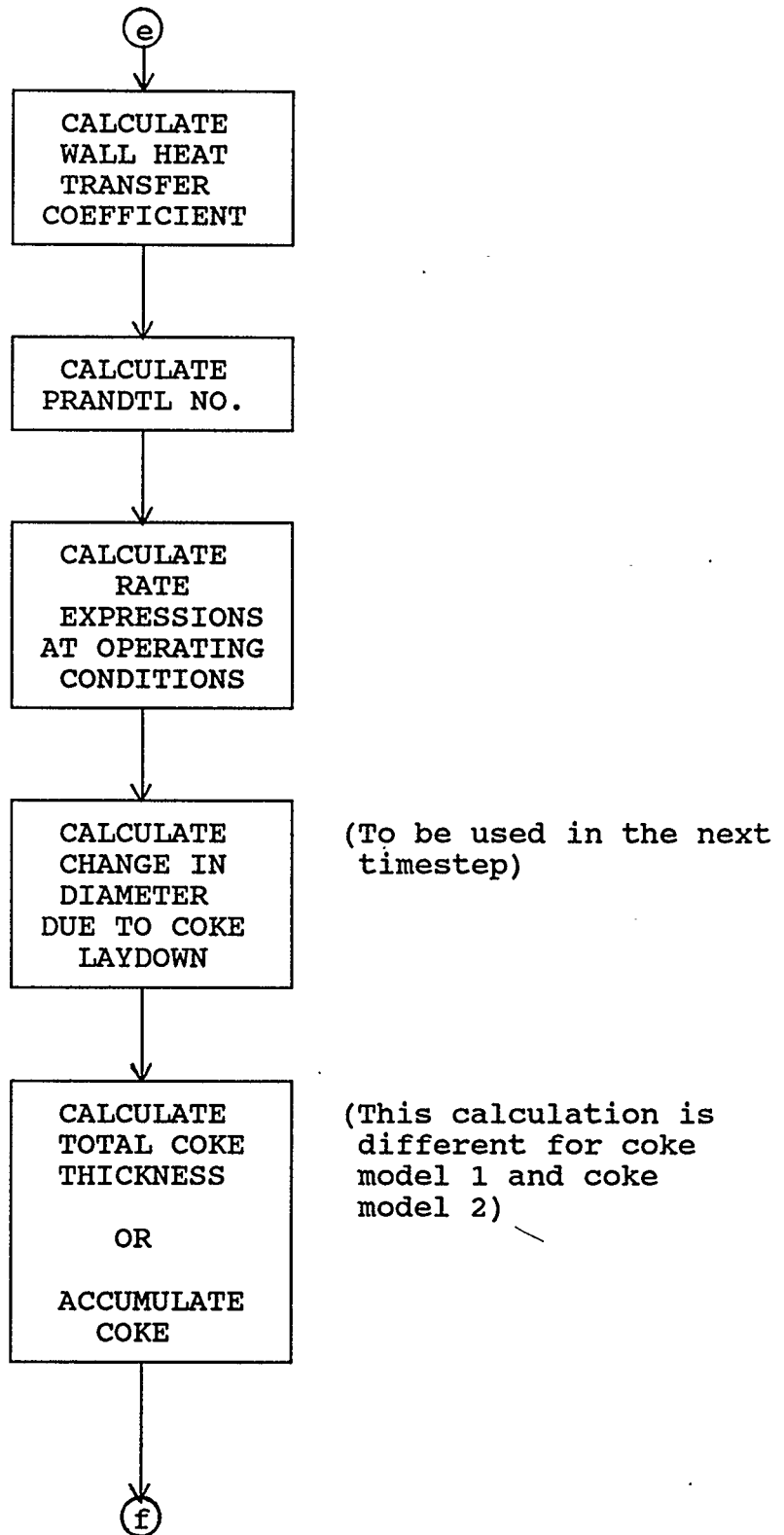


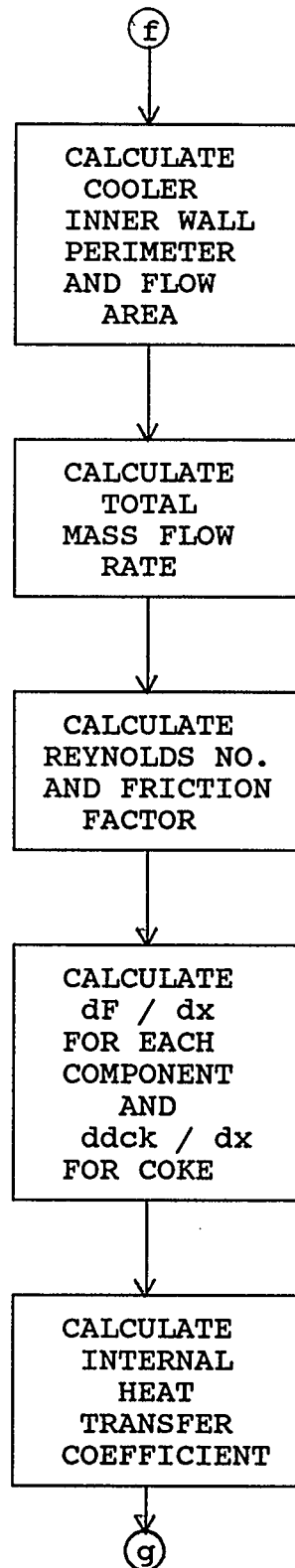
(Initial calculations made by the program to set up all variables required by the iterative portion of the program)



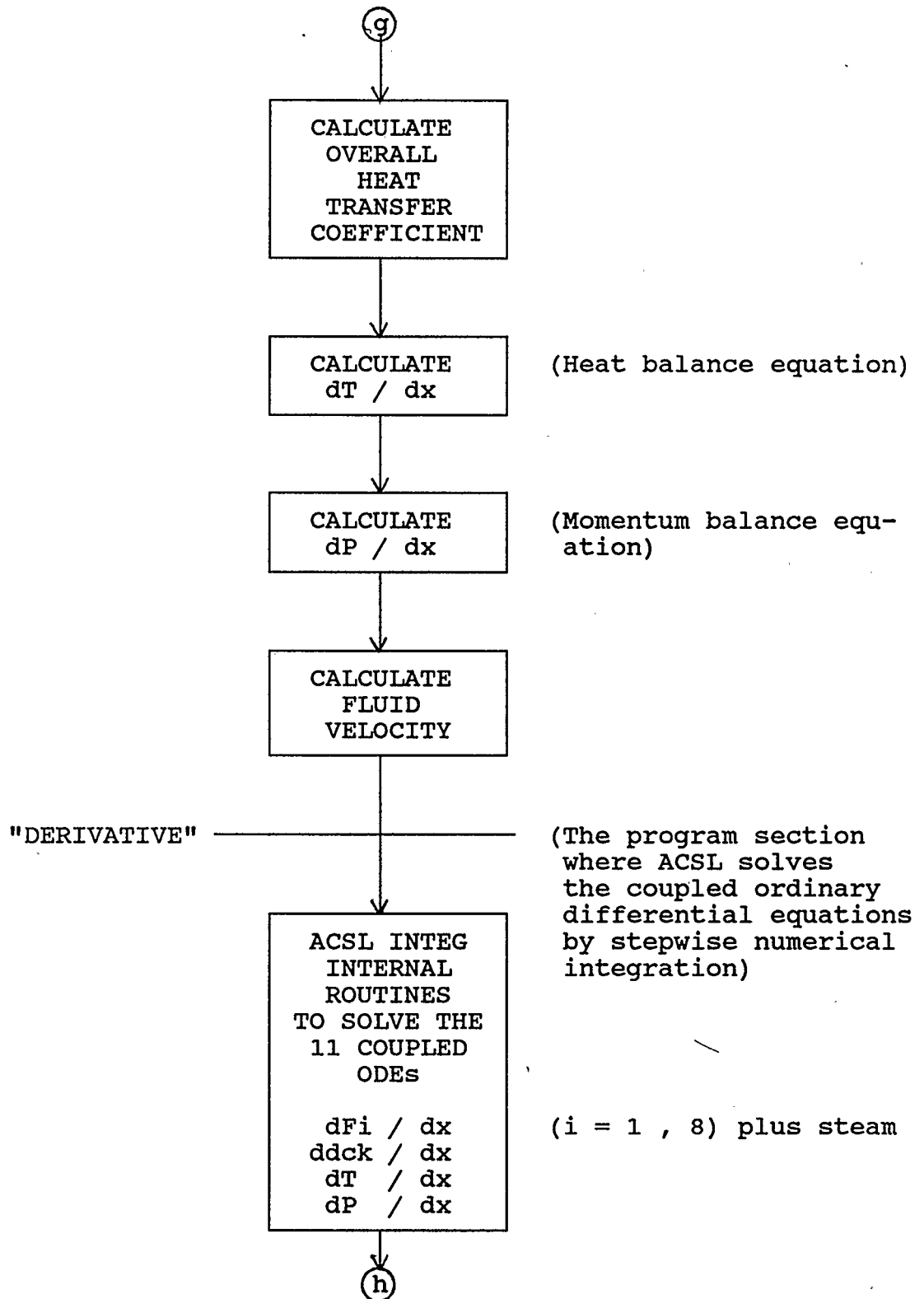


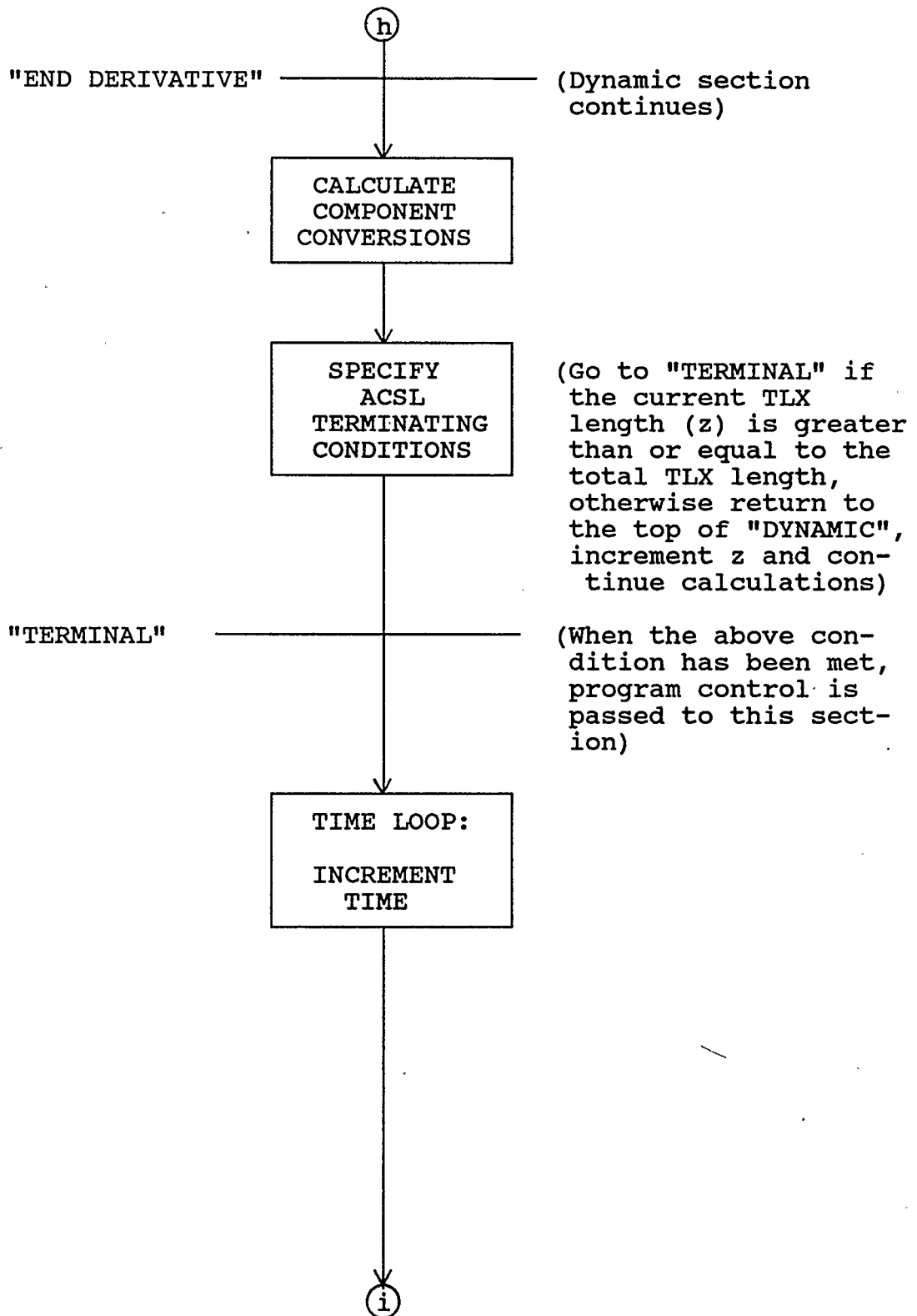


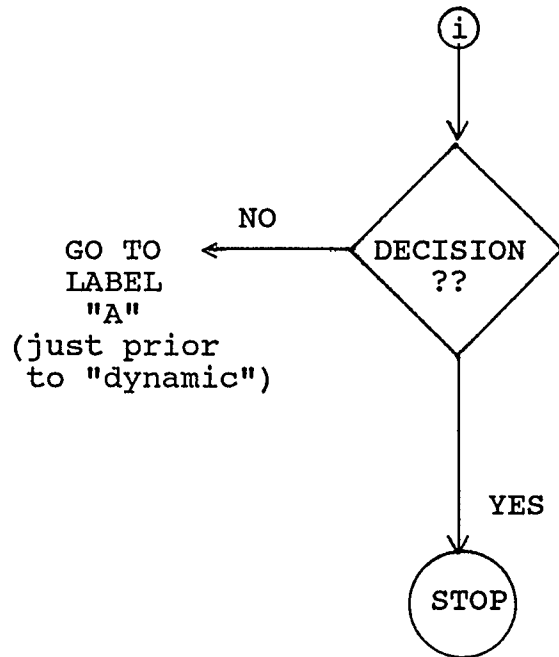




(Mass balance equation)







(Does the new value of the total elapsed operational time exceed the specified end of run time?
-OR-
Does the new total coke thickness exceed the maximum allowed?)

Appendix H. Summary of Computer Runs and Results

Table H.1 Description of Parametric Simulation CasesA. Effect of Time on Coke Formation

<u>CASE</u>	<u>Description</u>
1	Base case for coke model 1. Simulation time = 0 days
2	Base case for coke model 1. Simulation time = 6 days
3	Base case for coke model 1. Simulation time = 12 days
4	Base case for coke model 1. Simulation time = 18 days
5	Base case for coke model 1. Simulation time = 24 days
6	Base case for coke model 2. Simulation time = 0 days
7	Base case for coke model 2. Simulation time = 6 days
8	Base case for coke model 2. Simulation time = 12 days

B. Parametric Study of Model Parameters

<u>CASE</u>	<u>Description</u>	<u>Variable</u>	<u>Time</u>	<u>Coke Model</u>
9	Base case	Defaults	0 days	1
10	Base case	Defaults	0 days	2
11	Base case	Defaults	12 days	1
12	Base case	Defaults	12 days	2
13	Feed mass flux	FLOWI = 10.0	0 days	1
14	Feed mass flux	FLOWI = 10.0	0 days	2
15	Feed mass flux	FLOWI = 100.0	0 days	1
16	Feed mass flux	FLOWI = 100.0	0 days	2
17	Feed mass flux	FLOWI = 200.0	0 days	1
18	Feed mass flux	FLOWI = 200.0	0 days	2
19	Tube inside diameter	DIAI = 50.0	0 days	1
20	Tube inside diameter	DIAI = 50.0	0 days	2
21	Tube inside diameter	DIAI = 100.0	0 days	1
22	Tube inside diameter	DIAI = 100.0	0 days	2
23	Steam dilution	FRST = 0.0	0 days	1
24	Steam dilution	FRST = 0.0	0 days	2
25	Steam dilution	FRST = 0.5	0 days	1
26	Steam dilution	FRST = 0.5	0 days	2
27	Steam dilution	FRST = 1.0	0 days	1
28	Steam dilution	FRST = 1.0	0 days	2
29	Steam dilution	FRST = 2.0	0 days	1
30	Steam dilution	FRST = 2.0	0 days	2
31	Steam temperature	TSTM = 373.15	0 days	1
32	Steam temperature	TSTM = 373.15	0 days	2
33	Steam temperature	TSTM = 700.00	0 days	1
34	Steam temperature	TSTM = 700.00	0 days	2
35	Steam heat transfer coefficient	HO = 2839.0	0 days	1
36	Steam heat transfer coefficient	HO = 2839.0	0 days	2
37	Steam heat transfer coefficient	HO = 19874.0	0 days	1
38	Steam heat transfer coefficient	HO = 19874.0	0 days	2
39	Coke laydown parameter	ACK = 0.1	12 days	1
40	Coke laydown parameter	ACK = 0.1	12 days	2
41	Coke laydown parameter	ACK = 0.5	12 days	1
42	Coke laydown parameter	ACK = 0.5	12 days	2
43	Coke thermal conductivity	KCK = 0.55	12 days	1
44	Coke thermal conductivity	KCK = 0.55	12 days	2
45	Coke thermal conductivity	KCK = 76.0	12 days	1
46	Coke thermal conductivity	KCK = 76.0	12 days	2

Table H.2 Parametric Simulation Results - Part 1

CASE	Temp.	Press.	F _{c1}	F _{c2}	F _{c3}	F _{c4}	F _{c5}	F _{c6}	F _{c7}	F _{c8}
1	643.963	2.011	.39142	.05320	.00497	.31188	.21834	.01372	.01832	.00421
2	648.872	1.974	.39105	.05286	.00475	.31162	.21878	.01396	.01832	.00414
3	654.851	1.851	.39088	.05250	.00454	.31158	.21901	.01422	.01831	.00405
4	659.681	1.494	.39091	.05198	.00424	.31185	.21905	.01458	.01831	.00391
5	658.847	.869	.39094	.05126	.00378	.31217	.21909	.01511	.01830	.00376
6	643.963	2.011	.39142	.05320	.00497	.31188	.21834	.01372	.01832	.00421
7	648.206	1.977	.39103	.05287	.00476	.31159	.21880	.01395	.01832	.00414
8	653.145	1.743	.39090	.05236	.00447	.31169	.21902	.01430	.01831	.00400
9	643.963	2.011	.39142	.05320	.00497	.31188	.21834	.01372	.01832	.00421
10	643.963	2.011	.39142	.05320	.00497	.31188	.21834	.01372	.01832	.00421
11	654.851	1.851	.39088	.05250	.00454	.31158	.21901	.01422	.01831	.00405
12	653.145	1.743	.39090	.05236	.00447	.31169	.21902	.01430	.01831	.00400
13	607.907	2.115	.07925	.01192	.00162	.06265	.04255	.00182	.00368	.00129
14	607.907	2.115	.07925	.01192	.00162	.06265	.04255	.00182	.00368	.00129
15	672.062	1.691	.78132	.10363	.00807	.62321	.43847	.02959	.03661	.00787
16	672.062	1.691	.78132	.10363	.00807	.62321	.43847	.02959	.03661	.00787
17	713.455	1.090	1.56118	.20359	.01353	1.24606	.87876	.06206	.07318	.01515
18	713.455	1.090	1.56118	.20359	.01353	1.24606	.87876	.06206	.07318	.01515
19	761.154	2.067	1.61478	.22975	.02636	1.28255	.89509	.04829	.07557	.02083
20	761.154	2.067	1.61478	.22975	.02636	1.28255	.89509	.04829	.07557	.02083
21	899.536	2.094	6.47637	.98637	.12807	5.10330	3.55281	.14430	.30317	.11827
22	899.536	2.094	6.47637	.98637	.12807	5.10330	3.55281	.14430	.30317	.11827
23	646.353	2.012	.49780	.06804	.00617	.39601	.27928	.01757	.02335	.00560
24	646.353	2.012	.49780	.06804	.00617	.39601	.27928	.01757	.02335	.00560
25	642.760	2.011	.33588	.04553	.00432	.26783	.18681	.01173	.01570	.00353
26	642.760	2.011	.33588	.04553	.00432	.26783	.18681	.01173	.01570	.00353
27	641.022	2.010	.25342	.03423	.00333	.20231	.14035	.00880	.01183	.00258
28	641.022	2.010	.25342	.03423	.00333	.20231	.14035	.00880	.01183	.00258
29	639.311	2.010	.16997	.02288	.00228	.13584	.09373	.00586	.00792	.00167
30	639.311	2.010	.16997	.02288	.00228	.13584	.09373	.00586	.00792	.00167
31	441.210	2.034	.39116	.05212	.00425	.31201	.21869	.01459	.01831	.00398
32	441.210	2.034	.39116	.05212	.00425	.31201	.21869	.01459	.01831	.00398
33	838.271	1.990	.39173	.05562	.00634	.31104	.21787	.01180	.01835	.00496
34	838.271	1.990	.39173	.05562	.00634	.31104	.21787	.01180	.01835	.00496
35	656.092	2.009	.39154	.05354	.00518	.31186	.21819	.01346	.01832	.00430
36	656.092	2.009	.39154	.05354	.00518	.31186	.21819	.01346	.01832	.00430
37	642.360	2.012	.39141	.05316	.00494	.31188	.21836	.01376	.01832	.00420
38	642.360	2.012	.39141	.05316	.00494	.31188	.21836	.01376	.01832	.00420
39	644.848	2.007	.39133	.05313	.00492	.31181	.21845	.01377	.01832	.00420
40	644.833	2.007	.39133	.05313	.00492	.31181	.21845	.01377	.01832	.00420
41	648.872	1.974	.39105	.05286	.00475	.31162	.21878	.01396	.01832	.00414
42	648.450	1.975	.39102	.05286	.00475	.31159	.21881	.01396	.01832	.00414
43	803.797	1.434	.39519	.05698	.00727	.31399	.21432	.01075	.01837	.00518
44	681.633	1.633	.39432	.05550	.00645	.31388	.21527	.01190	.01836	.00473
45	646.381	1.905	.39027	.05170	.00398	.31124	.21970	.01484	.01830	.00391
46	646.768	1.772	.39012	.05142	.00380	.31120	.21988	.01504	.01830	.00385

NOTE: All results reported for the TLX tube exit (z = 6.1 m)

Table H.2 Parametric Simulation Results - Part 2

CASE	U_o	f	ρ_f	U_m	G	Re	b_{ck}
1	.007713	.020224	.737313	7169.7	5.0036	62344.0	0.000E+00
2	.007787	.020245	.737498	7356.3	5.0035	62021.0	5.396E-05
3	.007877	.020270	.737711	7916.1	5.0037	61637.0	1.198E-04
4	.007949	.020290	.737880	9881.7	5.0039	61332.5	1.629E-04
5	.007937	.020287	.737867	16966.3	5.0032	61382.3	1.182E-04
6	.007713	.020224	.737313	7169.7	5.0036	62344.0	0.000E+00
7	.007777	.020242	.737476	7340.4	5.0034	62063.6	4.765E-05
8	.007851	.020263	.737656	8386.1	5.0035	61745.1	1.006E-04
9	.007713	.020224	.737313	7169.7	5.0036	62344.0	0.000E+00
10	.007713	.020224	.737313	7169.7	5.0036	62344.0	0.000E+00
11	.007877	.020270	.737711	7916.1	5.0037	61637.0	1.198E-04
12	.007851	.020263	.737656	8386.1	5.0035	61745.1	1.006E-04
13	.002116	.027680	.735781	1295.3	1.0018	12979.2	0.000E+00
14	.002116	.027680	.735781	1295.3	1.0018	12979.2	0.000E+00
15	.013218	.017709	.738297	17773.4	10.0046	121111.4	0.000E+00
16	.013218	.017709	.738297	17773.4	10.0046	121111.4	0.000E+00
17	.021996	.015542	.739590	58519.7	20.0062	232594.4	0.000E+00
18	.021996	.015542	.739590	58519.7	20.0062	232594.4	0.000E+00
19	.008852	.017955	.740749	8260.0	5.0053	113010.5	0.000E+00
20	.008852	.017955	.740749	8260.0	5.0053	113010.5	0.000E+00
21	.009404	.015987	.743799	9651.4	5.0072	201945.4	0.000E+00
22	.009404	.015987	.743799	9651.4	5.0072	201945.4	0.000E+00
23	.008319	.020100	.741528	7152.4	4.9995	64290.3	0.000E+00
24	.008319	.020100	.741528	7152.4	4.9995	64290.3	0.000E+00
25	.007394	.020284	.734835	7177.7	5.0053	61421.0	0.000E+00
26	.007394	.020284	.734835	7177.7	5.0053	61421.0	0.000E+00
27	.006915	.020369	.730729	7188.1	5.0071	60146.4	0.000E+00
28	.006915	.020369	.730729	7188.1	5.0071	60146.4	0.000E+00
29	.006426	.020451	.725944	7197.1	5.0072	58952.2	0.000E+00
30	.006426	.020451	.725944	7197.1	5.0072	58952.2	0.000E+00
31	.006525	.019215	.728133	4853.2	5.0029	80525.5	0.000E+00
32	.006525	.019215	.728133	4853.2	5.0029	80525.5	0.000E+00
33	.008663	.020958	.742611	9446.4	5.0045	52156.6	0.000E+00
34	.008663	.020958	.742611	9446.4	5.0045	52156.6	0.000E+00
35	.007258	.020275	.737712	7315.9	5.0038	61563.3	0.000E+00
36	.007258	.020275	.737712	7315.9	5.0038	61563.3	0.000E+00
37	.007780	.020217	.737259	7150.3	5.0035	62449.0	0.000E+00
38	.007780	.020217	.737259	7150.3	5.0035	62449.0	0.000E+00
39	.007727	.020227	.737348	7194.6	5.0035	62285.1	9.756E-06
40	.007726	.020227	.737347	7194.2	5.0035	62286.0	9.585E-06
41	.007787	.020245	.737498	7356.3	5.0035	62021.0	5.396E-05
42	.007780	.020243	.737485	7350.9	5.0034	62047.8	4.902E-05
43	.009668	.020819	.741690	12721.1	5.0516	53931.5	5.363E-03
44	.008276	.020377	.738412	9382.2	5.0079	60033.3	1.389E-04
45	.007749	.020235	.737462	7588.0	5.0026	62172.6	9.076E-05
46	.007755	.020237	.737486	8158.7	5.0024	62145.3	9.431E-05

NOTE: All results reported for the TLX tube exit ($z = 6.1$ m)

Table H.2 Parametric Simulation Results - Part 3

CASE	X _{c1}	X _{c2}	X _{c3}	X _{c4}	X _{c5}	X _{c6}	X _{c7}	X _{c8}
1	-.00504	-.07712	-1.25569	-.00276	.01053	.17949	-.00224	-.16052
2	-.00407	-.07014	-1.15528	-.00190	.00852	.16506	-.00194	-.14089
3	-.00364	-.06293	-1.05885	-.00180	.00747	.15000	-.00169	-.11601
4	-.00373	-.05241	-.92528	-.00266	.00730	.12819	-.00140	-.07712
5	-.00381	-.03769	-.71636	-.00369	.00709	.09646	-.00103	-.03448
6	-.00504	-.07712	-1.25569	-.00276	.01053	.17949	-.00224	-.16052
7	-.00402	-.07031	-1.15823	-.00184	.00843	.16561	-.00194	-.14154
8	-.00369	-.05994	-1.02919	-.00215	.00745	.14483	-.00160	-.10273
9	-.00504	-.07712	-1.25569	-.00276	.01053	.17949	-.00224	-.16052
10	-.00504	-.07712	-1.25569	-.00276	.01053	.17949	-.00224	-.16052
11	-.00364	-.06293	-1.05885	-.00180	.00747	.15000	-.00169	-.11601
12	-.00369	-.05994	-1.02919	-.00215	.00745	.14483	-.00160	-.10273
13	-.01745	-.20704	-2.67871	-.00709	.03582	.45490	-.00735	-.77454
14	-.01745	-.20704	-2.67871	-.00709	.03582	.45490	-.00735	-.77454
15	-.00309	-.04896	-.83175	-.00186	.00645	.11532	-.00136	-.08462
16	-.00309	-.04896	-.83175	-.00186	.00645	.11532	-.00136	-.08462
17	-.00214	-.03039	-.53446	-.00158	.00439	.07227	-.00084	-.04334
18	-.00214	-.03039	-.53446	-.00158	.00439	.07227	-.00084	-.04334
19	-.00675	-.12938	-1.90403	-.00127	.01504	.29887	-.00379	-.39319
20	-.00675	-.12938	-1.90403	-.00127	.01504	.29887	-.00379	-.39319
21	-.00944	-.21217	-2.52725	.00398	.02263	.47623	-.00674	-.97764
22	-.00944	-.21217	-2.52725	.00398	.02263	.47623	-.00674	-.97764
23	-.00277	-.08069	-1.19698	.00108	.00705	.17577	-.00229	-.21127
24	-.00277	-.08069	-1.19698	.00108	.00705	.17577	-.00229	-.21127
25	-.00618	-.07547	-1.28746	-.00468	.01229	.18165	-.00222	-.13525
26	-.00618	-.07547	-1.28746	-.00468	.01229	.18165	-.00222	-.13525
27	-.00785	-.07329	-1.33701	-.00747	.01486	.18524	-.00220	-.09898
28	-.00785	-.07329	-1.33701	-.00747	.01486	.18524	-.00220	-.09898
29	-.00952	-.07145	-1.39165	-.01026	.01746	.18951	-.00219	-.06337
30	-.00952	-.07145	-1.39165	-.01026	.01746	.18951	-.00219	-.06337
31	-.00436	-.05513	-.92741	-.00316	.00894	.12745	-.00167	-.09534
32	-.00436	-.05513	-.92741	-.00316	.00894	.12745	-.00167	-.09534
33	-.00582	-.12603	-1.87540	-.00005	.01266	.29419	-.00354	-.36710
34	-.00582	-.12603	-1.87540	-.00005	.01266	.29419	-.00354	-.36710
35	-.00533	-.08396	-1.35141	-.00269	.01118	.19535	-.00243	-.18386
36	-.00533	-.08396	-1.35141	-.00269	.01118	.19535	-.00243	-.18386
37	-.00500	-.07618	-1.24225	-.00277	.01044	.17729	-.00221	-.15742
38	-.00500	-.07618	-1.24225	-.00277	.01044	.17729	-.00221	-.15742
39	-.00480	-.07562	-1.23365	-.00252	.01003	.17641	-.00217	-.15663
40	-.00479	-.07561	-1.23356	-.00252	.01002	.17641	-.00217	-.15663
41	-.00407	-.07014	-1.15528	-.00190	.00852	.16506	-.00194	-.14089
42	-.00401	-.07008	-1.15499	-.00183	.00840	.16511	-.00193	-.14082
43	-.01472	-.15350	-2.29847	-.00955	.02872	.35703	-.00504	-.42730
44	-.01248	-.12360	-1.92777	-.00918	.02443	.28835	-.00410	-.30392
45	-.00207	-.04656	-.80422	-.00070	.00437	.11245	-.00116	-.07690
46	-.00171	-.04094	-.72482	-.00058	.00355	.10076	-.00096	-.06103

NOTE: All results reported for the TLX tube exit (z = 6.1 m)

Table H.3 Alberta Gas Ethylene Plant Simulation Results -
Part 1

Part 1. Flow Rate History Match Results:

0 days total elapsed operational time

A. TLX Identity: H143

CASE	Feed Flow Geometry Factor	Steam Feed Flow Factor	Outlet Temperature (K)	Outlet Pressure (kPa)	Total Feed Flow (kg/m ² ·s)
1	2/108	1/2	530.33	200.0	38.545
2	2/108	1	531.03	198.6	47.677
3	4/108	1/2	550.91	188.1	67.958
4	4/108	1	551.80	185.4	77.091
5	4/108	2	553.91	180.1	95.355

AGE Supplied Outlet Temperature = 557.650 K

AGE Supplied Outlet Pressure = 171.4 kPa to 181.4 kPa

B. TLX Identity: HAVG

CASE	Feed Flow Geometry Factor	Steam Feed Flow Factor	Outlet Temperature (K)	Outlet Pressure (kPa)	Total Feed Flow (kg/m ² ·s)
1	2/108	1/2	533.15	224.5	43.052
2	2/108	1	533.98	223.0	53.190
3	4/108	1/2	555.14	211.5	75.967
4	4/108	1	556.18	208.6	86.104
5	4/108	2	558.59	202.7	106.378
6	4/108	3	561.27	196.6	126.652
7	4/108	4	564.10	190.2	146.926

AGE Supplied Outlet Temperature = 564.238 K

AGE Supplied Outlet Pressure = 196.3 kPa to 206.3 kPa

Table H.3 Alberta Gas Ethylene Plant Simulation Results -
Part 2

Part 2. Results at 42 days total elapsed operational time

B. TLX Identity: HAVG

CASE	Coke Deposition Ratio (α)	Outlet Temperature (K)	Outlet Pressure (kPa)	Shutdown Time (days)
1	0.10	563.66	199.7	60
2	0.20	567.09	193.3	60
3	0.30	570.05	186.8	54
4	0.33	569.86	182.4	48
5	0.34	570.14	180.7	48
6	0.35	570.43	179.0	48
7	0.40	573.78	129.5	42

AGE Supplied Outlet Temperature = 572.425 K

AGE Supplied Outlet Pressure = none

Appendix I. Typical Computer Run Output Listing - Run 6

ACSL RUN-TIME EXEC VERSION 1 LEVEL 8D

SET TIMES = 0.0

SET TITLE= "ETHYLENE QUENCH COOLER (TLE)"

PREPAR Z,TEMP,PRES,FC1,FC2,FC3,FC4,FC5,FC6,FC7,FC8,DELBCK,BCK,VELF

PREPAR CVC1,CVC2,CVC3,CVC4,CVC5,CVC6,CVC7,CVC8,UO,FRIC,PRM,GTOT,RE

PREPAR TRES

START

PRINT

ETHYLENE QUENCH COOLER (TLE)

LINE	Z	TEMP	PRES	FC1	FC2	FC3	FC4	FC5	FC6	FC7
0	0.	1133.7000	2.1200000	0.3894597	0.0493955	0.0022040	0.3110232	0.2206592	0.0167245	0.0182802
1	10.000000	1108.0126	2.1173911	0.3910459	0.0506191	0.0031336	0.3123138	0.2188958	0.0158400	0.0182990
2	20.000000	1085.4388	2.1148403	0.3916822	0.0514049	0.0037089	0.3127331	0.2181671	0.0152421	0.0183087
3	30.000000	1064.7637	2.1123427	0.3919056	0.0519347	0.0040881	0.3127985	0.2178937	0.0148220	0.0183140
4	40.000000	1045.4337	2.1098949	0.3919430	0.0523017	0.0043475	0.3127209	0.2178294	0.0145206	0.0183170
5	50.000000	1027.1599	2.1074940	0.3919004	0.0525603	0.0045290	0.3125946	0.2178579	0.0143019	0.0183187
6	60.000000	1009.7776	2.1051377	0.3918292	0.0527445	0.0046580	0.3124624	0.2179221	0.0141422	0.0183197
7	70.000000	993.18557	2.1028240	0.3917538	0.0528767	0.0047505	0.3123423	0.2179946	0.0140252	0.0183203
8	80.000000	977.31660	2.1005509	0.3916848	0.0529720	0.0048172	0.3122406	0.2180627	0.0139393	0.0183206
9	90.000000	962.12234	2.0983165	0.3916263	0.0530409	0.0048654	0.3121580	0.2181216	0.0138763	0.0183208
10	100.000000	947.56509	2.0961193	0.3915786	0.0530907	0.0049002	0.3120925	0.2181701	0.0138302	0.0183210
11	110.000000	933.61333	2.0939575	0.3915410	0.0531268	0.0049253	0.3120416	0.2182089	0.0137964	0.0183210
12	120.000000	920.23922	2.0918296	0.3915117	0.0531529	0.0049433	0.3120024	0.2182392	0.0137719	0.0183211
13	130.000000	907.41728	2.0897342	0.3914894	0.0531716	0.0049562	0.3119726	0.2182626	0.0137541	0.0183211
14	140.000000	895.12362	2.0876699	0.3914724	0.0531851	0.0049652	0.3119500	0.2182805	0.0137413	0.0183211
15	150.000000	883.33558	2.0856353	0.3914597	0.0531946	0.0049715	0.3119330	0.2182941	0.0137321	0.0183211
16	160.000000	872.03149	2.0836292	0.3914502	0.0532013	0.0049758	0.3119202	0.2183043	0.0137257	0.0183211
17	170.000000	861.19059	2.0816503	0.3914431	0.0532059	0.0049786	0.3119106	0.2183120	0.0137213	0.0183211
18	180.000000	850.79293	2.0796974	0.3914378	0.0532090	0.0049803	0.3119034	0.2183178	0.0137183	0.0183211
19	190.000000	840.81942	2.0777695	0.3914339	0.0532110	0.0049813	0.3118980	0.2183221	0.0137163	0.0183212
20	200.000000	831.25170	2.0758655	0.3914310	0.0532123	0.0049817	0.3118939	0.2183254	0.0137151	0.0183212
21	210.000000	822.07222	2.0739843	0.3914289	0.0532129	0.0049818	0.3118909	0.2183278	0.0137145	0.0183212
22	220.000000	813.26414	2.0721251	0.3914273	0.0532132	0.0049816	0.3118886	0.2183297	0.0137142	0.0183212
23	230.000000	804.81139	2.0702868	0.3914262	0.0532132	0.0049813	0.3118868	0.2183310	0.0137142	0.0183212
24	240.000000	796.69855	2.0684685	0.3914253	0.0532130	0.0049808	0.3118855	0.2183321	0.0137144	0.0183212
25	250.000000	788.91093	2.0666695	0.3914247	0.0532127	0.0049803	0.3118845	0.2183329	0.0137147	0.0183212
26	260.000000	781.43447	2.0648889	0.3914242	0.0532124	0.0049797	0.3118837	0.2183335	0.0137151	0.0183212
27	270.000000	774.25574	2.0631259	0.3914239	0.0532119	0.0049792	0.3118831	0.2183339	0.0137155	0.0183212
28	280.000000	767.36192	2.0613798	0.3914236	0.0532115	0.0049786	0.3118826	0.2183343	0.0137160	0.0183212
29	290.000000	760.74078	2.0596499	0.3914234	0.0532110	0.0049781	0.3118823	0.2183345	0.0137164	0.0183212
30	300.000000	754.38064	2.0579355	0.3914233	0.0532106	0.0049776	0.3118820	0.2183347	0.0137169	0.0183212
31	310.000000	748.27034	2.0562359	0.3914232	0.0532102	0.0049771	0.3118818	0.2183349	0.0137173	0.0183212
32	320.000000	742.39923	2.0545506	0.3914231	0.0532098	0.0049766	0.3118816	0.2183350	0.0137177	0.0183212
33	330.000000	736.75716	2.0528789	0.3914231	0.0532094	0.0049762	0.3118815	0.2183351	0.0137181	0.0183212
34	340.000000	731.33442	2.0512202	0.3914231	0.0532090	0.0049758	0.3118814	0.2183352	0.0137185	0.0183212

35	350.00000	726.12176	2.0495741	0.3914230	0.0532087	0.0049754	0.3118813	0.2183352	0.0137188	0.0183212
36	360.00000	721.11034	2.0479400	0.3914230	0.0532083	0.0049751	0.3118812	0.2183353	0.0137191	0.0183212
37	370.00000	716.29172	2.0463174	0.3914230	0.0532080	0.0049748	0.3118812	0.2183353	0.0137194	0.0183212
38	380.00000	711.65784	2.0447058	0.3914230	0.0532078	0.0049745	0.3118812	0.2183354	0.0137197	0.0183212
39	390.00000	707.20102	2.0431048	0.3914230	0.0532075	0.0049742	0.3118811	0.2183354	0.0137200	0.0183212
40	400.00000	702.91391	2.0415140	0.3914230	0.0532073	0.0049740	0.3118811	0.2183354	0.0137202	0.0183212
41	410.00000	698.78949	2.0399328	0.3914230	0.0532071	0.0049738	0.3118811	0.2183354	0.0137204	0.0183212
42	420.00000	694.82106	2.0383610	0.3914230	0.0532069	0.0049736	0.3118810	0.2183354	0.0137206	0.0183212
43	430.00000	691.00222	2.0367981	0.3914230	0.0532067	0.0049734	0.3118810	0.2183354	0.0137208	0.0183212
44	440.00000	687.32686	2.0352437	0.3914230	0.0532065	0.0049732	0.3118810	0.2183355	0.0137210	0.0183212
45	450.00000	683.78913	2.0336976	0.3914230	0.0532063	0.0049730	0.3118810	0.2183355	0.0137211	0.0183212
46	460.00000	680.38345	2.0321593	0.3914230	0.0532062	0.0049729	0.3118810	0.2183355	0.0137213	0.0183212
47	470.00000	677.10447	2.0306286	0.3914230	0.0532060	0.0049727	0.3118810	0.2183355	0.0137214	0.0183212
48	480.00000	673.94710	2.0291050	0.3914230	0.0532059	0.0049726	0.3118810	0.2183355	0.0137216	0.0183212
49	490.00000	670.90646	2.0275884	0.3914230	0.0532058	0.0049725	0.3118810	0.2183355	0.0137217	0.0183212
50	500.00000	667.97788	2.0260785	0.3914230	0.0532057	0.0049723	0.3118810	0.2183355	0.0137218	0.0183212
51	510.00000	665.15689	2.0245749	0.3914230	0.0532056	0.0049722	0.3118810	0.2183355	0.0137219	0.0183212
52	520.00000	662.43924	2.0230774	0.3914230	0.0532055	0.0049721	0.3118810	0.2183355	0.0137220	0.0183212
53	530.00000	659.82083	2.0215857	0.3914231	0.0532054	0.0049720	0.3118810	0.2183355	0.0137221	0.0183212
54	540.00000	657.29777	2.0200997	0.3914231	0.0532053	0.0049720	0.3118810	0.2183355	0.0137222	0.0183212
55	550.00000	654.86630	2.0186190	0.3914231	0.0532052	0.0049719	0.3118809	0.2183355	0.0137223	0.0183212
56	560.00000	652.52285	2.0171434	0.3914231	0.0532052	0.0049718	0.3118809	0.2183355	0.0137223	0.0183212
57	570.00000	650.26400	2.0156728	0.3914231	0.0532051	0.0049717	0.3118809	0.2183355	0.0137224	0.0183212
58	580.00000	648.08645	2.0142069	0.3914231	0.0532050	0.0049717	0.3118809	0.2183355	0.0137225	0.0183212
59	590.00000	645.98708	2.0127454	0.3914231	0.0532050	0.0049716	0.3118809	0.2183355	0.0137225	0.0183212
60	600.00000	643.96286	2.0112883	0.3914231	0.0532049	0.0049715	0.3118809	0.2183355	0.0137226	0.0183212
61	610.00000	642.01091	2.0098354	0.3914231	0.0532048	0.0049715	0.3118809	0.2183355	0.0137226	0.0183212

ETHYLENE QUENCH COOLER (TLE)

LINE	FC8	DELBCK	BCK	VELF	CVC1	CVC2	CVC3	CVC4	CVC5	CVC6
0	0.0036301	0.3421305	0.	11931.803	0.	0.	0.	0.	0.	0.
1	0.0037383	0.2686984	0.	11698.416	-0.0040728	-0.0247709	-0.4217821	-0.0041494	0.0079917	0.0528845
2	0.0038447	0.2155618	0.	11484.558	-0.0057066	-0.0406795	-0.6827862	-0.0054977	0.0112942	0.0886330
3	0.0039335	0.1740472	0.	11284.315	-0.0062803	-0.0514041	-0.8548490	-0.0057079	0.0125330	0.1137542
4	0.0040033	0.1407480	0.	11094.812	-0.0063763	-0.0588340	-0.9725401	-0.0054583	0.0128244	0.1317740
5	0.0040568	0.1138259	0.	10914.440	-0.0062670	-0.0640692	-1.0549213	-0.0050523	0.0126956	0.1448496
6	0.0040970	0.0920354	0.	10742.206	-0.0060842	-0.0677988	-1.1134449	-0.0046271	0.0124045	0.1543990
7	0.0041270	0.0744189	0.	10577.445	-0.0058905	-0.0704751	-1.1554083	-0.0042410	0.0120759	0.1613966
8	0.0041492	0.0602005	0.	10419.674	-0.0057134	-0.0724046	-1.1856608	-0.0039141	0.0117671	0.1665310
9	0.0041657	0.0487408	0.	10268.512	-0.0055631	-0.0737994	-1.2075238	-0.0036484	0.0115002	0.1702978
10	0.0041778	0.0395126	0.	10123.640	-0.0054408	-0.0748090	-1.2233235	-0.0034379	0.0112804	0.1730576
11	0.0041868	0.0320840	0.	9984.7764	-0.0053440	-0.0755394	-1.2347153	-0.0032741	0.0111048	0.1750746
12	0.0041934	0.0261028	0.	9851.6649	-0.0052690	-0.0760669	-1.2428908	-0.0031483	0.0109673	0.1765433
13	0.0041983	0.0212837	0.	9724.0646	-0.0052115	-0.0764465	-1.2487152	-0.0030524	0.0108612	0.1776075
14	0.0042020	0.0173967	0.	9601.7469	-0.0051680	-0.0767181	-1.2528205	-0.0029799	0.0107801	0.1783733
15	0.0042047	0.0142570	0.	9484.4936	-0.0051353	-0.0769110	-1.2556698	-0.0029252	0.0107187	0.1789193
16	0.0042067	0.0117166	0.	9372.0950	-0.0051108	-0.0770464	-1.2576040	-0.0028840	0.0106722	0.1793037

17	0.0042082	0.0096571	0.	9264.3497	-0.0050926	-0.0771398	-1.2588737	-0.0028531	0.0106373	0.1795697
18	0.0042093	0.0079838	0.	9161.0639	-0.0050791	-0.0772028	-1.2596639	-0.0028299	0.0106111	0.1797492
19	0.0042102	0.0066211	0.	9062.0515	-0.0050691	-0.0772438	-1.2601105	-0.0028125	0.0105915	0.1798657
20	0.0042108	0.0055086	0.	8967.1337	-0.0050617	-0.0772689	-1.2603138	-0.0027995	0.0105768	0.1799369
21	0.0042113	0.0045981	0.	8876.1388	-0.0050562	-0.0772827	-1.2603472	-0.0027896	0.0105657	0.1799756
22	0.0042116	0.0038509	0.	8788.9021	-0.0050522	-0.0772884	-1.2602645	-0.0027822	0.0105574	0.1799912
23	0.0042119	0.0032359	0.	8705.2660	-0.0050492	-0.0772886	-1.2601048	-0.0027766	0.0105511	0.1799908
24	0.0042121	0.0027284	0.	8625.0792	-0.0050470	-0.0772850	-1.2598964	-0.0027723	0.0105464	0.1799795
25	0.0042123	0.0023084	0.	8548.1970	-0.0050454	-0.0772788	-1.2596597	-0.0027691	0.0105429	0.1799609
26	0.0042124	0.0019598	0.	8474.4808	-0.0050442	-0.0772711	-1.2594092	-0.0027666	0.0105401	0.1799379
27	0.0042125	0.0016695	0.	8403.7982	-0.0050434	-0.0772625	-1.2591550	-0.0027647	0.0105381	0.1799123
28	0.0042126	0.0014272	0.	8336.0222	-0.0050427	-0.0772535	-1.2589039	-0.0027632	0.0105365	0.1798855
29	0.0042126	0.0012242	0.	8271.0317	-0.0050423	-0.0772444	-1.2586607	-0.0027621	0.0105353	0.1798585
30	0.0042127	0.0010537	0.	8208.7106	-0.0050419	-0.0772354	-1.2584283	-0.0027612	0.0105344	0.1798319
31	0.0042127	9.100E-04	0.	8148.9481	-0.0050417	-0.0772268	-1.2582083	-0.0027605	0.0105337	0.1798062
32	0.0042127	7.886E-04	0.	8091.6383	-0.0050415	-0.0772184	-1.2580017	-0.0027600	0.0105331	0.1797816
33	0.0042128	6.857E-04	0.	8036.6797	-0.0050414	-0.0772106	-1.2578086	-0.0027595	0.0105327	0.1797583
34	0.0042128	5.982E-04	0.	7983.9754	-0.0050413	-0.0772032	-1.2576290	-0.0027592	0.0105323	0.1797364
35	0.0042128	5.236E-04	0.	7933.4330	-0.0050412	-0.0771962	-1.2574624	-0.0027589	0.0105321	0.1797159
36	0.0042128	4.598E-04	0.	7884.9638	-0.0050412	-0.0771898	-1.2573083	-0.0027587	0.0105319	0.1796968
37	0.0042128	4.051E-04	0.	7838.4832	-0.0050412	-0.0771837	-1.2571658	-0.0027585	0.0105317	0.1796790
38	0.0042128	3.580E-04	0.	7793.9103	-0.0050412	-0.0771782	-1.2570342	-0.0027584	0.0105316	0.1796625
39	0.0042128	3.174E-04	0.	7751.1677	-0.0050412	-0.0771730	-1.2569129	-0.0027583	0.0105314	0.1796472
40	0.0042128	2.823E-04	0.	7710.1815	-0.0050412	-0.0771682	-1.2568009	-0.0027582	0.0105314	0.1796331
41	0.0042128	2.518E-04	0.	7670.8809	-0.0050412	-0.0771637	-1.2566976	-0.0027581	0.0105313	0.1796200
42	0.0042128	2.253E-04	0.	7633.1983	-0.0050412	-0.0771596	-1.2566023	-0.0027580	0.0105312	0.1796078
43	0.0042128	2.021E-04	0.	7597.0691	-0.0050412	-0.0771558	-1.2565142	-0.0027580	0.0105312	0.1795966
44	0.0042128	1.819E-04	0.	7562.4312	-0.0050412	-0.0771523	-1.2564329	-0.0027579	0.0105311	0.1795862
45	0.0042128	1.642E-04	0.	7529.2256	-0.0050412	-0.0771490	-1.2563576	-0.0027579	0.0105311	0.1795765
46	0.0042128	1.486E-04	0.	7497.3957	-0.0050412	-0.0771460	-1.2562879	-0.0027579	0.0105311	0.1795675
47	0.0042128	1.348E-04	0.	7466.8871	-0.0050412	-0.0771432	-1.2562233	-0.0027579	0.0105311	0.1795592
48	0.0042128	1.227E-04	0.	7437.6482	-0.0050412	-0.0771406	-1.2561634	-0.0027578	0.0105310	0.1795515
49	0.0042128	1.119E-04	0.	7409.6292	-0.0050412	-0.0771381	-1.2561077	-0.0027578	0.0105310	0.1795443
50	0.0042128	1.023E-04	0.	7382.7827	-0.0050412	-0.0771359	-1.2560559	-0.0027578	0.0105310	0.1795376
51	0.0042128	9.384E-05	0.	7357.0632	-0.0050413	-0.0771338	-1.2560076	-0.0027578	0.0105310	0.1795314
52	0.0042128	8.625E-05	0.	7332.4272	-0.0050413	-0.0771318	-1.2559626	-0.0027578	0.0105310	0.1795255
53	0.0042128	7.946E-05	0.	7308.8329	-0.0050413	-0.0771299	-1.2559206	-0.0027578	0.0105310	0.1795201
54	0.0042128	7.338E-05	0.	7286.2405	-0.0050413	-0.0771282	-1.2558812	-0.0027577	0.0105310	0.1795150
55	0.0042128	6.792E-05	0.	7264.6118	-0.0050413	-0.0771266	-1.2558444	-0.0027577	0.0105310	0.1795102
56	0.0042128	6.300E-05	0.	7243.9100	-0.0050413	-0.0771251	-1.2558098	-0.0027577	0.0105310	0.1795057
57	0.0042128	5.857E-05	0.	7224.1000	-0.0050413	-0.0771236	-1.2557773	-0.0027577	0.0105310	0.1795015
58	0.0042128	5.457E-05	0.	7205.1483	-0.0050413	-0.0771223	-1.2557467	-0.0027577	0.0105310	0.1794975
59	0.0042128	5.094E-05	0.	7187.0226	-0.0050413	-0.0771210	-1.2557179	-0.0027577	0.0105310	0.1794938
60	0.0042128	4.765E-05	0.	7169.6919	-0.0050413	-0.0771198	-1.2556908	-0.0027577	0.0105310	0.1794902
61	0.0042128	4.466E-05	0.	7153.1267	-0.0050413	-0.0771187	-1.2556651	-0.0027577	0.0105310	0.1794869

ETHYLENE QUENCH COOLER (TLE)

LINE	CVC7	CVC8	UO	FRIC	PRM	GTOT	RE	TRES
0	0.	0.	0.0116800	0.0218354	0.7477906	5.0000000	42489.624	0.
1	-0.0010253	-0.0298144	0.0115265	0.0217662	0.7473792	5.0020162	43169.328	8.548E-04
2	-0.0015553	-0.0591237	0.0113918	0.0217050	0.7470345	5.0029646	43781.735	0.0017415
3	-0.0018458	-0.0835772	0.0112672	0.0216483	0.7467230	5.0034186	44358.172	0.0026586
4	-0.0020099	-0.1028142	0.0111486	0.0215946	0.7464302	5.0036274	44912.599	0.0036053
5	-0.0021043	-0.1175265	0.0110342	0.0215431	0.7461487	5.0037123	45451.925	0.0045811
6	-0.0021591	-0.1286040	0.0109229	0.0214934	0.7458749	5.0037356	45979.711	0.0055854
7	-0.0021913	-0.1368682	0.0108143	0.0214453	0.7456067	5.0037298	46497.778	0.0066179
8	-0.0022102	-0.1429996	0.0107080	0.0213986	0.7453432	5.0037117	47007.019	0.0076778
9	-0.0022215	-0.1475344	0.0106041	0.0213533	0.7450840	5.0036900	47507.817	0.0087647
10	-0.0022282	-0.1508833	0.0105023	0.0213093	0.7448287	5.0036688	48000.281	0.0098779
11	-0.0022323	-0.1533557	0.0104027	0.0212666	0.7445775	5.0036498	48484.382	0.0110168
12	-0.0022347	-0.1551821	0.0103052	0.0212251	0.7443303	5.0036335	48960.026	0.0121807
13	-0.0022362	-0.1565329	0.0102100	0.0211848	0.7440872	5.0036199	49427.095	0.0133689
14	-0.0022371	-0.1575337	0.0101169	0.0211457	0.7438484	5.0036087	49885.476	0.0145807
15	-0.0022377	-0.1582769	0.0100260	0.0211078	0.7436138	5.0035996	50335.063	0.0158153
16	-0.0022380	-0.1588301	0.0099373	0.0210711	0.7433837	5.0035921	50775.771	0.0170720
17	-0.0022382	-0.1592430	0.0098508	0.0210354	0.7431579	5.0035860	51207.537	0.0183499
18	-0.0022384	-0.1595520	0.0097664	0.0210008	0.7429367	5.0035810	51630.316	0.0196484
19	-0.0022384	-0.1597841	0.0096841	0.0209674	0.7427200	5.0035768	52044.084	0.0209666
20	-0.0022385	-0.1599588	0.0096040	0.0209349	0.7425079	5.0035734	52448.835	0.0223037
21	-0.0022385	-0.1600909	0.0095259	0.0209034	0.7423003	5.0035704	52844.582	0.0236589
22	-0.0022386	-0.1601909	0.0094499	0.0208730	0.7420974	5.0035680	53231.353	0.0250316
23	-0.0022386	-0.1602670	0.0093759	0.0208435	0.7418990	5.0035659	53609.189	0.0264208
24	-0.0022386	-0.1603250	0.0093039	0.0208149	0.7417053	5.0035641	53978.146	0.0278258
25	-0.0022386	-0.1603694	0.0092339	0.0207872	0.7415160	5.0035626	54338.291	0.0292459
26	-0.0022386	-0.1604035	0.0091657	0.0207604	0.7413314	5.0035612	54689.703	0.0306803
27	-0.0022386	-0.1604296	0.0090995	0.0207345	0.7411512	5.0035600	55032.469	0.0321283
28	-0.0022386	-0.1604498	0.0090350	0.0207094	0.7409755	5.0035590	55366.687	0.0335892
29	-0.0022386	-0.1604655	0.0089724	0.0206851	0.7408042	5.0035581	55692.461	0.0350621
30	-0.0022386	-0.1604776	0.0089115	0.0206616	0.7406373	5.0035573	56009.903	0.0365465
31	-0.0022386	-0.1604869	0.0088524	0.0206389	0.7404747	5.0035566	56319.133	0.0380417
32	-0.0022386	-0.1604943	0.0087949	0.0206169	0.7403163	5.0035560	56620.273	0.0395470
33	-0.0022386	-0.1604999	0.0087391	0.0205956	0.7401621	5.0035554	56913.453	0.0410617
34	-0.0022386	-0.1605044	0.0086848	0.0205750	0.7400121	5.0035549	57198.806	0.0425853
35	-0.0022386	-0.1605078	0.0086321	0.0205551	0.7398661	5.0035544	57476.471	0.0441171
36	-0.0022386	-0.1605105	0.0085809	0.0205358	0.7397241	5.0035540	57746.585	0.0456565
37	-0.0022386	-0.1605126	0.0085312	0.0205172	0.7395860	5.0035537	58009.294	0.0472030
38	-0.0022386	-0.1605142	0.0084829	0.0204992	0.7394517	5.0035533	58264.741	0.0487560
39	-0.0022386	-0.1605155	0.0084361	0.0204818	0.7393212	5.0035530	58513.073	0.0503150
40	-0.0022386	-0.1605165	0.0083905	0.0204649	0.7391944	5.0035527	58754.438	0.0518795
41	-0.0022386	-0.1605172	0.0083463	0.0204486	0.7390712	5.0035525	58988.986	0.0534489
42	-0.0022386	-0.1605178	0.0083034	0.0204328	0.7389515	5.0035523	59216.864	0.0550228
43	-0.0022386	-0.1605182	0.0082618	0.0204176	0.7388353	5.0035521	59438.223	0.0566008
44	-0.0022386	-0.1605185	0.0082213	0.0204029	0.7387225	5.0035519	59653.212	0.0581823
45	-0.0022386	-0.1605187	0.0081820	0.0203886	0.7386129	5.0035517	59861.978	0.0597671


```

122.0000 E.....F.....D.....*.....C.....
E      F      .      D      .      *      C.
.
E      .      F      .      D      .      BA C .
.
E      .      F      .      D      .      BA C .
E      .      F      .      D      .      B A C .
.
E      .      F      .      D      .      B A C .
.
E      .      F      .      D      B A C .
E      .      .F      .      D      B. A C .
.
E      .      .      F      .      D      B .A C .
E      .      .      F      .      D      B .A C .
.
E      .      .      F      .      D      B .A C .
E      .      .      F      .      D      B .A C .
.
E      .      .      F      .      D      B .A C .
E      .      .      F      .      D      B .A C .
.
244.0000 E.....F.....*.....A.....C.....
E      .      .      .      F. *      A. C .
.
E      .      .      .      .FBD      A. C .
E      .      .      .      *D      A. C .
.
E      .      .      .      .B DF      A . C .
.
E      .      .      .      B D F      A . C .
E      .      .      .      B. D      FA . C .
.
E      .      .      .      B . D      AF . C .
E      .      .      .      B . D      A F C .
.
E      .      .      .      B . D      A .F C .
.
E      .      .      .      B . D      A . FC .
E      .      .      .      B . D      A . * .
.
E      .      .      .      B . D      A . C F .
.
366.0000 E      .      .      B      .      D A      .      C F .
E      .      .      .      B      .      D A      .      C F.
.
E      .      .      .      B      .      D A      .      C F .
.
E      .      .      .      .B      .      D A      .      C . F .

```

```

E . . . B . . . D A . . . C . . . F . . . . . . . . . . . .
. E . . . B. . . . D A . . . C . . . F . . . . . . . . . . . .
. E . . . B . . . . D A . . . C . . . F . . . . . . . . . . . .
. E . . . B . . . . DA . . . C . . . F . . . . . . . . . . . .
. E . . . B . . . . DA . . . C . . . F . . . . . . . . . . . .
. E . . . B . . . . DA . . . C . . . F . . . . . . . . . . . .
. E . . . B . . . . DA . . . C . . . F . . . . . . . . . . . .
488.0000 E . . . B . . . . DA . . . C . . . F . . . . . . . . . . . .
. E . . . B . . . . * . . . C . . . F . . . . . . . . . . . .
. E . . . B . . . . * . . . C . . . F . . . . . . . . . . . .
. E . . . B . . . . * . . . C . . . F . . . . . . . . . . . .
. E . . . B . . . . * . . . C . . . F . . . . . . . . . . . .
. E . . . B. . . . * . . . C . . . F . . . . . . . . . . . .
. E . . . B. . . . * . . . C . . . F . . . . . . . . . . . .
. E . . . B . . . . * . . . C . . . F . . . . . . . . . . . .
. E . . . B . . . . * . . . C . . . F . . . . . . . . . . . .
. E . . . B . . . . AD . . . C . . . . . . . . . . . . . . . .
. E . . . B . . . . AD . . . C . . . . . . . . . . . . . . . .
. E . . . B . . . . AD . . . C . . . . . . . . . . . . . . . .
610.0000 E . . . B . . . . AD . . . C . . . . . . . . . . . . F . . .

```

STOP
2545 WORDS TABL SPAC US D

Appendix J. Quench Cooler ACSL Program Listings

- Listing 1: Simulation Program for Coke Model 1
- Listing 2: Simulation Program for Coke Model 2
- Listing 3: Alberta Gas Ethylene Simulation Program

```

program tle
*****
" ETHANE TO ETHYLENE PYROLYSIS QUENCH COOLER"
" Richard Huntrods P. Eng."
" University of Calgary Masters of Engineering Thesis"
" July 1988"
*****
" MODEL 1 - Integrated form of the COKE equation"
*****
***** initial conditions"
constant timei = 0.0           $" days"
constant times = 60.0         $" end time - days"
constant tstep = 6.0          $" days"
constant tempi = 1133.7        $" feed temperature - K"
constant presi = 2.12         $" feed pressure - atm"
constant flowi = 5.0          $" feed flow rate - gm / cm2 sec"
constant xc1i = 0.3004        $" feed composition - mole fraction"
constant xc2i = 0.0381
constant xc3i = 0.0017
constant xc4i = 0.2399
constant xc5i = 0.1702
constant xc6i = 0.0129
constant xc7i = 0.0141
constant xc8i = 0.0028
constant frst = 0.2819        $" steam dilution ratio"
constant dcki = 0.0           $" initial coke deposition"
***** definition of reactor parameters"
constant ztot = 610.0         $" reactor length - cm (= 20 ft)"
constant delz = 10.0          $" cm"
constant diai = 2.4638        $" tube diameter - cm (= 0.97 in)"
constant xwall = 0.3556       $" tube thickness - cm (= 9/64 in.)"
constant kck = 3.2            $" Btu / hr ft F"
constant bck = 0.0            $" initial coke thickness - cm."
constant bcksv = 0.0          $" stored coke thickness"
constant delbck = 0.0         $" initial delta coke thickness"
constant bckmax = 1.00        $" maximum coke thickness allowed"
constant alpck = 1.0           $" fraction of coke deposited"
constant tw = 586.48          $" steam temperature - K"
constant ho = 2040.0          $" Btu / hr ft2 F"
***** definition of constant data"
constant tref = 298.0         $" K"
constant rconst = 1.987       $" cal/g-mol K"
constant rgas = 82.05         $" cm3 atm / g-mol K"
constant factp = 4.9343e-7    $" ( gm / cm2 to atm ) * 1 / 2gc"
constant factu = 1.3550e-4    $" Btu / hr ft2 F to cal / sec cm2 K"
constant tfact = 8.64e+4      $" time from days to sec."
constant pi = 3.1416
constant rneg1 = -1.0
***** definition of component data"
" H2 = C1 (hydrogen)"
" CH4 = C2 (methane)"
" C2H2 = C3 (acetylene)"
" C2H4 = C4 (ethylene)"
" C2H6 = C5 (ethane)"
" C3H6 = C6 (propylene)"
" C3H8 = C7 (propane)"
" C4H6 = C8 (1,3-butadiene)"
" C = C9 (coke)"
***** H2"
constant mwc1 = 2.016         $" molecular weight - gm / g-mol"
constant tcc1 = 33.2          $" critical temperature - K"
constant pcc1 = 12.8          $" critical pressure - atm"
constant cpac1 = 6.483        $" Cp coeff. - cal / g-mol K"
constant cpbc1 = 2.215e-3     $" Cp coeff. - cal / g-mol K**2"
constant cpcc1 = -3.298e-6    $" Cp coeff. - cal / g-mol K**3"
constant cpdc1 = 1.826e-9     $" Cp coeff. - cal / g-mol K**4"
constant delhc1 = 0.0         $" heat of formation - cal / g-mol"
***** CH4"
constant mwc2 = 16.043
constant tcc2 = 190.6

```

```

constant pcc2 = 45.4
constant cpac2 = 4.598
constant cpbc2 = 1.245e-2
constant cpcc2 = 2.860e-6
constant cpdc2 = -2.703e-9
constant delhc2 = -17890.0
***** C2H2"
constant mwc3 = 26.038
constant tcc3 = 308.3
constant pcc3 = 60.6
constant cpac3 = 6.406
constant cpbc3 = 1.810e-2
constant cpcc3 = -1.196e-5
constant cpdc3 = 3.363e-9
constant delhc3 = 54190.0
***** C2H4"
constant mwc4 = 28.054
constant tcc4 = 282.4
constant pcc4 = 49.7
constant cpac4 = 0.909
constant cpbc4 = 3.740e-2
constant cpcc4 = -1.994e-5
constant cpdc4 = 4.192e-9
constant delhc4 = 12500.0
***** C2H6"
constant mwc5 = 30.070
constant tcc5 = 305.4
constant pcc5 = 48.2
constant cpac5 = 1.292
constant cpbc5 = 4.254e-2
constant cpcc5 = -1.657e-5
constant cpdc5 = 2.081e-9
constant delhc5 = -20240.0
***** C3H6"
constant mwc6 = 42.081
constant tcc6 = 365.0
constant pcc6 = 45.6
constant cpac6 = 0.886
constant cpbc6 = 5.602e-2
constant cpcc6 = -2.771e-5
constant cpdc6 = 5.266e-9
constant delhc6 = 4880.0
***** C3H8"
constant mwc7 = 44.097
constant tcc7 = 369.8
constant pcc7 = 41.9
constant cpac7 = -1.009
constant cpbc7 = 7.315e-2
constant cpcc7 = -3.789e-5
constant cpdc7 = 7.678e-9
constant delhc7 = -24820.0
***** C4H6"
constant mwc8 = 54.092
constant tcc8 = 425.0
constant pcc8 = 42.7
constant cpac8 = -0.403
constant cpbc8 = 8.165e-2
constant cpcc8 = -5.589e-5
constant cpdc8 = 1.513e-8
constant delhc8 = 26330.0
***** coke"
constant mwck = 12.0
constant cpack = 2.673
constant cpbck = 2.617e-3
constant cpccck = 0.0
constant cpdck = 0.0
constant delhck = 0.0
constant rhock = 1.6
***** steam"
constant mwst = 18.015

```

\$" density - g / cm3"

```

constant tcst = 647.3
constant pcst = 217.6
constant cpast = 7.701
constant cpbst = 4.595e-4
constant cpcst = 2.521e-6
constant cpdst = -0.859e-9
***** definition of reaction data"
" rx1: C2H6 <-> C2H4 + H2"
" rx2: 2 C2H6 -> C3H8 + CH4"
" rx3: C3H6 <-> C2H2 + CH4"
" rx4: C2H2 + C2H4 -> C4H6"
" rx5: C2H4 + C2H6 -> C3H6 + CH4"
" rx6: C4H6 -> 4 C + 3 H2"
constant prrx1 = 4.652e13          $" 1 / sec"
constant actrx1 = 65200.0         $" cal / g-mol"
constant prrx2 = 3.850e11
constant actrx2 = 65250.0
constant prrx3 = 9.814e08
constant actrx3 = 36920.0
constant prrx4 = 1.026e15        $" cm3 / g-mol sec"
constant actrx4 = 41260.0
constant prrx5 = 7.083e16        $" cm3 / g-mol sec"
constant actrx5 = 60430.0
constant prrx6 = 8.55e4          $" gm coke cm / gm c4 sec"
constant actrx6 = 28250.0
***** equilibrium constants f(T)"
constant eqbrx1 = -19.496
constant eqsrx1 = 1.4098e-2
constant eqbrx3 = -18.286
constant eqsrx3 = 1.3040e-2
*****
***** initial calculations and setup"
initial
***** change the variable from t to z (length)"
variable z=0.
cinterval ci = 10.0
***** calculate tube outer diameter - cm."
diao = diai + 2.0 * xwall
***** calculate initial flow conditions"
areai = pi * diai * diai * 0.25
hctot = xc1i + xc2i + xc3i + xc4i + xc5i + xc6i + xc7i + xc8i
xstm = hctot * frst
xtot = hctot + xstm
yc1i = xc1i / xtot
yc2i = xc2i / xtot
yc3i = xc3i / xtot
yc4i = xc4i / xtot
yc5i = xc5i / xtot
yc6i = xc6i / xtot
yc7i = xc7i / xtot
yc8i = xc8i / xtot
ystm = xstm / xtot
mwavi = yc1i * mwc1 + yc2i * mwc2 + yc3i * mwc3 + yc4i * mwc4 + ...
        yc5i * mwc5 + yc6i * mwc6 + yc7i * mwc7 + yc8i * mwc8 + ...
        ystm * mwst
ftoti = flowi * areai / mwavi
fc1i = yc1i * ftoti
fc2i = yc2i * ftoti
fc3i = yc3i * ftoti
fc4i = yc4i * ftoti
fc5i = yc5i * ftoti
fc6i = yc6i * ftoti
fc7i = yc7i * ftoti
fc8i = yc8i * ftoti
fstm = ystm * ftoti
***** calculate viscosity term 1"
vcrc1 = 7.70 * mwc1 ** 0.5 * pcc1 ** (2./3.) * tcc1 ** (-1./6.)
vcrc2 = 7.70 * mwc2 ** 0.5 * pcc2 ** (2./3.) * tcc2 ** (-1./6.)
vcrc3 = 7.70 * mwc3 ** 0.5 * pcc3 ** (2./3.) * tcc3 ** (-1./6.)
vcrc4 = 7.70 * mwc4 ** 0.5 * pcc4 ** (2./3.) * tcc4 ** (-1./6.)

```

```

vcrc5 = 7.70 * mwc5 ** 0.5 * pcc5 ** (2./3.) * tcc5 ** (-1./6.)
vcrc6 = 7.70 * mwc6 ** 0.5 * pcc6 ** (2./3.) * tcc6 ** (-1./6.)
vcrc7 = 7.70 * mwc7 ** 0.5 * pcc7 ** (2./3.) * tcc7 ** (-1./6.)
vcrc8 = 7.70 * mwc8 ** 0.5 * pcc8 ** (2./3.) * tcc8 ** (-1./6.)
vcrst = 7.70 * mwst ** 0.5 * pcst ** (2./3.) * tcst ** (-1./6.)
***** calculate heat of reaction at 298K - cal / g-mol"
dhrx1 = delhc4 + delhc1 - delhc5
dhrx2 = delhc7 + delhc2 - 2 * delhc5
dhrx3 = delhc3 + delhc2 - delhc6
dhrx4 = delhc8 - delhc3 - delhc4
dhrx5 = delhc6 + delhc2 - delhc4 - delhc5
dhrx6 = 4 * delhc4 + 3 * delhc1 - delhc8
***** calculate delcp for reactions - cal / g-mol K"
cparx1 = cpac4 + cpac1 - cpac5
cparx2 = cpac7 + cpac2 - 2 * cpac5
cparx3 = cpac3 + cpac2 - cpac6
cparx4 = cpac8 - cpac3 - cpac4
cparx5 = cpac6 + cpac2 - cpac4 - cpac5
cparx6 = 4 * cpac4 + 3 * cpac1 - cpac8
cpbrx1 = ( cpbc4 + cpbc1 - cpbc5 ) * 0.5
cpbrx2 = ( cpbc7 + cpbc2 - 2 * cpbc5 ) * 0.5
cpbrx3 = ( cpbc3 + cpbc2 - cpbc6 ) * 0.5
cpbrx4 = ( cpbc8 - cpbc3 - cpbc4 ) * 0.5
cpbrx5 = ( cpbc6 + cpbc2 - cpbc4 - cpbc5 ) * 0.5
cpbrx6 = ( 4 * cpbc4 + 3 * cpbc1 - cpbc8 ) * 0.5
cpcrx1 = ( cpcc4 + cpcc1 - cpcc5 ) / 3.0
cpcrx2 = ( cpcc7 + cpcc2 - 2 * cpcc5 ) / 3.0
cpcrx3 = ( cpcc3 + cpcc2 - cpcc6 ) / 3.0
cpcrx4 = ( cpcc8 - cpcc3 - cpcc4 ) / 3.0
cpcrx5 = ( cpcc6 + cpcc2 - cpcc4 - cpcc5 ) / 3.0
cpcrx6 = ( 4 * cpcc4 + 3 * cpcc1 - cpcc8 ) / 3.0
cpdrx1 = ( cpdc4 + cpdc1 - cpdc5 ) * 0.25
cpdrx2 = ( cpdc7 + cpdc2 - 2 * cpdc5 ) * 0.25
cpdrx3 = ( cpdc3 + cpdc2 - cpdc6 ) * 0.25
cpdrx4 = ( cpdc8 - cpdc3 - cpdc4 ) * 0.25
cpdrx5 = ( cpdc6 + cpdc2 - cpdc4 - cpdc5 ) * 0.25
cpdrx6 = ( 4 * cpdc4 + 3 * cpdc1 - cpdc8 ) * 0.25
***** initialize time loop"
time = timei
label1.. continue
end $"initial"
dynamic
***** calculate total feed - g-mol / sec"
ftot = fc1 + fc2 + fc3 + fc4 + fc5 + fc6 + fc7 + fc8 + fstm
***** calculate mole fractions"
yc1 = fc1 / ftot
yc2 = fc2 / ftot
yc3 = fc3 / ftot
yc4 = fc4 / ftot
yc5 = fc5 / ftot
yc6 = fc6 / ftot
yc7 = fc7 / ftot
yc8 = fc8 / ftot
yst = fstm / ftot
***** evaluate rate constants"
denom = rconst * temp * rneg1
***** ( 1 / sec )"
rkrx1 = prrx1 * exp ( actrx1 / denom )
rkrx2 = prrx2 * exp ( actrx2 / denom )
rkrx3 = prrx3 * exp ( actrx3 / denom )
***** ( cm3 / g-mol sec )"
rkrx4 = prrx4 * exp ( actrx4 / denom )
rkrx5 = prrx5 * exp ( actrx5 / denom )
***** ( gm coke cm / gm c4 sec )"
rkrx6 = prrx6 * exp ( actrx6 / denom )
***** evaluate equilibrium constants - g-mol / cm3"
***** (convert g-mol / l to g-mol / cm3)"
eqrx1 = ( exp ( eqbrx1 + eqsrx1 * temp ) ) * 0.001
eqrx3 = ( exp ( eqbrx3 + eqsrx3 * temp ) ) * 0.001
***** calculate viscosity - cp"

```

```

vrc1 = exp (( -0.1208 + 0.1354 * alog ( temp / tcc1 )) * 5.0 )
vrc2 = exp (( -0.1208 + 0.1354 * alog ( temp / tcc2 )) * 5.0 )
vrc3 = exp (( -0.1208 + 0.1354 * alog ( temp / tcc3 )) * 5.0 )
vrc4 = exp (( -0.1208 + 0.1354 * alog ( temp / tcc4 )) * 5.0 )
vrc5 = exp (( -0.1208 + 0.1354 * alog ( temp / tcc5 )) * 5.0 )
vrc6 = exp (( -0.1208 + 0.1354 * alog ( temp / tcc6 )) * 5.0 )
vrc7 = exp (( -0.1208 + 0.1354 * alog ( temp / tcc7 )) * 5.0 )
vrc8 = exp (( -0.1208 + 0.1354 * alog ( temp / tcc8 )) * 5.0 )
vrst = exp (( -0.1208 + 0.1354 * alog ( temp / tcst )) * 5.0 )
***** (convert from micropoise to cP)
visc1 = 0.0001 * vcrc1 * vrc1
visc2 = 0.0001 * vcrc2 * vrc2
visc3 = 0.0001 * vcrc3 * vrc3
visc4 = 0.0001 * vcrc4 * vrc4
visc5 = 0.0001 * vcrc5 * vrc5
visc6 = 0.0001 * vcrc6 * vrc6
visc7 = 0.0001 * vcrc7 * vrc7
visc8 = 0.0001 * vcrc8 * vrc8
visst = 0.0001 * vcrst * vrst
***** calculate average viscosity - cP
ymvc1 = yc1 * sqrt( mvc1 )
ymvc2 = yc2 * sqrt( mvc2 )
ymvc3 = yc3 * sqrt( mvc3 )
ymvc4 = yc4 * sqrt( mvc4 )
ymvc5 = yc5 * sqrt( mvc5 )
ymvc6 = yc6 * sqrt( mvc6 )
ymvc7 = yc7 * sqrt( mvc7 )
ymvc8 = yc8 * sqrt( mvc8 )
ymvst = yst * sqrt( mvst )
vnum = ymvc1 * visc1 + ymvc2 * visc2 + ymvc3 * visc3 + ...
      ymvc4 * visc4 + ymvc5 * visc5 + ymvc6 * visc6 + ...
      ymvc7 * visc7 + ymvc8 * visc8 + ymst * visst
vden = ymvc1 + ymvc2 + ymvc3 + ymvc4 + ymvc5 + ymvc6 + ymvc7 + ...
      ymvc8 + ymst
vism = vnum / vden
***** calculate average molecular weight - gm / g-mol
mnav = yc1 * mvc1 + yc2 * mvc2 + yc3 * mvc3 + yc4 * mvc4 + ...
      yc5 * mvc5 + yc6 * mvc6 + yc7 * mvc7 + yc8 * mvc8 + ...
      ystm * mvst
***** calculate heat capacities - cal / g-mol K
temp2 = temp * temp
temp3 = temp2 * temp
cpc1 = cpac1 + cpbc1 * temp + cpcc1 * temp2 + cpdc1 * temp3
cpc2 = cpac2 + cpbc2 * temp + cpcc2 * temp2 + cpdc2 * temp3
cpc3 = cpac3 + cpbc3 * temp + cpcc3 * temp2 + cpdc3 * temp3
cpc4 = cpac4 + cpbc4 * temp + cpcc4 * temp2 + cpdc4 * temp3
cpc5 = cpac5 + cpbc5 * temp + cpcc5 * temp2 + cpdc5 * temp3
cpc6 = cpac6 + cpbc6 * temp + cpcc6 * temp2 + cpdc6 * temp3
cpc7 = cpac7 + cpbc7 * temp + cpcc7 * temp2 + cpdc7 * temp3
cpc8 = cpac8 + cpbc8 * temp + cpcc8 * temp2 + cpdc8 * temp3
cpst = cpast + cpbst * temp + cpccst * temp2 + cpdst * temp3
***** calculate average heat capacity - cal / g-mol K
cpav = yc1 * cpc1 + yc2 * cpc2 + yc3 * cpc3 + yc4 * cpc4 + ...
      yc5 * cpc5 + yc6 * cpc6 + yc7 * cpc7 + yc8 * cpc8 + ...
      yst * cpst
***** calculate integrated delta heat capacity - cal / g-mol
tt = temp - tref
tt2 = tt * tt
tt3 = tt2 * tt
tt4 = tt3 * tt
cprx1 = cparx1 * tt + cpbrx1 * tt2 + cpcrx1 * tt3 + cpdrx1 * tt4
cprx2 = cparx2 * tt + cpbrx2 * tt2 + cpcrx2 * tt3 + cpdrx2 * tt4
cprx3 = cparx3 * tt + cpbrx3 * tt2 + cpcrx3 * tt3 + cpdrx3 * tt4
cprx4 = cparx4 * tt + cpbrx4 * tt2 + cpcrx4 * tt3 + cpdrx4 * tt4
cprx5 = cparx5 * tt + cpbrx5 * tt2 + cpcrx5 * tt3 + cpdrx5 * tt4
cprx6 = cparx6 * tt + cpbrx6 * tt2 + cpcrx6 * tt3 + cpdrx6 * tt4
***** calculate heat of reaction - cal / g-mol
hrx1 = dhrx1 + cprx1
hrx2 = dhrx2 + cprx2
hrx3 = dhrx3 + cprx3

```

```

hrx4 = dhrx4 + cprx4
hrx5 = dhrx5 + cprx5
hrx6 = dhrx6 + cprx6
***** calculate gas thermal conductivity - Btu / hr ft F"
***** (convert viscosity from cP to lb / hr ft)"
cvav = cpav - 1.99
vismb = vism * 2.42
kfm = vismb * cvav * ( 3.670 / cvav + 1.272 ) / mwav
***** calculate wall heat transfer coefficient - Btu / hr ft F"
tfar = ( temp * 1.8 ) - 459.67
kwall = 14.1 + 0.00433 * ( tfar - 1300.0 )
***** calculate Prandtl no. - dimensionless"
prm = cpav * vismb / ( kfm * mwav )
***** evaluate rate expressions - g-mol / cm3 sec"
prt = pres / ( rgas * temp )
ypc1 = yc1 * prt
ypc2 = yc2 * prt
ypc3 = yc3 * prt
ypc4 = yc4 * prt
ypc5 = yc5 * prt
ypc6 = yc6 * prt
ypc7 = yc7 * prt
ypc8 = yc8 * prt
rtrx1 = rkrx1 * ( ypc5 - ypc4 * ypc1 / eqrx1 )
rtrx2 = rkrx2 * ( ypc5 )
rtrx3 = rkrx3 * ( ypc6 - ypc3 * ypc2 / eqrx3 )
rtrx4 = rkrx4 * ( ypc3 * ypc4 )
rtrx5 = rkrx5 * ( ypc4 * ypc5 )
***** ( mole coke / cm2 sec )"
rtrx6z = rkrx6 * ( ypc8 ) * ( mwc8 / mwck )
***** calculate the change in diameter due to coke - cm."
bterm = rneg1 * rtrx6z * mwck * time * tfact * 2.0 / ( rhock * diai )
bck = 0.5 * diai * ( 1.0 - exp ( bterm * alpck ) )
delbck=bck-bcksv
bcksv = amax1 ( bcksv , bck )
dia = diai - 2.0 * bck
***** calculate the perimeter and area - cm and cm2"
per = pi * dia
area = pi * dia * dia * 0.25
***** convert rtrx6 from mol / cm2 sec to mol / cm3 sec"
rtrx6 = rtrx6z * per / area
***** calculate mass flow rate - gm / cm2 sec"
gtot = ftot * mwav / area
***** calculate Reynold's no. - dimensionless"
re = dia * gtot / ( vism * 0.01 )
***** calculate friction term - 1 / cm"
fric = 0.184 * re ** (-0.2)
***** calculate dF/dx terms - g-mol / cm sec"
dfc1 = area * ( rtrx1 + 3 * rtrx6 )
dfc2 = area * ( rtrx2 + rtrx3 + rtrx5 )
dfc3 = area * ( rtrx3 - rtrx4 )
dfc4 = area * ( rtrx1 - rtrx4 - rtrx5 )
dfc5 = area * ( rtrx1 + 2 * rtrx2 + rtrx5 ) * rneg1
dfc6 = area * ( rtrx5 - rtrx3 )
dfc7 = area * ( rtrx2 )
dfc8 = area * ( rtrx4 - rtrx6 )
ddck = area * ( 4 * rtrx6 )
***** calculate internal heat transfer coeff - Btu / hr ft2 F"
teff = ( tw / temp ) ** ( 0.29 + 0.0019 * z / dia )
hi = 0.021 * re ** 0.8 * prm ** 0.4 * kfm * 30.48 / ( teff * dia )
***** calculate overall heat transfer coefficient - Btu / hr ft2 F"
dialw = diai + xwall
dialc = diai - bck
hoi = 1.0 / ho
hii = diao / ( dia * hi )
hwi = diao * 0.03281 * xwall / ( dialw * kwall )
hci = diao * 0.03281 * bck / ( dialc * kck )
uoi = hii + hwi + hci + hoi
uo = ( 1.0 / uoi ) * factu
***** calculate temperature derivative"

```

```

t den = cpav * ftot
sumr = ( rtrx1 * hrx1 + rtrx2 * hrx2 + rtrx3 * hrx3 + rtrx4 * ...
        hrx4 + rtrx5 * hrx5 + rtrx6 * hrx6 ) * rneg1
dt = ( per * uo * ( tw - temp ) + area * sumr ) / tden
***** calculate pressure drop derivative ( fanning )"
rho f = pres * mwav / ( rgas * temp )
dp = rneg1 * factp * gtot * gtot * fric / ( dia * rho f )
***** calculate fluid velocity"
velf = gtot / rho f
derivative
***** integrate for quantities"
fc1 = integ( dfc1 , fc1i )
fc2 = integ( dfc2 , fc2i )
fc3 = integ( dfc3 , fc3i )
fc4 = integ( dfc4 , fc4i )
fc5 = integ( dfc5 , fc5i )
fc6 = integ( dfc6 , fc6i )
fc7 = integ( dfc7 , fc7i )
fc8 = integ( dfc8 , fc8i )
dck = integ( ddck , dcki )
temp = integ( dt , tempi )
pres = integ( dp , presi )
end $"derivative"
***** calculate conversions"
cvc1 = ( fc1i - fc1 ) / fc1i
cvc2 = ( fc2i - fc2 ) / fc2i
cvc3 = ( fc3i - fc3 ) / fc3i
cvc4 = ( fc4i - fc4 ) / fc4i
cvc5 = ( fc5i - fc5 ) / fc5i
cvc6 = ( fc6i - fc6 ) / fc6i
cvc7 = ( fc7i - fc7 ) / fc7i
cvc8 = ( fc8i - fc8 ) / fc8i
***** calculate residence time"
tres = z / velf
***** specify terminating conditions"
termt ( z . ge . ztot )
end $"dynamic"
*****
terminal
***** time loop"
time = time + tstep
if( time.le.times .and. bcksv.le.bckmax ) go to label1
end $"terminal"
end $"program"

```

```

program tle
*****
" ETHANE TO ETHYLENE PYROLYSIS QUENCH COOLER"
" Richard Huntruds P. Eng."
" University of Calgary Masters of Engineering Thesis"
" July 1988"
*****
" MODEL 2 - Differential form of the COKE equation"
*****
***** declarations"
integer ipos, int, npos
array tcoke(100)
***** initial conditions"
constant timei = 0.0           $" days"
constant times = 60.0         $" end time - days"
constant tstep = 6.0          $" days"
constant tempi = 1133.7        $" feed temperature - K"
constant presi = 2.12         $" feed pressure - atm"
constant flowi = 5.0          $" feed flow rate - gm / cm2 sec"
constant xc1i = 0.3004        $" feed composition - mole fraction"
constant xc2i = 0.0381
constant xc3i = 0.0017
constant xc4i = 0.2399
constant xc5i = 0.1702
constant xc6i = 0.0129
constant xc7i = 0.0141
constant xc8i = 0.0028
constant frst = 0.2819        $" steam dilution ratio"
constant dcki = 0.0           $" initial coke deposition"
***** definition of reactor parameters"
constant npos = 61            $" number of reactor grid blocks"
constant ztot = 610.0         $" reactor length - cm (= 20 ft)"
constant delz = 10.0          $" cm"
constant diai = 2.4638        $" tube diameter - cm (= 0.97 in)"
constant xwall = 0.3556       $" tube thickness - cm (= 9/64 in.)"
constant kck = 3.2            $" Btu / hr ft F"
constant bck = 0.0            $" initial coke thickness - cm."
constant delbck = 0.0         $" initial delta coke thickness"
constant bckmax = 1.0         $" maximum coke thickness allowed"
constant alpck = 1.0          $" fraction of coke deposited"
constant tw = 586.48          $" steam temperature - K"
constant ho = 2040.0          $" Btu / hr ft2 F"
***** definition of constant data"
constant tref = 298.0         $" K"
constant rconst = 1.987       $" cal/g-mol K"
constant rgas = 82.05         $" cm3 atm / g-mol K"
constant factp = 4.9343e-7    $" ( gm / cm2 to atm ) * 1 / 2gc"
constant factu = 1.3550e-4     $" Btu / hr ft2 F to cal / sec cm2 K"
constant tfact = 8.64e+4       $" time from days to sec."
constant pi = 3.1416
constant rneg1 = -1.0
***** definition of component data"
" H2 = C1 (hydrogen)"
" CH4 = C2 (methane)"
" C2H2 = C3 (acetylene)"
" C2H4 = C4 (ethylene)"
" C2H6 = C5 (ethane)"
" C3H6 = C6 (propylene)"
" C3H8 = C7 (propane)"
" C4H6 = C8 (1,3-butadiene)"
" C = C9 (coke)"
***** H2"
constant mwc1 = 2.016          $" molecular weight - gm / g-mol"
constant tcc1 = 33.2           $" critical temperature - K"
constant pcc1 = 12.8           $" critical pressure - atm"
constant cpac1 = 6.483         $" Cp coeff. - cal / g-mol K"
constant cpbc1 = 2.215e-3      $" Cp coeff. - cal / g-mol K**2"
constant cpcc1 = -3.298e-6     $" Cp coeff. - cal / g-mol K**3"
constant cpdc1 = 1.826e-9      $" Cp coeff. - cal / g-mol K**4"
constant delhc1 = 0.0          $" heat of formation - cal / g-mol"

```

```

***** CH4"
constant mwc2 = 16.043
constant tcc2 = 190.6
constant pcc2 = 45.4
constant cpac2 = 4.598
constant cpbc2 = 1.245e-2
constant cpcc2 = 2.860e-6
constant cpdc2 = -2.703e-9
constant delhc2 = -17890.0
***** C2H2"
constant mwc3 = 26.038
constant tcc3 = 308.3
constant pcc3 = 60.6
constant cpac3 = 6.406
constant cpbc3 = 1.810e-2
constant cpcc3 = -1.196e-5
constant cpdc3 = 3.363e-9
constant delhc3 = 54190.0
***** C2H4"
constant mwc4 = 28.054
constant tcc4 = 282.4
constant pcc4 = 49.7
constant cpac4 = 0.909
constant cpbc4 = 3.740e-2
constant cpcc4 = -1.994e-5
constant cpdc4 = 4.192e-9
constant delhc4 = 12500.0
***** C2H6"
constant mwc5 = 30.070
constant tcc5 = 305.4
constant pcc5 = 48.2
constant cpac5 = 1.292
constant cpbc5 = 4.254e-2
constant cpcc5 = -1.657e-5
constant cpdc5 = 2.081e-9
constant delhc5 = -20240.0
***** C3H6"
constant mwc6 = 42.081
constant tcc6 = 365.0
constant pcc6 = 45.6
constant cpac6 = 0.886
constant cpbc6 = 5.602e-2
constant cpcc6 = -2.771e-5
constant cpdc6 = 5.266e-9
constant delhc6 = 4880.0
***** C3H8"
constant mwc7 = 44.097
constant tcc7 = 369.8
constant pcc7 = 41.9
constant cpac7 = -1.009
constant cpbc7 = 7.315e-2
constant cpcc7 = -3.789e-5
constant cpdc7 = 7.678e-9
constant delhc7 = -24820.0
***** C4H6"
constant mwc8 = 54.092
constant tcc8 = 425.0
constant pcc8 = 42.7
constant cpac8 = -0.403
constant cpbc8 = 8.165e-2
constant cpcc8 = -5.589e-5
constant cpdc8 = 1.513e-8
constant delhc8 = 26330.0
***** coke"
constant mwck = 12.0
constant cpack = 2.673
constant cpbck = 2.617e-3
constant cpccck = 0.0
constant cpdck = 0.0
constant delhck = 0.0

```

```

constant rhock = 1.6          $" density - g / cm3"
***** steam"
constant mwst = 18.015
constant tcst = 647.3
constant pcst = 217.6
constant cpast = 7.701
constant cpbst = 4.595e-4
constant cpcst = 2.521e-6
constant cpdst = -0.859e-9
***** definition of reaction data"
" rx1: C2H6 <-> C2H4 + H2"
" rx2: 2 C2H6 -> C3H8 + CH4"
" rx3: C3H6 <-> C2H2 + CH4"
" rx4: C2H2 + C2H4 -> C4H6"
" rx5: C2H4 + C2H6 -> C3H6 + CH4"
" rx6: C4H6 -> 4 C + 3 H2"
constant prrx1 = 4.652e13      $" 1 / sec"
constant actrx1 = 65200.0     $" cal / g-mol"
constant prrx2 = 3.850e11
constant actrx2 = 65250.0
constant prrx3 = 9.814e08
constant actrx3 = 36920.0
constant prrx4 = 1.026e15     $" cm3 / g-mol sec"
constant actrx4 = 41260.0
constant prrx5 = 7.083e16     $" cm3 / g-mol sec"
constant actrx5 = 60430.0
constant prrx6 = 8.55e4       $" gm coke cm / gm c4 sec"
constant actrx6 = 28250.0
***** equilibrium constants f(T)"
constant eqbrx1 = -19.496
constant eqsrx1 = 1.4098e-2
constant eqbrx3 = -18.286
constant eqsrx3 = 1.3040e-2
*****
***** initial calculations and setup"
initial
***** change the variable from t to z (length)"
variable z=0.
cinterval ci = 10.0
***** calculate tube outer diameter - cm."
diao = diai + 2.0 * xwall
***** calculate initial flow conditions"
areai = pi * diai * diai * 0.25
hctot = xc1i + xc2i + xc3i + xc4i + xc5i + xc6i + xc7i + xc8i
xstm = hctot * frst
xtot = hctot + xstm
yc1i = xc1i / xtot
yc2i = xc2i / xtot
yc3i = xc3i / xtot
yc4i = xc4i / xtot
yc5i = xc5i / xtot
yc6i = xc6i / xtot
yc7i = xc7i / xtot
yc8i = xc8i / xtot
ystm = xstm / xtot
mwavi = yc1i * mwc1 + yc2i * mwc2 + yc3i * mwc3 + yc4i * mwc4 + ...
        yc5i * mwc5 + yc6i * mwc6 + yc7i * mwc7 + yc8i * mwc8 + ...
        ystm * mwst
ftoti = flowi * areai / mwavi
fc1i = yc1i * ftoti
fc2i = yc2i * ftoti
fc3i = yc3i * ftoti
fc4i = yc4i * ftoti
fc5i = yc5i * ftoti
fc6i = yc6i * ftoti
fc7i = yc7i * ftoti
fc8i = yc8i * ftoti
fstm = ystm * ftoti
***** calculate viscosity term 1"
vcrc1 = 7.70 * mwc1 ** 0.5 * pcc1 ** (2./3.) * tcc1 ** (-1./6.)

```

```

vcrc2 = 7.70 * mnc2 ** 0.5 * pcc2 ** (2./3.) * tcc2 ** (-1./6.)
vcrc3 = 7.70 * mnc3 ** 0.5 * pcc3 ** (2./3.) * tcc3 ** (-1./6.)
vcrc4 = 7.70 * mnc4 ** 0.5 * pcc4 ** (2./3.) * tcc4 ** (-1./6.)
vcrc5 = 7.70 * mnc5 ** 0.5 * pcc5 ** (2./3.) * tcc5 ** (-1./6.)
vcrc6 = 7.70 * mnc6 ** 0.5 * pcc6 ** (2./3.) * tcc6 ** (-1./6.)
vcrc7 = 7.70 * mnc7 ** 0.5 * pcc7 ** (2./3.) * tcc7 ** (-1./6.)
vcrc8 = 7.70 * mnc8 ** 0.5 * pcc8 ** (2./3.) * tcc8 ** (-1./6.)
vcrst = 7.70 * mncst ** 0.5 * pcst ** (2./3.) * tcst ** (-1./6.)
***** calculate heat of reaction at 298K - cal / g-mol"
dhrx1 = delhc4 + delhc1 - delhc5
dhrx2 = delhc7 + delhc2 - 2 * delhc5
dhrx3 = delhc3 + delhc2 - delhc6
dhrx4 = delhc8 - delhc3 - delhc4
dhrx5 = delhc6 + delhc2 - delhc4 - delhc5
dhrx6 = 4 * delhc8 + 3 * delhc1 - delhc8
***** calculate delcp for reactions - cal / g-mol K"
cparx1 = cpac4 + cpac1 - cpac5
cparx2 = cpac7 + cpac2 - 2 * cpac5
cparx3 = cpac3 + cpac2 - cpac6
cparx4 = cpac8 - cpac3 - cpac4
cparx5 = cpac6 + cpac2 - cpac4 - cpac5
cparx6 = 4 * cpac8 + 3 * cpac1 - cpac8
cpbrx1 = ( cpbc4 + cpbc1 - cpbc5 ) * 0.5
cpbrx2 = ( cpbc7 + cpbc2 - 2 * cpbc5 ) * 0.5
cpbrx3 = ( cpbc3 + cpbc2 - cpbc6 ) * 0.5
cpbrx4 = ( cpbc8 - cpbc3 - cpbc4 ) * 0.5
cpbrx5 = ( cpbc6 + cpbc2 - cpbc4 - cpbc5 ) * 0.5
cpbrx6 = ( 4 * cpbc8 + 3 * cpbc1 - cpbc8 ) * 0.5
cpcrx1 = ( cpcc4 + cpcc1 - cpcc5 ) / 3.0
cpcrx2 = ( cpcc7 + cpcc2 - 2 * cpcc5 ) / 3.0
cpcrx3 = ( cpcc3 + cpcc2 - cpcc6 ) / 3.0
cpcrx4 = ( cpcc8 - cpcc3 - cpcc4 ) / 3.0
cpcrx5 = ( cpcc6 + cpcc2 - cpcc4 - cpcc5 ) / 3.0
cpcrx6 = ( 4 * cpcc8 + 3 * cpcc1 - cpcc8 ) / 3.0
cpdrx1 = ( cpdc4 + cpdc1 - cpdc5 ) * 0.25
cpdrx2 = ( cpdc7 + cpdc2 - 2 * cpdc5 ) * 0.25
cpdrx3 = ( cpdc3 + cpdc2 - cpdc6 ) * 0.25
cpdrx4 = ( cpdc8 - cpdc3 - cpdc4 ) * 0.25
cpdrx5 = ( cpdc6 + cpdc2 - cpdc4 - cpdc5 ) * 0.25
cpdrx6 = ( 4 * cpdc8 + 3 * cpdc1 - cpdc8 ) * 0.25
***** initialize coke accumulation"
do label2 ipos=1,npos
tcoke(ipos)=0.0
label2.. continue
***** initialize time loop"
time = timei
label1.. continue
end $"initial"
dynamic
***** calculate total feed - g-mol / sec"
ftot = fc1 + fc2 + fc3 + fc4 + fc5 + fc6 + fc7 + fc8 + fstm
***** calculate mole fractions"
yc1 = fc1 / ftot
yc2 = fc2 / ftot
yc3 = fc3 / ftot
yc4 = fc4 / ftot
yc5 = fc5 / ftot
yc6 = fc6 / ftot
yc7 = fc7 / ftot
yc8 = fc8 / ftot
yst = fstm / ftot
***** evaluate rate constants"
denom = rconst * temp * rneg1
***** ( 1 / sec )"
rkrx1 = prrx1 * exp ( actrx1 / denom )
rkrx2 = prrx2 * exp ( actrx2 / denom )
rkrx3 = prrx3 * exp ( actrx3 / denom )
***** ( cm3 / g-mol sec )"
rkrx4 = prrx4 * exp ( actrx4 / denom )
rkrx5 = prrx5 * exp ( actrx5 / denom )

```

```

***** ( gm coke cm / gm c4 sec )"
rkrx6 = prerx6 * exp ( actrx6 / denom )
***** evaluate equilibrium constants - g-mol / cm3"
***** (convert g-mol / l to g-mol / cm3)"
eqrx1 = ( exp ( eqbrx1 + eqsrx1 * temp ) ) * 0.001
eqrx3 = ( exp ( eqbrx3 + eqsrx3 * temp ) ) * 0.001
***** calculate viscosity - cP"
vrc1 = exp ( ( -0.1208 + 0.1354 * alog ( temp / tcc1 ) ) * 5.0 )
vrc2 = exp ( ( -0.1208 + 0.1354 * alog ( temp / tcc2 ) ) * 5.0 )
vrc3 = exp ( ( -0.1208 + 0.1354 * alog ( temp / tcc3 ) ) * 5.0 )
vrc4 = exp ( ( -0.1208 + 0.1354 * alog ( temp / tcc4 ) ) * 5.0 )
vrc5 = exp ( ( -0.1208 + 0.1354 * alog ( temp / tcc5 ) ) * 5.0 )
vrc6 = exp ( ( -0.1208 + 0.1354 * alog ( temp / tcc6 ) ) * 5.0 )
vrc7 = exp ( ( -0.1208 + 0.1354 * alog ( temp / tcc7 ) ) * 5.0 )
vrc8 = exp ( ( -0.1208 + 0.1354 * alog ( temp / tcc8 ) ) * 5.0 )
vrst = exp ( ( -0.1208 + 0.1354 * alog ( temp / tcst ) ) * 5.0 )
***** (convert from micropoise to cP)"
visc1 = 0.0001 * vrc1 * vrc1
visc2 = 0.0001 * vrc2 * vrc2
visc3 = 0.0001 * vrc3 * vrc3
visc4 = 0.0001 * vrc4 * vrc4
visc5 = 0.0001 * vrc5 * vrc5
visc6 = 0.0001 * vrc6 * vrc6
visc7 = 0.0001 * vrc7 * vrc7
visc8 = 0.0001 * vrc8 * vrc8
visst = 0.0001 * vrst * vrst
***** calculate average viscosity - cP"
ymwc1 = yc1 * sqrt( mwc1 )
ymwc2 = yc2 * sqrt( mwc2 )
ymwc3 = yc3 * sqrt( mwc3 )
ymwc4 = yc4 * sqrt( mwc4 )
ymwc5 = yc5 * sqrt( mwc5 )
ymwc6 = yc6 * sqrt( mwc6 )
ymwc7 = yc7 * sqrt( mwc7 )
ymwc8 = yc8 * sqrt( mwc8 )
ymwst = yst * sqrt( mwst )
vnum = ymwc1 * visc1 + ymwc2 * visc2 + ymwc3 * visc3 + ...
      ymwc4 * visc4 + ymwc5 * visc5 + ymwc6 * visc6 + ...
      ymwc7 * visc7 + ymwc8 * visc8 + ymwcst * visst
vden = ymwc1 + ymwc2 + ymwc3 + ymwc4 + ymwc5 + ymwc6 + ymwc7 + ...
      ymwc8 + ymwcst
vism = vnum / vden
***** calculate average molecular weight - gm / g-mol"
mwav = yc1 * mwc1 + yc2 * mwc2 + yc3 * mwc3 + yc4 * mwc4 + ...
      yc5 * mwc5 + yc6 * mwc6 + yc7 * mwc7 + yc8 * mwc8 + ...
      ystm * mwst
***** calculate heat capacities - cal / g-mol K"
temp2 = temp * temp
temp3 = temp2 * temp
cpc1 = cpac1 + cpbc1 * temp + cpcc1 * temp2 + cpdc1 * temp3
cpc2 = cpac2 + cpbc2 * temp + cpcc2 * temp2 + cpdc2 * temp3
cpc3 = cpac3 + cpbc3 * temp + cpcc3 * temp2 + cpdc3 * temp3
cpc4 = cpac4 + cpbc4 * temp + cpcc4 * temp2 + cpdc4 * temp3
cpc5 = cpac5 + cpbc5 * temp + cpcc5 * temp2 + cpdc5 * temp3
cpc6 = cpac6 + cpbc6 * temp + cpcc6 * temp2 + cpdc6 * temp3
cpc7 = cpac7 + cpbc7 * temp + cpcc7 * temp2 + cpdc7 * temp3
cpc8 = cpac8 + cpbc8 * temp + cpcc8 * temp2 + cpdc8 * temp3
cpst = cpast + cpbst * temp + cpcst * temp2 + cpdst * temp3
***** calculate average heat capacity - cal / g-mol K"
cpav = yc1 * cpc1 + yc2 * cpc2 + yc3 * cpc3 + yc4 * cpc4 + ...
      yc5 * cpc5 + yc6 * cpc6 + yc7 * cpc7 + yc8 * cpc8 + ...
      ystm * cpst
***** calculate integrated delta heat capacity - cal / g-mol"
tt = temp - tref
tt2 = tt * tt
tt3 = tt2 * tt
tt4 = tt3 * tt
cprx1 = cparx1 * tt + cpbrx1 * tt2 + cpcrx1 * tt3 + cpdrx1 * tt4
cprx2 = cparx2 * tt + cpbrx2 * tt2 + cpcrx2 * tt3 + cpdrx2 * tt4
cprx3 = cparx3 * tt + cpbrx3 * tt2 + cpcrx3 * tt3 + cpdrx3 * tt4

```

```

cprx4 = cparx4 * tt + cpbrx4 * tt2 + cpcrx4 * tt3 + cpdrx4 * tt4
cprx5 = cparx5 * tt + cpbrx5 * tt2 + cpcrx5 * tt3 + cpdrx5 * tt4
cprx6 = cparx6 * tt + cpbrx6 * tt2 + cpcrx6 * tt3 + cpdrx6 * tt4
***** calculate heat of reaction - cal / g-mol"
hrx1 = dhrx1 + cprx1
hrx2 = dhrx2 + cprx2
hrx3 = dhrx3 + cprx3
hrx4 = dhrx4 + cprx4
hrx5 = dhrx5 + cprx5
hrx6 = dhrx6 + cprx6
***** calculate gas thermal conductivity - Btu / hr ft F"
***** (convert viscosity from cP to lb / hr ft)"
cvav = cpav - 1.99
vismb = vism * 2.42
kfm = vismb * cvav * ( 3.670 / cvav + 1.272 ) / mwav
***** calculate wall heat transfer coefficient - Btu / hr ft F"
tfar = ( temp * 1.8 ) - 459.67
kwall = 14.1 + 0.00433 * ( tfar - 1300.0 )
***** calculate Prandtl no. - dimensionless"
prm = cpav * vismb / ( kfm * mwav )
***** evaluate rate expressions - g-mol / cm3 sec"
prt = pres / ( rgas * temp )
ypc1 = yc1 * prt
ypc2 = yc2 * prt
ypc3 = yc3 * prt
ypc4 = yc4 * prt
ypc5 = yc5 * prt
ypc6 = yc6 * prt
ypc7 = yc7 * prt
ypc8 = yc8 * prt
rtrx1 = rkrx1 * ( ypc5 - ypc4 * ypc1 / eqrx1 )
rtrx2 = rkrx2 * ( ypc5 )
rtrx3 = rkrx3 * ( ypc6 - ypc3 * ypc2 / eqrx3 )
rtrx4 = rkrx4 * ( ypc3 * ypc4 )
rtrx5 = rkrx5 * ( ypc4 * ypc5 )
***** ( mole coke / cm2 sec )"
rtrx6z = rkrx6 * ( ypc8 ) * ( mwc8 / mwck )
***** calculate the change in diameter due to coke - cm."
ipos = int ( z / delz ) + 1
bck = tcokel(ipos)
dia = diai - 2.0 * bck
***** accumulate coke"
delbck = alpck * rtrx6z * mwck * tstep * tfact / rhock
tcokel(ipos) = tcokel(ipos) + delbck
***** calculate the perimeter and area - cm and cm2"
per = pi * dia
area = pi * dia * dia * 0.25
***** convert rtrx6 from mol / cm2 sec to mol / cm3 sec"
rtrx6 = rtrx6z * per / area
***** calculate mass flow rate - gm / cm2 sec"
gtot = ftot * mwav / area
***** calculate Reynold's no. - dimensionless"
re = dia * gtot / ( vism * 0.01 )
***** calculate friction term - 1 / cm"
fric = 0.184 * re ** (-0.2)
***** calculate dF/dx terms - g-mol / cm sec"
dfc1 = area * ( rtrx1 + 3 * rtrx6 )
dfc2 = area * ( rtrx2 + rtrx3 + rtrx5 )
dfc3 = area * ( rtrx3 - rtrx4 )
dfc4 = area * ( rtrx1 - rtrx4 - rtrx5 )
dfc5 = area * ( rtrx1 + 2 * rtrx2 + rtrx5 ) * rneg1
dfc6 = area * ( rtrx5 - rtrx3 )
dfc7 = area * ( rtrx2 )
dfc8 = area * ( rtrx4 - rtrx6 )
ddck = area * ( 4 * rtrx6 )
***** calculate internal heat transfer coeff - Btu / hr ft2 F"
teff = ( tw / temp ) ** ( 0.29 + 0.0019 * z / dia )
hi = 0.021 * re ** 0.8 * prm ** 0.4 * kfm * 30.48 / ( teff * dia )
***** calculate overall heat transfer coefficient - Btu / hr ft2 F"
dialw = diai + xwall

```

```

dialc = diai - bck
hoi = 1.0 / ho
hii = diao / ( dia * hi )
hwi = diao * 0.03281 * xwall / ( dialw * kwall )
hci = diao * 0.03281 * bck / ( dialc * kck )
uoi = hii + hwi + hci + hoi
uo = ( 1.0 / uoi ) * factu
***** calculate temperature derivative"
tden = cpav * ftot
sumr = ( rtrx1 * hrx1 + rtrx2 * hrx2 + rtrx3 * hrx3 + rtrx4 * ...
        hrx4 + rtrx5 * hrx5 + rtrx6 * hrx6 ) * rneg1
dt = ( per * uo * ( tw - temp ) + area * sumr ) / tden
***** calculate pressure drop derivative ( fanning )"
rhof = pres * mwav / ( rgas * temp )
dp = rneg1 * factp * gtot * gtot * fric / ( dia * rhof )
***** calculate fluid velocity"
velf = gtot / rhof
derivative
***** integrate for quantities"
fc1 = integ( dfc1 , fc1i )
fc2 = integ( dfc2 , fc2i )
fc3 = integ( dfc3 , fc3i )
fc4 = integ( dfc4 , fc4i )
fc5 = integ( dfc5 , fc5i )
fc6 = integ( dfc6 , fc6i )
fc7 = integ( dfc7 , fc7i )
fc8 = integ( dfc8 , fc8i )
dck = integ( ddck , dcki )
temp = integ( dt , tempi )
pres = integ( dp , presi )
end $"derivative"
***** calculate conversions"
cvc1 = ( fc1i - fc1 ) / fc1i
cvc2 = ( fc2i - fc2 ) / fc2i
cvc3 = ( fc3i - fc3 ) / fc3i
cvc4 = ( fc4i - fc4 ) / fc4i
cvc5 = ( fc5i - fc5 ) / fc5i
cvc6 = ( fc6i - fc6 ) / fc6i
cvc7 = ( fc7i - fc7 ) / fc7i
cvc8 = ( fc8i - fc8 ) / fc8i
***** calculate residence time"
tres = z / velf
***** specify terminating conditions"
termt ( z . ge . ztot )
end $"dynamic"
*****
terminal
***** time loop"
time = time + tstep
do label3 ipos=1,npos
if( tcoke(ipos).ge.bckmax ) go to label4
label3.. continue
if( time.gt.times ) go to label4
go to label1
label4.. continue
end $"terminal"
end $"program"

```

```

program age
*****
" ALBERTA GAS ETHYLENE - ETHANE TO ETHYLENE PYROLYSIS QUENCH COOLER"
" Richard Huntrods P. Eng."
" University of Calgary Masters of Engineering Thesis"
" July 1988"
*****
" MODEL 2 - Differential form of the COKE equation"
*****
***** declarations"
integer ipos , int , npos
array tcoke(100)
***** initial conditions: DATA FOR TLX SIMULATOR: H143 (AVERAGE)"
constant timei = 0.0           $" days"
constant times = 60.0          $" end time - days"
constant tstep = 6.0           $" days"
constant tempi = 1109.200       $" feed temperature - K"
constant presi = 2.024920      $" feed pressure - atm"
constant xc1i = 0.354107       $" feed composition - mole fraction"
constant xc2i = 0.061365
constant xc3i = 0.001811
constant xc4i = 0.320909
constant xc5i = 0.250490
constant xc6i = 0.003244
constant xc7i = 0.003244
constant xc8i = 0.004829
constant dcki = 0.0             $" initial coke deposition"
***** new initial conditions"
constant flohci = 2.941323      $" mass flow rate - gm/cm**2 sec"
constant flosti = 0.913211     $" mass flow rate - gm/cm**2 sec"
***** definition of reactor parameters"
constant npos = 84              $" number of reactor grid blocks"
constant ztot = 838.2           $" reactor length - cm (= 27.6 ft)"
constant delz = 10.0            $" cm"
constant diai = 3.05816         $" tube diameter - cm (= 1.204 in.)"
constant xwall = 0.37592        $" tube thickness - cm (= 0.148 in.)"
constant kck = 3.2              $" Btu / hr ft F"
constant bck = 0.0              $" initial coke thickness - cm."
constant delbck = 0.0           $" initial delta coke thickness"
constant bckmax = 1.00          $" maximum coke thickness allowed"
constant alpck = 1.0            $" fraction of coke deposited"
constant tw = 493.40            $" steam temperature - K"
constant ho = 2040.0            $" Btu / hr ft2 F"
***** definition of constant data"
constant tref = 298.0           $" K"
constant rconst = 1.987         $" cal/g-mol K"
constant rgas = 82.05           $" cm3 atm / g-mol K"
constant factp = 4.9343e-7      $" ( gm / cm2 to atm ) * 1 / 2gc"
constant factu = 1.3550e-4      $" Btu / hr ft2 F to cal / sec cm2 K"
constant tfact = 8.64e+4        $" time from days to sec."
constant pi = 3.1416
constant rneg1 = -1.0
***** definition of component data"
" H2 = C1 (hydrogen)"
" CH4 = C2 (methane)"
" C2H2 = C3 (acetylene)"
" C2H4 = C4 (ethylene)"
" C2H6 = C5 (ethane)"
" C3H6 = C6 (propylene)"
" C3H8 = C7 (propane)"
" C4H6 = C8 (1,3-butadiene)"
" C = C9 (coke)"
***** H2"
constant mwc1 = 2.016           $" molecular weight - gm / g-mol"
constant tcc1 = 33.2            $" critical temperature - K"
constant pcc1 = 12.8            $" critical pressure - atm"
constant cpac1 = 6.483          $" Cp coeff. - cal / g-mol K"
constant cpbc1 = 2.215e-3       $" Cp coeff. - cal / g-mol K**2"
constant cpcc1 = -3.298e-6      $" Cp coeff. - cal / g-mol K**3"
constant cpdc1 = 1.826e-9       $" Cp coeff. - cal / g-mol K**4"

```

```

constant delhc1 = 0.0          $" heat of formation - cal / g-mol"
***** CH4"
constant mwc2 = 16.043
constant tcc2 = 190.6
constant pcc2 = 45.4
constant cpac2 = 4.598
constant cpbc2 = 1.245e-2
constant cpcc2 = 2.860e-6
constant cpdc2 = -2.703e-9
constant delhc2 = -17890.0
***** C2H2"
constant mwc3 = 26.038
constant tcc3 = 308.3
constant pcc3 = 60.6
constant cpac3 = 6.406
constant cpbc3 = 1.810e-2
constant cpcc3 = -1.196e-5
constant cpdc3 = 3.363e-9
constant delhc3 = 54190.0
***** C2H4"
constant mwc4 = 28.054
constant tcc4 = 282.4
constant pcc4 = 49.7
constant cpac4 = 0.909
constant cpbc4 = 3.740e-2
constant cpcc4 = -1.994e-5
constant cpdc4 = 4.192e-9
constant delhc4 = 12500.0
***** C2H6"
constant mwc5 = 30.070
constant tcc5 = 305.4
constant pcc5 = 48.2
constant cpac5 = 1.292
constant cpbc5 = 4.254e-2
constant cpcc5 = -1.657e-5
constant cpdc5 = 2.081e-9
constant delhc5 = -20240.0
***** C3H6"
constant mwc6 = 42.081
constant tcc6 = 365.0
constant pcc6 = 45.6
constant cpac6 = 0.886
constant cpbc6 = 5.602e-2
constant cpcc6 = -2.771e-5
constant cpdc6 = 5.266e-9
constant delhc6 = 4880.0
***** C3H8"
constant mwc7 = 44.097
constant tcc7 = 369.8
constant pcc7 = 41.9
constant cpac7 = -1.009
constant cpbc7 = 7.315e-2
constant cpcc7 = -3.789e-5
constant cpdc7 = 7.678e-9
constant delhc7 = -24820.0
***** C4H6"
constant mwc8 = 54.092
constant tcc8 = 425.0
constant pcc8 = 42.7
constant cpac8 = -0.403
constant cpbc8 = 8.165e-2
constant cpcc8 = -5.589e-5
constant cpdc8 = 1.513e-8
constant delhc8 = 26330.0
***** coke"
constant mwcck = 12.0
constant cpack = 2.673
constant cpbck = 2.617e-3
constant cpccck = 0.0
constant cpdck = 0.0

```

```

constant delhck = 0.0
constant rhock = 1.6          $" density - g / cm3"
***** steam"
constant mwst = 18.015
constant tcst = 647.3
constant pcst = 217.6
constant cpast = 7.701
constant cpbst = 4.595e-4
constant cpcst = 2.521e-6
constant cpdst = -0.859e-9
***** definition of reaction data"
" rx1: C2H6 <-> C2H4 + H2"
" rx2: 2 C2H6 -> C3H8 + CH4"
" rx3: C3H6 <-> C2H2 + CH4"
" rx4: C2H2 + C2H4 -> C4H6"
" rx5: C2H4 + C2H6 -> C3H6 + CH4"
" rx6: C4H6 -> 4 C + 3 H2"
constant prerx1 = 4.652e13      $" 1 / sec"
constant actrx1 = 65200.0      $" cal / g-mol"
constant prerx2 = 3.850e11
constant actrx2 = 65250.0
constant prerx3 = 9.814e08
constant actrx3 = 36920.0
constant prerx4 = 1.026e15      $" cm3 / g-mol sec"
constant actrx4 = 41260.0
constant prerx5 = 7.083e16      $" cm3 / g-mol sec"
constant actrx5 = 60430.0
constant prerx6 = 8.55e4        $" gm coke cm / gm c4 sec"
constant actrx6 = 28250.0
***** equilibrium constants f(T)"
constant eqbrx1 = -19.496
constant eqsrx1 = 1.4098e-2
constant eqbrx3 = -18.286
constant eqsrx3 = 1.3040e-2
*****
***** initial calculations and setup"
initial
***** change the variable from t to z (length)"
variable z=0.
cinterval ci = 10.0
***** calculate tube outer diameter - cm."
diao = diai + 2.0 * xwall
***** calculate initial flow conditions"
areai = pi * diai * diai * 0.25
hctot = xc1i + xc2i + xc3i + xc4i + xc5i + xc6i + xc7i + xc8i
yc1i = xc1i / hctot
yc2i = xc2i / hctot
yc3i = xc3i / hctot
yc4i = xc4i / hctot
yc5i = xc5i / hctot
yc6i = xc6i / hctot
yc7i = xc7i / hctot
yc8i = xc8i / hctot
ystm = xstm / hctot
mwhci = yc1i * mwci + yc2i * mwci + yc3i * mwci + yc4i * mwci + ...
        yc5i * mwci + yc6i * mwci + yc7i * mwci + yc8i * mwci
fhci = flohci * areai / mwhci
fci = yc1i * fhci
fci2 = yc2i * fhci
fci3 = yc3i * fhci
fci4 = yc4i * fhci
fci5 = yc5i * fhci
fci6 = yc6i * fhci
fci7 = yc7i * fhci
fci8 = yc8i * fhci
fstm = flosti * areai / mwst
***** calculate viscosity term 1"
vcrc1 = 7.70 * mwci ** 0.5 * pcc1 ** (2./3.) * tcc1 ** (-1./6.)
vcrc2 = 7.70 * mwci ** 0.5 * pcc2 ** (2./3.) * tcc2 ** (-1./6.)
vcrc3 = 7.70 * mwci ** 0.5 * pcc3 ** (2./3.) * tcc3 ** (-1./6.)

```

```

vcrc4 = 7.70 * mwc4 ** 0.5 * pcc4 ** (2./3.) * tcc4 ** (-1./6.)
vcrc5 = 7.70 * mwc5 ** 0.5 * pcc5 ** (2./3.) * tcc5 ** (-1./6.)
vcrc6 = 7.70 * mwc6 ** 0.5 * pcc6 ** (2./3.) * tcc6 ** (-1./6.)
vcrc7 = 7.70 * mwc7 ** 0.5 * pcc7 ** (2./3.) * tcc7 ** (-1./6.)
vcrc8 = 7.70 * mwc8 ** 0.5 * pcc8 ** (2./3.) * tcc8 ** (-1./6.)
vcrst = 7.70 * mwst ** 0.5 * pcst ** (2./3.) * tcst ** (-1./6.)
***** calculate heat of reaction at 298K - cal / g-mol"
dhrx1 = delhc4 + delhc1 - delhc5
dhrx2 = delhc7 + delhc2 - 2 * delhc5
dhrx3 = delhc3 + delhc2 - delhc6
dhrx4 = delhc8 - delhc3 - delhc4
dhrx5 = delhc6 + delhc2 - delhc4 - delhc5
dhrx6 = 4 * delhc8 + 3 * delhc1 - delhc8
***** calculate delcp for reactions - cal / g-mol K"
cparx1 = cpac4 + cpac1 - cpac5
cparx2 = cpac7 + cpac2 - 2 * cpac5
cparx3 = cpac3 + cpac2 - cpac6
cparx4 = cpac8 - cpac3 - cpac4
cparx5 = cpac6 + cpac2 - cpac4 - cpac5
cparx6 = 4 * cpac8 + 3 * cpac1 - cpac8
cpbrx1 = ( cpbc4 + cpbc1 - cpbc5 ) * 0.5
cpbrx2 = ( cpbc7 + cpbc2 - 2 * cpbc5 ) * 0.5
cpbrx3 = ( cpbc3 + cpbc2 - cpbc6 ) * 0.5
cpbrx4 = ( cpbc8 - cpbc3 - cpbc4 ) * 0.5
cpbrx5 = ( cpbc6 + cpbc2 - cpbc4 - cpbc5 ) * 0.5
cpbrx6 = ( 4 * cpbc8 + 3 * cpbc1 - cpbc8 ) * 0.5
cpcrx1 = ( cpcc4 + cpcc1 - cpcc5 ) / 3.0
cpcrx2 = ( cpcc7 + cpcc2 - 2 * cpcc5 ) / 3.0
cpcrx3 = ( cpcc3 + cpcc2 - cpcc6 ) / 3.0
cpcrx4 = ( cpcc8 - cpcc3 - cpcc4 ) / 3.0
cpcrx5 = ( cpcc6 + cpcc2 - cpcc4 - cpcc5 ) / 3.0
cpcrx6 = ( 4 * cpcc8 + 3 * cpcc1 - cpcc8 ) / 3.0
cpdrx1 = ( cpdc4 + cpdc1 - cpdc5 ) * 0.25
cpdrx2 = ( cpdc7 + cpdc2 - 2 * cpdc5 ) * 0.25
cpdrx3 = ( cpdc3 + cpdc2 - cpdc6 ) * 0.25
cpdrx4 = ( cpdc8 - cpdc3 - cpdc4 ) * 0.25
cpdrx5 = ( cpdc6 + cpdc2 - cpdc4 - cpdc5 ) * 0.25
cpdrx6 = ( 4 * cpdc8 + 3 * cpdc1 - cpdc8 ) * 0.25
***** initialize coke accumulation"
do label2 ipos=1,npos
tcoke(ipos)=0.0
label2.. continue
***** initialize time loop"
time = timei
label1.. continue
end $"initial"
dynamic
***** calculate total feed - g-mol / sec"
ftot = fc1 + fc2 + fc3 + fc4 + fc5 + fc6 + fc7 + fc8 + fstm
***** calculate mole fractions"
yc1 = fc1 / ftot
yc2 = fc2 / ftot
yc3 = fc3 / ftot
yc4 = fc4 / ftot
yc5 = fc5 / ftot
yc6 = fc6 / ftot
yc7 = fc7 / ftot
yc8 = fc8 / ftot
yst = fstm / ftot
***** evaluate rate constants"
denom = rconst * temp * rneg1
***** ( 1 / sec )"
rkrx1 = prrx1 * exp ( actrx1 / denom )
rkrx2 = prrx2 * exp ( actrx2 / denom )
rkrx3 = prrx3 * exp ( actrx3 / denom )
***** ( cm3 / g-mol sec )"
rkrx4 = prrx4 * exp ( actrx4 / denom )
rkrx5 = prrx5 * exp ( actrx5 / denom )
***** ( gm coke cm / gm c4 sec )"
rkrx6 = prrx6 * exp ( actrx6 / denom )

```

```

***** evaluate equilibrium constants - g-mol / cm3"
***** (convert g-mol / l to g-mol / cm3)"
  eqrx1 = ( exp ( eqbrx1 + eqsrx1 * temp )) * 0.001
  eqrx3 = ( exp ( eqbrx3 + eqsrx3 * temp )) * 0.001
***** calculate viscosity - cP"
  vrc1 = exp (( -0.1208 + 0.1354 * alog ( temp / tcc1 )) * 5.0 )
  vrc2 = exp (( -0.1208 + 0.1354 * alog ( temp / tcc2 )) * 5.0 )
  vrc3 = exp (( -0.1208 + 0.1354 * alog ( temp / tcc3 )) * 5.0 )
  vrc4 = exp (( -0.1208 + 0.1354 * alog ( temp / tcc4 )) * 5.0 )
  vrc5 = exp (( -0.1208 + 0.1354 * alog ( temp / tcc5 )) * 5.0 )
  vrc6 = exp (( -0.1208 + 0.1354 * alog ( temp / tcc6 )) * 5.0 )
  vrc7 = exp (( -0.1208 + 0.1354 * alog ( temp / tcc7 )) * 5.0 )
  vrc8 = exp (( -0.1208 + 0.1354 * alog ( temp / tcc8 )) * 5.0 )
  vrst = exp (( -0.1208 + 0.1354 * alog ( temp / tcst )) * 5.0 )
***** (convert from micropoise to cP)"
  visc1 = 0.0001 * vcrc1 * vrc1
  visc2 = 0.0001 * vcrc2 * vrc2
  visc3 = 0.0001 * vcrc3 * vrc3
  visc4 = 0.0001 * vcrc4 * vrc4
  visc5 = 0.0001 * vcrc5 * vrc5
  visc6 = 0.0001 * vcrc6 * vrc6
  visc7 = 0.0001 * vcrc7 * vrc7
  visc8 = 0.0001 * vcrc8 * vrc8
  visst = 0.0001 * vcrst * vrst
***** calculate average viscosity - cP"
  ymwc1 = yc1 * sqrt( mwc1 )
  ymwc2 = yc2 * sqrt( mwc2 )
  ymwc3 = yc3 * sqrt( mwc3 )
  ymwc4 = yc4 * sqrt( mwc4 )
  ymwc5 = yc5 * sqrt( mwc5 )
  ymwc6 = yc6 * sqrt( mwc6 )
  ymwc7 = yc7 * sqrt( mwc7 )
  ymwc8 = yc8 * sqrt( mwc8 )
  ymwt = yst * sqrt( mwst )
  vnum = ymwc1 * visc1 + ymwc2 * visc2 + ymwc3 * visc3 + ...
        ymwc4 * visc4 + ymwc5 * visc5 + ymwc6 * visc6 + ...
        ymwc7 * visc7 + ymwc8 * visc8 + ymwt * visst
  vden = ymwc1 + ymwc2 + ymwc3 + ymwc4 + ymwc5 + ymwc6 + ymwc7 + ...
        ymwc8 + ymwt
  vism = vnum / vden
***** calculate average molecular weight - gm / g-mol"
  mwav = yc1 * mwc1 + yc2 * mwc2 + yc3 * mwc3 + yc4 * mwc4 + ...
        yc5 * mwc5 + yc6 * mwc6 + yc7 * mwc7 + yc8 * mwc8 + ...
        ystm * mwst
***** calculate heat capacities - cal / g-mol K"
  temp2 = temp * temp
  temp3 = temp2 * temp
  cpc1 = cpac1 + cpbc1 * temp + cpcc1 * temp2 + cpdc1 * temp3
  cpc2 = cpac2 + cpbc2 * temp + cpcc2 * temp2 + cpdc2 * temp3
  cpc3 = cpac3 + cpbc3 * temp + cpcc3 * temp2 + cpdc3 * temp3
  cpc4 = cpac4 + cpbc4 * temp + cpcc4 * temp2 + cpdc4 * temp3
  cpc5 = cpac5 + cpbc5 * temp + cpcc5 * temp2 + cpdc5 * temp3
  cpc6 = cpac6 + cpbc6 * temp + cpcc6 * temp2 + cpdc6 * temp3
  cpc7 = cpac7 + cpbc7 * temp + cpcc7 * temp2 + cpdc7 * temp3
  cpc8 = cpac8 + cpbc8 * temp + cpcc8 * temp2 + cpdc8 * temp3
  cpst = cpast + cpbst * temp + cpcst * temp2 + cpdst * temp3
***** calculate average heat capacity - cal / g-mol K"
  cpav = yc1 * cpc1 + yc2 * cpc2 + yc3 * cpc3 + yc4 * cpc4 + ...
        yc5 * cpc5 + yc6 * cpc6 + yc7 * cpc7 + yc8 * cpc8 + ...
        yst * cpst
***** calculate integrated delta heat capacity - cal / g-mol"
  tt = temp - tref
  tt2 = tt * tt
  tt3 = tt2 * tt
  tt4 = tt3 * tt
  cprx1 = cparx1 * tt + cpbrx1 * tt2 + cpcrx1 * tt3 + cpdrx1 * tt4
  cprx2 = cparx2 * tt + cpbrx2 * tt2 + cpcrx2 * tt3 + cpdrx2 * tt4
  cprx3 = cparx3 * tt + cpbrx3 * tt2 + cpcrx3 * tt3 + cpdrx3 * tt4
  cprx4 = cparx4 * tt + cpbrx4 * tt2 + cpcrx4 * tt3 + cpdrx4 * tt4
  cprx5 = cparx5 * tt + cpbrx5 * tt2 + cpcrx5 * tt3 + cpdrx5 * tt4

```

```

cprx6 = cparx6 * tt + cpbrx6 * tt2 + cpcrx6 * tt3 + cpdrx6 * tt4
***** calculate heat of reaction - cal / g-mol"
hrx1 = dhrx1 + cprx1
hrx2 = dhrx2 + cprx2
hrx3 = dhrx3 + cprx3
hrx4 = dhrx4 + cprx4
hrx5 = dhrx5 + cprx5
hrx6 = dhrx6 + cprx6
***** calculate gas thermal conductivity - Btu / hr ft F"
***** (convert viscosity from cP to lb / hr ft)"
cvav = cpav - 1.99
vismb = vism * 2.42
kfm = vismb * cvav * ( 3.670 / cvav + 1.272 ) / mwav
***** calculate wall heat transfer coefficient - Btu / hr ft F"
tfar = ( temp * 1.8 ) - 459.67
kwall = 14.1 + 0.00433 * ( tfar - 1300.0 )
***** calculate Prandtl no. - dimensionless"
prm = cpav * vismb / ( kfm * mwav )
***** evaluate rate expressions - g-mol / cm3 sec"
prt = pres / ( rgas * temp )
ypc1 = yc1 * prt
ypc2 = yc2 * prt
ypc3 = yc3 * prt
ypc4 = yc4 * prt
ypc5 = yc5 * prt
ypc6 = yc6 * prt
ypc7 = yc7 * prt
ypc8 = yc8 * prt
rtrx1 = rkrx1 * ( ypc5 - ypc4 * ypc1 / eqrx1 )
rtrx2 = rkrx2 * ( ypc5 )
rtrx3 = rkrx3 * ( ypc6 - ypc3 * ypc2 / eqrx3 )
rtrx4 = rkrx4 * ( ypc3 * ypc4 )
rtrx5 = rkrx5 * ( ypc4 * ypc5 )
***** ( mole coke / cm2 sec )"
rtrx6z = rkrx6 * ( ypc8 ) * ( mwc8 / mwck )
***** calculate the change in diameter due to coke - cm."
ipos = int ( z / delz ) + 1
bck = tcoke(ipos)
dia = diai - 2.0 * bck
***** accumulate coke"
delbck = alpck * rtrx6z * mwck * tstep * tfact / rhock
tcoke(ipos) = tcoke(ipos) + delbck
***** calculate the perimeter and area - cm and cm2"
per = pi * dia
area = pi * dia * dia * 0.25
***** convert rtrx6 from mol / cm2 sec to mol / cm3 sec"
rtrx6 = rtrx6z * per / area
***** calculate mass flow rate - gm / cm2 sec"
gtot = ftot * mwav / area
***** calculate Reynold's no. - dimensionless"
re = dia * gtot / ( vism * 0.01 )
***** calculate friction term - 1 / cm"
fric = 0.184 * re ** (-0.2)
***** calculate dF/dx terms - g-mol / cm sec"
dfc1 = area * ( rtrx1 + 3 * rtrx6 )
dfc2 = area * ( rtrx2 + rtrx3 + rtrx5 )
dfc3 = area * ( rtrx3 - rtrx4 )
dfc4 = area * ( rtrx1 - rtrx4 - rtrx5 )
dfc5 = area * ( rtrx1 + 2 * rtrx2 + rtrx5 ) * rneg1
dfc6 = area * ( rtrx5 - rtrx3 )
dfc7 = area * ( rtrx2 )
dfc8 = area * ( rtrx4 - rtrx6 )
ddck = area * ( 4 * rtrx6 )
***** calculate internal heat transfer coeff - Btu / hr ft2 F"
teff = ( tw / temp ) ** ( 0.29 + 0.0019 * z / dia )
hj = 0.021 * re ** 0.8 * prm ** 0.4 * kfm * 30.48 / ( teff * dia )
***** calculate overall heat transfer coefficient - Btu / hr ft2 F"
dialw = diai + xwall
dialc = diai - bck
hoi = 1.0 / ho

```

```

hii = diao / ( dia * hi )
hwi = diao * 0.03281 * xwall / ( dialw * kwall )
hci = diao * 0.03281 * bck / ( dialc * kck )
uoi = hii + hwi + hci + hoi
uo = ( 1.0 / uoi ) * factu
***** calculate temperature derivative"
tden = cpav * ftot
sumr = ( rtrx1 * hrx1 + rtrx2 * hrx2 + rtrx3 * hrx3 + rtrx4 * ...
        hrx4 + rtrx5 * hrx5 + rtrx6 * hrx6 ) * rneg1
dt = ( per * uo * ( tw - temp ) + area * sumr ) / tden
***** calculate pressure drop derivative ( fanning )"
rhof = pres * mwav / ( rgas * temp )
dp = rneg1 * factp * gtot * fric / ( dia * rhof )
***** calculate fluid velocity"
velf = gtot / rhof
derivative
***** integrate for quantities"
fc1 = integ( dfc1 , fc1i )
fc2 = integ( dfc2 , fc2i )
fc3 = integ( dfc3 , fc3i )
fc4 = integ( dfc4 , fc4i )
fc5 = integ( dfc5 , fc5i )
fc6 = integ( dfc6 , fc6i )
fc7 = integ( dfc7 , fc7i )
fc8 = integ( dfc8 , fc8i )
dck = integ( ddck , dcki )
temp = integ( dt , tempi )
pres = integ( dp , presi )
end $"derivative"
***** calculate conversions"
cvc1 = ( fc1i - fc1 ) / fc1i
cvc2 = ( fc2i - fc2 ) / fc2i
cvc3 = ( fc3i - fc3 ) / fc3i
cvc4 = ( fc4i - fc4 ) / fc4i
cvc5 = ( fc5i - fc5 ) / fc5i
cvc6 = ( fc6i - fc6 ) / fc6i
cvc7 = ( fc7i - fc7 ) / fc7i
cvc8 = ( fc8i - fc8 ) / fc8i
***** output values"
hctot = yc1 + yc2 + yc3 + yc4 + yc5 + yc6 + yc7 + yc8
frst = yst / hctot
xc1 = yc1 / hctot
xc2 = yc2 / hctot
xc3 = yc3 / hctot
xc4 = yc4 / hctot
xc5 = yc5 / hctot
xc6 = yc6 / hctot
xc7 = yc7 / hctot
xc8 = yc8 / hctot
***** calculate residence time"
tres = z / velf
***** specify terminating conditions"
termt ( z . ge . ztot )
end $"dynamic"
*****
terminal
***** time loop"
time = time + tstep
do label3 ipos=1,npos
if( tcoke(ipos).ge.bckmax ) go to label4
label3.. continue
if( time.gt.times ) go to label4
go to label1
label4.. continue
end $"terminal"
end $"program"

```

Appendix K. Program Run Post Processing

The simulation computer runs were performed on the University of Calgary Cyber 860 computer. Data was transferred to the Cyber from an IBM PC compatible computer, via the University of Calgary Honeywell Multics computer. Simulation results were transferred from the Cyber to the Honeywell, and then to the PC. Post-processing of the simulation results files on the PC was accomplished using a number of FORTRAN programs which I wrote for this work. These programs read the simulation results files, reformatted the data, and produced both the output summaries found in Appendix H. The plots found in the body of the report were produced using three FORTRAN programs which I wrote for this task. These programs ran on Canadian Hunter's Prime 6350 computer (with data transferred from the PC), and produced the plots using the DIPLOT plotting subroutine package developed for Canadian Hunter by Enigma Software.